REARING *Mesostoma ehrenbergii* AND STUDYING CHROMOSOME MOVEMENTS DURING MEIOSIS IN THEIR SPERMATOCYTES

JESSICA FERRARO-GIDEON

A DISSERTATION SUBMITTED TO
THE FACULTY OF GRADUATE STUDIES
IN PARTIAL FULFILLMENT OF THE REQUIREMENTS
FOR THE DEGREE OF
DOCTOR OF PHILOSOPHY

GRADUATE PROGRAM IN BIOLOGY
YORK UNIVERSITY
TORONTO, ONTARIO

AUGUST 2013

ABSTRACT

The *Mesostoma ehrenbergii* spermatocyte is an advantageous cell for studying meiosis. Its many unique features include regular and persistent bivalent kinetochore oscillations, distance segregation of univalents and the presence of a precocious cleavage furrow. In studying these unconventional aspects of meiosis in one cell, I concentrated on studying which components are involved in the force production driving chromosome movement, using bivalent kinetochore oscillations as a measurable conversion. *Mesostoma* spermatocytes had not been well studied and there are only a handful of articles in the literature that describe them so I first had to characterize their normal behaviour. I determined that kinetochore movement to the pole is faster than kinetochore movement away from the pole; bivalents enter into anaphase in the middle of an oscillation cycle as there is no definable metaphase; bivalents reorient (and kinetochores switch poles) after achieving bipolar orientation; and univalents move multiple times between spindle poles. After characterizing kinetochore oscillations in these spermatocytes, I used an ultraviolet microbeam, an optical cutting laser and an optical trapping laser as tools to study the components involved in driving kinetochore movements to and away from the pole. The results from my UV microbeam and laser microbeam experiments suggest that different mechanisms are required to produce kinetochore movement to the pole versus away from the pole, and that non-microtubule components and/or a spindle matrix are involved as kinetochores still moved to the pole in the absence of microtubule continuity between kinetochore and pole. Comparisons of normal bivalent reorientations, where partner kinetochores switch poles, with laser-induced reorientations, where partners retain their original orientations, suggest that the segregation of bivalents is non-random. UV irradiations indicated that the cleavage furrow changes positions in response to alterations in spindle components. Severed chromosome arms moved to the other arm, indicating that there is a connection ("tether") between bivalent arms. The results from my optical trapping experiments determined that the force produced by the spindle to move chromosomes to the pole is one one-hundredth of 700pN that was originally measured and is close to the theoretical values.

ACKNOWLEDGMENTS

I am sincerely honoured to have been given the privilege to conduct my PhD dissertation in the Forer laboratory. Words cannot express how grateful I am to have Dr. Arthur Forer as my supervisor. Dr. Forer goes above and beyond his role as a supervisor; he is a teacher, a leader, a mentor, an excellent proofreader and a fountain of information. His continual guidance and support has helped me develop the ability to think critically, to solve problems, to ask questions, and to write clearly and concisely. Dr. Forer's strong beliefs on how chromosome move and his enthusiasm for research are qualities that I respect and will take with me as I start the next chapter of my research career.

I would like to thank my supervisory committee, Dr. Barry Loughton and Dr. Patricia Lakin-Thomas, who have provided me with continual guidance and direction over the past six years. I would like to thank Dr. Paula Wilson and Dr. Leocadia Paliulis for our stimulating discussions and their positive reassurance that my controversial optical trapping laser paper would be published. I would also like to thank Dr. Suzanne McDonald for enthusiastically agreeing to be on my examining committee.

I would sincerely like to thank the members of the Forer' laboratory, in particular Rozhan Sheykhani and Carina Hoang. You both have been amazing colleagues, friends and roommates, and I could not have asked for two better people to have shared this experience with. To Karen Rethoret, thank you very much for teaching me everything I need to know about electron microscopy and confocal microscopy. I am also very grateful to you for the numerous hours you spent sectioning and preparing grids for EM.

To my husband, Sami Gideon, thank you for being extremely supportive and understanding. You were always there to lift my spirits when I had a bad day in the lab or when I received notification that one of my articles had been rejected. Your constant reassurance and continual guidance gave me the extra motivation I needed to continue to strive for success. To my parents, you have instilled in me the importance of education since I was a child and because of this, I continued to strive for a higher education. Dad, your creative science fair project ideas sparked my initial fascination for science and our many science-related discussions continued to drive my passion. I would like to thank you both for giving me the passion and desire to complete my PhD. To my sisters, you have both been very supportive throughout the many years I have spent in school. Michele, your help and guidance on how to format my thesis allowed me to complete it right on time and for that, I am extremely grateful to you. To the Gideon family, thank you for your constant words of encouragement. To my mother-in-law, Dr. Salva Gideon, thank you for showing me that a woman can complete a degree, be extremely successful in her career and raise a wonderful family. You have been my role model. To my two beautiful babies, Mia and Joseph, you are my precious bundles of joy. Thank you for giving me the inspiration to strive for greatness.

TABLE OF CONTENTS

CHAPTERS

LIST OF TABLES

LIST OF FIGURES

CHAPTER 1

Introduction

1.1 Meiosis: The Conventional Process

Meiosis is the process that converts diploid cells to haploid cells and is the basis for sexual reproduction in most eukaryotic organisms. I will first be describing the "conventional" or "textbook" process of meiosis and then I will describe the unconventional processes of meiosis that occur in a variety of different cell types.

Meiosis only occurs in small populations of germ cells which, in a common manner, undergo a single round of chromosome duplication followed by two consecutive rounds of division, meiosis I and meiosis II (Morgan, 2007). Meiosis I and meiosis II result in the segregation of homologous chromosomes and the segregation of sister chromatids, respectively (Morgan, 2007).

Meiosis is controlled by a series of cell cycle checkpoints that ensure that one phase is completed before another phase begins (Morgan, 2007; Page and Orr-Weaver, 1997). The G1 and S phase are divisions of interphase which precede the commencement of meiosis. These phases initiate DNA replication and centrosome duplication and either commit the cell to continue division or exit the cell cycle (Morgan, 2007). Once the cell commits to division, the onset of meiosis occurs. The first phase of meiosis is prophase. During this phase there are numerous changes in chromosome structure: homologous chromosomes pair and form synaptonemal complex near the future sites of crossover (Morgan, 2007; Vogt et al., 2008); genetic information is exchanged through the

recombination of DNA (Meier and Gartner, 2006; Burgoyne and Mahadevaiah, 2007); physical linkages of chromatin called chiasmata are created once recombination is complete (Roeder and Baillis, 2000; Hochwagen and Amon, 2006); and bivalents become dispersed throughout the nucleus in preparation for spindle formation (Swanson et al., 2001). In prometaphase, chromosome motion usually commences following nuclear envelope breakdown to allow microtubules to interact with chromosomes (Pickett-Heaps et al., 1984). Upon capture of microtubules by kinetochores, chromosomes exhibit irregular oscillations throughout prometaphase until the directed motion of the oscillations towards the equator results in the proper metaphase configuration (Pickett-Heaps et al., 1984). Therefore, by metaphase, the homologous chromosomes align at the spindle equator and form a bipolar attachment (Page and Orr-Weaver, 1997; Tyson and Novak, 2008). Bi-polar orientation of homologous chromosomes and a stable attachment to the spindle are required for the progression into anaphase (Page and Orr-Weaver, 1997).

Tension at the kinetochore is required for chromosome segregation to occur: in praying mantid spermatocytes, the absence of tension at the kinetochore prevents chromosome segregation from occurring (Li and Nicklas, 1995). When trivalent chromosomes were oriented incorrectly, there was a lack of tension on the chromosomes so Li and Nicklas (1995) mimicked the tension that would be present on the chromosome by pulling the X-univalent with a microneedle toward the unattached pole. This resulted in anaphase onset after approximately an hour, showing that tension is an important cue for anaphase to begin and for proper chromosome segregation to occur. In anaphase I,

cohesions, which hold chromosomes together as bivalents, are removed, allowing homologous chromosomes to segregate to opposite poles (Tyson and Novak, 2008). The end of meiosis I generates two haploid daughter cells with replicated chromosomes (Tyson and Novak, 2008). Meiosis II begins without an intervening S phase and results in the segregation of sister chromatids to opposite poles, forming four nuclei, each with a haploid set of chromosomes.

Meiosis in males and females differs (Albertini and Carabatsos, 1998; Vogt et al., 2008), across most species. Using humans as an example, male spermatogenesis is initiated at puberty and continues uninterrupted in the testis (Austin and Short, 1982). Spermatogonia double their DNA content and proceed directly from the end of prophase into two meiotic divisions without pausing or arresting at a cell cycle checkpoint (Handel et al., 1999; Vogt et al., 2008). The second meiotic division of spermatogenesis yields four haploid spermatids from each spermatocyte. In human females, on the other hand, meiosis begins in the embryonic ovary prior to birth (Vogt et al., 2008) and meiosis then is arrested until ovulation at the time of puberty (Austin and Short, 1982; Vogt *et al.* 2008). Oocytes undergo a selection process prior to completing meiosis known as folliculogenesis which recruits, nurtures and marks a specific oocyte suitable to complete meiosis and reach meiotic competency for maturation (Albertini and Carabatsos, 1998; Vogt et al., 2008). Upon reaching full competency, the oocyte re-enters meiosis, generating a large oocyte and a small cell known as a polar body and then arrests at metaphase II (Albertini and Carabatsos, 1998). The cells finish meiosis II after fertilization and produce an ovum and three polar bodies (Vogt et al., 2008).

Meiosis in many eukaryotes differs, however, from this standard textbook picture. Differences from the stereotypical meiosis include: equational division (no change in the number of chromosomes at the end of division) followed by a reductional division (reduction or decrease in the number of chromosomes at the end of division), only an equational division or only a reductional division or non-random chromosome segregation. Some of these examples will be discussed later in the introduction.

1.2 The Components Involved in Cell Motility

Meiosis and mitosis are essential processes for cells to successfully divide and replicate; the components involved in chromosome segregation, a key event in cell division, play a vital role in the successful completion of these processes. Chromosome segregation is just one form of motility that occurs within a cell. In general, motility within a cell is driven by the cytoskeleton (Bray, 2001). Comprised of a meshwork of protein filaments including microtubules, microfilaments and intermediate filaments, the cytoskeleton extends throughout the cytoplasm in plant and animal cells, functioning as a structural support, an internal framework responsible for positioning and directing the movements of organelles, as well as serving as essential components for cell division. The motor proteins associated with microtubules and actin filaments are responsible for almost all the movements that occur in eukaryotic cells (Bray, 2001). Microtubules and actin filaments have distinct structural polarities that dictate the direction of motion.

Microtubules present in plant and animal cells, serve as tracks to direct the movement of vesicles, organelles and other components of the cell (Bray, 2001; Karp,

2003). The assembly of microtubules from the protein tubulin generally occurs in association with a microtubule organizing center (MTOC) (Pickett-Heaps, 1969) that controls the number of microtubules assembled, the polarity of the microtubule and the time and location in which microtubule assembly takes place in the cytoplasm (Karp, 2003). As microtubules are usually assembled from an organizing center, the polarity of a microtubule can be determined in relation to the organizing center, with the minus end attached to the organizing center and the plus end opposite the organizing center (Haimo, 1997). When a microtubule polymerizes the tubulin subunits add more rapidly to one end of the microtubule than the other. The fast growing end is called the plus end and the other end the minus end (Bergen and Borisy, 1980). Microtubules have phases of steady growth and phases of rapid shortening, known as dynamic instability (Mitchison and Kirschner, 1987). GTP subunits are incorporated into a microtubule and are hydrolyzed to GDP during polymerization and GDP subunits are released from a microtubule during depolymerization (Kirschner, 1980). The polarity of a microtubule influences the directed movement of cellular components throughout the cell because the microtubule-associated motor proteins, kinesin and cytoplasmic dynein, direct attached cargo, in general, towards the plus end of the microtubule and towards the minus end of the microtubule, respectively (Hyman and Mitchison, 1991). Cargo attachment is specific to the motor protein as each motor protein has a different tail and associated light chains that allow for the appropriate organelle to attach (Alberts et al., 2008). Microtubules provide an elaborate linear network that allows the directed transport of intracellular components via

the motor proteins, kinesin and dynein, throughout the cytoskeleton of the eukaryotic cell.

Actin microfilaments are also important filamentous cytoskeleton components that allow cells to undergo remarkable forms of motility. Microfilaments containing F-actin are composed of globular subunits of G-actin (Dominguez, 2004). Similar to microtubules, each actin subunit has its own polarity and each subunit is pointed in the same direction providing polarity to the actin filament (Mooseker and Tilney, 1975). The structural polarity of an actin filament can be experimentally determined by the interaction of actin with purified myosin that has been cleaved into fragments, referred to as heavy meromyosin (HMM) or S1 fragments, which decorate an actin filament with arrowheads (Moore et al., 1969). The pointed end of the arrowhead specifies the minus end of an actin filament, the end which adds G-actin subunits slowly, whereas, the barbed end of the arrowhead specifies the plus end of an actin filament, the fast growing end; this is determined by labelling with arrowheads, removing HMM, adding G-actin, and seeing which end is longer when you look via negative staining (Holmes et al., 1990). During polymerization, when the G-actin monomer and its unassembled ATP is incorporated in the filament the ATP is hydrolyzed to ADP. An actin filament contains a cap at the barbed end of the filament which prevents disassembly as well as provides important contributions to actin-based motility (Pollard and Borisy, 2003).

In order for actin to function in motility, it requires an actin-based motor, myosin. Myosin motors are involved in muscle contraction, cell movement, cytokinesis and membrane transport (Vale and Milligan, 2000), amongst others. There are two major

classes of myosins, conventional myosin and unconventional myosin. Myosin-2, a conventional myosin, powers both muscle contractions and non-muscle contractions (Bray, 2001; Karp, 2003). Myosin-2 functions in cell contractility, cytokinesis and locomotion (Even-Ram et al., 2007). Myosin-10, an unconventional myosin, on the other hand is required for meiotic spindle assembly and mitotic spindle positioning and may also be involved in actin-microtubule interactions in the spindle as myosin-10 can bind to both actin and microtubules (Woolner et al., 2008). The polarity of an actin filament will direct the movement of myosin as myosin moves toward the barbed end (plus end) of the actin filament causing the pointed end (minus end) to lead the direction of the movement (Huxley, 1973). Therefore, the polarity of actin filaments allows contraction to take place through the attachment of each myosin head in different directions on actin filaments of opposite polarity, producing force that pulls the actin filaments together (Bray, 2001).

Microtubules and actin filaments are separate systems of cell motility but they often interact with one another (Rodriguez et al., 2003). Myosin-2A is believed to play a role in the coupling of microtubule and actin filament systems (Even-Ram et al., 2007). The best examples of microtubule-actin interactions occur in cell division during spindle positioning, chromosome movement and cytokinesis (Rodriguez et al., 2003). Spindle positioning occurs via the interactions of actin and astral microtubules (Wuhr et al., 2008) as microtubules are often linked to the cell cortex containing actin, to ensure the future metaphase plate is properly placed for division (Rodriguez et al., 2003). Microtubule-actin interactions have been shown to be necessary for cytokinesis to occur as the disruption of the spindle before furrow formation prevents cytokinesis from occurring

(Rodriguez et al., 2003). At the onset of anaphase, astral microtubules grow from the centrosome to the cortex, a process that is necessary for the initiation of cytokinesis in some cells (Burgess and Chang, 2005). Microtubule-actin interactions involved in spindle positioning and cytokinesis are widely accepted (Rodriguez et al., 2003); however, whether microtubule-actin interactions are involved in chromosome movement has been debated as many models propose that microtubules are the sole component driving chromosome movement. Fabian and Forer (2005) used drug inhibitors to show that actin and myosin must be involved in chromosome movement as the inhibition of these components temporarily blocked chromosome movement. Whether microtubules and actin filaments interact with one another to produce motility within a cell or whether microtubules and actin filaments work as separate motile systems, their presence is required for many cell motility processes to occur. Microtubule-actin interactions and their involvement in chromosome movement will be discussed later in greater detail.

1.3 Chromosome Movement: The Components and Mechanisms Involved

The mechanisms underlying chromosome-to-pole motion in anaphase of mitosis have been heavily debated in cell biology. Cell biologists originally believed that the spindle was structureless because spindle fibres could only be seen following fixation and could not be seen in living cells with a conventional microscope. It was not until the work of Inoué (1953) using the polarization microscope that cell biologists realized that the spindle was composed of weakly birefringent fibres. Inoué (1953) demonstrated that the birefringent spindle fibres he could see in living cells resembled the same structures that

were observed by researchers in fixed and stained cells. This provided the first set of evidence that spindle fibres exist in living cells. Since then, many models were developed to answer the question, "How do chromosomes move?" Most models propose that anaphase chromosomes move by action of the kinetochore fibre (Mitchison et al., 1986). The kinetochore fibre, which is composed of kinetochore microtubules that extend the full length of the fibre from the kinetochore to the poles (Cameron et al., 2006), is thought to produce the force driving chromosome motion. Early ultraviolet (UV) microbeam experiments conducted by Forer (1966) demonstrated, however, that kinetochore fibres may not cause chromosome movement. Chromosomes moved to the pole with areas of reduced birefringence (ARB) in their kinethochore fibres following irradiation (Forer, 1966; Sillers and Forer, 1983); ARBs are regions of kinetochore fibres in which microtubules have been depolymerized (Snyder et al., 1991). Regardless of these results, early models still considered that kinetochore microtubules are solely responsible for chromosome-to-pole motion. For example, the dynamic equilibrium theory describes chromosome-to-pole motion as occurring when microtubules assemble at the kinetochore and shorten at the poles (Inuoé and Sato, 1967) while the sliding model describes chromosome-to-pole motion as occurring when microtubule sliding takes place between microtubules of opposite polarity (McIntosh et al., 1969).

More recent models consider kinetochore fibres in different ways. The Pac-Man model describes chromosome-to-pole motion as occurring when the kinetochore "chews" its way to the spindle pole with microtubule depolymerization occurring at the kinetochore (Rieder and Salmon, 1994). The Pac-Man model also proposes that the force

required to produce chromosome-to-pole motion is driven by minus end directed motors (e.g.. dynein) at the kinetochore (Rieder and Salmon, 1994). Early evidence to support the Pac-Man model derived from experiments conducted by Gorbsky and his colleagues (1987). They observed that when an area of a kinetochore fibre was photobleached during metaphase, the photobleached region remained stationary. However, at anaphase, the chromosome moved poleward past the photobleached region (Gorbsky, 1987). In another set of experiments, Hyman and Mitchison (1991) observed that kinetochores can slide in either direction along microtubules *in vitro* depending on whether a plus end motor or a minus end motor was present.

The traction fibre model, on the other hand, describes chromosome-to-pole motion as occurring when kinetochore fibre depolymerization at the spindle poles drags chromosomes anchored to kinetochore fibres poleward (Cornman, 1944; Pickett-Heaps et al., 1996). The traction fibre model also proposes that the force required to produce chromosome-to-pole motion is driven by a plus end directed motor (Mitchison and Sawin, 1990). The traction fibre model later became known as the "flux" model as microinjection and photoactivation studies revealed that kinetochore fibres are continuously formed prior to the onset of anaphase as microtubule subunits are constantly added to the plus end of microtubules and removed from the minus end of microtubules and when microtubule subunit addition at the kinetochore ceases, chromosomes move poleward (Mitchison, 1989).

The mechanism for chromosome-to-pole motion, however, can vary between different cell types. In *Xenopus* oocytes (Desai et al., 1998) and crane fly spermatocytes

(Wilson and Forer, 1989), when chromosomes move to the pole there is solely microtubule depolymerization at the spindle pole; therefore only the "flux" model could explain chromosome-to-pole motion in these organisms. In vertebrate somatic cells, on the other hand, when chromosomes move to the pole microtubules depolymerize both at the spindle pole and at the kinetochore (Mitchison and Salmon, 1992). Therefore, both "flux" and Pac-Man are required for chromosome-to-pole motion as flux accounts for approximately 25% of chromosome movement and Pac-Man accounts for approximately 75% of chromosome movement during early anaphase in this cell (Mitchison and Salmon, 1992). Both the Pac-Man model and the "flux" model assume that microtubules and their associated motor proteins are the only components responsible for chromosome-to-pole motion (Pickett-Heaps and Forer, 2009).

Other models can explain the same results. Forer and colleagues argue that the forces driving both flux and chromosome-to-pole motion arise from a spindle matrix that utilizes actin and its motor myosin to exert external forces on kinetochore microtubules (Forer et al., 2008). The spindle matrix model considers microtubules as rigid fibres, "governors", that limit the rate of movement and whose rate of depolymerization, a consequence of force production, not its cause, governs the velocity of chromosome-to-pole motion (Forer et al., 2003; Forer et al., 2008; Pickett-Heaps and Forer, 2009). The spindle matrix model developed by Forer and his colleagues has led to decades of controversy within the cell biology community; the issue of whether the kinetochore fibre produces the force driving chromosome-to-pole motion or whether the kinetochore fibre

solely governs the velocity of chromosome-to-motion remains unresolved (Maiato and Lince-Faria, 2010).

Although this controversy still divides cell biologists, many years of evidence support the existence of a spindle matrix. Early studies on diatoms revealed that diatoms have a central spindle, known as a "collar" that consists of interconnecting microtubules that extend between kinetochores and poles (Pickett-Heaps and Tippit, 1980; Pickett-Heaps et al., 1982). When kinetochore microtubules were partially or completely severed, the central spindle either buckled or collapsed, indicating that there is compressive force acting on the spindle. Based on these results, Pickett-Heaps and Tippit (1980) concluded that the "collar" in diatoms acts as an elastic matrix and is responsible for the proper segregation of chromosomes. Experiments using the ultraviolet (UV) microbeam have also provided evidence that a spindle matrix exists. Briefly, following UV irradiation across the entire half spindle of newt and PtK fibroblasts that severed microtubules, the spindle pole associated with the irradiation moved towards the equator (Spurck et al., 1990; Snyder et al., 1991); this shows that interpolar forces persist without microtubule continuity between the spindle poles. When kinetochore microtubules were irradiated in metaphase in newt fibroblasts, the chromosome attached to the irradiated kinetochore fibre moved to the pole associated with the irradiation (Spurck et al., 1997), indicating that chromosomes can continue to move after their kinetochore microtubules are severed. In addition, newt fibroblast chromosomes continued to move to the pole and even accelerated poleward when kinetochore microtubules were severed in anaphase (Forer et al., 2008); this shows that kinetochore microtubules act as governors for velocity and

poleward movement is due to forces generated from a spindle matrix acting on kinetochore microtubules. A cut kinetochore stub (remnants of the kinetochore fibre that remains attached to the kinetochore but is severed from the pole following irradiation) continued to grow poleward while its associated chromosome also continued to move poleward during anaphase (Pickett-Heaps et al., 1996; Spurck et al., 1997). Based on these experiments, Forer and his colleagues concluded that kinetochore microtubules are rigid structures that are pulled by the spindle matrix, and that the forces acting on the kinetochore microtubules cause them to disassemble (Forer et al., 2007, 2008). Additional UV microbeam experiments will be described later in greater detail.

In addition to microtubules, kinetochore fibres contain non-microtubule components that might be involved in force production (Forer, 1988) and microtubule flux (Forer et al., 2007). One such component, actin, was identified using fluorescently labelled phalloidin (Czaban and Forer, 1994; Fabian and Forer, 2005). In addition, anti-actin drugs (Cytochalasin D and Latrunculin B) cause chromosome movement in crane-fly spermatocytes to be temporarily blocked or slowed, indicating that cells generally use spindle actin to cause chromosomes to move (Forer and Pickett-Heaps, 1998). In metaphase cells, anti-actin drugs (Cytochalasin D and Latrunculin B) block or slow elongation of kinetochore stubs produced from severing a kinetochore fibre with the ultraviolet microbeam (Forer et al., 2007). The stub elongates because tubulin subunits are added at the kinetochore and flux toward the severed end of the kinetochore stub, so the temporary blockage of elongation indicates that flux is derived from actin associated with the spindle matrix (Forer et al., 2007). Anti-myosin drugs (BDM and Y-27632) also

cause chromosome movement in crane-fly spermatoctyes to be temporarily blocked or slowed (Silverman-Gavrila and Forer, 2001). Based on these experiments, actin and myosin have been considered components of the spindle matrix which may act along the length of the kinetochore fibre to aid in producing the force driving chromosome-to-pole motion (Pickett-Heaps et al., 1997).

Molecular evidence for a spindle matrix arose in other laboratories. In *Drosophila*, nuclear proteins were found to reorganize during prophase into a spindle-like structure (Johansen and Johansen, 2007, 2009). The nuclear proteins, Megator, Skeletor, Chromator and EAST, form a spindle-like structure in the absence of microtubules (Walker et al., 2000; Rath et al., 2004). When microtubules are disassembled following cold treatment, Skeleton and Megator persist in the shape of the spindle, indicating that the spindle is an independent structure from the spindle matrix (Johansen et al., 2011). In addition, when microtubules were disassembled, the spindle-like structure that remained was compressed; this suggests that the spindle matrix is an elastic and not a rigid structure (Qi et al., 2004; Johansen et al., 2011). Defects in the mitotic spindle were also evident following the loss of Megator, Chromator and EAST in *Drosophila* (Johansen and Johansen, 2007). The structure of the diatom spindle, UV microbeam experiments in crane-fly spermatocytes and newt fibroblasts, the presence of non-microtubule components in the spindle and the existence of a spindle-like structure composed of nuclear proteins in *Drosophila* provides evidence for the existence of a spindle matrix.

1.4 The Ultraviolet Microbeam and its Applications in Cell Biology

The ultraviolet (UV) microbeam was one of the earliest tools used to test models that try to explain how chromosomes move. It was first used by Tchackotine in as early as 1912 and then was later pioneered throughout the 1950s and 1960s by a variety of different researchers (Urtez et al., 1954; Bloom et al., 1955; Zirkle et al., 1960; Bajer and Mole-Bajer, 1961; Zirkle and Urtez, 1963). The UV microbeam is a useful tool for cell biologists as certain components in the cell can be irradiated, leaving other components still functional, without damaging the surrounding area, without killing the cell and without ablating all of the components in the focussed spot, as laser microbeam ablations do. The basic principle of the UV microbeam is to focus high-intensity ultraviolet light emitted from a mercury arc lamp onto a pinhole; the light passing through the pinhole is then focussed onto a cell using a microscope objective lens (Wilson and Forer, 1987). In order to ensure that the appropriate wavelength of UV (between 260nm-290nm) is transmitted to the cell, a monochromator is placed between the mercury arc lamp and the pinhole so only a single wavelength of light is transmitted (Wilson and Forer, 1987). Different wavelengths of UV light have been shown to have different effects on the cell as each wavelength of light corresponds to a different absorption peak for a particular chromophore (part of a molecule that absorbs light for a particular wavelength); therefore, different wavelengths are absorbed by different proteins in the cell (Sillers and Forer, 1983). For example, when spindle fibres of anaphase chromosomes in crane fly spermatocytes were irradiated with light at a wavelength of 260nm, chromosome movement was not affected but there was a decrease in birefringence of the irradiated

fibre; when a wavelength of 290nm was used, chromosome movement was affected but there was no effect on the birefringence of the irradiated fibre; and when wavelengths of 270nm and 280nm were used, there was an effect on chromosome movement as well as a decrease in the birefringence of the irradiated fibre (Sillers and Forer, 1981a; Sillers and Forer, 1983). Based on these experiments, Sillers and Forer (1981a) created an action spectrum that determined the effects of different wavelengths on chromosome movement and birefringence.

In early UV microbeam experiments, researchers noticed that irradiated chromosomes appeared 'paled' in the irradiated region compared to their normal black appearance when observed using phase contrast microscopy, indicating that UV irradiations change the index of refraction of chromosomes (Urtez et al., 1954; Bloom et al., 1955; Bajer and Mole-Bajer, 1961), most likely due to a loss in both protein and DNA (Zirkle and Uretz, 1963). Later observation established that an area of reduced birefringence (ARB) of the spindle was correlated with a loss of microtubules in the irradiated region (Forer, 1965; Bajer, 1972) as a result of the depolymerization of the microtubules (Wilson and Forer, 1988; Synder et al., 1991).

In addition to studying the dynamics of microtubules, the UV microbeam has been used to conduct experiments to demonstrate that force does not arise solely from spindle microtubules and that non-microtubule components are involved in chromosome-to-pole motion. Following irradiation of kinetochore fibres, chromosomes still moved to the pole even though kinetochore microtubules were severed and an ARB was produced (Sillers and Forer, 1983; Forer and Wilson 1994; Picket-Heaps *et al.* 1996). Forer and

colleagues (1997) also observed that following irradiation of kinetochore microtubules in crane fly spermatocytes, the kinetochore stub elongated at a constant velocity toward the pole, indicating that tubulin subunits are added at the kinetochore and flux toward the pole. In later experiments, Forer et al. (2007) created kinetochore stubs in crane fly spermatocytes using the UV microbeam and then treated the cells with actin and myosin inhibitors, which blocked the elongation of the kinetochore stub, indicating that flux requires active actin and myosin. Non-microtubule components were also suggested to be involved in driving chromosome movement to the pole as chromosome movement stopped following irradiations with wavelengths that match the absorption peaks for actin and myosin (270nm and 290nm) (Sillers and Forer, 1981a; Forer, 1988); this was later confirmed by the absence of kinetochore microfilaments in the irradiated region as shown by the absence of phallodin staining (Czaban and Forer, 1994; Forer et al., 2003). The UV microbeam has also provided evidence that forces for movement arise from a spindle matrix. In newt and PtK fibroblasts, spindle poles moved closer together after microtubules across the entire half-spindle were severed (Spurck et al., 1990; Snyder et al., 1991) which indicates that there is a tensile element that extends throughout the spindle in the absence of microtubule continuity (Forer et al., 2008). In other experiments, newt fibroblast chromosomes accelerated to the pole when kinetochore microtubules were severed (Forer et al., 2008), as would be expected in the absence of microtubules, if microtubules do not provide the force but act as governors.

The UV microbeam has proven to be a useful tool for cell biologists; however, there are certain limitations to the UV microbeam (Forer, 1966). Irradiation of one area of

the spindle may result in the irradiation of a different area of the spindle as the UV light can shift its position of focus because of varying thicknesses of cell between coverslip and target or inhomogeneities that could exist in the cell preparation (Forer, 1966). Also, the spindle components that are out of focus could be irradiated with greater energy per area than the spindle components that are in focus and are targeted to be irradiated because of variations in the thickness of the preparation (Forer, 1966). As discussed by Forer (1966), these limitations result because the focus of the lens is corrected to be immediately after leaving the coverslip, therefore, if there is much medium or cytoplasm between the coverslip and the target, then the UV beam can shift in focus both vertically and horizontally. Nonetheless, the UV microbeam has proven to be a useful tool for cell biologists from its initial development in 1912 until the present day; researchers continue to use the UV microbeam to study chromosome movement and the mitotic spindle.

1.5 The Optical Cutting Laser and its Applications in Cell Biology

Laser microbeams, also known as "optical cutting lasers" or "optical scissors", are a fairly new tool when compared to the long history of the UV microbeam. Laser is an acronym for "Light Amplification by Stimulated Emission of Radiation" (Berns and Greulich, 2007). Using the principles of stimulated emission, a laser forces the photons emitted from a specific wavelength of light into a tightly bound range of phase, frequency, polarization and direction (Berns and Greulich, 2007). For this to occur however, a laser must consist of a gain medium that is placed in an optical resonator as well as an energy source to excite the molecules within the gain medium (Berns and

Greulich, 2007). Since a laser microbeam can be attached to conventional microscopes, a high power, submicron sized spot is created in the focal plane when the laser is focussed by a high numerical aperture objective lens (Berns and Greulich, 2007).

Laser microbeams allow cell biologists to target specific cellular structures in a variety of living and fixed cells with greater precision than earlier microbeams. The first laser was built in 1960 by Theodore Maiman and based on the original design by Maiman, in 1962 Marcel Bessis developed the ruby laser microbeam (Berns and Greulich, 2007). The blue-green argon laser, using wavelengths of 488nm and 514nm, was the next laser used to perform micromanipulation and ablation studies (Berns et al., 1969) on chromosomes in live cells (Berns et al., 1969). Using this high power, tightly focussed laser Berns and his colleagues (1969) created micron sized lesions in the chromosomes of salamander lung tissue cells to study chromosome injury and repair. The lesions created by the laser microbeam were similar to the paling that was observed following UV microbeam irradiation of chromosomes. Even though UV microbeam irradiations and laser microbeam irradiations both produce paling, the laser microbeam, unlike the UV microbeam, has the ability to ablate part of a single mitotic chromosome (Berns et al., 1971), or to remove chromosomes from the mitotic spindle by destroying the kinetochore/microtubule attachment (McNeill and Berns, 1981) and sever chromosome arms to study chromosome movements (Rieder et al., 1986). The subsequent development of the laser microbeam allowed researchers to ablate or completely sever and remove individual components of chromosomes and the mitotic spindle to study chromosome movement and cell division.

Further advances have been made to laser microbeams in the past decade or so. In addition to the development of nanosecond and picosecond lasers, femtosecond lasers (which were most recently developed) use ultrashort laser pulses which lead to very high peak powers to micromanipulate nanoscale structures in living cells (Konig et al., 1999). Femtosecond lasers which typically use wavelengths in the near infrared region of the light spectrum (ex. 800nm) have become widely popular for their ability to perform precise ablations, reduce thermal side effects of the laser and for their ability to be used in cell imaging (Berns and Greulich, 2007). All laser microbeam irradiation studies that will be described later in this thesis use a femtosecond laser.

1.6 The Optical Trapping Laser and its Applications in Cell Biology

The development of a variety of laser microbeam systems gave cell biologists new tools to study living cells. In addition to laser microbeams which could ablate and sever chromosomes and spindle components, an optical trapping laser (also known as optical tweezers) was developed by Arthur Ashkin in 1970 that could manipulate, hold, and move biological objects *in vivo*. When Ashkin (1970) discovered that he could hold freely suspended particles by the force generated from the radiation pressure emitted from visible laser light, he developed a new type of laser microbeam. This was a single-beam optical trap using a high numerical aperture objective to tightly focus a laser beam (Ashkin et al., 1989). By tightly focusing the laser beam, a transfer of momentum occurs from the scattering of photons from the laser beam to create a scattering force and a gradient force (Neuman and Block, 2004). The scattering force helps to push the particle or the object in the direction of light; whereas, the gradient force helps to keep the

particle trapped or held in place. However, for the trap to work, there must be a difference in the index of refraction between the object and the surrounding medium. The index of refraction of the particle or object must be greater than the index of refraction of the surrounding medium to create the required change in momentum to hold a particle or object within the laser beam (Neuman and Block, 2004). Although Ashkin first discovered that he could use an optical trap to hold and manipulate dielectric particles, he soon realized that he could use an optical trap to manipulate biological particles, such as viruses, bacteria (Ashkin and Dziedzic, 1987) and organelles inside single cells (Ashkin et al., 1989). Ashkin's development of the optical trap provides a non-invasive tool that researchers can use to: (1) directly trap single or groups of living cells (Ashkin and Dziedzic, 1989); (2) directly trap and manipulate organelles within cells without disrupting the cell membrane or causing damage to the cell (Ashkin and Dziedzic, 1989); and (3) trap beads to measure the force of motor molecules (Kuo and Sheetz, 1993).

This new and novel technique was not widely accepted, at first, as researchers were skeptical that the optical trapping laser would cause physiological damage to biological specimens by 'opticution', death by light (Ashkin and Dziedzic, 1989). However, the possibilities of damage were thoroughly investigated by researchers who determined that some wavelengths produced very little if any damage. Liu et al. (1996) determined that using a wavelength of 1064nm from the infrared spectrum of light was safe, non-invasive and minimized light-induced damage to Chinese hamster ovary cells and motile spermatozoa as no damge to DNA was observed following trapping. *E.coli* bacteria and yeast cells were able to reproduce in the presence of the trap while being

held in the trap for hours (Ashkin et al., 1987; Ashkin and Dziedzic, 1989). Therefore, a wavelength of 1064nm is commonly used for optical trapping.

Since the discovery by Ashkin (1970), the optical trap has produced many advances in cell biology. In plant cells, the optical trap has been used to study cytoplasmic streaming and internal cell membranes (Ashkin and Dziedzic, 1989). Berns and colleagues were the first to demonstrate that they could study the complexities of mitosis using an optical trap instead of a micromanipulation needle to manipulate and hold chromosomes *in vivo*. By varying the power in the trap to hold a chromosome, Berns and colleagues demonstrated that they could estimate the force acting on chromosomes (Berns et al., 1989; Liang et al., 1991; Liang et al., 1994). Following the work of Berns and colleagues, the optical trap has been used to measure the force of mitochondria moving along microtubules (Ashkin et al., 1990), the force of a single kinesin molecule (Kuo and Sheetz, 1993; Svoboda and Block, 1994), the unbinding force between an actin filament and its motor myosin (Nishizaka et al., 1995), the force produced by a single myosin head (Molloy et al., 1995) and the force generated by a motile sperm head (Konig et al., 1996; Nascimento et al., 2008). Although many of these force experiments were conducted *in vitro* on coated beads (Kuo and Sheetz, 1993; Svoboda and Block, 1994; Nishizaka et al., 1995; Molloy et al., 1995), these experiments allow researchers to use these force values to develop models to better understand the basic structure and function of cells.

1.7 The Advantages of Using *Mesostoma ehrenbergii* as a Model Organism for Studying Meiosis

The UV microbeam, the optical cutting laser and the optical trapping laser are very useful tools for studying meiosis and mitosis. They have allowed cell biologists to test a variety of different models that have arisen to predict how chromosomes move to the pole during anaphase as well as to determine which spindle components are involved in the force production driving chromosome-to-pole movement. These tools however would not be useful if researchers did not have a variety of different model organisms to use them on. Despite the unique and advantageous features found in *Mesostoma ehrenbergii* spermatocytes, *Mesostoma* are not well studied by cell biologists. Only a handful of papers published by Oakley (1982; 1983; 1985), Fuge (1987; 1989; 1991) and Forer and Pickett-Heaps (2010) describe these features, which include: (1) regular and persistent kinetochore oscillations; (2) distance segregation (and perhaps non-random segregation) of univalents; and (3) the presence of a precocious "pre-anaphase" cleavage furrow. Based on their unique features, *Mesostoma* make an ideal organism to study a variety of different processes of cell division and tools such as the UV microbeam, optical cutting laser and optical trapping laser aid these studies.

Although *Mesostoma* has not received much attention from cell biologists, they have received considerable attention from ecologists. *Mesostoma ehrenbergii* is a hermaphroditic aquatic flatworm from the order Rhabdocoela and the class Turbellaria. *Mesostoma* are widely distributed across Europe, Africa, Asia, North America and South America (Husted et al., 1973; Kolasa and Mead, 1981). Anatomical differences in the subspecies of *Mesostoma* from the various localities in which they inhabit have been

previously described; in general, most subspecies of *Mesostoma* have an oval shaped, transparent body that can grow to approximately 1.5 cm in length by the time of maturity (Ferguson and Hayes Jr, 1941; Kolasa and Schwartz, 1988; Bedini and Lanfranchi, 1990; Kalita and Goswami, 2012). They have pairs of lobed testes which occupy approximately one half of their body length and lie along either side of the pharynx (Croft and Jones, 1989). *Mesostoma* are well known voracious predators of zooplankton, *Daphnia*, mosquito larvae and copepods because of their abilities to contort and twist themselves in a variety of configurations, detect and respond to moving objects several millimeters away and secrete sticky mucus that immobilizes prey (Kolasa, 1984; Kolasa et al., 1985; Blaustein, 1990; Blaustein and Dumont, 1990; DeRoeck et al., 2005; Trochine et al., 2005; Trochine et al., 2006; Tranchida et al. 2009). Following the capture of prey, *Mesostoma* wrap their bodies around the prey and use their proboscis to suck out the body contents (Schwartz and Herbert, 1981; Wrona and Koopowitz, 1998).

They are well known for their ability to produce both embryos and dormant eggs (Bresslau 1903; Fiore and Ioalè, 1973; Domenici and Gremigni, 1977; Heitkamp, 1977). Subitaneous eggs or S eggs (embryos) and dormant eggs or D eggs can be produced through self-fertilization or through mating and the production of these eggs is thought to be influenced by environmental factors such as temperature, amount of food, oxygen content in the water and pH (Fiore and Ioalè, 1973). Therefore, egg production in nature corresponds to the appropriate season: S eggs are abundantly produced in the warmer seasons and D eggs are abundantly produced closer to the end of the warm season to ensure the survival of the population during the cold seasons (Heitkamp, 1977). The

abundance of *Mesostoma* throughout various localities around the world as well as their voracious predatory nature, unique feeding behaviours, possible use in pest control of mosquito larvae and their ability to produce both embryos and dormant eggs make them an attractive organisms for ecologists to study.

In addition to the anatomical differences that exist between species of *Mesotoma*, differences also exist in the morphology and number of meiotic chromosomes in the spermatocytes of *M. ehrenbergii* from Europe (Luther, 1904; Bresslau, 1904; Voss, 1914) and North America (Husted et al., 1939; Husted and Ruebush, 1940). Early researchers differentiated between the spermatocytes of *M. ehrenbergii* from Europe and *M. ehrenbergii* from North America based on the length of each chromosome, the position of the centromere and the number of chromosomes; the European worms have spermatocytes with 3 bivalents and 4 univalents. The North American worms were originally observed to have spermatocytes with 3 bivalents and 2 univalents (Husted and Ruebush, 1940), but subsequent work of Hebert and Beaton (1990) showed that North American worms have the same number of chromosomes (n=10) as the European worms; 3 homologues present as bivalents and 4 unpaired univalents (Fuge, 1987). In addition, the three bivalents from both the North American and European spermatocytes of *M. ehrenbergii* each possess a single distally located chiasma (Husted and Ruebush, 1940). Although *M. ehrenbergii* spermatocytes from Europe and North America share the same number of chromosomes and posses bivalents with distally located chiasma, the karyotype of these worms are different in that chromosomes in *M. ehrenbergii* spermatocytes from North America are much shorter than chromosomes in *M.*

ehrenbergii spermatocytes from Europe (Hebert and Beaton, 1990) and two of the bivalents are metacentric (with kinetochores in the centre of the arms) and one is acrocentric (with a kinetochore near the end of the arms) whereas in the European spermatocytes 1 bivalent is a metacentric pair and 2 are acrocentric pairs (Oakley and Jones (1982). Differences in karyotype not only exist between North American and European populations but also between European populations, since some European forms have three metacentric bivalents (Husted et al., 1939).

I will now describe in greater detail the three unique and advantageous features of *Mesostoma* spermatocytes and how these features compare to: (1) prometaphase chromosome oscillations in other cell types; (2) other cells that exhibit either distance segregation or non-random chromosome segregation; and (3) the conventional process of cytokinesis.

1.8 Prometaphase Chromosome Oscillations in *Mesostoma* spermatocytes and Other Mitotic and Meiotic Cells

Continuous, vigorous and regular chromosome oscillations are a feature unique to *Mesostoma* spermatocytes. Bivalent chromosome movements in living *Mesostoma* spermatoctyes were described by Fuge (1987, 1989). He described the unique kinetochore oscillations of the three bipolarly oriented bivalents that occur during prometaphase/metaphase. From the short sequences of film that he originally analyzed, Fuge (1987) was able to determine that the kinetochore oscillations are regular, rapid, and coordinated. In the cells he studied, kinetochores oscillated for a period of approximately one hour, the maximum time that he studied them, with velocities of 8-10 μm/min to

maximum velocities of up to 17 μm/min. Fuge determined that kinetochores move 5-7 μm away from the pole and then back to the pole, repeating this every 100s.

To better understand how kinetochores move to and from the spindle poles, Fuge conducted electron microscopy studies (Fuge, 1987, 1989; Fuge and Falke, 1991), from which he determined that *Mesostoma* kinetochores have a cup-like invagination for insertion of kinetochore microtubules (Fuge, 1987), and that chromosomal fibres are several μm in length, well-developed, and contain kinetochore microtubules that insert into the kinetochore as well as non-kinetochore microtubules that surround the kinetochores and bivalents (Fuge, 1989). These results could explain kinetochore movement to the pole by shortening of kinetochore microtubules, but not the backward movement of the entire chromosome and the away from pole movement of kinetochores and arms. In a subsequent article, Fuge and Falke (1991) suggested that chromosome spindle fibres resemble a "microtubular fir-tree", composed of kinetochore microtubules and non-kinetochore microtubules that associate with both bivalents and kinetochores. Although Fuge and Falke (1991) were able to provide an intricate picture of the spindle of *Mesostoma* spermatocytes, they still could only speculate as to how kinetochores oscillate to and away from the pole.

Although kinetochore oscillations in *Mesostoma* spermatocytes were only described in a few articles by Fuge, prometaphase kinetochore oscillations in other cell types have been well described in the literature. Kinetochore oscillations of mono-oriented and bi-oriented chromosomes occur during prometaphase and metaphase as chromosomes congress to the metaphase plate prior to the onset of anaphase in meiosis

and mitosis. Oscillations have been observed in a variety of different cell types including: diatoms (Pickett-Heaps et al., 1979; Pickett-Heaps and Tippit, 1980), newt lung culture cells (Bajer 1982; Ault et al., 1991; Skibbens et al., 1993, 1995; Cassimeris et al., 1994; Ke et al., 2009), PtK cells (Khodjakov et al., 1997), *Drosophila* embryos (Civelekoglu-Scholey et al., 2006) and HeLa cells (Amaro et al., 2010; Jaqaman et al., 2010). In most of these cells, kinetochore oscillations appear as saw-toothed wave patterns consisting of abrupt switches between to the pole and away from pole motion, with small amplitude (1-2μm), irregular oscillations that last for only a short time (up to 10-25 minutes) and relatively low speeds (1-3μm/min) (Skibbens et al., 1993; Jaqaman et al., 2010). Kinetochore oscillations of mono-oriented chromosomes however, can last for a period of approximately 45 minutes (Bajer, 1982). On the other hand, oscillations in diatoms and *Drosophila* embryos are very rapid but last for a very short period of time. (Pickett-Heaps et al., 1979; Pickett-Heaps and Tippit, 1980; Civelekoglu-Scholey et al., 2006). In diatoms, mono-oriented chromosomes exhibit kinetochore oscillations that are irregular in amplitude and period, actively oscillating between spindle poles with a velocity of 5 μm/s, ceasing oscillations after approximately 5 minutes once the chromosomes have achieved bi-polar attachment (Pickett-Heaps and Tippit, 1980). Similarly, in early *Drosophila* embryo cells, chromosomes exhibit small amplitude kinetochore oscillations of 0.5-2 μm, oscillating between spindle poles with an average velocity of 3.6-6.6 μm/min (Maddox et al., 2002) but which last for only 50-100s (Civelekoglu-Scholey et al. 2006). Oscillations in most of these cell types are irregular either exhibiting small amplitude oscillations that persist for a maximum of 45 minutes but with a slow velocity

or small amplitude oscillations that persist for a maximum of 5 minutes but with a very rapid velocity. *Mesostoma* spermatocytes, on the other hand, have bi-oriented chromosomes with kinetochore oscillations that are regular, rapid and coordinated and last for a period of 1 to 2 hours during prometaphase/metaphase before entering into anaphase (Fuge, 1987; Fuge, 1989). The velocity of kinetochore movement in *Mesostoma* spermatocytes is comparable to the velocity of kinetochore movement in early *Drosophila* embryo cells but the length of time oscillatory movement takes place and the distance of each excursion are much greater than that seen in early *Drosophila* embryos. I studied kinetochore oscillations in *Mesostoma* spermatocytes to better understand how chromosomes move, to determine the force required to move chromosomes and to determine which components are involved in producing the forces that drive chromosome movement.

Many models have been proposed to explain how chromosome kinetochores oscillate. Researchers have developed these models to explain how kinetochores switch abruptly between poleward movement and away from pole movement, movement which they have termed directional instability. One model proposes that poleward movement and away-from-pole movement is generated by tension in the kinetochore (Skibbens et al., 1993; Skibbens et al., 1995); a second model proposes that away-from-pole movement is generated by polar ejection forces acting on the chromosome arms (Ault et al., 1991; Khodjakov and Rieder, 1996; Liu et al., 2007; Campas and Sens, 2006; Ke et al., 2009).

The kinetochore motor/tensiometer model hypothesizes that tension at the kinetochore controls directional instability and determines when the kinetochore switches between to-the-pole and away-from-the-pole movement (Skibbens et al., 1995; Waters et al., 1996). Tension is thought to increase the frequency of kinetochore switching; a decrease in tension would promote poleward movement whereas an increase in tension would promote switching to movement away from the pole (Skibbens et al., 1993; Skibbens et al., 1995). Skibbens and colleagues (1995) tested this model by severing bi-oriented chromosomes in half with a laser microbeam; severed chromosomes ceased oscillating and moved to opposite poles, suggesting that tension is required for chromosome oscillations. Waters and colleagues (1996) also confirmed that tension is required for chromosome oscillations of mono-oriented and bi-oriented chromosomes by determining that centromeres remain stretched rather than compressed during both poleward movement and away from the pole movement.

The polar/ejection model assumes that kinetochores only produce a pulling force and away from pole movement is produced by an antagonistic force such as an ejection force acting on chromosome arms (Bajer, 1982; Skibbens et al., 1993) and/or a polar ejection force exerted by astral microtubules (Ault et al., 1991). In order for this model to be plausible, chromosome arms must be covered in chromokinesins (Liu et al., 2007) composed of microtubule plus end directed motors and that when these motors interact with astral microtubules, the growing astral microtubules push the chromosome away from the pole (Ault et al., 1991). Khodjakov and Rieder (1996) tested this model by removing the pole-moving kinetochore with a laser microbeam; the kinetochore moving

away from the pole continued to move away from the pole, suggesting that the chromosome was being pushed away from the pole by polar ejection forces. Campas and Sens (2006) used computer modeling to recreate chromosome oscillations based on a variety of different parameters; using an estimate of chromokinesin velocity, they determined that chromosome oscillations could be a result of opposing polar ejection forces of astral microtubules.

The kinetochore motor/tensiometer model and the polar/ejection model can both be used to explain why kinetochores switch between poleward and away from pole movement during kinetochore oscillations; however, the kinetochore motor/tensiometer model is readily used to describe kinetochore oscillations of bi-oriented chromosomes, whereas, the polar/ejection model is readily used to describe kinetochore oscillations of mono-oriented chromosomes (Khodjakov et al., 1997).

1.9 Distance Segregation and Non-Random Segregation of Chromosomes

Another unique feature of *Mesostoma* spermatocytes is the distance segregation (and perhaps) non-random segregation of univalents which was originally observed and described by Oakley (1983, 1985). Univalents in *Mesostoma* spermatocytes segregate by 'distance segregation', which was defined by Hughes-Schrader (1969) as the segregation to opposite poles of partner chromosomes that are not conjoined.

Distance segregation has not been well studied except for a few cells. In crane-fly spermatocytes, the three autosomal bivalents disjoin and move to opposite poles during anaphase I, while the two unpaired sex chromosome univalents remain at the metaphase

plate (Forer, 1966). It is not until approximately 20-30 minutes after the autosomes have reached the spindle poles that the unpaired sex chromosome univalents, which are amphitelically oriented with kinetochore fibre attachments to both poles, move to opposite spindle poles (Fuge, 1972; Schaap and Forer, 1979). To try to understand the mechanism by which distance segregation of sex chromosome univalents takes place in crane fly spermatoctyes, Forer and Koch (1973) used micromanipulation to detach half-bivalents during anaphase and to change the positions of the sex chromosomes. When detached half-bivalents became amphitelically oriented, the half-bivalent and one sex chromosome univalent moved to opposite spindle poles while the other sex chromosome remained at the equator (Forer and Koch, 1973). During sex chromosome segregation, Forer and Koch (1973) pushed sex chromosome 1 to move ahead of sex chromosome 2 after which both sex chromosome univalents changed their direction of motion and moved to the other spindle poles. In another set of experiments to understand the mechanism by which distance segregation of sex chromosome univalents takes place in crane fly spermatocytes, Sillers and Forer (1983) irradiated single autosomal spindle fibres with an ultraviolet microbeam during autosomal anaphase. Following the irradiation of single autosomal spindle fibres adjacent to sex chromosome spindle fibres, either one sex chromosome remained at the equator while the other sex chromosome moved normally to its associated spindle pole or the two sex chromosome univalents moved to the pole not associated with the irradiation (Sillers and Forer, 1983). These experiments demonstrate that distance segregation of sex chromosome univalents in

crane fly spermatocytes can be dependent on the univalent's ability to "read" adjacent autosomal spindle fibres (Sillers and Forer, 1983).

Non-random segregation of chromosomes has been observed in the spermatocytes of Sciarid flies (Gerbi, 1986; Fuge 1997), of *Gryllotalpa hexadactyla*, mole crickets (Camenzind and Nicklas, 1968), and mealy bugs (Brown and Nur, 1956). By non-random I mean that the half-bivalents or sex chromosomes segregating in anaphase do not have random orientation on the spindle -- for example, male derived chromosomes all go to the same pole and female derived chromosomes go to the opposite pole, in direct contradiction to the "random assortment" required by Mendelian genetics treatments of gene transmission. Therefore at the end of meiosis I, there is always the same combination of chromosomes in the two daughter cells. In Sciarid flies, spermatogenesis results in the elimination of paternal chromosomes in different numbers and at different times during the first and second meiotic divisions (Fuge, 1997; Goday and Esteban, 2001), which is non-random transmission of chromosomes. In the first meiotic division, there is no true metaphase as chromosomes do not align at the metaphase plate but instead move poleward on a monopolar spindle (Gerbi, 1986). In this division, the maternal chromosomes move poleward while the paternal chromosomes are eliminated in a cytoplasmic bud (Kubai, 1987). The second meiotic division is a normal equational division that generates only one functional spermatazoan with all chromosomes of maternal origin (Goday and Esteban. 2001).

Non-random chromosome segregation also occurs in spermatocytes of the mole cricket, *Gryllotalpa hexadactyla*. The eleventh chromosome pair is characterized by two

homologues which differ in size, one homologue being several times the size of the other (Camenzind and Nicklas, 1968). At anaphase I, the larger homologue of the eleventh pair and the X chromosome always segregate to the same pole (Payne, 1912; White, 1951; Camenzind and Nicklas, 1968). In the second meiotic division, all the chromosomes divide equationally so half the spermatozoa contain the X chromosome and the larger homologue (and ordinary chromosomes) and the other half contain the smaller homologue (and ordinary chromosomes) (Camenzind and Nicklas, 1968). The mechanism of non-random chromosome segregation was tested in *Gryllotalpa* by Camenzind and Nicklas (1968) using micromanipulation. From these micromanipulation experiments, Camenzind and Nicklas (1968) wanted to determine if (1) there is a physical connection between the larger homologue and the X chromosome and (2) if the larger homologue and the X chromosome always move to the same spindle pole. First they moved a needle between the two chromosomes and from this experiment they confirmed that no attachment exists between the X chromosome and the larger homologue. Second, they moved the X chromosome to the spindle pole to which the smaller homologue was oriented. Or they reoriented the bivalent so that the smaller homologue and larger homolog switched poles. Following both of these experiments, the X chromosome moved to the spindle pole to which the larger homologue was oriented, while the bivalent was passive. From these experiments, they confirmed that segregation of the larger homologue and X-chromosome always occurs to the same pole and that the X chromosome is the active element which makes chromosome segregation non-random in this organism.

In mealy bugs, the non-random segregation of chromosomes also occurs in the spermatocytes of males. In the blastula stage of this organism, half of the chromosomes become heterochromatic in those embryos destined to be males (Brown and Nur, 1956). Chromosomes that become heterochromatic become genetically inactive during development (Brown and Nur, 1956). In male coccids, various different meiotic systems exist, including the *diaspidid* system, the *lecanoid* system and the *Comstockiella* system (Cimino, 1972). In *diaspidid* meiosis, which occurs in spermatogenesis in mealy bugs, a single haploid meiosis generates two functional spermatozoa that contain only maternal chromosomes as the heterochromatic paternal chromosomes are lost during the cleavage division (Brown and Nur 1956). In *lecanoid* meiosis, the first spermatocyte division is equational and the second spermatocyte division is reductional with no pairing or genetic recombination taking place (Schrader, 1921; Brown and Nur, 1956). The distribution of the chromosomes in the reductional division of each cell generates four nuclei; two nuclei contain the euchromatic chromosomes and two nuclei contain the heterochromatic chromosomes (Brown and Nur, 1956). The two nuclei containing the heterochromatic chromosomes gradually disintegrate (Brown and Nur, 1956). The heterochromatic derivatives are of paternal origin; therefore, males only express and transmit genes they receive from their mothers (Brown and Nur, 1956). In *Comstockiella* meiosis, the paternal set of chromosomes becomes heterochromatic in the males, but prior to the onset of spermatogenesis, all but one heterochromatic chromosome is destroyed (Nur, 1982). Spermatogenesis consists of one division in which the remaining heterochromatic chromosome is eliminated from spermatids by lagging at anaphase or by ejection after

telophase (Nur, 1982). In all of these examples there is non-random segregation of chromosomes, but with different mechanisms to achieve this in the different division systems.

In *Mesostoma* spermatocytes, univalents segregate via distance segregation and perhaps non-random segregation as well. Early in division, univalents position themselves at the spindle poles where they usually remain until the onset of anaphase I; univalents however can also move from pole-to-pole prior to the onset of anaphase (Oakley, 1983; Oakley, 1985). Oakley (1983) suggested that univalents move from pole-to-pole to achieve the "correct" distribution of univalents at the spindle poles. In her early experiments, Oakley (1983, 1985) determined from squash preparations of fixed and stained *Mesostoma* spermatocytes that the 4 univalents are actually two morphologically identical pairs; for example X1,X2 and Y1,Y2, that are identical to each other but different from the other pair. She also determined that prior to anaphase there can be different numbers of univalents at the spindle poles; there could be X1,X2,Y1 at one pole and Y2 at the other pole, X1,X2,Y1,Y2 at one pole and no univalents at the other pole or X1,Y2 at one pole and X2,Y1 at the other pole. Therefore, by moving between spindle poles during prometaphase I, univalents try to assort themselves properly so by anaphase I there is one of each kind at each pole, either X1,Y1 at one pole and X2,Y2 at the other pole, or X1,Y2 at one pole and X2,Y1 at the other, assuming that there is random segeregation of the univalents. Oakley (1983, 1985) characterized the pole-to-pole movements of univalents in later experiments. From these experiments, Oakley determined that achieving the correct distribution of univalents at the spindle poles did

not always lead to a stable state, as univalents moved from pole to pole more often than needed to obtain the correct assortment of univalents at the poles. Based on these observations, Oakley (1983, 1985) suggested that univalent segregation was non-random, that not only is there one X chromosome and one Y chromosome at each pole, there must be X1 and Y1 at the same pole and X2 and Y2 are at the other pole. The segregation of univalents between spindle poles in *Mesostoma* spermatocytes is an example of distance segregation, and if the cell requires X1,Y1 and X2,Y2 at the two poles, that would be an example of non-random segregation. The mechanism, however, of how univalent chromosomes achieve distance segregation in *Mesostoma* spermatocytes is completely unknown, nor is it known whether or why there is non-random assortment of univalent chromosomes as suggested by Oakley (1985).

1.10 Precocious "pre-anaphase" Cleavage Furrow in Mesostoma spermatoctyes versus Conventional Cytokinesis in Other Cells

Yet another unusual feature of *Mesostoma* spermatocytes is the presence of a precocious, "pre-anaphase", cleavage furrow. Oakley and Fuge originally described the appearance of *Mesostoma* spermatocytes as "dumbbell-shaped" and although they did not describe this as a cleavage furrow and did not describe cytokinesis in this organism, their description of the cell shape alluded to the notion that a precocious furrow exists. The presence of a precocious cleavage furrow in *Mesostoma* spermatocytes was not described in detail until the work of Forer and Pickett-Heaps (2010) more than 20 years after the initial observations made by Fuge and Oakley. In *Mesostoma* spermatocytes, indentations arise very early in prometaphase at the equator of the spindle and resemble the initial

ingressions of a cleavage furrow (Forer and Pickett-Heaps, 2010). Following the initial formation of these indentations, the ingression of the furrow may continue somewhat but it eventually becomes arrested and only in late prometaphase prior to anaphase onset do these indentations become more prominent and accentuated at the spindle equator. To determine if the initial ingressions observed in early prometaphase were in fact the early formation of a furrow and the future site of cleavage, Forer and Pickett-Heaps (2010) followed *Mesostoma* spermatocytes from early prometaphase through to telophase. They observed that the initial ingressions at the equator of the spindle were in fact the presence of a precocious furrow and marked the eventual site of cleavage; when chromosomes separated and reached the poles in anaphase, these initial indentations quickly ingressed and cleaved the cell into two equal daughter cells. Although the initial and final ingressions of the furrow occur at the spindle equator, Forer and Pickett-Heaps (2010), observed that the furrow actually shifts its position along the length of the cell throughout prometaphase. Shifts in the position of the furrow occurred in response to imbalances in chromosome numbers at the spindle poles. When univalents segregated between poles to obtain the correct distribution of univalents at each spindle pole, prior to the onset of anaphase, the furrow responded to the imbalance in chromosome number by shifting its position toward the pole with the fewer number of univalents. Once the imbalance in chromosome number at the poles was restored, the furrow responded by shifting back to its original position at the equator (Forer and Pickett-Heaps, 2010). The furrow also shifted its position in response to an imbalance in chromosome numbers when half-bivalent kinetochores detached from one pole and moved to the opposite pole, following

nocodazole treatment. Based on these results, Forer and Pickett-Heaps (2010) determined that shifts in the position of the furrow can occur in the absence of microtubules as nocodazole depolymerises microtubules in the spindle and cell cortex that could potentially be involved in furrow positioning. From further drug experiments with actin and myosin inhibitors, Forer and Pickett-Heaps (2010) determined that actin and myosin are necessary for the formation of a cleavage furrow as the addition of these inhibitors caused the furrow to either relax or completely disappear. The observations made by Forer and Pickett-Heaps (2010) on *Mesostoma* spermatocytes present new data on cleavage furrows and the process of cytokinesis as the presence of a precocious, "pre-anaphase", cleavage furrow presents a new phenomenon that could potentially shed light on the formation of cleavage furrows in other cells types.

Precocious cleavage furrows are uncommon but are not restricted to *Mesostoma* spermatocytes as they have also been described in diatoms (Pickett-Heaps et al., 1979; Pickett-Heaps and Tippet, 1980). From electron microscopy studies on diatoms, Pickett-Heaps and his colleagues (1979, 1980) observed that microfilaments were positioned around the cell periphery by late prophase. By metaphase, these microfilaments are activated and the initial indentation of a cleavage furrow can be observed. Cleavage furrow formation during metaphase involves a slow initial ingression of the furrow while during late anaphase the final ingression of the furrow is very rapid (Pickett-Heaps et al., 1979; Pickett-Heaps and Tippet, 1980). *Mesostoma* spermatocytes and diatoms are two examples in which cleavage furrows form prior to anaphase; this phenomenon is unique to these two cells, as cleavage furrows in most cells form after the onset of anaphase.

The presence of a precocious, "pre-anaphase" cleavage furrow in *Mesostoma* spermatocytes and diatoms challenges the current understanding of when cleavage furrows form to complete the process of cytokinesis. In general, cytokinesis remains a challenging process for cell biologists to understand how cells assemble the necessary machinery to cleave themselves into two cells at the end of mitosis (Pollard, 2010) and why cleavage furrows form at the same place on the spindle (Canman and Wells, 2004). In cell division, cytokinesis is the process that occurs at the end of the mitosis which physically splits the cytoplasm of a cell into two (Barr and Gruneberg, 2007). Cytokinesis occurs in a multitude of organisms including amoebas, fungi, yeast, plants and animals and although common proteins involved in cytokinesis are shared amongst these organisms, the process of cytokineis and the formation of the cleavage furrow vary between cell types (Barr and Gruneberg, 2007; Pollard, 2010). I will now briefly describe the process of cytokinesis in animal cells.

The first step of cytokinesis is for the cell to determine the future position of the cleavage furrow to ensure that it is located between segregating chromosomes (Barr and Gruneberg, 2007) so two equal daughter cells are formed. Since the anaphase midzone is positioned between the chromosomes, many models predict that the mitotic spindle is important for positioning the furrow (Canman and Wells, 2004) and that the anaphase midzone transmits signals through spindle microtubules from the chromosomes to the cell cortex to active furrow formation (Glotzer, 2004). Another model however predicts that the mitotic spindle in combination with spindle asters is involved in positioning the furrow (Barr and Gruneberg, 2007). Therefore it is still under debate exactly how the

furrow is positioned at the equator. Once the furrow is correctly positioned between segregating chromosomes, a contractile ring composed of actin and myosin-II forms at the anaphase midzone (equator) and like strings on a purse, these contractile filaments are drawn together by the action of myosin-II (Canman and Wells, 2004; Wang, 2005; Wolfe and Gould, 2005). The contraction of the ring generates enough force to cleave the cell into two (Wolfe and Gould, 2005). Although this description is "easy", there are over 100 proteins involved (Pollard, 2010), and the timing in which these proteins are recruited to the furrow is especially important to ensure the successful completion of cytokinesis (Wu et al., 2003). The process of cytokinesis is complicated and although many advances have been made, there are many questions that remain unanswered. The presence of a precocious cleavage furrow in *Mesostoma* spermatocytes may help us better understand how the furrow is positioned during anaphase in other cells and which proteins are necessary for the successful completion of cytokinesis and the formation of two new daughter cells.

1.11 References

Albertini, J.D. and Carabatsos, M.J. (1998). Comparative aspects of meiotic cell cycle control in mammals. Journal of Molecular Medicine. **76**, 795-799.

Alberts, B., Johnson, A., Lewis, J., Raff, M., Roberts, K. and Walter, P. (2008). Molecular biology of the cell. New York: Garland Science.

Amaro, A.C., Samora, C.P., Holtackers, R., Wang, E., Kingston, I.J., Alonso, M., Lampson, M., McAinsh, A.D. and Meraldi, P. (2010). Molecular control of kinetochore-microtubule dynamics and chromosome oscillations. Nat Cell Bio. **12**, 319-329.

Askin, A. (1970). Acceleration and trapping of particles by radiation pressure. Phys Rev Lett. **24**, 156-159.

Ashkin, A. and Dziedzic, J.M. (1987). Optical trapping and manipulation of viruses and bacteria. Science. **235**, 1517-1520.

Ashkin, A., Dziedzic, J.M. and Yamane, T. (1987). Optical trapping and manipulation of single cells using infrared laser beams. Nature. **330**, 769-771.

Ashkin, A. and Dziedzic, J.M. (1989). Internal cell manipulation using infrared laser traps. Proc Natl Acad Sci. **86**, 7914-7918.

Ashkin, A., Schutze, K., Dziedzic, J.M., Euteneuer, U. and Schliwa, M. (1989). Force generation of organelle transport measured *in vivo* by an infrared laser trap. Nature. **22**, 346-348.

Ault, J.G., Demarco, A.J., Salmon, E.D. and Rieder, C.L. (1991) Studies on the ejection properties of asters: astral microtubule turnover influences the oscillatory behavior and positioning of mono-oriented chromosomes. J Cell Sci. **99**, 701-710.

Austin, C.R. and Short, R.V. (1982). Reproduction in mammals: Germ cells and fertilization. Cambridge: Cambridge University Press.

Bajer, A. (1972). Influence of UV microbeam on spindle fine structure and anaphase chromosome movements.

Bajer, A.S. (1982). Functional autonomy of monopolar spindle and evidence for oscillatory movement in mitosis. J Cell Biol. **93**, 33-48.

Bajer, A. and Mole-Bajer, J. (1961). UV microbeam irradiation of chromosomes during mitosis in endosperm. Exp Cell Res. **25**, 251-267.

Barr, F.A. and Gruneberg, U. (2007). Cytokinesis: Placing and making the final cut. Cell. **131**, 847-860.

Bedini, C. and Lanfranchi, A. (1990). The eyes of *Mesostoma ehrenbergii* (Focke, 1836) (Platyhelminthes, Rhabdocoela). Fine structure and photoreceptor membrane turnover. Acta Zool. **71**, 125-133.

Bergen, L.G. and Borisy, G.G. (1980). Head-to-tail polymerization of microtubules in vitro. Electron microscopy analysis of seeded assembly. J Cell Biol. **84**, 141-150.

Berns, M.W. and Greulich, K.O. (2007). Laser micromanipulation of cells and tissues. Methods in Cell Biology. San Diego (CA): Academic Press.

Berns, M.W., Cheng, W.K., Floyd, A.D. and Ohnuki, Y. (1971) Cell division after laser microirradition of mitotic chromosomes. Nature. **233**, 122-123.

Berns, M.W., Olsen, R.S. and Rounds, D.E. (1969). *In vitro* production of chromosome lesions using an argon laser microbeam. Nature. **221**, 74-75.

Berns, M.W., Wright, W.H., Tromberg, B.J., Profeta, G.A., Andrews, J.J. and Walter, R.J. (1998). Use of a laser-induced optical force trap to study chromosome movement on the mitotic spindle. Proc Natl Acad Sci. **86**, 4539-4543.

Blaustein, L. (1990). Evidence for predatory flatworms as organizers of zooplankton and mosquito community structure in rice fields. Hydrobiologia. **199**, 179-191.

Blaustein, L. and Dumont, H.J. (1990). Typhloplanid flatworms (*Mesostoma* and related genera): Mechanisms of predation and evidence that they structure aquatic invertebrate communities. Hydrobiologia. **198**, 61-77.

Bloom, W., Zirkle, R.E. and Uretz, R.B. (1955). Irradiation of parts of individual cells. III. Effects of chromosomal and extrachromosomal irradiation on chromosome movements. Ann NY Acad Sci. **59**, 503-513.

Bray, D. (2001). Cell movements from molecules to motility. New York: Garland Publishing.

Bresslau, E. (1903). Die sommer und wintereier der Rhabdocoelen sussen wassers und ihre biologischebedeutung. Verh Dt Zool Ges. **1903**, 126-139.

Bresslau, E. (1904). Beitrage zu entwicklungsgeschichte der Turbellarien. I. Die entwicklung der Rhabdocoelen und alloiocoelen. Zoologie. **76**, 213-332.

Brown, S.W. and Nur, U. (1956). Heterochromatic chromosomes in the coccids. Science.. **45**, 130-145.

Burgess, D.R. and Chang F. (2005). Site selection for the cleavage furrow at cytokinesis. Trends in Cell Biol. **15,** 156-162.

Burgoyne, P.S. and Mahadevaiah, S.K. (2007). The management of DNA double-stranded breaks in mitotic G2 and in mammalian meiosis viewed from a mitotic G2 perspective. BioEssays. **29**, 974-986.

Camenzind, R. and Nicklas, R.B. (1968). The non-random chromosome segregation in spermatocytes of *Gryllotalpa hexadactyla*. Chromosoma (Berl.). **24**, 324-335.

Cameron, L.A., Yang, G, Cimini, D., Canman, J.C., Kisurina-Evgenieva, O., Khodjakov, A., Danuser, G. and Salmon, E.D. (2006). Kinesin 5-independent poleward flux of kinetochore microtubules in PtK1 cells. J Cell Biol. **173**, 173-179.

Campas, O. and Sens, P. (2006). Chromosome oscillations in mitosis. Phys Rev Lett. **97**, 1-4.

Canman, J.C. and Wells, W.A. (2004). Rappaport furrows our mind. The ASCB cytokinesis meeting. Burlington, VT July 22-25, 2004. J Cell Biol. **166**:943-948.

Cassimeris, L., Rieder, C.L. and Salmon, E.D. (1994). Microtubule assembly and kinetochore directional instability in vertebrate monopolar spindles: implications for the mechanism of chromosome congressions. J Cell Sci. **107**, 285-297.

Civelekoglu-Scholey, G., Sharp, D.J., Mogilner, A. and Scholey, J.M. (2006). Model of chromosome motility in *Drosophila* embryos: Adaptation of a general mechanism for rapid mitosis. Biophys J. **90**, 3966-3986.

Cimino, M.C. (1972). Egg production, polyploidization and evolution in a diploid all-female fish of the genus *Poeciliopsis*. Evolution. **26**, 294-306.

Cornman, I. (1944). A summary of evidence in favor of the traction fiber in mitosis. Amer Naturalist. **78**, 410-422.

Croft, J.A. nd Jones, G.H. (1989). Meiosis in *Mesostoma ehrenbergii ehrenbergii*. IV. Recombination nodules in spermatocytes and a test of the correspondence of late recombination nodules and chiasmata. Genetics. **121**, 255-262.

Czaban, B.B. and Forer, A. (1994). Rhodamine-phalloidin and anti-tubulin antibody staining of spindle fibres that were irradiated with an ultraviolet microbeam. Protoplasma. **178**, 18-27.

Desai, A., Maddox, P.S., Mitchison, T.J. and Salmon, E.D. (1998). Anapahse A chromosome movement and poleward spindle microtubule flux occur at similar rates in *Xenopus* extract spindles. J Cell Biol. **141**, 703-713.

Domenici, L. and Gremigni, V. (1977). Fine structure and functional role of the coverings of the eggs in *Mesostoma ehrenbergii* (Focke). Zoomorphology. **88**, 247-257.

Dominguez, R. (2004). Actin-binding proteins-a unifying hypothesis. Trends Biochem Sci. **29**, 572-578.

Even-Ram, S., Doyle, A.D., Conti, M.A., Matsumoto, K., Adelstein, R.S. and Yamada, K.M. Myosin IIA regulates cell motility and actomyosin-microtubule crosstalk. Nature Cell Biol. **9**, 299-309.

Ferguson, F.F. and Hayes Jr, W.J. (1941). A synopsis of the genus *Mesostoma ehrenbergii* 1835. J Elisha Mitchell Sc Soc. **57**, 1-37.

Fiore, L. and Ioalè, P. (1973). Regulation of the production of subitaneous and dormant eggs in the Turbellarian *Mesostoma ehrenbergii* (Focke). Monit Zool Ital. **7**, 203-224.

Forer, A. (1965). Local reduction of spindle birefringence in living *Nephrotoma suturalis* (Loew) spermatocytes induced by ultraviolet microbeam irradiation. J Cell Bio. **25**, 95-117.

Forer, A. (1966). Characterization of the mitotic traction system, and evidence that birefringent spindle fibres neither produce nor transmit force for chromosome movement. Chromosoma. **19**, 44-98.

Forer, A. (1988). Do anaphase chromosomes chew their way to the pole or are they pulled by actin? J Cell Sci. **91**, 449-453.

Forer, A. and Koch, C. (1973). Influence of autosome movements of sex-chromosome movements on sex-chromosome segregation in crane fly spermatocytes. Chromosoma. **40**, 417-442.

Forer, A. and Pickett-Heaps, J.D. (1998). Cytochalasin D and latrunculin effect chromosome behaviour during meiosis in crane-fly spermatocytes. Chromosome Res. **6**, 533-549.

Forer, A. and Pickett-Heaps, J. (2010). Precocious (pre-anaphase) cleavage furrows in *Mesostoma* spermatocytes. Eur J Cell Biol. **89**, 607-618.

Forer, A., Spurck, T., and Pickett-Heaps, J.D. (1997). Ultraviolet microbeam irradiations of spindle fibres in crane-fly spermatocytes and newt epithelial cells: resolution of previously conflicting observations. Protoplasma. **197,** 230–240.

Forer, A., Spurck, J.D. and Pickett-Heaps, J.D. (2007). Actin and myosin inhibitors block elongation of kinetochore fibre stubs in metaphase crane-fly spermatocytes. Protoplasma. **232**, 79-85.

Forer, A., Pickett-Heaps, J.D. and Spurck, T. (2008). What generates flux of tubulin in kinetochore microtubules? Protoplasma. **232**, 137-141.

Forer, A., Spurck, T., Pickett-Heaps, J.D. and Wilson, P.J. (2003). Structure of kinetochore fibres in crane-fly spermatocytes after irradiation with an ultraviolet microbeam: neither microtubules nor actin filaments remain in the irradiated region. Cell Motil Cytoskeleton. **56**, 173-192.

Forer, A. and Wilson, P.J. (1994). A model for chromosome movement during mitosis. Protoplasma. **179**, 95-105.

Fuge, H. (1972). Morphological studies on the structure of univalent sex chromosomes during anaphase movement in spermatocytes of the crane fly *Pales ferruginea*. Chromosoma (Berl.). **39**, 403-417.

Fuge, H. (1987). Oscillatory movement of bipolar-oriented bivalent kinetochores and spindle forces in male meiosis of *Mesostoma ehrenbergii*. Euro J Cell Bio. **44**, 294-298.

Fuge, H. (1989). Rapid kinetochore movements in *Mesostoma ehrenbergii* spermatocytes: action of antagonistic chromosome fibre. Cell Motil Cytoskeleton. **13**, 212-220.

Fuge, H. (1997). Nonrandom chromosome segregation in male meiosis of a sciarid flies: elimination of paternal chromosomes in first division is mediated by non-kinetochore microtubules. Cell Motil Cytoskeleton. **36**, 84-94.

Fuge, H. and Falke, D. (1991). Morphological aspects of chromosome spindle fibres in *Mesostoma*: "microtubular fir-tree" structures and microtubule association with kinetochores and chromatin. Protoplasma. **160**, 39-48.

Gerbi, S.A. (1986). Unusual chromosome movements in sciarid flies. Results Probl Cell Differ. **13**, 71-104.

Goday, C. and Esteban, M.R. (2001). Chromosome elimination in sciarid flies. BioEssays. **23**, 242-250.

Gorbsky, G.J., Sammak, P.J. and Borisy, G.G. (1987). Chromosomes move poleward in anaphase along stationary microtubules that coordinately disassemble from their kinetochore ends. J Cell Biol. **104**, 9-18.

Glotzer, M. (2004). Cleavage furrow positioning. J Cell Biol. **164**, 347-351.

Haimo, L.T. (1997). Ordering microtubules. BioEssays. **19**, 547-550.

Hebert, P.D.N and Beaton, M.J. (1990). Breeding system and genome size of the rhabdocoel turbellarian *Mesostoma ehrenbergii*. Genome. **33**, 719-724.

Heitkamp, U. (1977). Zur fortpflanzungsbiologie von *Mesostoma ehrenbergii* (Focke, 1836) (Turbellaria). Hydrobiologia. **55**, 21-31.

Hochwagen, A. and Amon, A. (2006). Checking your breaks: Surveillance mechanisms of meiotic recombination. Curr Biol. **16,** R217-R228.

Holmes, K.C., Popp, D., Gebhard, W. and Kabsch, W. (1990). Atomic model of the actin filament. Nature. **347**, 44-49.

Husted, L. and Ruebush, T.K. (1940). A comparative cytological and morphological study of *Mesostoma ehrenbergii ehrenbergii* and *Mesostoma ehrenbergii wardii*. J Morphol. **67**, 387-410.

Husted, L., Ferguson, F.F. and Stirewalt, M.A. (1939). Chromosome association in *Mesostoma ehrenbergii* (Focke) *schmidt*. Am Nat. **73**, 180-184.

Huxley, H.E. (1973). Muscular contraction and cell motility. Nature. **243**, 445-449.

Hyman, A.A. and Mitchison, T.J. (1991). Two different microtubule-based motor activities with opposite polarities in kinetochores. Nature. **351**, 206-211.

Inoué, S. (1953). Polarization optical studies of the mitotic spindle. I Demonstration of spindle fibres in living cells. Chromosome. **5**, 487-500.

Inoué, S. and Sato, H. (1967). Cell motility by labile association of molecules. The nature of mitotic spindle fibres and their role in chromosome movement. J Gen Physiol. **50**, 259-292.

Jaqaman, K., King, E.M., Amaro, A.C., Winter, J.R., Dorn, J.F., Elliot, H.L., et al. (2010). Kinetochore alignment within the metaphase plate is regulated by centromere stiffness and microtubule depolymerases. J Cell Biol. **188**, 665-679.

Johansen, K.M. and Johansen, J. (2007). Cell and molecular biology of the spindle matrix. Int Rev Cytol. **263**, 155–206.

Johansen, J and Johansen, K.M. (2009). The spindle matrix through the cell cycle in Drosophila. Fly. **3**, 1–8.

Johansen, K.M., Forer, A., Yao, C., Girton, J. and Johansen, J. (2011). Do nuclear envelope and intranuclear proteins reorganize during mitosis to form an elastic, hydrogel-like spindle matrix? Chromsome Res. **19**, 345-365.

Kalita, G. and Goswami, M.M. (2012). Occurrence of *Mesostoma tetragonum* (Muller) (Turbellaria) in the Deepar wetlands of Assam, India. J Threat Taxa. **4**, 2609-2613.

Karp, G. (2003). Cell and molecular biology: Concepts and experiments. Danvers: John Wiley and Sons Inc.

Ke, K., Cheng, J. and Hunt, A.J. (2009). The distribution of polar ejection forces determines the amplitude of chromosome directional stability. Curr Bio. **19**, 807-815.

Khodjakov, A. and Rieder, C.L. (1996). Kinetochores moving away from their associated pole do not exert a significant pushing force on the chromosome. J Cell Biol. **135**, 315-327.

Khodjakov, A., Cole, R.W., McEwen, B.F., Buttle, K.F. and Rieder, C.L. (1997). Chromosome fragments possessing only one kinetochore can congress to the spindle equator. J Cell Bio. **136**: 22-240.

Kirschner, M.W. (1980). Implications of treadmilling for the stability and polarity of actin and tubulin polymers in vivo. J Cell Biol. **86**, 330-334.

Kolasa, J. (1984). Predation on mosquitoes by juveniles of *Mesostoma* spp. (Turbellaria). Freshwater Invertebrate Biology. **3**, 42-47.

Kolasa, J. and Mead, A.P. (1981). A new species of freshwater turbellarian from Africa, predatory on mosquitoes: *Mesostoma zariae* n. sp. (Typhloplanoida). Hydrobiologia. **84**, 19-22.

Kolasa, J. and Schwartz, S.S. (1988). Two new *Mesostoma* species (Turbellaria, Rhabdocoela) from Australia. Zool Scr. **17**, 329-335.

Kolasa, J., Fletcher, M. and Main, A.J. (1985). New records for two mosquito predators [Turbellaria: *Mesostoma*] in the northeastern United States. Entomophaga. **30**, 83-85.

Konig, K., Riemannm I., Fischer, P., and Halbhuber, K. (1999). Intracellular nanosurgery with near infrared femtosecond laser pulses. Cell Mol Biol. **45**, 192-201.

Konig, K., Svaasand, L., Liu, Y., Sonek, G., Patrizzio, P., Tadir, Y., Berns, M.W. and Tromberg, B.J. (1996). Determination of motility forces of human spermatozoa using an 800nm optical trap. Cellular and Molecular Biology. **42**, 501-509.

Kubai, D.F. (1987). Nonrandom chromosome arrangements in germ line nuclei of *Sciara coprophila* males: the basis for nonrandom chromosomes segregation on the meiosis I spindle. J Cell Biol. **105,** 2433-2446.

Kuo, S.C. and Sheetz, M.P. (1993). Force of single kinesin molecules measured with optical tweezers. Science. **260**, 232-234.

Li, X, and Nicklas, R.B. (1995). Mitotic forces control a cell-cycle checkpoint. Nature. **373**, 630-632.

Liang, H., Wright, W.H., He, W. and Berns, M.W. (1991). Micromanipulation of mitotic chromosomes in PtK_2 cells using laser-induced optical forces ("optical tweezers"). Exp Cell Res. **197**, 21-35.

Liang, H. Wright, W.H., Rieder, C.L., Salmon, E.D., Profeta, G., Andrews, J., Liu, Y., Sonek, G. and Berns, M.W. (1994). Directed movement of chromosome arms and fragments in mitotic newt lung cells using optical scissors and optical tweezers. Exp Cell Res. **213**, 308-312.

Liu, J., Desai, A., Onuchic, J.W. and Hwa, T. (2007). A mechanobiochemical mechanism for monooriented chromosome oscillation n mitosis. PNAS. **104**, 16104-16109.

Liu, Y., Sonek, G.J., Berns, M.W. and Tromberg, B.J. (1996). Physiological monitoring of optically trapped cells: assessing the effects of confinement by 1064-nm laser tweezers using microfluorometry. Biophys J. **71**, 2158-2167.

Luther, A. (1904). Die eumesostominen. Zoologie. **77**, 1-273.

Maddox, P., Desai, A., Oegema, K., Mitchison, T. and Salmon, E. (2002). Poleward microtubule flux is a major component of spindle dynamics and anaphase A in mitotic Drosophila embryos. Curr Biol. **12**, 1670-1674.

Maiato, H. and Lince-Faria, M. (2010). The perpetual movements of anaphase. Cell Mol Life Sci. **67**: 2251-2269.

McIntosh, J.R., Hepler, P.K. and Van Wie, D.G. (1969). Model for mitosis. Nature. **224**, 659-663.

McNeill, P.A. and Berns, M.W. (1981). Chromosome behavior after laser microirradiation of a single kinetochore in mitotic PTK2 cells. J Cell Biol. **88**, 543-553.

Meier, B. and Gartner, A. (2006). Meiosis: Checking chromosomes pair up properly. Curr Biol. **16**, 249-251.

Mitchison, T.J. (1989). Polewards flux in the mitotic spindle evidence from photoactivation of fluorescence. J Cell Biol. **109**, 637-652.

Mitchison, T.J. and Kirschner, M.W. (1987). Some thoughts on the portioning of tubulin between monomer and polymer under conditions of dynamic instability. Cell Biophys. **11,** 35-55.

Mitchison, T.J. and Salmon, E.D. (1992). Poleward kinetochore fiber movement occurs during both metaphase and anaphase A in newt lung cell mitosis. J Cell Biol. **119**, 569-582.

Mitchison, T.J. and Sawin, K.E. (1990). Tubulin flux in the mitotic spindle: where does it come from, where is it going? Cell Motil Cytoskeleton. **16**, 93-98.

Mitchison, T.J., Evans, L., Schulze, E. and Kirschner, M. (1986). Sites of microtubule assembly and disassembly in the mitotic spindle. Cell. **45**, 515-527.

Molloy, J.E., Burns, J.E., Kendrick-Jones, J., Tregear, R.T. and White, D.C.S. (1995). Movement and force produced by a single myosin head. Nature. **379**, 209-212.

Moore, P.B., Huxley, H.E. and DeRosier, D.J. (1969). Three-dimensional reconstruction of F-actin, thin filaments and decorated thin filaments. J Mol Biol. **50**, 279-295.

Mooseker, M.S. and Tilney, L.G. (1975). Organization of an actin filament-membrane complex. Filament polarity and membrane attachment in the microvilli of intestinal epithelial cells. J Cell Biol. **67**, 725-743.

Morgan, D.O. (2007). The cell cycle: principles of control. London: New Science Press Ltd.

Nascimento, J.M., Shi, L.Z., Meyers, S., Gagneux, P., Loskutoff, N.M., Botvinick, E.L. and Berns, M.W. (2008). The use of optical tweezers to study sperm competition and motility in primates. J.R. Soc Interface. **5**, 297-302.

Neuman, K.C. and Block, S.M. (2004). Optical trapping. Review of Scientific Instruments. **75**, 2787-2809.

Nishizaka, T., Miyata, H., Yoshikawa, H., Ishiwata, S. and Kinosita Jr, K. (1995). Unbinding force of a single motor molecule of muscle measured using optical tweezers. Nature. **377**, 251-254.

Nur, U. (1982). Destruction of specific heterochromatic chromosomes during spermatogenesis in the *Comstockiella* chromosome system (Coccoidea: Homoptera). Chromosoma (Berl.). **85**, 519-530.

Oakley, H.A. and Jones, G.H. (1982). Meiosis in *Mesostoma ehrenbergii ehrenbergii* (Turbellaria, Rhabdocoela). I. Chromosome pairing, synaptonemal complexes and chiama localization in spermatogenesis. Chromosoma. **85**, 311-322.

Oakley, H.A. (1983). Male meiosis in *Mesostoma ehrenbergii ehrenbergii*. Kew Chromosome Conference II Editors PE Brandham, MD Bennett. George Allen and Unwin, London (Boston, Sydney) pp 195-199.

Oakley, H.A. (1985). Meiosis in *Mesostoma ehrenbergii ehrenbergii* (Turbellaria, Rhabdocoela) III. univalent chromosome segregation during the first meiotic division in spermatocytes. Chromosoma. **91,** 95-100.

Page, A.W. and Orr-Weaver, T.L. (1997). Stopping and starting the meiotic cell cycle. Curr Opin Genetics and Dev. **7**, 23-31.

Payne, F. (1912). The chromosomes of *Gryllotalpa borealis*. Arch Zellforsch. **9**, 141-148.

Pickett-Heaps, J. D. (1969). The evolution of the mitotic apparatus, an attempt at comparative ultrastructural cytology in dividing cell plants. Cytobios. **1**, 257–280.

Pickett-Heaps, J.D. and Forer, A. (2009). Mitosis: spindle evolution and the matrix model. Protoplasma. **235**, 91-99.

Pickett-Heap, J.D. and Tippit, D.H. (1980). Light and electron microscopic oberservations on cell division in two large pinnate diatoms, Hantzschia and Nitzschia. I. Mitosis in vivo. Eur J Cell Bio. **21**, 1-11.

Pickett-Heaps, J.D., Forer, A. and Spurck, T. (1996). Rethinking anaphase:where "PAC-MAN" fails and why a role for the spindle matrix is likely. Protoplasma. **192**, 1–10.

Pickett-Heaps, J.D., Forer, A. and Spurck, T. (1997). Traction fibre: toward a "tensegral model of the spindle". Cell Motil Cytoskeleton. **37**, 1-6.

Pickett-Heaps, J.D., Spruck, T. And Tippit, D. (1984). Chromosome motion and the spindle matrix. J Cell Biol. **99**, 137-143.

Pickett-Heaps, J.D., Tippit, D.H. and Andreozzi, J.A. (1979). Cell division in the pinnate diatom Pinnularia. V- Observations on live cells. Biol Cellulaire. **35**, 295-304.

Pickett-Heaps, J.D., Tippit, D.N. and Porter, K.R. (1982). Rethinking mitosis. Cell. **29**: 729-744.

Pollard, T.D. (2010). Mechanics of cytokinesis in eukaryotes. Curr Opin Cell Biol. **22**, 50-56.

Pollard, T.D. and Borisy, G.G. (2003). Cellular motility driven by assembly and disassembly of actin filaments. Cell. **12,** 452-465.

Rath, U., Wang, D., Ding, Y., Xu, Y.Z., Blacketer, M.J., Girton, J., Johansen, J. and Johansen, K.M. (2004). Chromator, a novel and essential chromodomain protein interacts directly with the spindle matrix protein skeletor in Drosophila. J Cell Biochem. **93**, 1033–1047.

Rieder, C.L. and Salmon, E.D. (1994). Motile kinetochores and polar ejection forces dictate chromosome position on the vertebrate mitotic spindle. J Cell Biol **124**, 223-233.

Rieder, C.L., Davison, E.A., Jensen, L.C., Cassimeris, L. and Salmon, E.D. (1986). Oscillatory movements of monooriented chromosomes and their positions relative to the spindle pole result from the ejection properties of the aster and half-spindle. J Cell Biol. **103**, 581-591.

Rodriguez, O.C., Schaefer, A.W., Mandato, C.A., Forscher, P., Bement, W.M. and Waterman-Storer, C.M. (2003). Conserved microtubule-actin interactions in cell movement and morphogenesis. Nature Cell Biol. **5**, 599-609.

Roeder, G.S. and Baillis, J.M. (2000). The pachytene checkpoint. Trends Genet. **16**, 395-402.

Schaap, C.J. and Forer, A. (1979). Temperature effects on anaphase chromosome movement in the spermatoctyes of two species of crane flies (*Nephrotoma suturalis* Loew and *Nephrotoma ferruginea* Fabricius). J Cell Sci. **39**, 29-52.

Schwartz, S.S. and Herbert, P.D.N. (1981). A laboratory study of the feeding behaviour of the rhabdocoel *Mesostoma ehrenbergii* on pond Cladocera. Can J Zool. **60**, 1305-1307.

Schrader, F. (1921). The chromosomes of *Pseudococcus nipae*. Biological Bulletin. **40**, 259-270.

Sillers, P.J. and Forer, A. (1981a). Analysis of chromosome movement in crane fly spermatocytes by ultraviolet microbeam irradiation of individual chromosomal spindle fibres. II. Action spectra for stopping chromosome movement and for blocking ciliary beating and myofibril contraction. Can J Biochem. **59**, 777-792.

Sillers, P.J. and Forer, A. (1981b). Autosomal spindle fibres influence subsequent sex-chromsome movements in crane-fly spermatocytes. J Cell Sci. **49**, 51-67.

Sillers, P.J. and Forer, A. (1983). Action spectrum for changes in spindle birefringence after ultraviolet microbeam irradiations of single chromosomal spindle fibres in crane-fly spermatocytes. J Cell Sci. **62**, 1-15.

Silverman-Gavrila, R.V. and Forer, A. (2001). Effects of anti-myosin drugs on anaphase chromosome movement and cytokinesis in crane-fly spermatocyts. Cell Motil Cytoskeleton. **50**, 180-197.

Skibbens, R.V., Skeen, V.P. and Salmon, E.D. (1993). Directional instability of kinetochore motility during chromosome congression and segregation in mitotic newt lung cells: a push-pull mechanism. J Cell Biol. 122, 859-875.

Skibbens, R.V., Rieder, C.L. and Salmon, E.D. (1995). Kinetochore motility after severing between sister centromeres using laser microsurgery: evidence that kinetochore directional instability and position is regulated by tension. J Cell Sci. **108**, 2537-2548.

Snyder, J.A., Armstrong, L., Stonington, G.O., Spurck, T.P., Pickett-Heaps, J.D. (1991). UV-microbeam irradiations of the mitotic spindle: spindle forces and structural analysis of lesions. Eur J Ceil Biol. **55**, 122-132.

Spurck, T., Forer, A. and Pickett-Heaps, J.D. (1997). Ultraviolet microbeam irradiations of epithelial and spermatocyte spindles suggest that forces act on the kinetochore fibre, and are not generated by its disassembly. Cell Motil Cytoskeleton. **36,** 136–148.

Spurck, T.P., Stonington, O.G., Snyder, J.A., Pickett-Heaps, J.D., Bajer, A. and Mole-Bajer, J. (1990). UV microbeam irradiation of the mitotic spindle. II. Spindle fiber dynamics and force production. J Cell Sci. **111**, 1505-1518.

Svoboda, K. and Block, S.M. (1994). Force and velocity measured for single kinesin molecules.

Swanson, C.P., Merz, T. and Young, W.J. (1981). Cytogenetics: The chromosome in division, inheritance and evolution. Englewood Cliffs: Prentice Hall Inc.

Tranchida, M.C., Macia, A., Brusa, F., Micieli, M.V. and Garcia, J.J. (2009). Predation potential of three flatworm species (Platyhelminthes: Turbellaria) on mosquitoes (Diptera: Culicidae). Biological Control. **49**, 270-276.

Trochine, C., Modenutti, B. and Balseiro, E. (2005). When prey mating increases predation risk: the relationship between the flatworm *Mesostoma ehrenbergii* and the copepod *Boekella gracilis*. Arch Hydrobiol. **163**, 555-569.

Trochine, C., Modenutti, B. and Balseiro, E. (2006). Influence of spatial heterogeneity on predation by the flatworm *Mesostoma ehrenbergii* (Focke) on calanoid and cyclopoid copepods. J Plankton Res. **28**, 267-274.

Tyson, J.J. and Novak, B. (2008). Temporal organization of the cell cycle. Curr Biol. **18**, R759-R768.

Uretz, R.B., Bloom, W. and Zirkle, R.E. (1954). Irradiation of parts of individual cells. II. Effects of an ultraviolet microbeam focused on parts of chromosomes. Science. **120**, 197-199.

Vogt, E., Kirsch-Volders, M., Pary, J. and Eichenlaug-Ritter, U. (2008). Spindle formation, chromosome segregation and the spindle checkpoint in mammalian oocytes and susceptibility to meiotic error. Mutat Res. **651**, 14-29.

Voss, von H. (1914). Cytologische studien an *Mesostoma ehrenbergii*. Arch für Zellforschung. **12**, 159-194.

Walker, D.L.,Wang, D,, Jin, Y., Rath, U.,Wang, Y., Johansen, J. and Johansen, K.M. (2000). Skeletor, a novel chromosomal protein that redistributes during mitosis provides evidence for the formation of a spindle matrix. J Cell Biol. **151**, 1401–1411.

Wang, Y.L. (2005). The mechanism of cortical ingression during early cytokinesis: thinking beyond the contractile ring hypothesis. Trends Cell Biol. **15**, 581-588.

Waters, J.C., Skibbens, R.V. and Salmon, E.D. (1996).Oscillating mitotic newt lung cell kinetochores are, on average, under tension and rarely pushed. J Cell Sci. **109**, 2823-2831.

White, M.J.D. (1951). Cytogenetics of orthopteroid insecta. Advance Genet. **4**, 267-330.

Wilson, P. and Forer, A. (1987). Irradiations of rabbit myofibrils with an ultraviolet microbeam. I. Effects of ultraviolet light on the myofibril components necessary for contraction. Biochem Cell Bio. **65**, 363-375.

Wilson, P. and Forer, A. (1988). Ultraviolet microbeam irradiation of chromosomal spindle fibres shears microtubules and permits study of the new free ends *in vivo*. J. Cell Sci. **91**, 455-468.

Wilson, P.J., and Forer, A. (1989). Acetylated-tubulin in spermatogenic cells of the crane fly *Nephrotoma suturalis*: kinetochore microtubules are selectively acetylated. Cell Motil Cytoskeleton **14**, 237–250.

Wolfe, B.A. and Gould, K.L. (2005). Split decisions: coordinating cytokinesis in yeast. Trends Cell Biol. **15**, 10-18.

Woolner, S., O'Brien, L.L., Wiese, C. and Bement, W.M. (2008). Myosin-10 and actin filaments are essential for mitotic spindle function. J Cell Biol. **182**, 77-88.

Wrona, F.J. and Koopowitz, H. (1998). Behavior of the rhabdocoel flatworm *Mesostoma ehrenbergii* in prey capture and feeding. Hydrobiologia. **383**, 35-40.

Wu, J.Q., Kuhn, J.R., Kovar, D.R. and Pollard, T.D. (2003). Spatial and temporal pathway for assembly and constriction of the contractile ring in fission yeast cytokinesis. Dev Cell. **5**, 723-734.

Wuhr, M., Mitchison, T. and Field, C.M. (2008). Mitosis: New roles for myosin-X and actin at the spindle. Curr Biol. **18**, R912-R914.

Zirkle, R.E. and Uretz, R.B. (1963). Action spectrum for paling (decrease in refractive index) of ultraviolet-irradiated chromosome segments. PNAS. **49**, 45-52.

Zirkle, R.E., Uretz, R.B. and Haynes, R.H. (1960). Disappearance of spindles and phragmoplasts after microbeam irradiation of cytoplasm. Ann NY Acad Sci. **90**, 435-439.

CHAPTER 2

TITLE: *Mesostoma ehrenbergii* spermatocytes - a unique and advantageous cell for studying meiosis

AUTHORS: Jessica Ferraro-Gideon[1], Carina Hoang [1] and Arthur Forer[1]

AUTHORS AFFILIATIONS: [1]Department of Biology, York University, Toronto, ON M3J 1P3, Canada

CORRESPONDENCE INFORMATION:
Arthur Forer
Biology Department, York University
4700 Keele St.
Toronto, ON
M3J1P3
(905) 736-2100 ext 44643
aforer@yorku.ca

RUNNING TITLE: Meiosis in *Mesostoma* spermatocytes (44 Characters)

KEYWORDS: distance segregation, meiosis, *Mesostoma ehrenbergii*, oscillations, precocious cleavage furrow, non-random chromosome assortment

WORD COUNT (not including references): 3326

DATE OF ACCEPTANCE: May 17, 2013 (Available on the Cell Biology International Website at doi: 10.1002/cbin.10130)

2.1 Summary

Mesostoma ehrenbergii have a unique male meiosis: their spermatocytes have three large bivalents that oscillate for 1-2 hours before entering into anaphase without having formed a metaphase plate, have a precocious ("pre-anaphase") cleavage furrow, and have four univalents that segregate between spindle poles without physical interaction between them, i.e., via "distance segregation". These unique and unconventional features make *Mesostoma* spermatocytes an ideal organism for studying the force produced by the spindle to move chromosomes, and to study cleavage furrow control and 'distance segregation'. In the present article we review the literature on meiosis in *Mesostoma* spermatocytes and describe the current research that we are doing using *Mesostoma* spermatocytes, rearing the animals in the laboratory using methods that we describe in our companion article (Hoang et al., 2013).

2.2 Introduction

In the present article, we review the literature on male meiosis in *Mesostoma ehrenbergii* and describe features of *Mesostoma* spermatocytes that make them valuable tools for studying cell division. *Mesostoma* spermatocytes are useful for studying cell division because they have few bivalents and a large spindle. In addition, they have many unique features that are not present in conventional meiotic systems including: (1) extensive chromosome oscillations, (2) the absence of a metaphase plate, (3) distance segregation of univalents and (4) a precocious "pre-anaphase" cleavage furrow. Chromosome oscillations in mitotic and meiotic cells are fairly common but these

oscillations are irregular, have low amplitudes, moderate velocities and last for a short periods of time. In *Mesostoma* spermatocytes on the other hand, oscillations are regular and coordinated, have larger amplitudes, rapid velocities and last for periods of 1-2 hours, from early prometaphase until anaphase onset, without formation of a metaphase plate. The cells contain 4 univalents, 2 each of 2 different kinds, that segregate to the two poles without physical contact between them ("distance segregation", Hughes-Schrader, 1969). Finally these cells have "precocious" cleavage furrows, cleavage furrows that form in early prometaphse, begin cleavage, arrest, and continue to cleave the cells in two only after anaphase. *Mesostoma* spermatocytes provide a single system for studying these rare aspects of meiosis that originally would have required a variety of different cell types to study each of these phenomena separately. In the accompanying article (Hoang et al., 2013) we present our methods for how to rear *Mesostoma* and how to make preparations of living spermatocytes for those who may want to study these cells.

2.2.1 Previous work on Mesostoma spermatocytes

Mesostoma ehrenbergii, a hermaphroditic aquatic flatworm from the order Rhabdocoela and the class Turbellaria, has been well-described anatomically by ecologists for decades (Ferguson and Hayes Jr, 1941; Kolasa and Schwartz, 1988; Bedini and Lanfranchi, 1990; Kalita and Goswami, 2012). The voracious predatory nature of *Mesostoma* (Blaustein and Dumont, 1990; DeRoeck et al., 2005; Trochine et al., 2005; Trochine et al., 2006), its unique feeding behaviours (Schwartz and Herbert, 1981; Wrona and Koopowitz, 1998), its possible use in control of mosquito larvae (Case and Washino,

1979; Kolasa and Mead, 1981; Kolasa, 1984; Kolasa et al., 1985; Blaustein, 1990; Tranchida et al. 2009), and its ability to produce both viviparous embryos and dormant eggs (Bresslau 1903; Fiore and Ioalè, 1973; Domenici and Gremigni, 1977; Heitkamp, 1977) have been well documented. Unfortunately, these worms have not received as much attention from cell biologists.

M. ehrenbergii was first reported in Europe by Focke in 1836 and later in different localities around the world (Woodworth 1897; Graff 1913). Early researchers who looked at their cells were primarily interested in determining the number and morphology of meiotic chromosomes in the European (Luther, 1904; Bresslau, 1904; Voss, 1914) and North American (Husted et al., 1939; Husted and Ruebush, 1940) variants of *M. ehrenbergii.* Husted and Ruebush (1940) were amongst the first researchers to illustrate the karyotype of *Mesostoma* spermatocytes (as seen in Figure 2.1) and to document the length of each chromosome and the differences in centromere positions in both the European and North American worms. Husted and Ruebush (1940) determined that the European *M. ehrenbergii* (subspecies: *ehrenbergii*) has spermatocytes with 3 bivalents and 4 univalents (n=10) (Figure 2.1A), whereas the North American *M. ehrenbergii* (subspecies: *wardii*) has spermatocytes with 3 bivalents and 2 univalents (n=8) (Figure 2.1B). This observation was later contradicted by Hebert and Beaton (1990) who found that the North American subspecies of *M. ehrenbergii* have spermatocytes with the same number of chromosomes (n=10) as the European worms.

Husted and Ruebush (1940) were also amongst the first researchers to describe that each of the three bivalents have a single distally located chiasma.

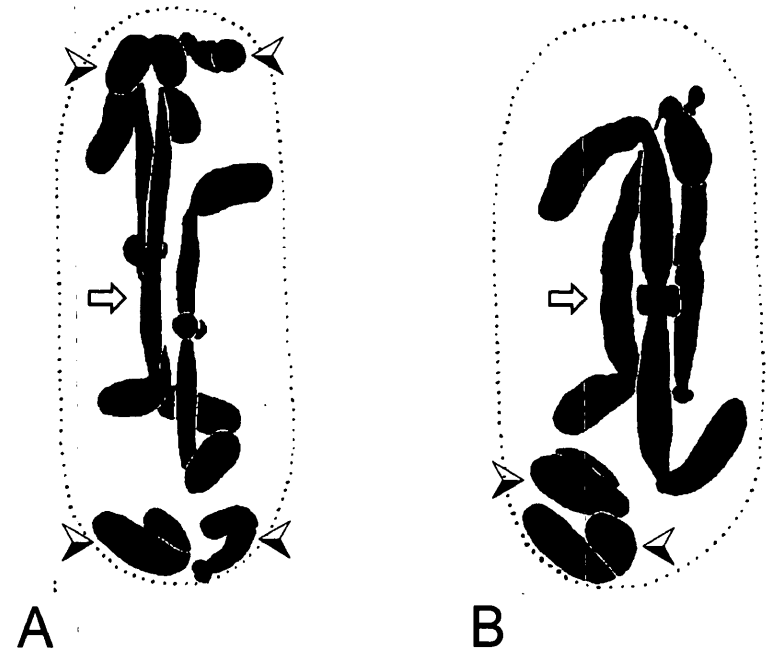

Figure 2.1 Picture of fixed and sectioned *M. ehrenbergii* spermatocytes modified from Husted and Ruebush (1940). (A) European form of *M. ehrenbergii* (*ehrenbergii*) showing 3 bivalents and 4 univalents, n=10. (B) North American form of *M. ehrenbergii* (*wardii*) showing 3 bivalents and 2 univalents, n=8. The open white arrows (⇨) illustrate the positions of one bivalent in each spermatocyte and the arrowheads (➢) illustrate the positions of each of the univalents at the poles in each spermatocyte.

This was later confirmed by electron microscopy studies performed by Oakley and Jones (1982) and Croft and Jones (1989). Oakley and Jones (1982) identified that chromosome pairing in *M. ehrenbergii* is incomplete, as synaptonemal complex (SC) formation is restricted to the lobed region of the nucleus which limits each of the three bivalents to short SC sequences. Jones and Croft (1989) further examined this

phenomenon and determined that chromosome pairing is indeed incomplete, synaptonemal complexes are in fact only short segments on each of the bivalents. But unlike Oakley and Jones (1982), they determined that each synaptonemal complex contains one recombination nodule.

After the work of Husted and Ruebush in 1940 on fixed preparations, there were no further studies of chromosomes during meiosis I in *Mesostoma* spermatocytes until almost 40 years later (Oakley and Jones, 1982; Oakley, 1983; Oakley, 1985; Fuge, 1987; Croft and Jones, 1989; Fuge, 1989 and Fuge and Falke 1991).

2.2.2 Non-Random Distance Segregation of Univalents

Oakley and Fuge studied chromosome movements in living spermatocytes. Oakley focused her research on the pole-to-pole univalent movements during prometaphase I in *Mesostoma* spermatocytes (Oakley, 1983; 1985). In early prometaphase, univalents are present at the spindle poles. They remain there until anaphase, but sometimes individual univalents move from one pole to the opposite pole. From squash preparations, Oakley determined that the four univalents are actually two pairs of two and that members of each pair are morphologically identical to each other but morphologically different from the other pair. Prior to anaphase, there can be different numbers of univalents at each pole or there can be two of the same kind at each pole; but by anaphase I there is one of each kind at each pole. So, if the two univalent pairs in *Mesostoma* spermatocytes consist of X1,X2 and Y1,Y2 chromosomes, the end result by the start of anaphase is one X and one Y chromosome at each pole. The

univalents seem to segregate properly by anaphase, an example of 'distance segregation', as described by Hughes-Schrader (1969), in which partners segregate to opposite poles without having first been conjoined.

From observations of living cells Oakley described univalents moving from pole to pole, and she presumed that the movements were necessary to obtain one X and one Y univalent at each pole. Her observations suggested to her that there was non-random assortment of the univalents. If assortment were random, then the two poles in any given cell would have X1, Y2 and X2, Y1 or would have X1,Y1 and X2,Y2 chromosomes. She noticed, however, that the univalents moved from pole to pole more often than needed in order to obtain one random X and one random Y at each pole, and she noticed that members of one univalent pair often changed poles (e.g., X1 and X2 changing poles); neither of these would occur if the required end point was only that there be one of each kind of univalent at each pole. Thus she suggested that there is non-random assortment of univalents in these cells, resulting, e.g., in the two poles having only X1, Y1 and X2,Y2 chromosomes.

In addition to her discovery that univalents undergo distance segregation and possible non-random assortment, Oakley characterized the pole-to-pole movements of these univalents (Oakley, 1983, 1985). The univalents move rapidly, moving from one spindle pole to the other in about 1-2 minutes (Oakley, 1983), as seen in Figure 2.2A-F, with the kinetochores always leading the way (Oakley, 1985). Univalents moved one at a time, with intervals as short as 5-10 minutes before the next univalent excursion

(Oakley, 1983), as illustrated graphically in Figure 2.2G.

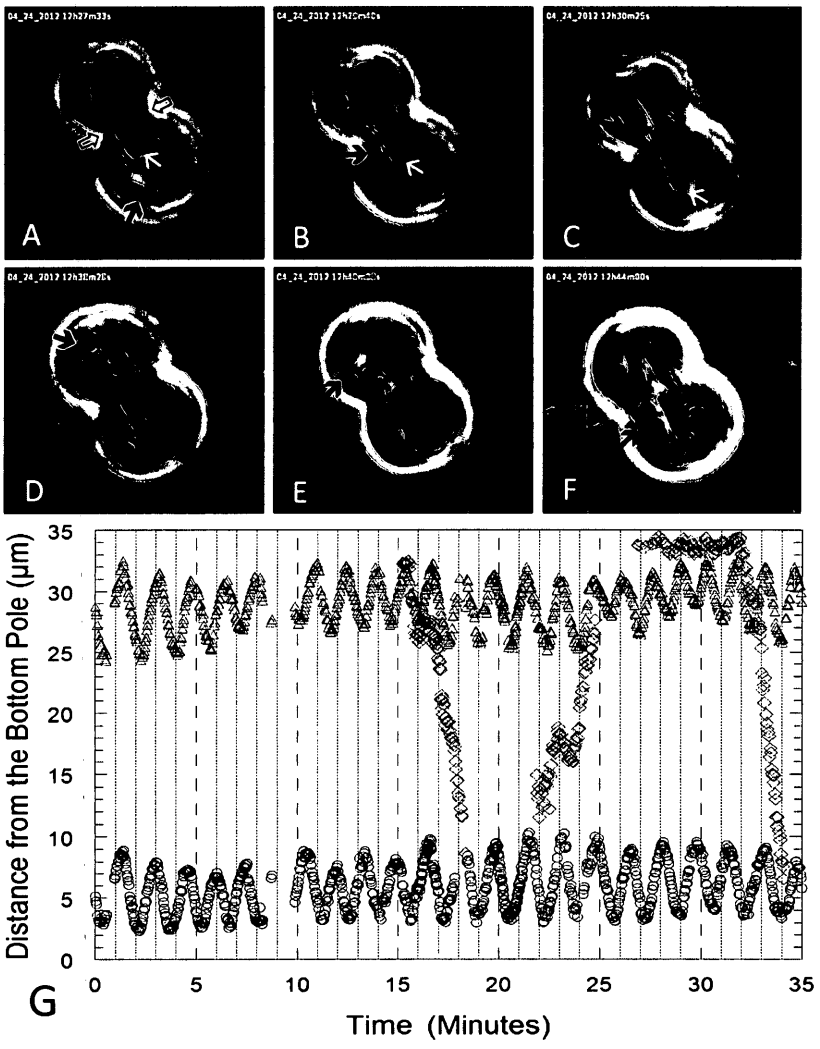

Figure 2.2 Montage of phase contrast microscope images of a *Mesostoma* spermatocyte illustrating a univalent as it moves between spindle poles during prometaphase/metaphase and bivalent kinetochore oscillations. (A-C) The univalent moves from the lower pole to the upper pole. The lower half-bivalent kinetochore as depicted by the white arrow moves towards its pole. (D-F) Approximately 10 minutes after the first univalent excursion, the same univalent moves from the upper pole to the lower pole. The black arrows in A point to the precocious cleavage furrow and the thick black arrows in A-E point to the positions of the univalent. (G) Graph of distance of the kinetochores of partner half bivalents (**O** and Δ) and of the kinetochores of a univalent (◊) from the bottom pole of the cell in µm, versus time in minutes in a *M. ehrenbergii* spermatocyte.

The mechanism of how univalent chromosomes achieve distance segregation is completely unknown, and it is not known whether there actually is non-random assortment of univalent chromosomes as suggested by Oakley (1985).

2.2.3 Kinetochore Oscillations of Autosomal Bivalents

Descriptions of bivalent chromosome movements in living *Mesostoma* spermatoctyes followed the work of Oakley. Fuge (1987, 1989) described the unique kinetochore oscillations of the three bipolarly oriented bivalents that occur during prometaphase/metaphase in *Mesostoma* spermatocytes. In his first article on the oscillatory movements of bivalent kinetochores in *Mesostoma* spermatoctyes, Fuge (1987) was able to analyze only short sequences (up to 8 minutes) of movement due to the short length of film that he had available. These short sequences of movement, however, were the first to illustrate the regular, rapid, and coordinated kinetochore oscillations that the bivalents in *Mesostoma* spermatocytes exhibit throughout prometaphase/metaphase (Figure 2.2A-C and Figure 2.2G). There is no defined 'metaphase' as commonly described, however, because the bivalents continually oscillate and do not align at the equator. In a later article, Fuge (1989) analysed longer sequences and was able to provide a more descriptive analysis of these kinetochore oscillations. In the cells he studied, kinetochores oscillated to and away from the spindle poles for the entire observation period, up to approximately one hour, with average kinetochore velocities of 8-10 μm/min and maximum velocities of up to 17 μm/min. Fuge determined that kinetochores move 5-7 μm away from the pole and then back to the pole, and repeat

this every 100s with the two kinetochores of any given bivalent moving either in phase or out of phase (Fuge, 1989, 1991). (He classified kinetochores as moving in-phase when partner kinetochores moved to the pole at the same time and away from the pole at the same time; partner kinetochores were classified as moving out-of-phase when one kinetochore moved to the pole and the other kinetochore moved away from pole.) In order to better understand how kinetochores move to and from the pole, electron microscopy studies were undertaken (Fuge, 1987, 1989; Fuge and Falke, 1991). The electron microscope images showed that *Mesostoma* kinetochores have a cup-like invagination that allow the deep insertion of kinetochore microtubules (Fuge 1987), and that chromosomal fibres are several μm in length, well-developed, and contain kinetochore microtubules that insert into the kinetochore and contained as well as non-kinetochore microtubules that surround the kinetochores and bivalents (Fuge 1989). These results could explain kinetochore movement to the pole by shortening of kinetochore microtubules but not the backward movement of the entire chromosome and the away from pole movement of kinetochores. In a subsequent article Fuge and Falke (1991) suggested that chromosome spindle fibres resemble a "microtubular fir-tree", composed of kinetochore microtubules and non-kinetochore microtubules that associate with both bivalents and kinetochores. Although Fuge and Falke (1991) were able to provide a more intricate picture of the spindle of *Mesostoma* spermatocytes, they still could only speculate as to how kinetochores oscillate to and away from the pole. And neither Fuge nor Oakley described anaphase in these spermatocytes.

The research conducted by Husted and Ruebush (1940), Oakley (1983, 1985) and Fuge (1987, 1989, 1991) laid the groundwork for further study of chromosome movements in *Mesostoma* spermatocytes, which was then hindered for decades by the absence of laboratory stocks of these animals.

2.2.4 Precocious "pre-anaphase" Cleavage Furrow

Approximately 20 years after the last article published on *Mesostoma* spermatocytes, Forer and Pickett-Heaps (2010) published an article on yet another unique feature of *Mesostoma* spermatocytes: the presence of a precocious ("pre-anaphase") cleavage furrow. Cleavage furrows in a multitude of cell types begin ingression after the onset of anaphase (Burgess and Chang, 2005; Barr and Gruneberg, 2007). Forer and Pickett-Heaps (2010), however, described a different phenomenon. In *Mesotoma* spermatocytes, the precocious cleavage furrow begins ingression during prometaphase when the bivalents achieve bipolar orientation; the furrow then arrests until the start of anaphase, almost 1-2 hours later, when it cleaves the cell into two equal daughter cells (Forer and Pickett-Heaps, 2010). A well–developed precocious furrow can be seen in the cell shown in Figure 2.2A. Surprisingly, precocious furrows shift their positions along the length of the cell in response to imbalances in chromosome numbers associated with the two poles, which occur when univalents move between spindle poles trying to achieve proper segregation (Forer and Pickett-Heaps, 2010).

The furrow compensates for these imbalances by shifting from its primary position at the equator toward the spindle pole associated with the fewer number of

chromosomes. Changes in the position of the furrow can occur in the absence of microtubules but not in the absence of actin and myosin as the latter are required to maintain the shape of the furrow (Forer and Pickett-Heaps, 2010).In sum, *Mesostoma* spermatocytes present opportunities for studying several unique occurrences, namely distance segregation, possible non-random chromosome assortment, kinetochore oscillations, absence of a true metaphase, and precocious ("pre-anaphase") cleavage furrows. Although meiosis in this organism would be defined as "unconventional" according to textbook descriptions of meiosis, these 'unusual' phenomena all exist in this one cell, and need to be understood if we are to really understand cell division. We have tried to expand our understanding of these cells in recent experiments.

2.2.5 Our Current Studies using Mesostoma Spermatocytes

We have been able to expand on the previous work on *Mesostoma* spermatocytes because we are able to rear the animals in the laboratory, as described in our companion article (Hoang et al. 2013). The *Mesostoma* that we rear in the laboratory however, are different from the *Mesostoma* that Oakley and Fuge originally used. In the subspecies we study, the bivalents are metacentric and have only one chiasma, so each bivalent has one free arm, whereas in the subspecies that Oakley and Fuge studied two of the bivalents are acrocentric (and have no free arms) and one bivalent is metacentric. Although some variation exists in the morphology of the bivalents in the North American subspecies we study versus the European subspecies that Oakley and Fuge studied, the same phenomena of kinetochore oscillations, distance segregation and non-random assortment of

univalents and presence of a precocious cleavage furrow exist in our cells. Therefore, we have been able to expand on the previous literature on kinetochore oscillations and univalent movements, as well as providing a detailed description of anaphase chromosome movements, bivalent reorientations, and shifts in the position of the precocious furrow in response to alterations in spindle components. We primarily focused on the kinetochore oscillations that occur during prometaphase/metaphase.

Oscillatory kinetochore movements are rapid, regular, coordinated and last for periods of 1 to 2 hours, which is uncommon when compared to oscillatory kinetochore movements in other cells types that are usually slower, irregular, uncoordinated and last only for a short period of time (Bajer, 1982; Ault *et al.* 1991; Skibbens *et al.* 1993, 1995; Khodjakov *et al.* 1997; Jaqaman *et al.* 2010). In the cells we studied kinetochores oscillated to and from the pole with average excursions of 4.0μm and velocities of 6.2μm/min and 5.2μm/min, respectively, as based on analysis of approximately 1700 kinetochores. The velocities of these movements are much faster than the prometaphase oscillatory kinetochore movements in most cells, which are around 1.0μm/min to 3.0μm/min (Bajer, 1982; Ault *et al.* 1991; Skibbens *et al.* 1993, 1995; Khodjakov *et al.* 1997; Jaqaman *et al.* 2010), but they are similar to the rapid oscillatory movements in early *Drosophila* embryo cells which have average velocities of 3.6μm/min and 6.6μm/min, depending on temperature (Maddox *et al.* 2002), but which, however, last for only 50-100s and have excursions that are only 0.5-2μm away from the pole (Civelekoglu-Scholey *et al.* 2006). The velocities of kinetochore movements in

Mesostoma spermatocytes are comparable to the velocities of chromosome movement in early *Drosophila* embryo cells but the length of time oscillatory movements take place and the distance of each excursion are much greater than those in early *Drosophila* embryos.

Kinetochore oscillations in *Mesostoma* spermatocytes are unique and therefore allow us to use a variety of tools to manipulate different components of the spindle so we can better understand how chromosomes move. Through the use of an optical trapping laser (1064nm), an ultraviolet microbeam (290nm) and an optical cutting laser (730nm), we determined that kinetochore movement to the pole is different from kinetochore movement away from the pole. We measured the force required to stop chromosome movement by holding oscillating kinetochores with an optical trap (Ferraro-Gideon et al., 2013). The lengthy oscillation periods allowed us to perform multiple trapping experiments in the same spermatocyte and to collect a lot of data in a short period of time. We determined the power that would stop kinetochore movement in the presence of the trap but would allow kinetochore movement to resume when the trap was released, indicating that though motion was stopped, the laser did not damage the cell (Ferraro-Gideon et al., 2013). UV microbeam irradiations of kinetochore fibres suggested that movement mechanisms are different for oscillations to and from the pole (unpublished data): After irradiation of a kinetochore fibre, kinetochore movement continued until the kinetochore reached the pole (or the movement reversed direction so the kinetochore could move to the pole). Movement stopped when the kinetochore was at the pole, but

movement resumed only for chromosomes whose fibres were irradiated as the kinetochore moved to the pole. We still are investigating differences in the components and mechanisms between movement to the pole versus away from the pole.

Although most of our research has focused on using kinetochore oscillations in *Mesostoma* spermatocytes to better understand how chromosomes move, the same experiments showed that the position of the precocious cleavage furrow changes after various components of the spindle are altered. Following UV irradiation of a kinetochore fibre, the furrow shifts approximately 1μm, usually away from the site of irradiation; following UV irradiation of a kinetochore, the furrow immediately shifts its position either towards or away from the site of irradiation, but the furrow then completely loses its shape and the cells become rounded (unpublished data). The furrow also shifts its position in response to bivalent reorientation, when both kinetochores are temporarily associated with one spindle pole, the furrow shifts towards the pole with the fewer number of attached kinetochores (unpublished data).

2.3 Conclusion

Mesostoma spermatocytes offer a unique system for studying and better understanding why and how chromosome oscillations take place; the mechanisms of distance segregation (and possibly non-random chromosome assortment); and they provide new insight into cleavage furrow formation since the furrows form and contract in early prometaphase, one or more hours prior to anaphase. Not only are these cells large, with few chromosomes, in conventional meiotic systems a variety of different cell

types would have been required to study each of these phenomena separately, whereas each of these phenomena can be studied using a single cell type, spermatocytes from *Mesostoma.* This not only allows for the study of each of these phenomena individually but it also allows for the study of these phenomena as a whole. Although some of the features of *Mesostoma* spermatocytes are unconventional to most meiotic systems, these unconventional features can allow us to shed light on important features of cell division that often are ignored.

There are other advantages to using these animals. For example, the hermaphroditic *Mesostoma* will self-fertilize if reared in isolation, which could be quite useful for genetic studies. The animals are transparent (see illustrations and videos in the accompanying article) and can easily be injected through the body wall with a variety of labeled markers. Although much still is unknown about this organism, and molecular tools have not yet been developed, the unusual kinetochore oscillations, the presence of a precocious ("pre-anaphase") cleavage furrow, the distance segregation of univalents, the non-random assortment of univalents and bivalents and the lack of metaphase make the meiotic division in *Mesostoma* spermatocytes so different from the standard paradigm of cell division, that it really should be investigated more fully.

2.4 References

Ault JG, Demarco AJ, Salmon ED, Rieder CL. Studies on the ejection properties of asters: astral microtubule turnover influences the oscillatory behavior and positioning of mono-oriented chromosomes. J Cell Sci 1991;99:701-710.

Bajer AS. Functional autonomy of monopolar spindle and evidence for oscillatory movement in mitosis. J Cell Biol 1982;93:33-48.

Barr FA, Gruneberg U, Cytokinesis: placing and making the final cut. Cell 2007;131:847-860.

Bedini C, Lanfranchi A. The eyes of *Mesostoma ehrenbergii* (Focke, 1836) (Platyhelminthes, Rhabdocoela). Fine structure and photoreceptor membrane turnover. Acta Zool 1990;71:125-133.

Blaustein L. Evidence for predatory flatworms as organizers of zooplankton and mosquito community structure in rice fields. Hydrobiologia 1990;199:179-191.

Blaustein L, Dumont HJ. Typhloplanid flatworms (*Mesostoma* and related genera): Mechanisms of predation and evidence that they structure aquatic invertebrate communities. Hydrobiologia 1990;198:61-77.

Bresslau E. Die sommer und wintereier der Rhabdocoelen sussen wassers und ihre biologischebedeutung. Verh Dt Zool Ges 1903 ;1903:126-139.

Bresslau E. Beitrage zu entwicklungsgeschichte der Turbellarien. I. Die entwicklung der Rhabdocoelen und alloiocoelen. Zoologie 1904 ;76 :213-332.

Burgess DR, Chang F. Site selection for the cleavage furrow at cytokinesis. Trends Cell Biol. 2005;15:156-162.

Case TJ, Washin RK. Flatworm control of mosquito larvae in rice fields. Science 1979;206:1412-1414.

Civelekoglu-Scholey G, Sharp DJ, Mogilner A, Scholey JM. Model of chromosome motility in *Drosophila* embryos: Adaptation of a general mechanism for rapid mitosis. Biophys J 2006;90:3966-3986.

Croft JA, Jones GH. Meiosis in *Mesostoma ehrenbergii ehrenbergii*. IV. Recombination modules in spermatocytes and a test of the correspondence in late recombination nodules and chiasmata. Genetics 1989;121:255-262.

DeRoeck ERM, Artois T, Brendonck L. Consumptive and non-consumptive effects of turbellarian (*Mesostoma* sp.) predation on anostracans. Hydrobiologia 2005;542:103-111.

Domenici L, Gremigni V. Fine structure and functional role of the coverings of the eggs in *Mesostoma ehrenbergii* (Focke). Zoomorphology 1977;88:247-257.

Ferguson FF, Hayes Jr WJ. A synopsis of the genus *Mesostoma ehrenbergii* 1835. J Elisha Mitchell Sc Soc 1941;57:1-37.

Ferraro-Gideon J, Sheykhani R, Zhu Q, Duquette ML, Berns MW, Forer A. Measurements of forces produced by the mitotic spindle using optical tweezers. Mol Biol Cell 2013;24:1375-1386.

Fiore L, Ioalè P. Regulation of the production of subitaneous and dormant eggs in the Turbellarian *Mesostoma ehrenbergii* (Focke). Monit Zool Ital 1973;7:203-224.

Forer A, Pickett-Heaps J. Precocious (pre-anaphase) cleavage furrows in *Mesostoma* spermatocytes. Eur J Cell Biol 2010;89:607-618.

Fuge H. Oscillatory movements of bipolar-oriented bivalent kinetochores and spindle forces in male meiosis of *Mesostoma ehrenbergii*. Eur J Cell Biol 1987;44:294-298.

Fuge H. Rapid kinetochore movements in *Mesostoma ehrenbergii* spermatocytes: action of antagonistic chromosome fibre. Cell Motil Cytoskeleton 1989;13:212-220.

Fuge H, Falke D. Morphological aspects of chromosome spindle fibres in *Mesostoma*: "microtubular fir-tree" structures and microtubule association with kinetochores and chromatin. Protoplasma 1991;160:39-48.

Graff LQ. Turbellaria. II. Rhabdocoelida. In: Das Tierreich; 1913. p. 35.

Hebert PDN, Beaton MJ. Breeding systems and genome size of the rhabdocoel turbellarian *Mesostoma ehrenbergii.* Genome 1990;33:719-724.

Heitkamp U. Zur fortpflanzungsbiologie von *Mesostoma ehrenbergii* (Focke, 1836) (Turbellaria). Hydrobiologia 1977;55:21-31.

Hoang C, Ferraro-Gideon J, Gauthier K, Forer A. Methods for rearing *Mesostoma ehrenbergii* in the laboratory for cell biology experiments, including identification of factors that influence production of different egg types. Cell Biol Int 2013; Accepted.

Hughes-Schrader S. Distance segregation and compound sex chromosomes in Mantispids (*Neuroptera: Mantispidae*). Chromosoma 1969;27:109-129.

Husted L, Ferguson FF, Stirewalt MA. Chromosome association in *Mesostoma ehrenbergii* (Focke) *schmidt*. Am Nat 1939;73:180-184.

Husted L, Ruebush TK. A comparative cytological and morphological study of *Mesostoma ehrenbergii ehrenbergii* and *Mesostoma ehrenbergii wardii*. J Morphol 1940;67:387-410.

Jaqaman K, King EM, Amaro AC, Winter JR, Dorn JF, Elliot HL, et al. Kinetochore alignment within the metaphase plate is regulated by centromere stiffness and microtubule depolymerases. J Cell Biol 2010;188:665-679.

Kalita G, Goswami MM. Occurrence of *Mesostoma tetragonum* (Muller) (Turbellaria) in the Deepar wetlands of Assam, India. J Threat Taxa 2012;4:2609-2613.

Khodjakov A, Rieder CL. Kinetochores moving away from their associated pole do not exert a significant pushing force on the chromosome. J Cell Biol 1996;135:315-327.

Kolasa J, Mead AP. A new species of freshwater turbellarian from Africa, predatory on mosquitoes: *Mesostoma zariae* n. sp. (Typhloplanoida). Hydrobiologia 1981;84:19-22.

Kolasa J. Predation on mosquitoes by juveniles of *Mesostoma* spp. (Turbellaria). Freshwater Invertebrate Biology 1984;3:42-47.

Kolasa J, Fletcher M, Main AJ. New records for two mosquito predators [Turbellaria: *Mesostoma*] in the northeastern United States. Entomophaga 1985;30:83-85.

Kolasa J, Schwartz SS. Two new *Mesostoma* species (Turbellaria, Rhabdocoela) from Australia. Zool Scr 1988;17:329-335.

Luther A. Die eumesostominen. Zoologie 1904;77:1-273.

Maddox P, Desai A, Oegema K, Mitchison T, Salmon E. Poleward microtubule flux is a major component of spindle dynamics and anaphase A in mitotic Drosophila embryos. Curr Biol 2002;12:1670-1674.

Oakley HA and Jones GH. Meiosis in *Mesostoma ehrenbergii ehrenbergii* (Turbellaria, Rhabdocoela) I. chromosome pairing, synaptonemal complexes and chiasma localization in spermatogenesis. Chromosoma 1982;85: 311-322.

Oakley HA. Male meiosis in *Mesostoma ehrenbergii ehrenbergii*. Key Chromosome Conference II 1983.

Oakley HA. Meiosis in *Mesostoma ehrenbergii ehrenbergii* (Turbellaria, Rhabdocoela) III. univalent chromosome segregation during the first meiotic division in spermatocytes. Chromosoma 1985;91:95-100.

Schwartz SS, Herbert PDN. A laboratory study of the feeding behaviour of the rhabdocoel *Mesostoma ehrenbergii* on pond Cladocera. Can J Zool 1981;60:1305-1307.

Skibbens RV, Skeen VP, Salmon ED. Directional instability of kinetochore motility during chromosome congression and segregation in mitotic newt lung cells: a push-pull mechanism. J Cell Biol 1993;122:859-875.

Skibbens RV, Rieder CL, Salmon ED. Kinetochore motility after severing between sister centromeres using laser microsurgery: evidence that kinetochore directional instability and position is regulated by tension. J Cell Sci 1995;108:2537-2548.

Tranchida MC, Macia A, Brusa F, Micieli MV, Garcia JJ. Predation potential of three flatworm species (Platyhelminthes: Turbellaria) on mosquitoes (Dipter: Culicidae). Biological Control 2009;49:270-276.

Trochine C, Modenutti B, Balseiro E. When prey mating increases predation risk: the relationship between the flatworm *Mesostoma ehrenbergii* and the copepod *Boekella gracilis*. Arch Hydrobiol 2005;163:555-569.

Trochine C, Modenutti B, Balseiro E. Influence of spatial heterogeneity on predation by the flatworm *Mesostoma ehrenbergii* (Focke) on calanoid and cyclopoid copepods. J Plankton Res 2006;28:267-274.

Voss vonH. Cytologische studien an *Mesostoma ehrenbergii*. Arch F Zellforschung 1914;12:159-194.

Woodworth WM. Contribution to the morphology of the Turbellaria. II. On some Turbellaria from Illinois. Bull Mus Comp Zool 1897;31:1-16.

Wrona FJ, Koopowitz H. Behavior of the rhabdocoel flatworm *Mesostoma ehrenbergii* in prey capture and feeding. Hydrobiologia 1998;383:35-40.

CHAPTER 3

TITLE: Methods for rearing *Mesostoma ehrenbergii* in the laboratory for cell biology experiments, including identification of factors that influence production of different egg types

AUTHORS: Carina Hoang[1], Jessica Ferraro-Gideon[1], Kimberley Gauthier[1], Arthur Forer[1]

AUTHOR AFFILIATIONS: [1]Biology Department, York University, 4700 Keele St. Toronto, Ontario, Canada M3J 1P3

SHORT RUNNING TITLE (45 characters): Rearing *Mesostoma* in the lab for cell biology

CORRESPONDENCE INFORMATION:
Arthur Forer
Biology Department, York University
4700 Keele St.
Toronto, ON
M3J1P3
(905) 736-2100 ext 44643
aforer@yorku.ca

KEYWORDS: Mesostoma, cell division, egg type, meiosis, spermatocytes

WORD COUNT: 6786

DATE OF ACCEPTANCE: May 17, 2013 (Available on the Cell Biology International Website at doi: 10.1002/cbin.10129)

3.1 Abstract

Mesostoma ehrenbergii spermatocytes are uniquely useful to study various aspects of cell division. Their chromosomes are large in size and few in number, with only 3 bivalent and 4 univalent chromosomes. During prometaphase, bipolar bivalents oscillate regularly to and from the poles for 1-2 hours. The univalents remain at the poles but occasionally move from one pole to the other. In addition, a precocious cleavage furrow forms during prometaphase and remains partially constricted until anaphase. Attempts to rear these animals indefinitely in laboratory conditions, however, have been mostly unsuccessful because of their reproductive strategy. *M. ehrenbergii* are hermaphroditic flatworms that can produce viviparous offspring (termed S eggs) and/or diapausing eggs (termed D eggs) and they follow either one of two reproductive patterns: (1) they first form S eggs and following the delivery of these eggs produce D eggs, or (2) they only produce D eggs. When only D eggs are formed, which is common under laboratory conditions, the stocks die out until the diapausing eggs hatch, which is irregular and creates unpredictable wait times. Consequently, to maintain *M. ehrenbergii* stocks in order to study their spermatocytes, we studied various factors that might influence egg type production. We have found that feeding them daily and keeping them at 25°C favours S egg production. Currently, our cultures have reached the 45th generation. In this article we describe our rearing and dissection methods and describe experiments which led to our present rearing methods.

3.2 Introduction

Mesostoma ehrenbergii are hermaphroditic flatworms that have been used to study chromosome movements during male meiosis. The unique cytological attributes of these cells are described in detail in the accompanying paper (Ferraro-Gideon et al., 2013). Briefly, dividing spermatocytes of these animals have only 3 bivalent and 4 univalent chromosomes (Oakley and Jones, 1982). The bivalents oscillate at regular speeds throughout prometaphase for long periods of time (Fuge, 1987), in contrast to most other cell types where oscillations are more irregular and for much shorter periods of time (Skibbens et al., 1993). The univalents are usually at the poles but sometimes move from pole to pole until correct segregation is achieved (Oakley,1985). *M. ehrenbergii* also forms a precocious cleavage furrow during prometaphase that remains arrested until anaphase finishes (Forer and Pickett-Heaps, 2010), also different from most other cell types (Barr and Gruneberg, 2007). Taken together, the few and large chromosomes that are easily distinguishable, the regular bivalent oscillations, the unique univalent movements, and the precocious cleavage furrows, make these cells uniquely useful to study various aspects of cell division, as elaborated on in (Ferraro-Gideon et al., 2013).

To study these spermatocytes, one must have animals to dissect. However, the laboratory populations of these worms often die out and, currently, the literature does not describe a way to rear them indefinitely. In previous attempts, Steinmann and Bresslau (1913) were only able to rear *M. ehrenbergii* to 6 generations while De Beauchamp (1924) reared them only to 24 generations before extinction. Fiore and Ioalè (1973)

reported that they successfully reached the 100th generation; however, they did not fully describe their rearing methods. We set out to keep a permanent laboratory stock of *M. ehrenbergii*.

The apparent population instability is a consequence of the animal's life strategy. *M. ehrenbergii* can produce viviparous offspring and/or diapausing eggs (Figure 3.1; Ferguson and Hayes, 1941), similar to other flatworms in the Typhloplanidae family.

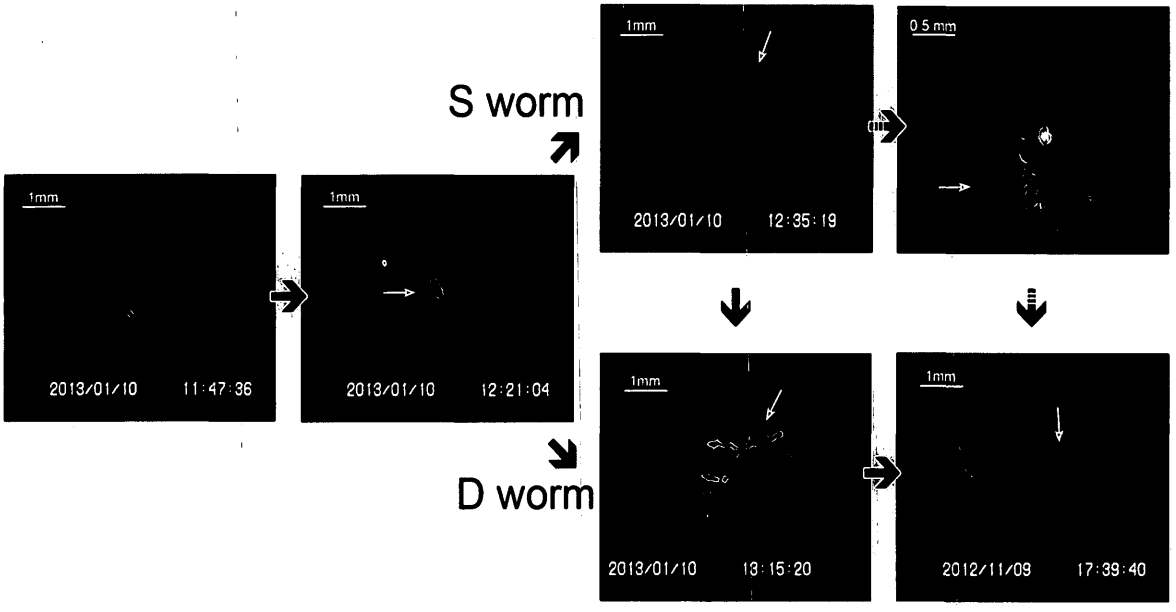

Figure 3.1: Physical appearance of *M. ehrenbergii* at different possible stages of life. The black arrows indicate the progression to a stage in life which usually occurs while the black dashed arrows indicate the progression to a stage in life which only periodically occurs. A newborn animal always first develops testes (white arrows) and then can either follow one of two reproductive patterns: (1) if it is to become an S worm, S eggs (blue arrow) form and ovaries (green arrows) either mature during pregnancy or after S eggs are laid. After ovaries mature, D eggs (red arrows) form. Periodically, ovaries will mature and D eggs will form while S eggs are still in the parental body. (2) if the juvenile is to become a D worm, ovaries mature and only D eggs are formed.

The viviparous eggs, termed subitaneous eggs (S eggs; Fiore and Ioalè, 1973) are thin-shelled, yolk-poor eggs that develop quickly in uteri; the diapausing eggs, termed dormant eggs (D eggs; Fiore and Ioalè, 1973), are thick-shelled, yolk-rich eggs that have a dormancy period before hatching in the water (Ferguson and Hayes, 1941). As a result, the viviparous S eggs cause a rapid population expansion while the diapausing D eggs allow the population to survive unfavourable conditions (Fiore and Ioalè, 1973). The reproductive cycle of these animals can follow either one of two patterns: they can first form S eggs and following the delivery of these eggs produce D eggs (termed S worms), or they only produce D eggs (termed D worms; Fiore and Ioalè, 1973). When only the D eggs are produced, laboratory stocks extinguish until some D eggs hatch, which has unpredictable wait times and sometimes does not even take place (e.g., Heitkamp, 1977). Consequently, in order to maintain animals for cell division experiments, it is important to raise the animals in conditions that allow for the continuous production of S eggs in successive generations.

Previous research into the conditions that influence egg type production have studied the various factors listed in Table A1, in the appendix, though the results were sometimes unclear or inconsistent between studies. In general, genetic propensity, higher temperatures, lower amounts of food, and rearing animals individually, seem to increase the likelihood of *M. ehrenbergii* bearing S eggs (Table A1, appendix; Fiore, 1971; Fiore and Ioalè, 1973; Heitkamp, 1977; Beisner et al., 1997). Fiore (1971) also observed that adult worms (defined as worms carrying S eggs or D eggs) inhibited the production of S

eggs in juveniles, even when they were separated by a net of nylon mesh, suggesting that a chemical substance produced by adult worms inhibits S egg production.

We wanted to maintain a constant supply of *M. ehrenbergii* for cell division experiments so we reared animals under different regimens of food, temperature and photoperiod and determined their influences on production of the different egg types, on the behaviour and growth rates of the worms, and on whether we could obtain living spermatocytes of the proper stage for study. We have been successful with our ultimate methods and are currently on our 45th generation, with more than 1000 animals in our lab at any given time. In this article, we describe in detail the rearing conditions we use to maintain our present stocks of *M. ehrenbergii* and the methods we use to obtain spermatocytes for cell division studies.

3.3 Materials and Methods

3.3.1 Our present methods for rearing *M. ehrenbergii* in the laboratory and making preparations of live spermatocytes

3.3.1.1 Rearing M. ehrenbergii

We started our *M. ehrenbergii* stock by hatching dormant eggs derived from animals collected from Lake Rondeau, Ontario by Hebert and Beaton (1990), from D worms kindly given to us by Dr. Hebert. We store diapausing eggs in water at 4°C until needed, generally more than several months. Oxygen deprivation aids in breaking diapause (J. Kolasa- personal communication) so we hatch D eggs under anaerobic conditions at room temperature by placing them in the dark in sealed, water-filled plastic jars containing algae, so that respiration from the algae removes oxygen from the water.

(To break diapause, Heitkamp (1977) put dormant eggs in mud, which also creates anaerobic conditions.) After several days, the jars are returned to light conditions and some of the water is removed to leave air space in the jar. The babies are fed brine shrimp or *Daphnia* once they appear. Hatched babies may be hard to see for untrained eyes because they are only 1-2mm long. We find it helpful to hold the jars against bright light when looking for them. Alternatively, one can add *Daphnia* to the jar of D eggs once the jars are removed from dark conditions, so when the babies hatch they can consume the *Daphnia* and grow to a size where they are more easily recognizable. (The *Daphnia* will survive in the jars since they eat algae.) Animals hatching from these D eggs constitute the first generation; subsequent generations will continue if the mature worms develop S eggs. We keep the worms in plastic jars (Figure 3.2A) with 5 animals per 200ml of dechlorinated water, at 25°C, and in a 16/8hr light/dark photoperiodic cycle, though from our data (described below) we are not sure that the light cycle matters. To control temperature and light cycles, we place jars containing *M. ehrenbergii* into one of two incubators: one from Environmental Growth Chambers (Model: TC-1) and the other from VWR (Model 2005; Serial #: 05037710). Lighting is provided by LED microlights (Microlites, Toronto) mounted in the incubators and programmed to turn on and off by a timer. We feed *M. ehrenbergii* daily (including weekends) with brine shrimp, although they are typically fed *Daphnia* by others (e.g., Table A1) and they also will consume mosquito or chironomid larvae (Blaustein and Dumont, 1990). However, we found it hard to maintain enough *Daphnia* and mosquito larvae to use as daily food for large

populations of *M. ehrenbergii* so we switched to brine shrimp, which is relatively easy to prepare in large quantities, as will be described in the next section.

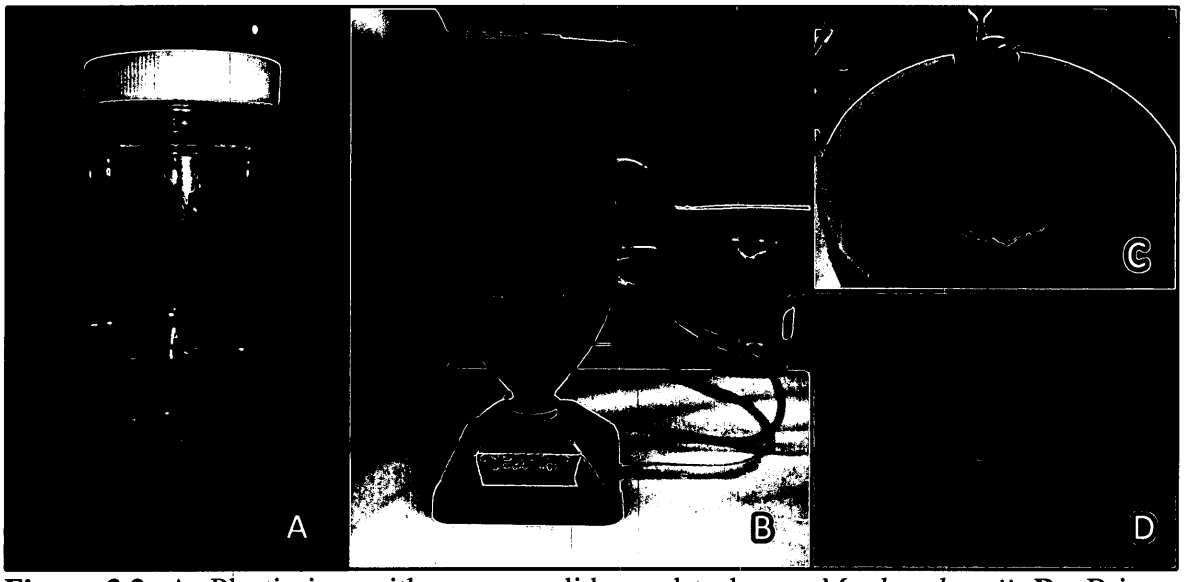

Figure 3.2: **A.** Plastic jars with screw-on lids used to house *M. ehrenbergii.* **B.** Brine shrimp hatchery set-up consisting of a 2L pop bottle inverted onto a platform connected to plastic tubing attached to air supply. **C.** Nylon mesh net filtering brine shrimp from the Oceanic water. **D.** Solution of brine shrimp in dechlorinated water.

There is no set time of the day when the worms are fed and therefore the time between each feeding varies slightly. When the animals die, their bodies disintegrate and their D eggs are released. We collect the D eggs and store them at 4°C in culture water in vials for at least one month before we try to hatch them.

Our rearing conditions were optimized to raise animals with a high likelihood of producing S eggs.Because we have so many animals, not all of them can be accommodated in the incubators. Consequently, we also keep many at room temperature in dechlorinated water in jars with 30 animals/400ml of water or *en masse* in rectangular

tanks; they are fed daily and survive almost as well as animals kept in the more controlled conditions, although not many produce S eggs, so that would not be recommended for maintaining a constant stock. We use animals raised outside the incubators primarily to collect D eggs when the animals die, though we sometimes dissect them for experiments.

3.3.1.2 Hatching brine shrimps and feeding M. ehrenbergii

We obtain brine shrimp eggs from a local aquarium supply store or from Brine Shrimp Direct (Ogden, UT, USA). We hatch brine shrimp from the eggs in a 'hatchery' consisting of a 2L plastic bottomless pop bottle mounted upside down on a platform (Big Al's Aquarium Supplies) which allows plastic tubing to supply air into the bottle (Figure 3.2B). To hatch the brine shrimp eggs, we connect the tubing to an air supply and fill the pop bottle with dechlorinated water and 2 tablespoons of Instant Ocean Sea Salt Mix (Big Al's Aquarium Supplies). The air flow is adjusted to give a constant stream of air bubbles to ensure that the brine shrimp eggs are properly aerated, and the eggs are allowed to deposit on the walls of the vessel. We typically wait 2 days for enough brine shrimp to hatch before straining them through a filter consisting of a fine nylon mesh (Fabricland) and washing them with dechlorinated water to remove the brine (Figure 3.2C). The washed brine shrimp are then put into dechlorinated water and we feed *M. ehrenbergii* from this solution of concentrated brine shrimp (Figure 3.2D) by pipetting a few drops into each jar; this seems to be more than enough food as evident from the full stomachs of the *M. ehrenbergii* and the leftover brine shrimp in the jars. We remove the excess brine shrimp detritus in the jars as necessary: the brine shrimp only survive a few hours in

non-ocean water and *M. ehrenbergii* do not eat the dead brine shrimp afterwards. If the brine shrimp detritus accumulates too much, the jars begin to smell and the animals die; prior to that stage we either remove the brine shrimp or transfer *M. ehrenbergii* to a new jar containing fresh dechlorinated water.

3.3.1.3 Dissection of M. ehrenbergii for preparations of live spermatocytes

We choose individual *M. ehrenbergii* for dissection based on their age and appearance of their testes. We dissect animals as young as when their ovaries first turn white in colour to when they develop D eggs (Figure 3.1). The age at which these events occur depend on their feeding regime and the temperature they are raised at, but in general it takes around 2 weeks for white-coloured ovaries to appear and around 3 weeks for D eggs to form in animals that do not carry S eggs, are fed daily, and are raised at 23-25°C. When S eggs develop, the formation of ovaries and D eggs are delayed by a few days to a week. We generally do not dissect S worms because we need their progeny to propagate the stock. For dissection we select animals (under a dissecting microscope) with testes that are clearish-white in colour and look plump and full, since these testes seem to contain the most dividing spermatocytes (Figure 3.3B). An example of an animal with a 'good' pair of testes, likely to contain dividing spermatocytes, is shown in Figure 3.3B beside an animal with a 'less good' pair of testes, less likely to contain dividing spermatocytes, shown in Figure 3.3A. To dissect the animals, we first rinse the chosen worm 3 times in *Mesostoma* Ringer's solution (61mM NaCl, 2.3mM KCl, 0.7mM $CaCl_2$, and 1.4mM phosphate buffer, pH6.8) by pipetting them into 3 subsequent Petri dishes

filled with Ringer's solution. This is to remove residual culture water. After the rinses, the worm is pipetted into a well on a microscope slide that is formed by vacuum grease squeezed from a syringe. Then, most of the Ringer's solution is sucked out from the animal's surroundings to limit their movement during dissection. Next, we use pulled 10μL needles (VWR International) to remove the testes.

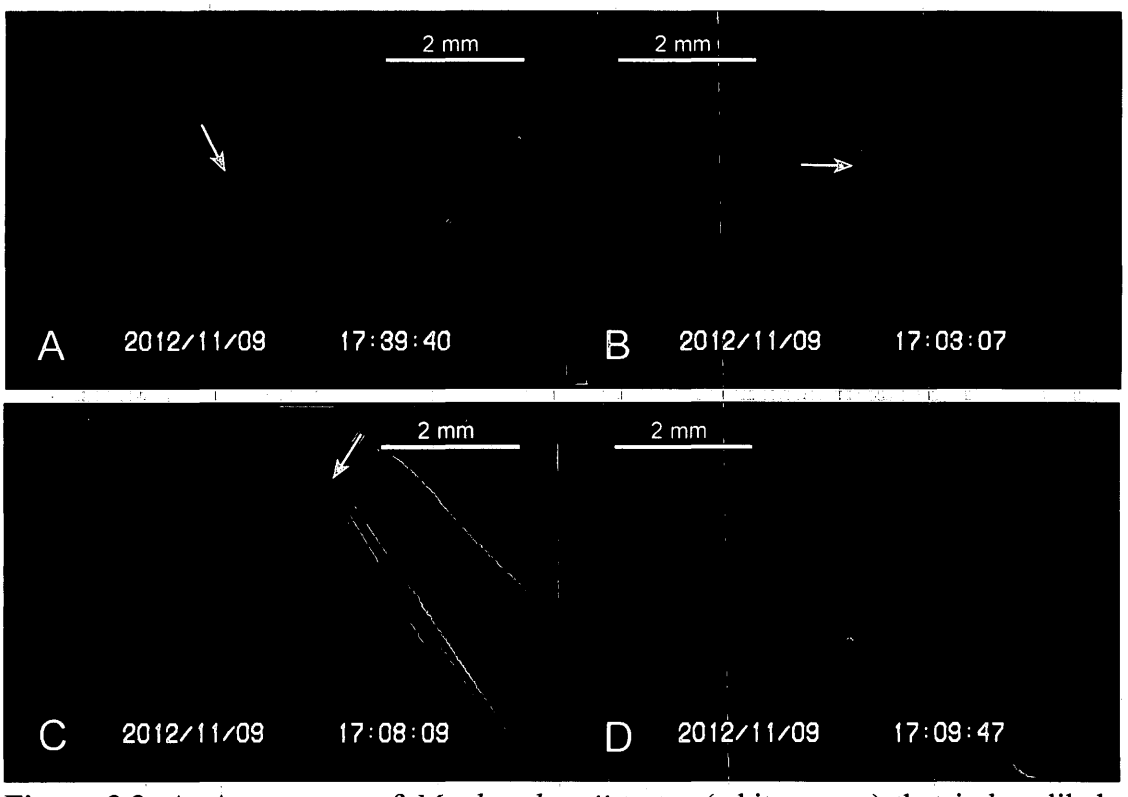

Figure 3.3: **A.** Appearance of *M. ehrenbergii* testes (white arrow) that is less likely to provide dividing spermatocytes. **B.** Appearance of *M. ehrenbergii* testes (white arrow) that is likely to provide dividing spermatocytes. **C.** Needle inserting into *M. ehrenbergii*'s body wall to siphon out the testes during dissection. **D.** Drop of testes and Ringer's solution mixture expelled onto a coverslip.

The wide blunt end of the needle is connected to Tygon tubing with a mouth piece on the other end and cotton wool in between to prevent contamination with mouth fluid, while the sharp end of the needle is inserted into the worm's body where the testes are (Figure 3.3C; Supplemental Video 1). The testes are then siphoned into the needle and expelled onto a coverslip (Figure 3.3D; Supplemental Video 1). After we estimate the size of the droplet of testes in Ringer's solution that was expelled, we add an equal amount of 20mg/mL fibrinogen and spread the mixture so a thin layer is formed on the coverslip. The same amount of 50units/ml thrombin as that of fibrinogen is then mixed into the layer to form a fibrin clot and the whole coverslip is mounted on a perfusion chamber containing *Mesostoma* Ringer's solution. The fibrin clot keeps the cells in place and the perfusion chamber allows us to perfuse the cells with Ringer's solution or drugs. Details of the clot and perfusion chamber procedures are given in Forer and Pickett-Heaps (2005).

3.3.2 Methods and procedures we used to study effects of environmental parameters on production of S and D eggs

To investigate factors that influence the type of egg produced by the worms, we reared *M. ehrenbergii* in conditions that varied in temperature, frequency of feeding, and photoperiod. We placed first generation worms (i.e., hatched from D eggs) into jars that housed 5 animals/400ml dechlorinated water in a 21°C or 17°C incubator, fed each jar either daily or once every three days, and put the jars into either a 16/8 hr light/dark photoperiod or 8/16hr light/dark photoperiod. (Note: these conditions are different from

our current conditions, which are 5 worms/200ml., 25°C and 16/8hr light/dark photoperiod.) Subsequent generations continued only when mature worms developed S eggs and delivered progeny. We removed the newborns from their parental jars usually on the day they were born and separated them into the same conditions that their parents were reared under. However, when the population in certain treatment groups went extinct or was low, we sometimes supplemented those groups with animals from other treatments to carry out the experiment for that generation. We sometimes also modified the treatment conditions in subsequent generations as we attempted to increase the number of S worms, as described in the results section. In a small population of *M. ehrenbergii,* we tested the effects of density by keeping some animals at a density of 15 worms/400ml of dechlorinated water and we tested the effect of isolation by keeping worms at the same original density (5 animals per 400 ml) but keeping them in isolation - i.e., 1 worm/ 80 ml of dechlorinated water. These were raised at 21°C and fed daily.

After the first set of D eggs that was hatched, we hatched a second set of D eggs when the first set was in the 9th generation; these were treated under the same treatment conditions as the animals in the first set, to confirm that the conclusions were not specific to the first isolate. We also hatched a third set of D eggs and reared them under our current optimal conditions to see whether trends still applied under these circumstances.

3.3.3 Data collection and analyses

We observed *M. ehrenbergii* at least twice a week by pipetting all of the animals out of each jar, putting them in a Petri dish, and studying them using a dissecting

microscope. We recorded each animal's reproductive state (i.e. whether we saw S eggs or D eggs), the age when the first S eggs were observed in the worms, and the lengths of two randomly chosen worms per jar (to determine growth rates). Lengths of worms of known ages were measured in a dissection microscope using a ruler placed under the Petri dish. The bodies of the animals stretch as they move (see Supplemental Video 2) so to standardize the lengths, all worms were measured while they were in a slow gliding motion. Jars with worms carrying S eggs were checked daily for the presence of newborns and we recorded the age of the parent worm when their S eggs hatched. We counted the number of newborns per jar and divided by the number of S worms in the jar to obtain the average number of S eggs produced per individual.

We tested for statistically significant differences in the growth and reproductive parameters between different treatment groups using the Student t-test. We performed linear regression analyses on the growth curves of *M. ehrenbergii* using a commercially available program (Slidewrite). We determined the growth rates as the least mean squares best fit slope of the curves of length versus time during the first 15 days after birth, the period before the growth slowed down and reached a plateau.

3.4 Results

Currently, under the conditions in which we feed *M. ehrenbergii* daily and rear them at 25°C as described above, we have raised animals up to their 45^{th} generation. The percentage of worms producing S eggs provides more than enough animals to dissect and the population does not show any signs of nearing extinction. In addition, we find it

easier to obtain spermatocytes when we keep the animals at 25°C and feed daily compared to when we kept them at lower temperatures and fed them less frequently. Though we are not able to quantify this impression, in previous rearing regimens it sometimes took many days of dissection before we found dividing spermatocytes whereas now we can find them in most worms that we dissect.

3.4.1 Factors that influence egg type production

Several factors influenced the egg type that was produced. The particular generation the animals were in, temperature, and feeding regime all affected whether the juveniles were more likely to become S worms and therefore produce S eggs first and then D eggs, or whether the juveniles were more likely to become D worms and therefore produce D eggs only. Photoperiod, on the other hand, did not seem to affect their reproductive behaviour, at least for the conditions we tried.

Some generational trends in the percentage of S worms occurred in all groups of animals, regardless of rearing conditions. Animals hatching from D eggs and their offspring (i.e. 1st and 2nd generation worms respectively) tended to produce S eggs while animals reaching their 4th or 5th generation tended to produce D eggs only, as indicated by the rapid decline in percentage of S worms in generations 4-5 (Figure 3.4 & Figure 3.6). These observations were independent of the environmental factors studied. Keeping these trends in mind, environmental factors that influence egg type production were only evaluated between generations 3-4 and/or after populations stabilized following the rapid decline of S worms (Figure 3.5 & Figure 3.6, for the two batches of hatched eggs).

Photoperiod did not seem to have an effect on the egg type produced. In the first 8 generations, animals reared in the 16/8hr light/dark photoperiod (light condition) and animals reared in the 8/16hr light/dark photoperiod (dark condition) had a similar percentage of worms that produced S eggs. There were no significant differences, and as a result data from these two conditions were combined. In generation 9 however, the percentage of juveniles becoming S worms in the dark condition was significantly higher than in the light condition ($p<0.05$; Figure 3.5), although we later determined that the effect was actually due to a temperature difference: one of the incubators did not properly regulate the set temperature and experimental tests (switching incubator photoperiod programs for the two incubators, switching animals, changing temperatures, etc.) verified that the differences seen were not due to photoperiod but to temperature.

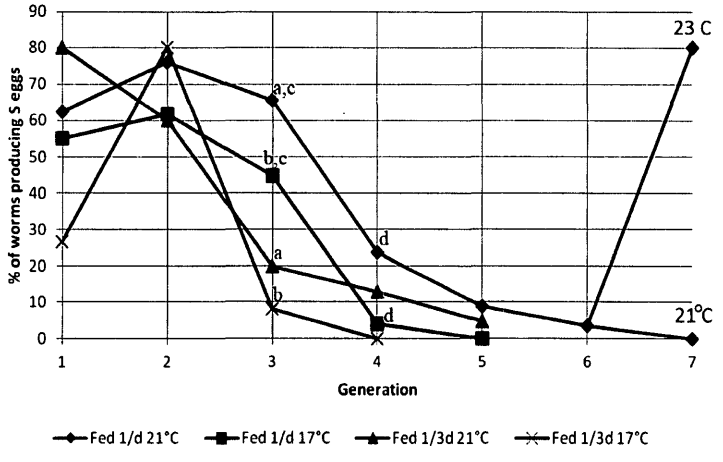

Figure 3.4: The percentage of worms that produced S eggs in different temperature and frequency of feeding conditions from generations 1-7 in the first batch of eggs hatched. Note: data from the two photoperiodic conditions were combined. Significant differences appeared in the third generation between animals fed daily vs. animals fed every three days at 21°C[a] and 17°C[b] and between daily fed animals that were reared at 21°C vs. 17°C[c] ($p<0.05$). Significance differences appeared in the fourth generation between daily fed animals that were reared at 21°C vs. 17°C[d] ($p< 0.05$).

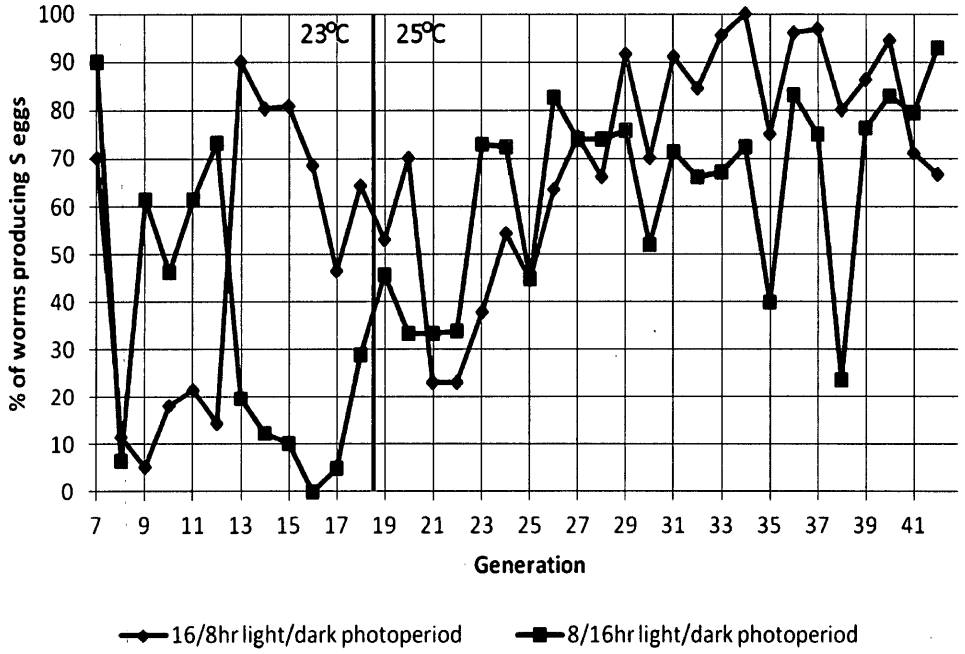

Figure 3.5: The percentage of worms that produced S eggs in different photoperiodic conditions from generations 7-42 in the first batch of eggs hatched. Note the temperature change before generation 19 from 23°C to 25°C. In generation 15 when the % of worms producing S eggs in the 8/16hr light/dark photoperiodic condition decreased to 0%, generation 16 was continued by taking babies born from generation 15 animals raised in the 16/8hr light/dark photoperiod.

Both temperature and frequency of feeding on the other hand, were important parameters in determining which egg type was produced. Well fed worms, given food daily, were more likely to produce S eggs compared to poorly fed worms that were given food only every three days ($p<0.05$; Figure 3.4). Because of the drop in S worms in generation 5, we stopped feeding animals poorly (i.e. every three days) in order to maintain the population. Similarly, temperature influenced egg type production: there was a significantly higher percentage of S worms produced at 21°C than at 17°C ($p<0.05$; Figure 3.4). We obtained further evidence for the importance of temperature when

animals reared at 21°C were switched to 23°C midway through generation 7 (Figure 3.4). In generations 4-5, the percent of S worms began decreasing drastically and the first worms with developed ovaries in the beginning of generation 7 all produced D eggs only.

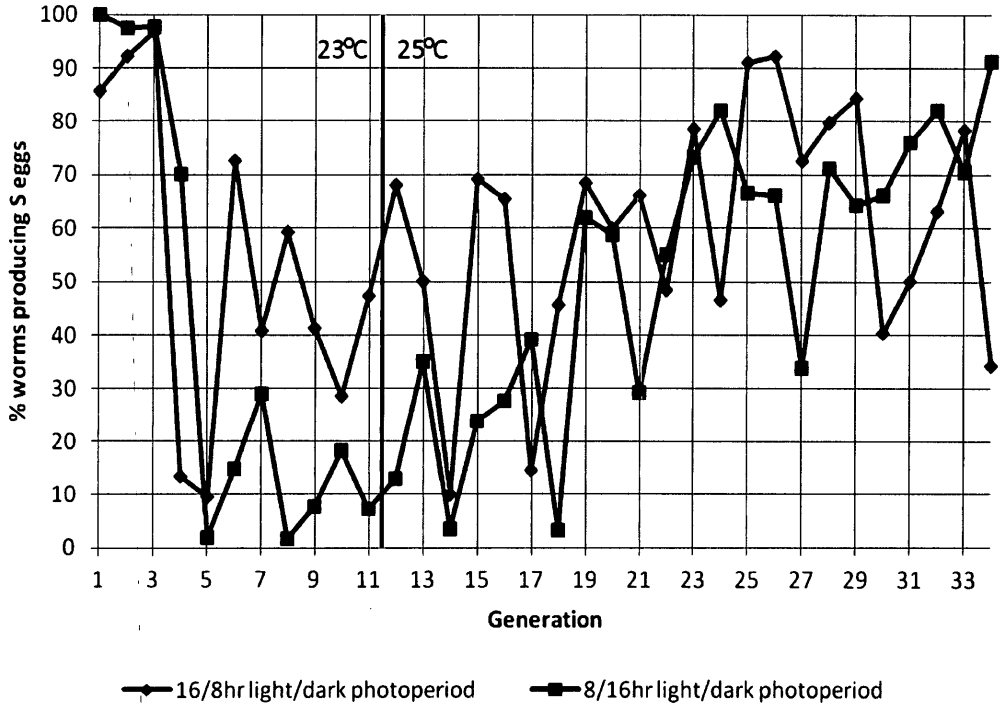

Figure 3.6: The percentage of worms that produced S eggs under different photoperiodic conditions from generations 1-34 in the second batch of hatched eggs. Note the temperature change before generation 12 from 23°C to 25°C.

We immediately switched the temperature to 23°C, however, and of animals maturing later in generation 7, after the increase in temperature to 23°C, 80% became S worms (Figure 3.4). Populations of worms raised at 17°C became extinct in the 4th and 5th generation for poorly and well- fed animals respectively, and attempts to use offspring

from other conditions to supplement the 17°C condition in generations 7 and 8 failed as worms produced D eggs only. As a result, we discontinued rearing animals at 17°C and all animals were reared at 23°C instead. As previously mentioned, there seemed to be a difference between animals raised in the light and dark conditions but we realized in generation 18 (Figure 3.5) that the temperature in the incubator with the higher percent of S worms was at 25°C, even though it was set at 23°C. Consequently, we changed the other incubator to 25°C so that from the middle of generation 18 onward, all animals were reared at 25°C (Figure 3.5). Following the increase to 25°C, the *M. ehrenbergii* populations in both incubators were stabilized with minimal effects of the different photoperiods and with 40-100% of worms in each generation forming S eggs (Figure 3.5). This is a relatively large range; the proportion of juveniles that become S worms cycles from high to low through different generations even when they are being raised in constant temperature and feeding regimens (Figure 3.5).

To confirm that the results we obtained were not unique to the one particular batch of *M. ehrenbergii*, a second batch of D eggs was hatched when the first batch was in the 9th generation. From Figure 3.6, it apparent that the two batches of worms responded similarly in the same environmental conditions, including the high propensity to become S worms in the first two generations, the rapid decline in generations 4-5, and the fluctuations in the later generations after populations were stabilized. A third batch of D eggs was also hatched but raised under our current optimal conditions. This set of animals is currently in their 9th generation and we have not seen any signs of a rapid

decline and recovery, although the percent of S eggs still fluctuate from one generation to another (data not shown).

3.4.2 Effect of temperature and feeding regime on developmental times and subitaneous clutch sizes

We also measured other reproductive parameters such as timing for the start of S egg formation, when the S eggs hatched, and the number of eggs produced by each worm. In all generations prior to and after the incubator temperature regulation problems, there was no significant difference between animals reared under the photoperiods in any of these parameters; thus the data were pooled. When the worms were fed less frequently, within each temperature group the ages at which the worms developed S eggs and when the S eggs were delivered were significantly delayed ($p<0.01$; Table 3.1). Similarly, lower temperatures caused significant delay in these events but the difference was only seen when the worms were fed daily ($p<0.01$; Table 3.1). Worms fed once every three days had similar developmental times at 17°C and 21°C (Table 3.1). In most cases, the worms first developed S eggs and then, following the birth of the S eggs, developed D eggs. On very rare occasions (1-2 worms out of 120 worms in each generation), in the current conditions of feeding daily at 25°C, we observed a second set of S eggs in the same animal following the delivery of the first set, before D eggs appeared. We have also periodically seen worms in which both S eggs and D eggs were present within the same animal (Figure 3.1). The temperature and feeding regimens also influenced the subitaneous clutch sizes per individual. Regardless of the temperature, when the worms

were fed more frequently, significantly higher numbers of S eggs were obtained ($p<0.05$; Figure 3.7).

Table 3.1: The effect of temperature and frequency of feeding on the age at which the first S eggs were observed and on the age of S egg hatching. Data from different generations and photoperiodic conditions were combined. The different letters, ^{a,b,c,d,e}, represent ages that were significantly different between the conditions compared ($p<0.01$).

	Temperature (°C)					
	17°C		21°C		25°C	
Frequency of Feeding	Age which first S eggs are observed (day ± standard error)	Age of S egg hatching (day ± standard error)	Age which first S eggs are observed (day ± standard error)	Age of S egg hatching (day ± standard error)	Age which first S eggs are observed (day ± standard error)	Age of S egg hatching (day ± standard error)
Fed daily	$10.5 \pm 0.24^{a,d}$	$25.2 \pm 0.60^{c,e}$	$8.6 \pm 0.17^{b,d}$	$21.4 \pm 0.22^{c,e}$	7.55 ± 0.35^{d}	18.23 ± 0.13^{e}
Fed once every three days	13.6 ± 0.40^{a}	31.7 ± 1.00^{c}	13.6 ± 0.38^{b}	30.8 ± 0.73^{c}	n/a	

Worms fed daily produced on average 5 more S eggs than worms fed once every three days (Figure 3.7). Moreover, worms reared at lower temperatures tended to produce more S eggs, although this effect was only seen when the worms were well fed ($p<0.05$; Figure 3.7). Worms reared at 17°C produced 3 more S eggs than worms reared at 21°C which produced 1 more S egg than worms reared at 25°C (Figure 3.7). We did not have enough data per generation to accurately compare the effects of different rearing densities on the

propensity to become S worms, but because the clutch sizes were similar between all generations, we were able to combine generational data in order to compare the effects of density on the number of S eggs delivered per individual (Figure 3.8).

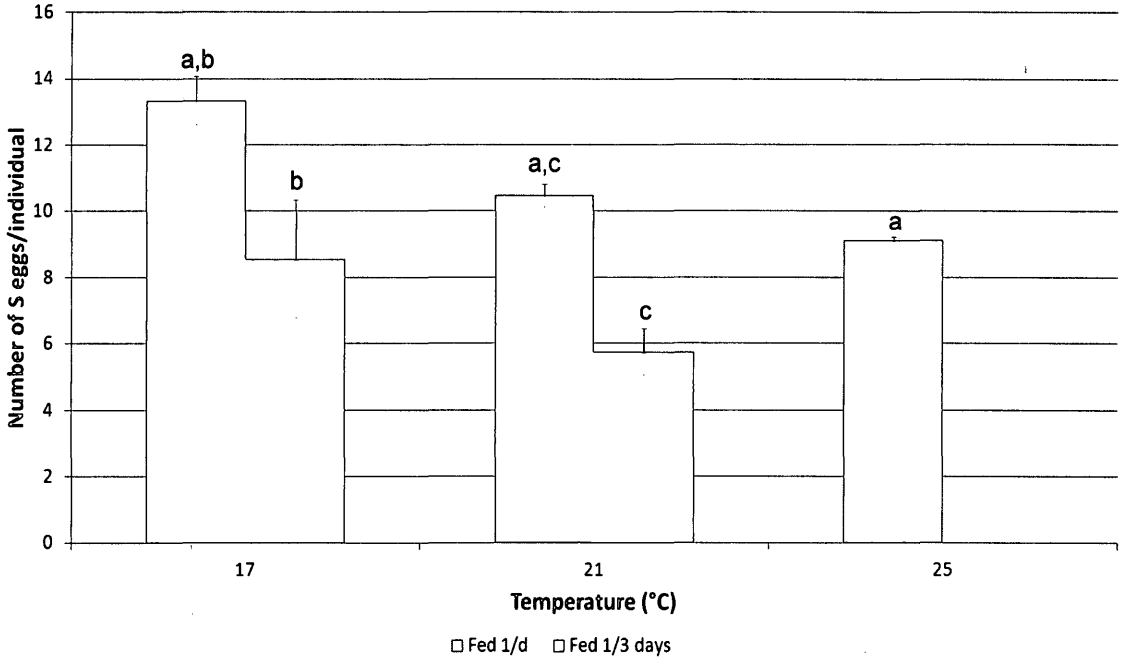

Figure 3.7: The effect of temperature and frequency of feeding on subitaneous clutch size. Note: data from different generations and photoperiodic conditions were combined. [a]Significant difference between daily fed animals at 17°C vs. 21°C vs. 25°C ($p<0.05$). [b,c]Significant difference between animals fed daily vs. once every three days ($p<0.05$).

From Figure 3.8, it is evident that the clutch sizes increased as the number of worms in the jar decreased; the greatest number of S eggs produced per individual was when the worms were isolated ($p<0.05$; Figure 3.8). As described in the introduction, these hermaphroditic worms are capable of self-fertilization when isolated, and they can produce both S eggs and D eggs by self-fertilization.

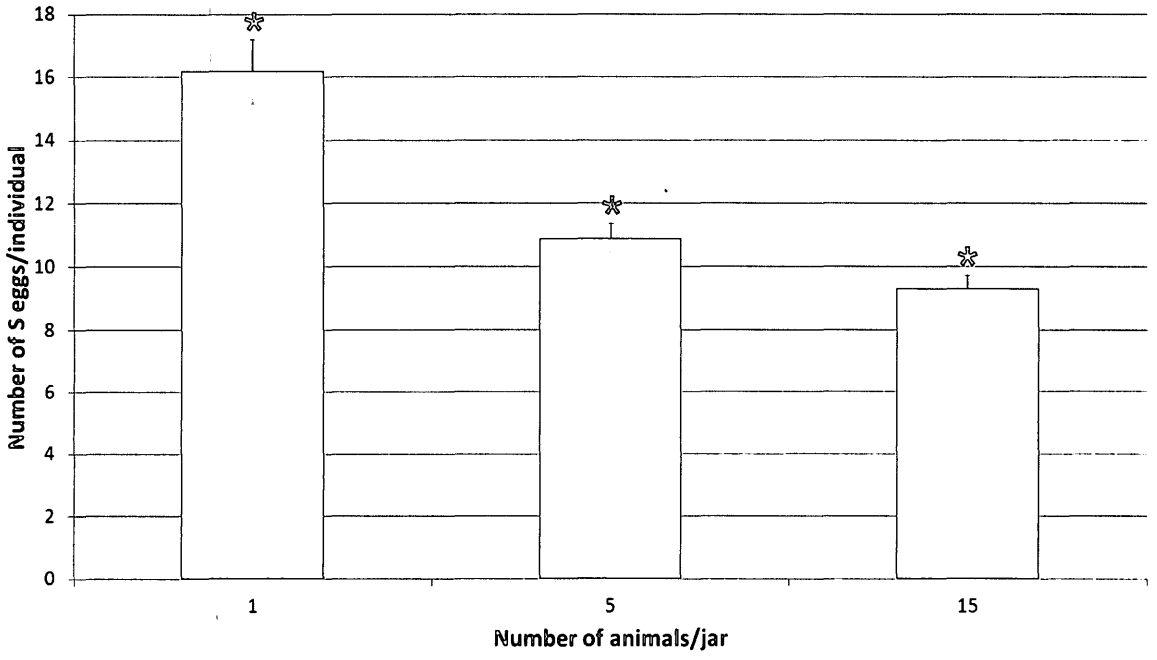

Figure 3.8: The effect of the number of *M. ehrenbergii* reared together per jar on subitaneous clutch size. Note: data from different generations and photoperiodic conditions were combined. *Significant difference in clutch sizes between 1 animal vs. 5 animals vs. 15 animals reared per jar ($p<0.05$).

3.4.3 Effect of temperature and feeding regime on *M. ehrenbergii* growth curves

M. ehrenbergii lengths were measured in the various conditions to determine their growth rates. There were no significant differences in length between the different generations and between the different photoperiodic treatments so those data were combined to generate the growth curves (Figure 3.9). In all treatments, the animals initially showed a linear increase in length with age (r^2 value from linear regression >0.90) and eventually reached a plateau, or final adult length (Figure 3.9). The growth rates ± standard errors are given in Table 3.2 together with the final adult lengths ±

standard error. At both 17°C and 21°C, growth rates of individuals fed daily were significantly higher than those of individuals fed once every three days, by about a factor of 2 ($p<0.01$). With the same frequency of feeding, *M. ehrenbergii* growth rates were similar at 17°C, 21°C, and 25°C (Table 3.2). Similarly, the final adult lengths of the worms that were fed daily were significantly greater than those of worms that were fed once every three days but there were no length differences between worms raised at the three temperatures ($p<0.01$; Table 3.2). The maximum length of the worms we observed was 12 mm.

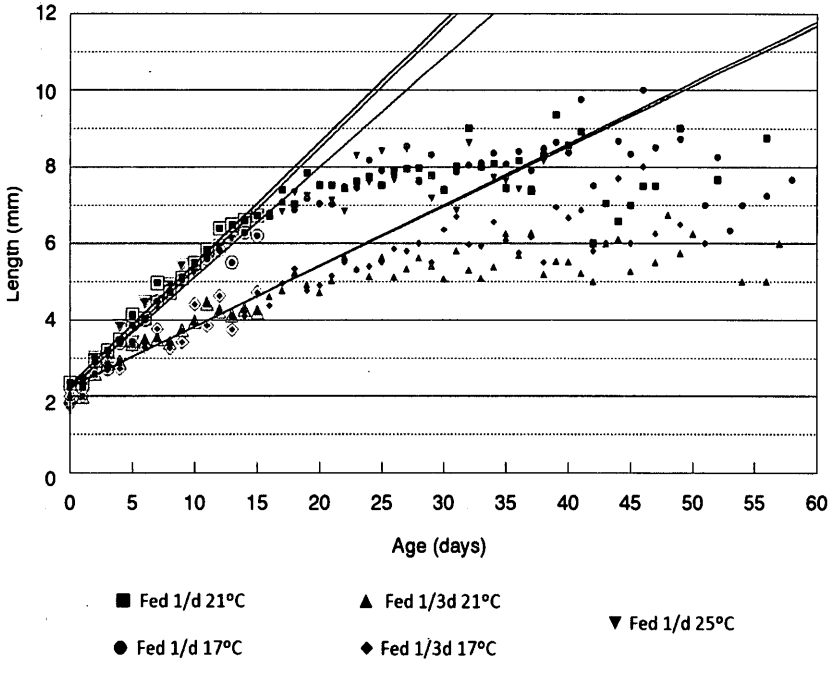

Figure 3.9: The effect of temperature and frequency of feeding on *M. ehrenbergii* growth curves. A linear regression was fit to the lengths corresponding to the first 15 days after birth ($r^2 > 0.9$). Note: data from different generations and photoperiodic conditions were combined. Each data point represents the average length of all animals measured at that condition and age ($n \geq 24$ for each condition). There is a significant difference in linear slopes between animals fed daily vs. animals fed once every three days at both temperatures ($p<0.01$).

Table 3.2: The effects of temperature and frequency of feeding on *M. ehrenbergii* growth rates (±standard error) and on final adult lengths reached (±standard error). Data from different generations and photoperiodic conditions were combined. The letters [a,b] represent significantly different growth rates between daily fed animals and animals fed once every three days ($p<0.01$). The letters [c,d] represent significantly different final adult lengths between daily fed animals and animals fed once every three days ($p<0.01$).

	Temperature (°C)					
	21°C		17 °C		25 °C	
Frequency of Feeding	Growth rate (mm/ day)	Final Adult Length (± standard error) (mm)	Growth rate (mm/ day)	Final Adult Length (± standard error) (mm)	Growth rate (mm/ day)	Final Adult Length (± standard error) (mm)
Fed daily	0.31±0.011[a]	8.1±0.13[c]	0.29±0.014[b]	8.2±0.14[d]	0.32±0.017	7.9±0.40
Fed once every three days	0.16 ±0.013[a]	5.6±0.10[c]	0.16±0.019[b]	6.2±0.1[d]	n/a	

3.4.3.1 Observations of M. ehrenbergii behaviour

Lastly, we would like to provide a general note on *M. ehrenbergii* behaviour. These worms are aggressive predators that secrete a web-like substance to trap their prey (Wrona and Koopowitz, 1998). With brine shrimp, they trap many at once, creating a mini ball of brine shrimp which are brought individually to their mouths to consume (Supplemental Video 2). They typically sink to the bottom of the jar or tank while eating.

We keep large numbers in a rectangular tank, where we noticed that the colonies of *M. ehrenbergii* form an organized net with the web-like sticky substance they produce and tend to aggregate at one corner or side of the tank, or on the surface; they rarely are found swimming in the middle of the tank (Figure 3.10).

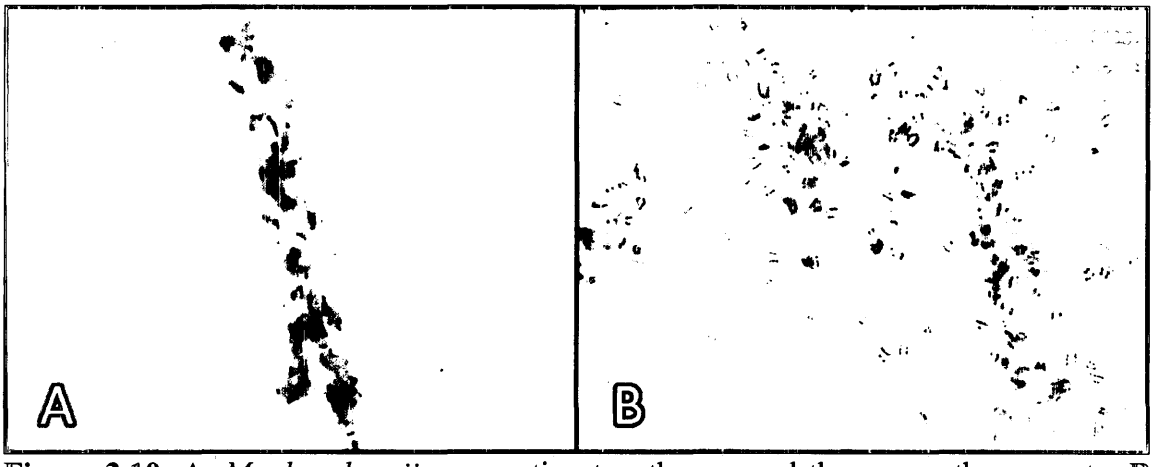

Figure 3.10: **A**. *M. ehrenbergii* aggregating together around the mucus they secrete. **B**. *M. ehrenbergii* spreading only on one side of the tank.

The location they aggregate in is not consistent; it varies from day to day and even during a day, and while the currents caused by daily feeding disrupt the integrity of the web, the communities are always reformed by the next day. When brine shrimp are put into the aquarium, they get caught in the web and the worms slowly glide to their prey and consume them on the web. They may also display aggressive behaviour to each other when many are crowded together because we have noticed that some animals from the aquarium seen in a dissecting microscope appear to be missing pieces of their body wall (Figure 3.11).

M. ehrenbergii deliver S eggs through their body wall and the newborns are released from the same position they are in inside the parent (Supplemental Video 3). The parental worm seems to move more actively during release of S eggs and we have not seen any damage or slit in the body wall. On the other hand, D eggs seem to be released only when individual *M. ehrenbergii* die and their body wall disintegrates, leaving behind the D eggs at the bottom of the jar. In quite a few occasions, we observed that when one worm in a jar dies, all of those in the same jar die. The other animals in the jar can be rescued only if we separate them in time from the dying *M. ehrenbergii*.

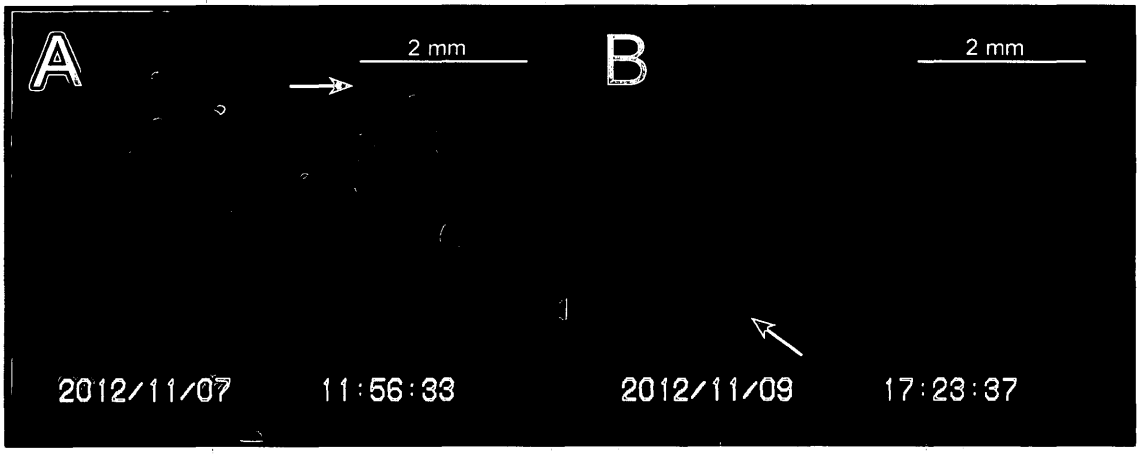

Figure 3.11: A. *M. ehrenbergii* with missing head (arrow). **B.** *M. ehrenbergii* with missing tail (arrow).

3.5 Discussion

We have described the methods we use to get sufficient stock of animals to dissect, and we described how to dissect the animals to obtain spermatocytes. We present

this information to help anyone wishing to study this unique meiotic system, and we are happy to provide animals to anyone who wishes to use them.

In learning how to rear *M. ehrenbergii* for our cell biological experiments we studied some of the parameters that influenced our choices of growth conditions. We now discuss how our observations compare with related observations in the literature.

The *M. ehrenbergii* stock we raised from D eggs usually either produced S eggs and following their delivery produced D eggs, or produced D eggs directly. However, we have periodically seen worms carrying both egg types, a situation never seen by Bresslau (1903), as cited by Fiore and Iaolè (1973). When we have seen this, the S eggs were liberated as babies, unlike the situations described by Fiore and Iaolè (1973) who reported that sometimes the D eggs prevented the release of the S eggs, which degenerated in uteri. Moreover, unlike *M. lingua* which may form S eggs again once D eggs are formed, neither we nor anyone in the literature that we are aware of has observed this in *M. ehrenbergii.* We have, however, seen animals produce a second batch of S eggs following the delivery of the first batch, but, similar to Fiore and Iaolè (1973), this occurs in only a small fraction of the animals that are reared in our current conditions.

The determinants for which egg type these worms produce seem to be a combination of endogenous and environmental factors. Similar to two previous studies, first generation worms hatching from D eggs had a high propensity to develop S eggs in a wide range of conditions (Heitkamp 1977; Fiore and Iaolè 1973) and in our experiments, this propensity extended to their offspring in the second generation as well. Beisner et al.

(1997) on the other hand, reported that *M. ehrenbergii* originating from D eggs were more likely to produce S eggs at lower temperatures of 18°C and produced D eggs only if given low amounts of food. A strong tendency of D egg-derived worms to become S worms regardless of conditions may be advantageous when the worms are trying to establish their populations in early spring.

Another generation-dependent observation we made was a sharp decline in percentage of S worms in generations 4 or 5, similar to the studies by Steinmann and Bresslau (1913) where they could not maintain stocks for more than 6 generations. As cited by Fiore and Iaolè (1973), Steinmann and Bresslau (1913) suggested that this corresponded to the natural time frame from when the worms would hatch from D eggs in the spring to the extinction of the population in the autumn and thus they concluded that endogenous factors which caused the worms to overwinter after a certain number of generations were mainly responsible for egg type production. However, this conclusion may perhaps only apply when the animals are raised under suboptimal conditions. In the third batch of eggs we hatched and raised under our current optimized conditions of 25°C and fed daily, we have not yet seen the sharp decline and the worms are currently in their 9^{th} generation.

Temperature and frequency of feeding influenced the egg type produced in animals from the 3rd generation onwards, although photoperiod did not, despite being the main cue for diapause induction in most aquatic invertebrates (Alekseev, 2006). This is consistent with Heitkamp's (1972) study on *M. lingua* which showed that length of day did not influence the production of S eggs. Higher temperatures and feeding worms daily,

on the other hand, significantly increased the proportion of S worms. Previous studies found similar effects of temperature where animals hatching from S eggs only became S worms in high frequencies when kept at temperatures above 20°C (De Beauchamp, 1926; Heitkamp, 1977; Beisner et al., 1997). This response to temperature may be advantageous since S-egg derived worms are born in the summer and cooler temperatures may signal the arrival of winter. However, opposite results were reported with respect to the feeding regime. Fiore and Iaolè (1973) and Beisner et al. (1997), studying *M. ehrenbergii,* and Heitkamp (1972), studying *M. lingua,* found that poorly fed worms were more likely to produce S eggs. The discrepancy in results concerning the worms' response to lower food levels may suggest that our frequency of feeding once every three days could be too 'low' since the Beisner et al. (1997) low food level regime is 1 Daphnia per day (the feeding regime Fiore and Iaolè (1973) used was not stated). Alternatively, it may be that *M. ehrenbergii* distinguishes the difference in food quality between the brine shrimp we used as food supply and the *Daphnia* which the other authors used as food supply.

Lastly, in our stable population of worms there is a wide fluctuation in the proportion of animals becoming S worms, ranging from 40-100%, even though they all are raised at consistent conditions of temperature and photoperiod (Figure 3.5 & Figure 3.6). Similar observations were reported by Fiore and Iaolè (1973); they raised worms for 100 generations and suggested that the variation may be due either to environmental conditions that are not controlled or to endogenous factors. Because of the regularity of this cycling between high and low proportions of S worms and the observation that both

we and another group have the same findings, we think it is possible that intrinsic factors play a role, although as Fiore and Iaolè pointed out, this is not advantageous. Having endogenous factors influence egg type production would decrease *M. ehrenbergii*'s ability to respond to different environments (Fiore and Iaolè, 1973).

M. ehrenbergii developmental times were dependent on temperature (Table 3.1), as expected for aquatic ectotherms whose body temperatures conform to its surroundings. The development times we observed seem comparable to the times reported in most of the literature, in most of which the animals were reared at slightly different temperatures (Table 3.3). However, because we only observed the worms for the presence of S eggs at most three times a week, the observed age for the first appearance of S eggs will be slightly higher than the actual age. The frequency of feeding also affected development times and worms that were fed once every three days developed significantly later than worms fed daily (Table 3.1). Fiore and Iaolè (1973) made similar observations; the delay most likely is due to the lack of energy and resources.

Table 3.3: The age at which first S eggs were observed and age of S egg hatching in *M. ehrenbergii* reported in literature. The temperatures the animals were reared at are also included. Other rearing conditions can be found in Table A1 in the appendix.

Study	**Age which first S eggs were observed (days)**	**Age of S egg hatching (days)**	**Temperature (°C)**
Beisner et al. 1997	n/a	16-17 23-24	Temp: 23°C Temp: 18°C
Fiore 1971	n/a	17	Temp: 23°C
Fiore and Iaolè 1973	5-6	17 28	Temp 23°C Temp: 17°C
Gremigni and Domenici 1977	5	14-15	Temp: 23°C

We also studied the number of S eggs produced in each clutch. Animals that were well fed and reared at lower temperatures produced the highest number of S eggs (Figure 3.7). *M. ehrenbergii* that were fed once per day at 17°C produced on average 3 more S eggs (13.3 S eggs/ individual) than those that were fed once per day at 21°C (10.5 S eggs/ individual; Figure 3.7). Beisner et al. (1997) also found a difference of 6 more S eggs per animal reared at 18°C compared to 24°C. As proposed by Beisner et al. (1997), the effects of temperature may be a result of the faster developmental times at 21°C compared to 17°C (Table 3.1) so that additional eggs do not have as much time to form. In addition, smaller clutch sizes were also observed when the worms were fed less. This is likely because there are fewer resources that can be allocated to form the S eggs. This conjecture is supported by the observation that animals that were fed every three days take longer to develop and do not reach the same length as ones that were fed daily (Table 3.1 and Table 3.2). We also found that one animal per jar produced more S eggs compared to 5 animals per jar which in turn produced more S eggs compared to 15 animals per jar (Figure 3.8). It may be reasonable to suppose that this could be due to the same chemical that is produced by worms that inhibit S egg production as discussed by Fiore (1971). With 15 animals per jar, there may be a higher concentration of the chemical that lowers the number of S eggs produced while isolated worms may not be affected by the chemical produced by themselves, as proposed by Fiore and Iaolè (1973) to explain why the chemical did not inhibit isolated worms from becoming S worms. It is unlikely that the reduction in number of S eggs produced by worms reared in larger

numbers is due to the lower levels of food each individual receives because in all three densities excess brine shrimp was present in the jars after feeding.

M. ehrenbergii growth rates were similar between different temperatures but were significantly slower when the worms were fed less (Figure 3.9; Table 3.2). Likewise, animals reached a similar maximum body length irrespective of temperature but were smaller when they were fed once every three days (Figure 3.9; Table 3.2). Beisner et al. (1997) found a similar effect of food level on growth rate and found that the final body sizes reached by *M. ehrenbergii* were the same at different temperatures. In contrast to our observation that the growth rates were also similar at both temperatures, however, they found that growth was slower at lower temperatures, a relationship that is found in other aquatic invertebrates as well (Angilletta et al. 2004). The final adult lengths of 8 mm reached by daily fed animals at both temperatures (Table 3.2) were slightly smaller than the usual 10-15 mm reported in literature although Husted and Ruebush (1940) and Ferguson and Hayes (1941) observed that North American species reach the size of only 5-7 mm (Table 3.4). Beisner et al. (1997) and Elvin and Koopowitz (1994) however, obtained their stock from Alberta and had worms attain a size between 10-15 mm (Table 3.4). Our stock came from Lake Rondeau in Ontario. The longest length we observed was approximately 12 mm while the reported maximum length of *M. ehrenbergii* in Canada is 15 mm (Elvin and Koopowitz 1994). The smaller size may have been due to the differences in the quality of food that was fed to the animals: *M. ehrenbergii* were fed with brine shrimp in our study but were fed *Daphnia* in the studies which reported the lengths (Table A1).

In conclusion, it seems apparent that these worms have an intrinsic system that causes them to produce S eggs in earlier generations and produce D eggs closer to the 4th or 5th generation where, in nature, they would encounter autumn. However, this system can be influenced by environmental factors and we found that higher temperatures and daily fed worms were more likely to produce S worms. However, lower temperatures produce the largest numbers of S eggs so there is a trade-off between raising more S worms that carry fewer S eggs or raising fewer S worms that carry more S eggs.

Table 3.4: The reported lengths of *M. ehrenbergii*. Note that some studies distinguished the difference between the lengths found at different locations.

Study	**Reported Lengths (mm)**	**Location**
Beisner et al. 1997	10-12	Alberta, Canada
Bresslau 1903	15	n/a
Elvin and Koopowitz 1994	15	Alberta, Canada
Ferguson and Hayes 1941	5 15	America Europe
Husted and Ruebush 1940	7 15	North America Europe
Stout 1958	7-8	New Zealand
Wrona and Koopowitz 1998	15	Alberta, Canada

Alternatively, if one wishes for more animals, one might grow the worms at 25°C and once they develop S eggs, transfer them to 17°C. We have not tried this, however, since with 8 S eggs per worm and 40-80% of the worms producing S eggs, we have more than enough animals to dissect for our experiments.

M. ehrenbergii are both easy to raise and to obtain spermatocytes from. This is a unique system that we believe will provide insight into the forces that cause chromosome movements, insight into control of cleavage furrow formation, and insight into other aspects of cell division in general.

3.6 Acknowledgements

We would like to thank Dr. Paul Hebert for kindly providing us with dormant eggs to start our *M. ehrenbergii* cultures. This work was supported by grants from the Natural Science and Engineering Research Council of Canada to AF.

3.7 References

Alekseev VR, Hwang JS, Tseng MH. Diapause in aquatic invertebrates: what's known and what's next in research and medical application? J Mar Sci Technol 2006;14:269-286.

Angilletta MJ, Steury TD, Sears MW. Temperature, growth rate, and body size in ectotherms: fitting pieces of a life-history puzzle. Integr Comp Biol 2004;44:498-509.

Barr FA, Gruneberg U. Cytokinesis: placing and making the final cut. Cell 2007;131:847-860.

Beisner BE, McCauley E, Wrona FJ. Predator-prey instability: individual-level mechanisms for population-level results. Funct Ecol 1997;11:112-120.

Blaustein L, Dumont HJ. Typhloplanid flatworms (*Mesostoma* and related genera) mechanisms of predation and evidence that they structure aquatic invertebrate communities. Hydrobiologia 1990;198:61-77.

Bresslau E. Die sommer und wintereier der Rhabdocoelen sussen wassers und ihre biologische bedeutung. Verh Dt Zool Ges 1903 ;1903:126-139.

De Beauchamp P. Obtention de 23 generations d'oeufs immediats chez *Mesostoma ehrenbergii* (Focke). Cr Séanc Soc Biol 1926;95:1435-1436.

Elvin M, Koopowitz H. Neuroanatomy of the rhabdocoel flatworm *Mesostoma ehrenbergii* (Focke, 1836). I. neuronal diversity in the brain. J Comp Neuro 1994;343:319-331.

Ferraro-Gideon J, Hoang C, Forer A. *Mesostoma ehrenbergii* spermatocytes have uniquefeatures and advantages: reasons why you should rear *Mesostoma* in your laboratory. Cell Biol Int 2013. Accepted.

Fiore L. A mechanism for self-inhibition of population growth in the flatworm *Mesostoma ehrenbergii* (Focke). Oecologia 1971;7:356-360.

Fiore L, Ioalè P. Regulation of the production of subitaneous and dormant eggs in theTurbellarian *Mesostoma ehrenbergii* (Focke). Monit Zool Ital 1973;7:203-224.

Forer A and Pickett-Heaps J. Fibrin clots keep non-adhering living cells in place on glass for perfusion or fixation. Cell Biol Int 2005;29:721-730.

Forer A, Pickett-Heaps J. Precocious (pre-anaphase) cleavage furrows in *Mesostoma* spermatocytes. Eur J Cell Biol 2010;89:607-618.

Ferguson FF, Hayes WJ. A synopsis of the genus *Mesostoma ehrenberg* 1835. J Elisha Mitchell Sci Soc 1941;57:1-52.

Fuge H. Oscillatory movements of bipolar-oriented bivalent kinetochores and spindle forces in male meiosis of *Mesostoma ehrenbergii*. Eur J Cell Biol 1987;44:294-298.

Gremigni V, Domenici L. Fine-structure of specialized cells involved in nutrient uptake in subitaneous eggs of *Mesostoma ehrenbergii*. J Submicrosc Cytol Pathol 1977;8:253-254.

Hebert PDN, Beaton MJ. Breeding systems and genome size of the rhabdocoel turbellarian *Mesostoma ehrenbergii.* Genome 1990;33:719-724.

Heitkamp U. Zur fortpflanzungsbiologie von *Mesostoma ehrenbergii* (Focke, 1836)(Turbellaria). Hydrobiologia 1977;55:21-31.

Heitkamp U. Die Mechanismen der Subitan- und Daurereibildung bei *Mesostoma lingua* (Abilgaard, 1798) (Turbellaria, Neorhabdocoela). Z Morph Tiere 1972;71:m203-389.

Husted L, Ruebush TK. A comparative cytological and morphological study of *Mesostoma ehrenbergii ehrenbergii* and *Mesostoma ehrenbergii wardii*. J Morphol 1940;67:387-410.

Oakley HA. Meiosis in *Mesostoma ehrenbergii ehrenbergii* (Turbellaria, Rhabdocoela) III. univalent chromosome segregation during the first meiotic division in spermatocytes. Chromosoma 1985;91:95-100.

Oakley HA, Jones GH. Meiosis in *Mesostoma ehrenbergii ehrenbergii* (Turbellaria, Rhabdocoela) 1. chromosome pairing, synaptonemal complexes and chiasma localisation in spermatogenesis. Chromosoma 1982;85: 311-322.

Skibbens RV, Skeen VP, Salmon ED. Directional instability of kinetochore motility during chromosome congression and segregation in mitotic newt lung cells: a push-pull mechanism. J Cell Biol 1993;122:859-875.

Steinmann P, Bresslau E. Die Strudelwürmer (Turbellaria). Monographien eiecheimischer Tiere. Bd. 5. Leipzig: Klinkhardt;1913.

Stout VM. A note on the occurrence in New Zealand of *Mesostoma ehrenbergii* (Focke) Schmidt, 1848 (Turbellaria, Rhabdocoela). Transactions of the Royal Society of New Zealand 1953; 81:295-301.

Wrona FJ, Koopowitz H. Behaviour of the rhabdocoel flatworm *Mesostoma ehrenbergii* in prey capture and feeding. Hydrobiologia 1998;383:35-40.

CHAPTER 4

TITLE: Meiosis-I in *Mesostoma ehrenbergii* spermatocytes includes distance segregation and inter-polar movements of univalents, and vigorous oscillations of bivalents

AUTHORS: Jessica Ferraro-Gideon[1], Carina Hoang [1] and Arthur Forer[1]

AUTHORS AFFILIATIONS: [1]Department of Biology, York University, Toronto, ON M3J 1P3, Canada

CORRESPONDENCE INFORMATION:
Arthur Forer
Biology Department, York University
4700 Keele St.
Toronto, ON
M3J1P3
(905) 736-2100 ext 44643
aforer@yorku.ca

KEYWORDS: Chromosome oscillations, Non-Random Segregation, Distance Segregation, Precocious cleavage furrow

WORD COUNT (not including references): 7050

DATE OF ACCEPTANCE: June 26 17, 2013 (Protoplasma)

4.1 Abstract

In this article, we describe meiosis-I in spermatocytes of *Mesostoma ehrenbergii*. We have expanded on the original observations of Oakley (1983, 1985) and Fuge (1987, 1989, 1991), the first to describe these cells, with the aim of laying the framework for experimental work on their various unique behaviours which challenge our understanding of cell division. These cells contain three bivalents and four (two pairs) univalent chromosomes. Bivalent kinetochores oscillate vigorously and regularly, throughout prometaphase, for up to several hours, until the start of anaphase. The onset of anaphase cannot be predicted and most often begins in the middle of the kinetochore oscillation cycle. Precocious cleavage furrows form at the start of prometaphase, ingress and then remain arrested until the end of anaphase. The four univalents do not pair, yet by anaphase they have segregated so there is one of each kind at each pole, an example of "distance segregation" (Hughes-Schrader, 1969). Until proper segregation is achieved, univalents move between spindle poles up to 7 times in an individual cell; they move with velocities averaging 9 μm/min, which is faster than the oscillatory motions of the bivalent kinetochores (5-6 μm/min), and much faster than the anaphase movements of the segregating half-bivalents (1 μm/min). Bipolar bivalents periodically reoriented, most often resulting in the partner kinetochores exchanging poles. We suggest that the large numbers of inter-polar movements of univalents, and the reorientations that lead to partners exchanging poles, might be because there is non-random segregation of chromosomes, as in other cell types.

4.2 Introduction

We have studied meiosis-I in *Mesostoma ehrenbergii* spermatocytes because several unique aspects of this division raise important questions that challenge our understanding of cell division. One of these aspects is *distance segregation*, the proper segregation of chromosomes that are not conjoined. The usual picture of meiosis is straightforward: chromosome partners are attached at chiasmata, they orient to opposite poles (bipolar, syntelic orientation), and once the partners disjoin the spindle fibres attached to each pole cause the partners to move to opposite poles. Chromosome partners are not attached to each other, however, in many cell types (Camenzind and Nicklas, 1968; Hughes-Schrader, 1969; Forer and Koch, 1973; Oakley, 1983; Oakley, 1985) yet their segregation nonetheless is accurate. In crane-fly spermatocytes, for example, the X and Y chromosomes are not attached, they move separately on the spindle during prometaphase, and when they reach the equator at metaphase both chromosomes have spindle fibre attachments to both poles (amphitelic orientation). As the two sex chromosomes move to opposite poles in anaphase (after the completion of autosomal anaphase) the spindle fibres to both poles persist: as each sex chromosome moves poleward during anaphase, one of its attached spindle fibres shortens and the other elongates (e.g., Forer, Ferraro-Gideon and Berns, 2013). Although it is not understood why sex-chromosome anaphase is temporally separated from autosomal anaphase in crane fly spermatocytes, the major puzzle of distance segregation is how each sex chromosome can segregate to its respective spindle pole despite them not having been paired. It is unclear what mechanism is utilized by the sex chromosomes to ensure that

movements are in opposite directions to opposite spindle poles, especially since the two sex chromosomes influence each other's movements throughout anaphase, as described by Forer and Koch, 1973 and Forer et al., 2013. This example, one of many, raises the issue of how movements of not-attached chromosomes are coordinated and how "communication" can occur between chromosomes that are not attached. An equally challenging univalent segregation pattern occurs in *Mesostoma* spermatocytes, as previously described by Oakley (1983, 1985), whose conclusions we now summarise.

Mesostoma spermatocytes have 3 autosomal bivalents and 4 univalents. The univalents appear as two pairs, two of each kind distinguishable by shape and position of their kinetochores (Husted and Ruebush, 1940). At the start of spindle formation, the univalents move to the two spindle poles as the bivalents become bipolarly oriented. The univalents remain at the spindle poles throughout prometaphase and metaphase but sometimes they move between the poles. As deduced by the chromosome complement in meiosis-II, at anaphase each pole is associated with one of each kind of univalent. Early in division, however, there often is "mis-segregation" of univalents: three at one pole and one at the other, or two of the same kind at each pole. The movements between poles thus seem to correct the mis-segregation and allow proper segregation of the univalents. Oakley speculated that not only do the univalents assort one of each kind at each pole, but they do so non-randomly (e.g., female derived univalents at one pole and male-derived univalents at the other), the kind of non-random segregation that is well documented in other cells [e.g., *Gryllotalpa hexadactyla* (mole crickets) (Camenzind and Nicklas, 1968); *Sciara* (Gerbi, 1986) and mealy-bugs (Nur, 1982; Schrader, 1921)].

Oakley based this suggestion on two observations: (1) that univalents seem to move between poles more often than necessary in order to achieve one of each kind at each pole, and (2) that in some cells univalents of the same kind changed poles after proper segregation had been achieved. In this article we describe inter-polar movements of univalents throughout prometaphase as they move from one spindle pole to the other, prior to the onset of anaphase. We describe the frequency of univalent movements, the velocity of univalent movements, and the effect of univalent movements on bivalent kinetochore oscillations.

A second remarkable feature of *Mesostoma* spermatocytes is the presence of a precocious cleavage furrow. The cleavage furrow begins ingression shortly after the bivalents become bipolarly oriented in prometaphase and the furrowing then becomes arrested shortly thereafter. The furrow can gradually become slightly more constricted as the cell gets closer to anaphase but only after anaphase does the furrow continue its ingression and cleave the cell (Forer and Pickett-Heaps, 2010). This seems remarkable in itself since most textbooks and articles assume that the stimulus for cleavage furrow ingression is released after anaphase onset. Almost more remarkable is that the position of the furrow along the length of the cell changes when a univalent moves from one pole to the other (Forer and Pickett-Heaps, 2010), when a bivalent re-orients, or when a component of the spindle is altered by UV microbeam irradiation (unpublished data). We do not deal with this phenomenon herein, except in passing.

A third noteworthy feature of *Mesostoma* spermatocytes is the vigorous and persistent oscillations of bivalent kinetochores, as described by Fuge (1987, 1989).

Oscillations of kinetochores in prometaphase and/or metaphase cells in other cell types generally are irregular, for short periods prior to anaphase (not more than 10-25 minutes), for short distances (at most 1-3 μm), perhaps tapering off as chromosomes approach the metaphase plate, and at moderate speeds of the order of 1-3μm/min (Skibbens et al., 1993; Ke et al., 2009; Jaqaman et al., 2010). Speeds and distances can be larger under unusual experimental conditions such as in monopolar spindles (Bajer, 1982; Ault et al., 1991; Skibbens et al., 1993; Cassimeris et al., 1994) or in chromosomes with only one kinetochore (e.g., Skibbens et al., 1995; Khodjakov and Rieder 1996; Khodjakov et al., 1997), and can be larger for oscillations of entire nuclei (e.g., Aist and Bayles, 1988). Compared with this usual description of oscillating chromosomes, oscillations in *Mesostoma* spermatocytes as described by Fuge (1987, 1989), are regular, cover longer distances, and take place throughout most of prometaphase such that the bipolar bivalents do not seem to reach a stable metaphase plate. According to Fuge, each kinetochore oscillated regularly to and from its spindle pole during the maximum observation period (up to an hour) with one kinetochore oscillation cycle to and from the pole taking about 100 seconds, encompassing distances of the order of 5-7 μm or more with velocities from 8-10μm/min. The oscillations lasted throughout prometaphase for as long as cells were followed. There was no real metaphase plate: individual bivalents centred at the metaphase plate only when the two kinetochores moved toward their respective poles at the same time. This sometimes happened but often did not, so when one kinetochore moved *toward* its pole and the other moved *away* from its pole, the bivalent shifted off the equator. The oscillation distances are so large that the chromosomes often are greatly

stretched: interkinetochore distances of the bivalents varied considerably during the oscillations from minimum lengths of around 27μm to up to 40μm (Fuge 1987, 1989). Fuge (1989) noted that kinetochores sometimes remain more-or-less motionless for varying periods, but that the oscillations generally are regular. Since he did not follow the cells into anaphase, there is no information about when or whether kinetochore oscillations stop prior to anaphase onset. Fuge (1989) also suggested (based on chromosome behaviour in a few cells) that there is some coordination between movements to the same pole: of the three bivalents in the cell, he suggested, two move in phase and the third moves in opposite phase. In this article we present extensive data on oscillatory movements of kinetochores in *Mesostoma* spermatocytes, including description of chromosome movements during anaphase.

4.3 Materials and Methods

4.3.1 Living Cell Preparations

We reared laboratory stocks of *Mesostoma ehrenbergii* and obtained spermatocytes from *Mesostoma* testes according to the protocol described by Hoang et al. 2013. Briefly, our *Mesostoma* stocks derived from animals hatched from diapausing (overwintering) eggs that were originally collected from Lake Rondeau, Ontario by Hebert and Beaton (1990). Approximately 5 to 15 animals were kept in plastic jars filled with dechlorinated water and we daily fed them laboratory-reared live brine shrimp (Brine Shrimp Direct, Ogden, Utah, USA). The jars were stored at 25°C in incubators with a 16 hour light: 8 hour dark cycle. We dissected 3- to 4-week old animals; we

removed the testes by inserting through the body wall of the animal a glass needle, pulled from 10 µl micropipettes (Fisher), and siphoning the testes using Tygon tubing (Fisher) attached to the needle. We expelled the testes from the needle onto a glass coverslip and added an equal-sized drop of *Mesostoma* Ringer's solution (61 mM NaCl, 2.3 mM KCl, 0.5 mM $CaCl_2$, and 2.3 mM phosphate buffer, pH 6.9) that contained 0.2mg/mL Fibrinogen (Calbiochem), as previously described (Forer and Pickett-Heaps, 2005). After evenly spreading the fibrogen/testes mixture on the coverslip we added a drop of thrombin (Sigma) to create a fibrin clot. The coverslip was then inverted into a perfusion chamber (Forer and Pickett-Heaps, 2010) that we sealed with wax and perfused with 2-3mL of *Mesostoma* Ringer's solution.

4.3.2 Data Analysis

Images of living cells were recorded on DVDs and then time-lapsed using Virtual Dub (http://www.virtualdub.org), a freeware program. Images were analysed as previously described by Wong and Forer (2003). Briefly, we created graphs using an in-house program developed by Raymond Wong in which we marked the position of a fixed point (the spindle pole) and then marked each kinetochore. The measured distances between pole and kinetochores were then imported into a commercially available program (SlideWrite) for analysis.

4.3.3 Statistical Analysis

Student's t-tests were conducted to determine if velocity to the pole and away from the pole was statistically different and to determine if the decreases in amplitude, period and velocity throughout prometaphase were different. Since the difference in amplitude, period and velocity were calculated as percentages, the percentages were first converted to proportions, the square root and arcsin-1 were then calculated using Excel, and the Student's t-tests were performed on the transformed values.

4.4 Results

4.4.1 Overview of *Mesostoma* spermatocytes

Mesostoma spermatocytes have 5 pairs of chromosomes, 3 bivalents with bipolar orientation and 4 unpaired univalents (Husted and Ruebush, 1940), as illustrated in Figure 4.1. The spermatocytes we study are different from those previously described by Oakley and Fuge in both karyotype and size. Both cells have 4 univalents, two of each kind, but the cells studied by Oakley and Fuge have 2 acrocentric bivalents (bivalents with no arms) plus one metacentric bivalent, whereas the cells we study have 3 metacentric bivalents. There is only one chiasma per bivalent so each of the half-bivalents in the cells we studied had a free arm. Additionally, their cells and chromosomes are considerably larger than ours; their cells have pole-to-pole distances of 40μm or greater, whereas in the cells we studied pole-to-pole distances were 30μm or

less; in their cells, chromosome lengths were 27-40 μm (Oakley, 1985; Fuge 1987) whereas in the cells we studied they were 20-25 μm.

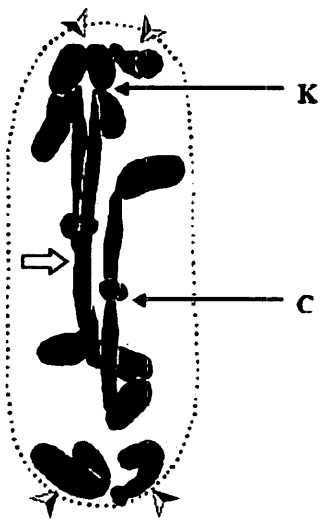

Figure 4.1 Illustrates a fixed and sectioned *Mesostoma* spermatocyte taken from Husted and Ruebush (1940) that has been modified using arrows to show the three bivalents (open arrow) and four univalents (arrowheads). The arrow labelled K points to the kinetochore of a bivalent and the arrow labelled C points to a chiasma.

These morphological differences may exist because Oakley and Fuge studied cells from *Mesostoma* populations that were originally derived from animals given to them by Professor Heitkamp in Germany whereas we studied cells from *Mesostoma* populations that were originally derived from animals from Lake Rondeau in Ontario, Canada, given to us by Dr. Paul Hebert (Hebert and Beaton, 1990). The chromosomal differences that exist between the European and North American subsepecies of *Mesostoma* are well known in the literature (Husted *et al.*, 1939; Husted and Ruebush, 1940; Hebert and Beaton, 1990).

Kinetochores of the 3 bivalents oscillate to and from the spindle poles throughout prometaphase (Fuge, 1987; Fuge, 1989; Fuge and Falke, 1991). The general impression from viewing time lapsed movies of these oscillations is that there is continuous and rapid movement of all kinetochores toward and away from the spindle poles throughout prometaphase and until the very start of anaphase, which occurs as long as 2 hours after the start of prometaphase. The oscillatory movements are so fast that one can easily see them in living cells when viewed on a TV screen. Univalents, on the other hand, do not oscillate. They remain at the spindle poles (Oakley, 1985), and only move from one pole to the other, presumably to achieve the proper distribution of two univalents at each pole, one of each kind, before the onset of anaphase (Oakley, 1985). Univalent movements between spindle poles can easily be seen in time lapsed movies and are more rapid than the oscillatory movements of the bivalents, as we describe in detail below.

Most *Mesostoma* spermatocytes have a dumbbell shaped appearance resulting from a precocious, "pre-anaphase", cleavage furrow that begins ingression once the bivalents have established bipolar orientation; ingression of the furrow then ceases until the onset of anaphase (Forer and Pickett-Heaps, 2010).

We now describe these phenomena in more detail, namely kinetochore oscillations; anaphase chromosome movement; bivalent reorientations; and univalent movements between spindle poles in *Mesostoma* spermatocytes.

4.4.2 Detailed Descriptions of *Mesostoma* spermatocytes

Oscillations in *Mesostoma* spermatocytes generally appear regular for any given kinetochore but sometimes there is no movement of one kinetochore, no movement of two or more kinetochores to the same pole, or no movement of partner kinetochores. From time-lapse movies of 152 kinetochores in 40 cells we determined that 42 kinetochores in 28 cells either did not move or "jiggled". By "jiggled" we mean that kinetochore movement is less than 1.0 μm to or from a pole and is not regular. In those cells in which kinetochores did not move, most often only 1 kinetochore did not move (16/28 cells) or 2 kinetochores associated with the same pole did not move (8/28 cells (Table 4.1). Of those 42 kinetochores from 28 cells that did not oscillate at the start of the observation period, only 5 kinetochores resumed movement. We now give detailed descriptions of those kinetochores that oscillated regularly.

Table 4.1 Summary of the number of kinetochores that oscillate throughout prometaphase compared to the number of kinetochores that remain stationary and do not move throughout prometaphase.

Total Number of KTs (n= number of cells)	Number of Moving KTs	Number of KTs **NOT** Moving	**Number of Cells with Kinetochores Not Moving**			
			One KT	Two KTs to the Same Pole	Partner KTs	KTs to Different Poles
152 (n=40)	110	42 (n=28)	16 (57%)	8 (29%)	3 (11%)	1 (3%)

4.4.3 Oscillations.

4.4.3.1 Average velocities, amplitudes and periods

Regular kinetochore oscillations in *Mesostoma* spermatocytes resemble a sawtooth, wave-like pattern when movement is plotted on a distance versus time graph (Figure 4.2a). From these graphs, we determined the average velocity for each kinetochore by measuring the slope of 5 sawtooth waves as the kinetochore moved to the spindle pole and 5 as they moved away from the spindle pole. From a total of 176 kinetochores (in 88 cells), the average velocity of kinetochore movement to the pole was 6.2 ±1.8 (SD) μm/min (range 0.9 to 12.5 μm/min) and the average velocity of kinetochore movement away from the pole was 5.2 ±2.2 μm/min (range 0.9 to 10.8 μm/min). The distribution is shown graphically in Figure 4.3a. The average velocity of kinetochore movement to the pole is statistically significantly faster than that of kinetochore movement away from the pole (Table 4.2).

Using the same 176 kinetochores, we determined the amplitudes of kinetochore movement by measuring the distance from the trough to the crest of each sawtooth wave, and we determined the periods by measuring the time interval between troughs of multiple waves. The average distance the kinetochores moved away from the pole was 4.0 μm (Table 4.2, Figure 4.3b). The average time it took a kinetochore to move away from the pole and then back to the pole was 92.5 seconds (Table 4.2, Figure 4.3c). At low time-resolution, kinetochores seem to reverse their directions immediately as the tips of the sawtooth waves appear pointed (Figure 4.2a), but at a higher time-resolution the tips of the sawtooth waves appear rounded (Figure 4.2b).

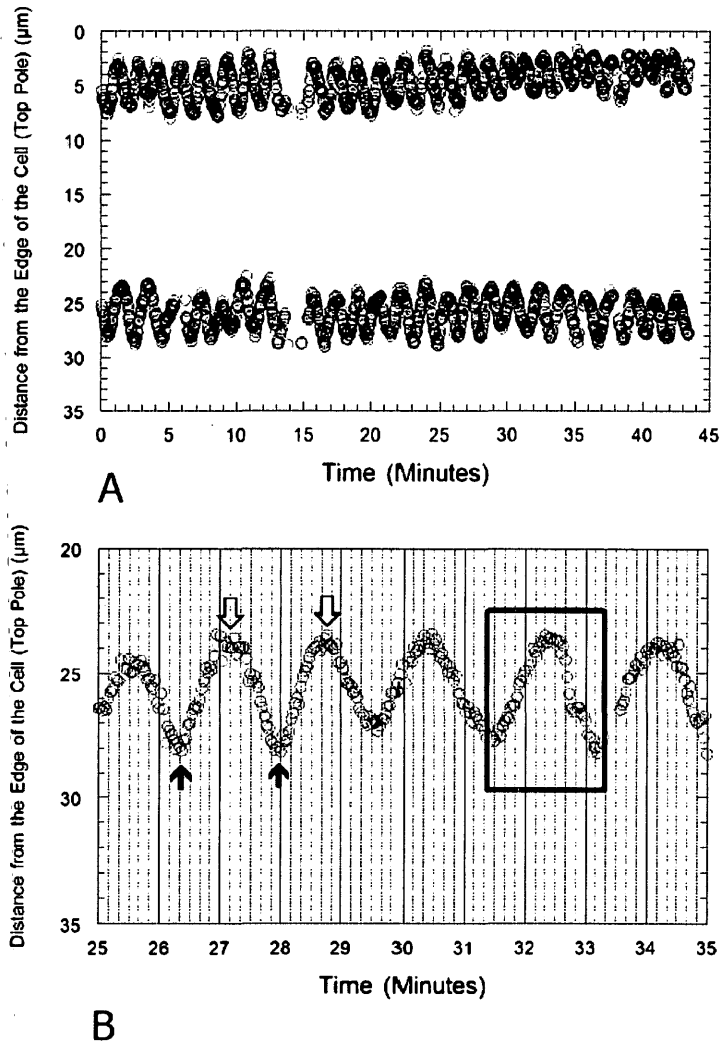

Figure 4.2 (a) Distance of the kinetochores of partner half-bivalents from the edge of the cell (top pole) in µm versus time in minutes in a *Mesostoma* spermatoctye. (b) Higher resolution of the distance from the graph of one kinetochore in Figure 4.2a. The dark black arrows point to the troughs of the sawtooth waves and the open arrows point to the peaks of the sawtooth waves. The distance from the trough to the peak represents the amplitude of the sawtooth wave and the distance between troughs or peaks represents the period of the sawtooth wave. The segment highlighted by the box illustrates that the peaks of the sawtooth waves are rounded and not pointed.

Table 4.2 Summary of the velocity, amplitude and period of kinetochore movement to the pole and away from the pole in *Mesostoma* primary spermatocytes and secondary spermatocyte.

***Mesostoma* Primary Spermatocytes**						
KT Movement	**Number of KT Measurements** (n= Number of Cells)	**Length of Time Series Analyzed**	**Range of Velocities** (μm/min)	**Average Velocities** (μm/min)	**Average Amplitude** (μm)	**Average Period** (sec)
Away from Pole*	880	2491.5 min (41.5 hr)	0.9-10.8	5.2±1.8	4.0±1.4 (1.0-9.0)	92.5±20 (50-180)
To the Pole*	880		0.9-12.4	6.2±2.2		
Combined	1760 (n=88)		0.9-12.4	5.7±2.0		
*Difference between to the pole and away from the pole kinetochore velocities, p=0.01						
***Mesostoma* Secondary Spermatocyte**						
KT Movement	**Number of KT Measurments** (n= Number of Cells)	**Length of Time Series Analyzed**	**Range of Velocities** (μm/min)	**Average Velocities** (μm/min)	**Average Amplitude** (μm)	**Average Period** (sec)
Away from Pole	20 (n=1)	15 min		5.3	4.3	83
To the Pole	20 (n=1)			6.5		
n= Number of cells, ± refers to standard deviation						

The lag time (i.e., the 'rounded' period between the two linear parts of the curve) for kinetochores at the pole was 11.4 ± 11.4 (SD) seconds (n=495) and for those away from the pole was 10.6 ± 10 seconds (n=509). These are not statistically different.

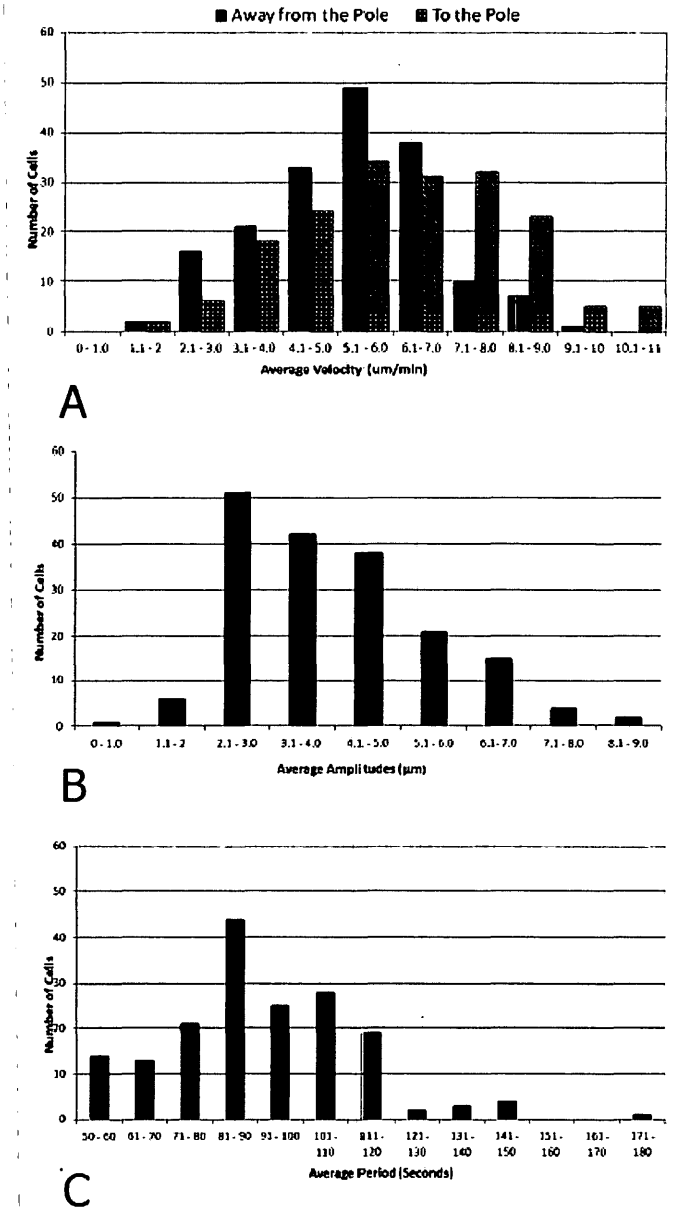

Figure 4.3 (a) Range of average velocities (in µm/min) to the pole and away from the pole. (b) Range of average amplitudes (in µm). (c) Range of average periods (in minutes).

We compared various oscillation parameters for kinetochores in the individual cells (Figure 4.4, Table 4.3). We recorded differences in the parameters in three groupings, 0-10% differences, 10-20% differences, or differences greater than 20%; we

consider that differences of 0-10% in any of the categories are not significant. Overall, neither velocities nor amplitudes nor periods in a cell are constant within 10% (Table 4.3): differences of 10% or less occur less than half the time for partner kinetochores, for kinetochores moving to the same pole, and for kinetochores moving to opposite poles. Even if we extend to 20% the differences that are not significant, more than 20% of the kinetochores were different for all parameters (Figure 4.4, Table 4.3). Thus, it appears that the movement parameters of each kinetochore's oscillation are individual, i.e., not necessarily the same as those of other kinetochores in the same cell.

We looked at the same parameters at different times during division, to see if those in early prometaphase were different from hours later, just before anaphase. Because many of our cells were observed for shorter time periods prior to experimentation of one kind or another, we had a smaller sample size for comparisons at different stages. We compared individual kinetochores in three different time intervals for each cell, usually 15 minute intervals, though sometimes 20 minutes or 35 minutes. The time intervals were different in different cells but were consistent within each cell. To determine if amplitude, period and velocity of kinetochore oscillations either increase or decrease as prometaphase progresses, we normalized the data by comparing the second and third time intervals to the first time interval. We compared the first and second time intervals in 20 cells and from those 20 cells we compared the first and third time intervals for 9 cells.

Table 4.3 Difference in the velocity of kinetochore movement away from the pole, velocity of kinetochore movement to the pole, amplitude of kinetochore movement to and away from the pole and period of kinetochore oscillations for partner kinetochores, kinetochores to the same pole and non-partner kinetochores moving to opposite poles in the same cell.

Type of Kinetochore	**Total Number of Cells**	**Difference in Velocity Away from Pole**			**Difference in Velocity To the Pole**		
		0-10%	10-20%	Greater than 20%	0-10%	10-20%	Greater than 20%
Partner KT	36	**22** (61%)	**5** (13%)	**9** (25%)	**12** (33%)	**10** (27%)	**14** (36%)
KTs to the same pole	34	**17** (50%)	**8** (24%)	**9** (26%)	**14** (42%)	**9** (27%)	**11** (32%)
Non-partner KTs moving to opposite poles	32	**17** (54%)	**9** (28%)	**6** (19%)	**12** (38%)	**7** (22%)	**13** (41%)
Type of Kinetochore	**Total Number of Cells**	**Difference in Amplitude**			**Difference in Period**		
		0-10%	10-20%	Greater than 20%	0-10%	10-20%	Greater than 20%
Partner KT	36	**14** (39%)	**11** (30.5%)	**11** (30.5%)	**22** (61%)	**6** (17%)	**8** (22%)
KTs to the same pole	34	**12** (35%)	**10** (29%)	**12** (35%)	**14** (41%)	**7** (21%)	**13** (38%)
Non-partner KTs moving to opposite poles	32	**12** (36%)	**7** (22%)	**13** (41%)	**18** (56%)	**7** (22%)	**7** (22%)

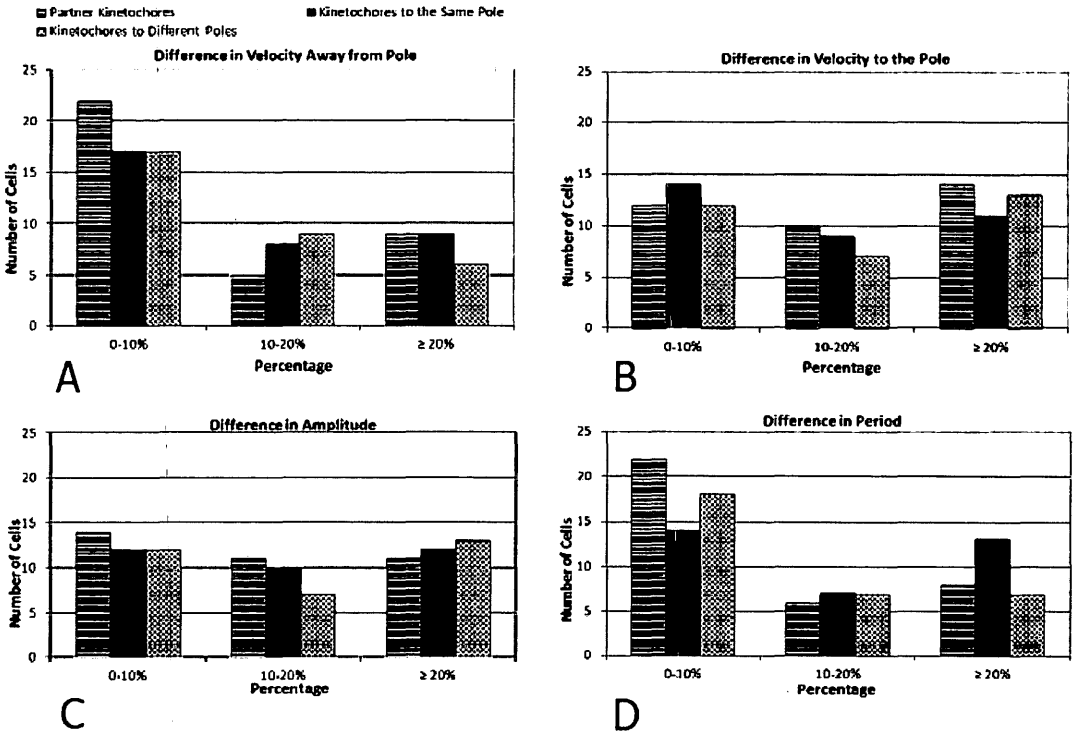

Figure 4.4 (a-d) Difference in the (a) velocity of kinetochore movement away from the pole, (b) velocity of kinetochore movement to the pole, (c) amplitude of kinetochore movement, and (d) period, for partner kinetochores, kinetochores to the same pole and kinetochores to different poles.

As seen in Figure 4.5, there is a small but gradual, statistically significant ($p<0.01$) decrease in the amplitude, period and velocity of kinetochore movement to the pole and away from the pole as prometaphase progresses for each time interval measured, with the largest decrease observed in the amplitude of kinetochore oscillations. The decrease in velocity of kinetochore movement away from the pole, however, was not statistically significant between the second and third time intervals. Each of these parameters seem to be 'labile', decreasing from prometaphase toward anaphase, as also seen in prometaphase chromosome behaviours in other cell types (e.g. Dietz, 1956).

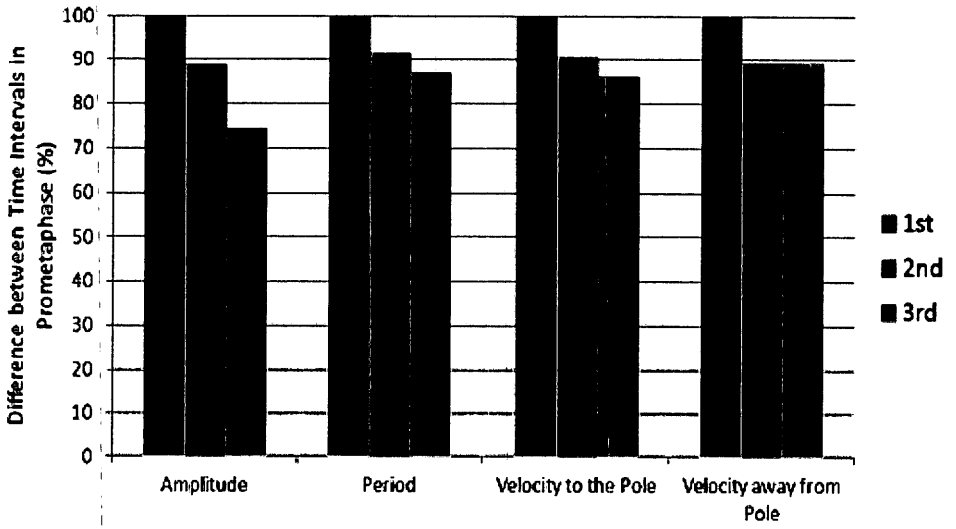

Figure 4.5 Difference between three time intervals of kinetochore movement throughout prometaphase (in percentage) for amplitude, period, velocity to the pole and velocity away from the pole. The difference between the three time intervals was statistically significant ($p<0.01$) for each parameter except the velocity of kinetochore movement away from the pole between the second and third time intervals.

Throughout prometaphase, kinetochores oscillate either in-phase or out-of-phase. Following the original definitions by Fuge (1987), we consider partner kinetochores as moving in-phase when both kinetochores move to their respective pole at the same time and away from the pole at the same time. Partner kinetochores are considered as moving out-of-phase when one kinetochore moves to its pole and the other kinetochore moves away from its pole. In the cells we studied, for any individual bivalent the two kinetochores sometimes moved in phase and sometimes moved out of phase. In individual cells one bivalent can oscillate in-phase while at the same time a different bivalent in the same cell can oscillate out-of-phase. Bivalents can shift between phases multiple times, and they always did so toward the termini of their oscillations, either at the pole or away from the pole; we illustrate on graphs of distance versus time two phase

shifts when the kinetochore was moving away from the pole (Figure 4.6a) and one when the kinetochore was at the pole (Figure 4.6b). In graphs encompassing 41.5 hours of kinetochore oscillations in 91 cells, partner kinetochores were in-phase 74% of the time (515/694 minutes). There were shifts of phase between partner kinetochores in 45 cells, and multiple phase shifts in 22/45 cells (Table 4.4). Of the 84 phase shifts observed, most (66/84) took place when the kinetochore was at the pole terminus of the oscillation (Figure 4.6b). We do not know why kinetochores oscillate in-phase versus out-of-phase, why bivalent kinetochores oscillate in-phase more often than out-of-phase, if different mechanisms are required for each type of movement, or why kinetochores change phases throughout prometaphase.

Table 4.4 Summary of the number of phase shifts that occur throughout prometaphase at the pole versus away from the pole and a summary of the length of time single bivalents oscillate in-phase versus out-of-phase.

	Phase Shifts			In-Phase vs Out-of-Phase		
	Length of Time Series Analyzed (min)	When KTs were at the pole (# of Phase Shifts)	When KTs were away from the pole (# of Phase Shifts)	Length of Time Series Analyzed (min)	Length of time **IN** phase (min)	Length of time **OUT** of phase (min)
Total	2491.5	66	18	690	508.5	181.5
Percentage (%)		79%	21%		73.7%	26.3%
Mean		1 in ~38 min	1 in ~138min			

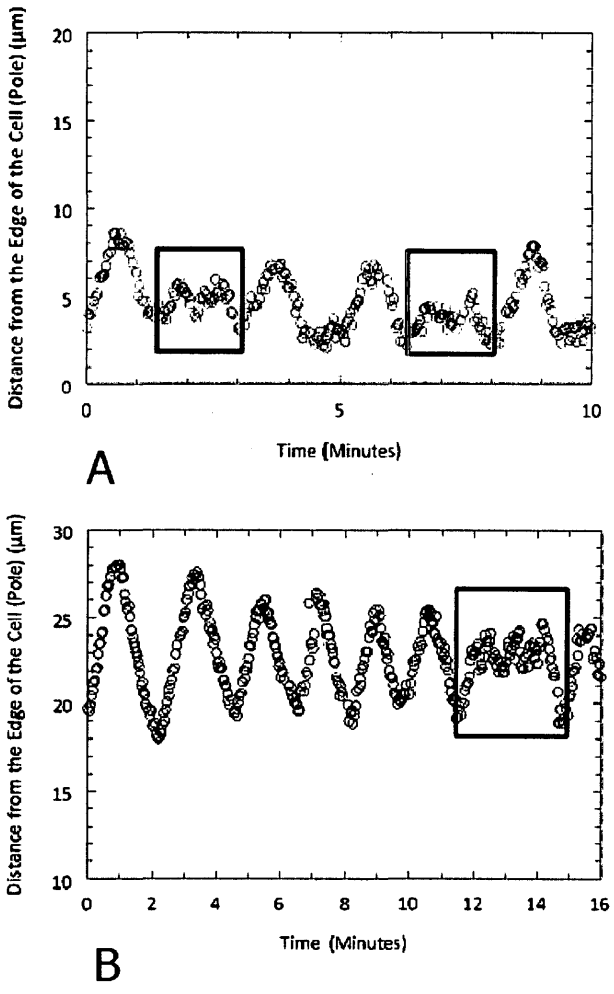

Figure 4.6 (a-b) Distance of the kinetochore of a half-bivalent from the edge of the cell (pole) in µm versus time in minutes. The segments highlighted by the boxes illustrate shifts in phase (a) as the kinetochore moved away from the pole and (b) when the kinetochore was at the pole.

Fuge (1987) suggested that tension in the bivalent was a driver of the kinetochore oscillations. When bivalent kinetochores oscillate in-phase both kinetochores move to the pole at the same time and away from the pole at the same time and therefore tension is built up as the chromosome stretches and is dissipated as the chromosome shortens. One might imagine that absence of tension induces force toward the pole and when the tension

in the chromosome is maximum the force releases and the tension pulls the two kinetochores toward each other. But when bivalent kinetochores oscillate out-of-phase, one kinetochore moves to the pole while the other kinetochore moves away from the pole and therefore tension is not built up. Rather, the chromosome remains at a more-or-less constant length, as seen in plots of interkinetochore distance versus time (Figure 4.7a). Since partner kinetochores move out of phase 26% of the time (181.5/690 minutes) (Table 4.4), changing tension in the chromosome would not seem to be the factor causing the oscillations. However, though bivalents maintain constant length when they move out of phase, as seen in boxed region in Figure 4.7, that constant length often is not the minimum length of the chromosomes seen on the same graphs, so there still can be some tension across the bivalent that is important for the oscillations to occur.

4.4.3.2 Arm movements

When kinetochores oscillate to and away from the pole, the arms of the bivalents usually move with the kinetochores, maintaining a constant angle from the kinetochore as the kinetochore moves, as if the same forces act on both the kinetochore and the arm. In some bivalents, in some cells, however, the tips of the arms remain stationary and thus the arms change angles as the kinetochore oscillates (Figure 4.8, Supplementary Movie). In time lapsed sequences of 130 *Mesostoma* spermatocytes, the arms moved with the kinetochores 87% (329/377 kinetochores) of the time. In the cells in which arms did not move with the kinetochore (48/377 kinetochores), the tips of the arms remained stationary. In some cells, partner kinetochores had one arm move with the kinetochore

and the other arm remain stationary. We do not know why some arms remain stationary and others move with their kinetochore.

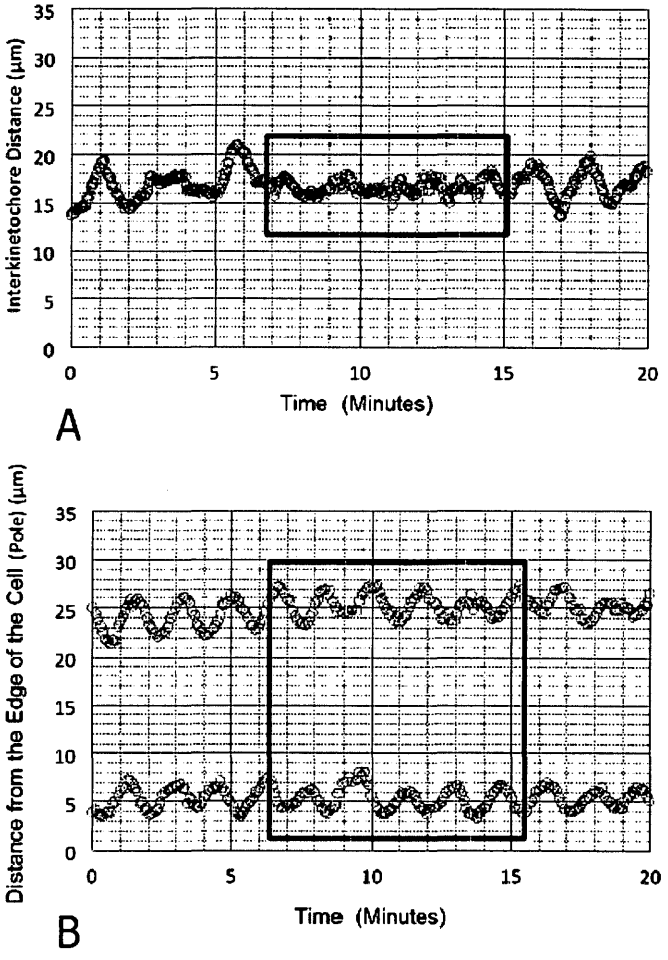

Figure 4.7 (a) Interkinetochore distance of partner half-bivalents in µm versus time in minutes. The segment highlighted by the box illustrates out-of-phase kinetochore movement where one half-bivalent kinetochore moves to the pole and its partner kinetochore moves away, maintaining a constant bivalent length. The segments outside of the box illustrate in-phase kinetochore movement where both half-bivalent kinetochores move to the pole and away from the pole at the same time, changing bivalent length. (b) Distance of the kinetochore of partner half-bivalents illustrated in Figure 4.7a from the edge of the cell (pole) in micrometers versus time in minutes. The segment highlighted by the box illustrates the same time series highlighted in 7(a) to demonstrate that partners continue to oscillate even when they are oscillating out-of-phase and the bivalent length remains constant.

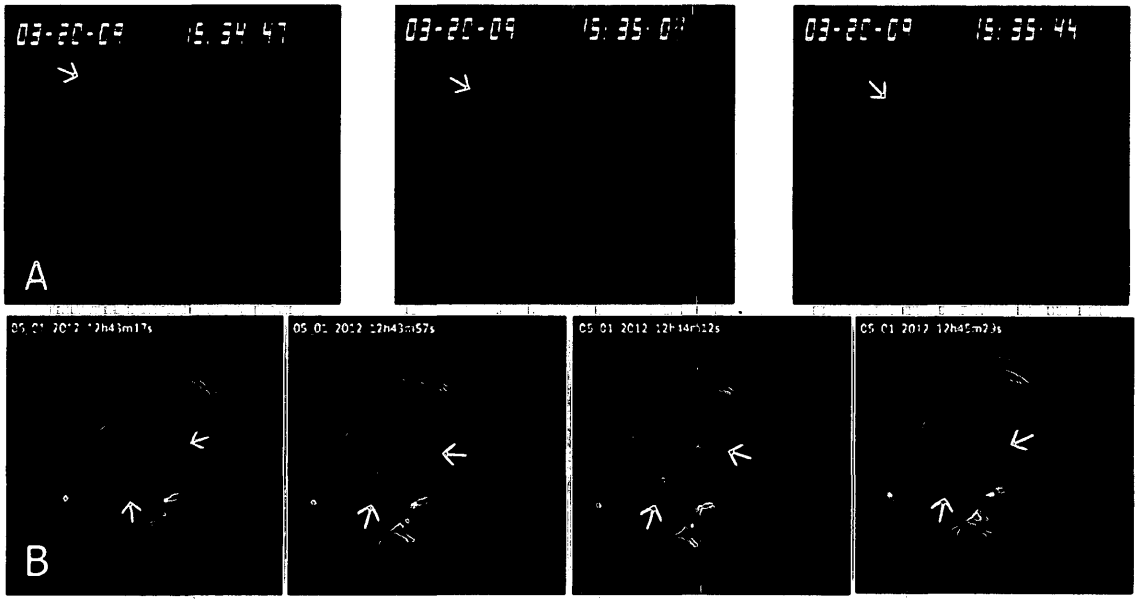

Figure 4.8 (a-b) Montage of phase contrast images of two *Mesostoma* spermatocytes whose bivalent arms do not move with their associated kinetochore and change angles as their kinetochore moves to the pole and away from the pole. The white arrows point to the bivalent arms that do not move with the kinetochore.

4.4.3.3 Granules in the spindle

Spindles do not contain granules in most cells (Nicklas, 1972). In *Mesostoma* spermatocytes, there are granules along the edges of either side of the cell and also in the centre of the spindle, intermixed with the bivalents. Granules in the spindle move short distances before reversing their direction, moving back and forth, in an undirected fashion, and are not transported to the pole or out of the spindle, as happens in other spindles (Nicklas, 1972). 'Granules' seen in electron microscopy images of spindles in *Mesostoma* spermatocytes appear to be mitochondria (Figure 4.9).

4.4.3.4 Phase dense fibres between kinetochores and poles

We have often seen phase dense "fibres" extending between kinetochores and pole (Figure 4.10). They are not always seen, and even when seen they often disappear as they change planes of focus. When seen, they extend between kinetochores and poles, and they seem to elongate as the kinetochores move away from the pole and shorten when the kinetochore moves towards the pole. They may represent the chromosomal spindle fibres.

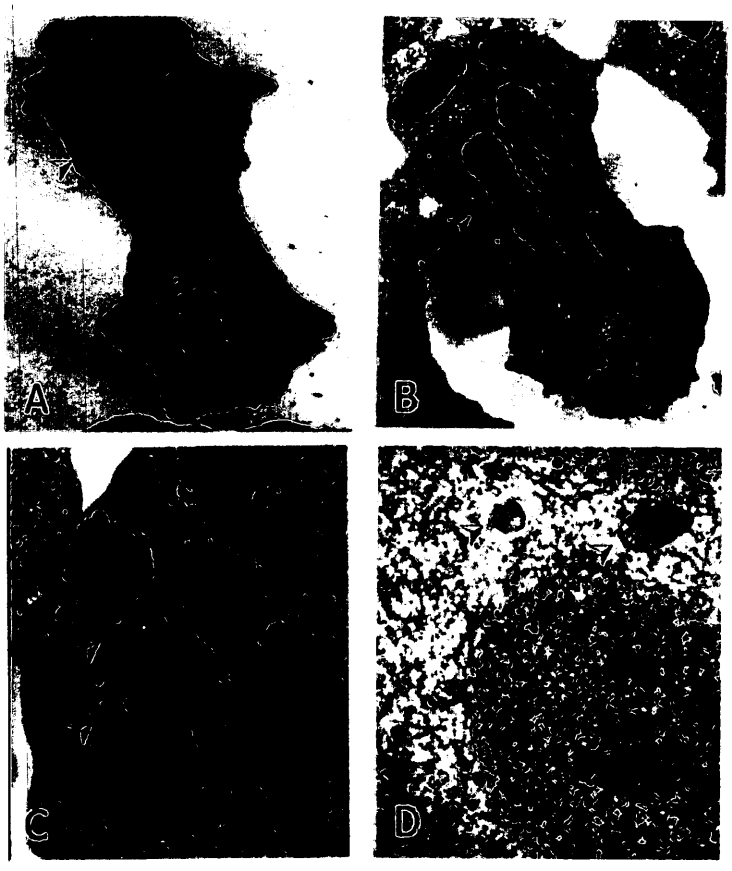

Figure 4.9 (a-d) Electron microscopy images at (a-b) low magnification, (c) medium magnification and (d) high magnification of a *Mesostma* spermatocyte, illustrating granules in the spindle that we identified as mitochondria. The arrowheads point to different mitochondria.

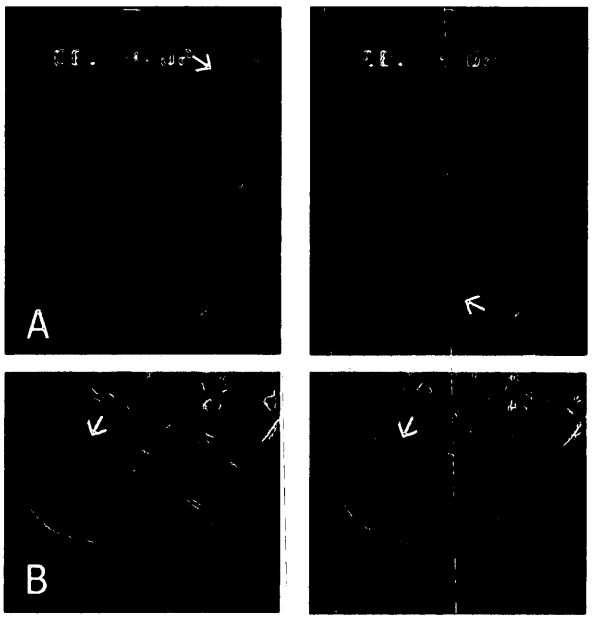

Figure 4.10 (a-b) Phase contrast images of two *Mesostoma* spermatocytes with visible phase dense fibres that could represent spindle fibres. The white arrows point to the possible phase dense fibres.

4.4.4 Anaphase.

Bivalents do not align at a metaphase plate prior to the onset of anaphase. Rather, in the apparent middle of an oscillation the half bivalents separate and move poleward (Figure 4.11). We do not know the exact length of time from prometaphase to anaphase, because we have not followed cells from nuclear membrane breakdown, and we generally experiment on cells before anaphase occurs, but several cells have been followed for over one and a half hours of continuous oscillations before they entered anaphase (Forer and Pickett-Heaps, 2010). The cells elongate an average of 1.3 μm (range 0 μm to 3 μm) from the onset of anaphase to the completion of anaphase and once the half-bivalents reach the poles, the cleavage furrow ingresses in the exact position of the arrested precocious cleavage furrow. In the cells in which we did see anaphase, half-

bivalents disjoined at the same time and moved an average of 1.9±1.2 (SD) μm (range 1 μm to 5 μm) toward their respective poles for approximately 165 s with constant velocities to the pole averaging 1.2± 0.9 μm/min (n = 37 half-bivalent pairs) (Table 4.5).

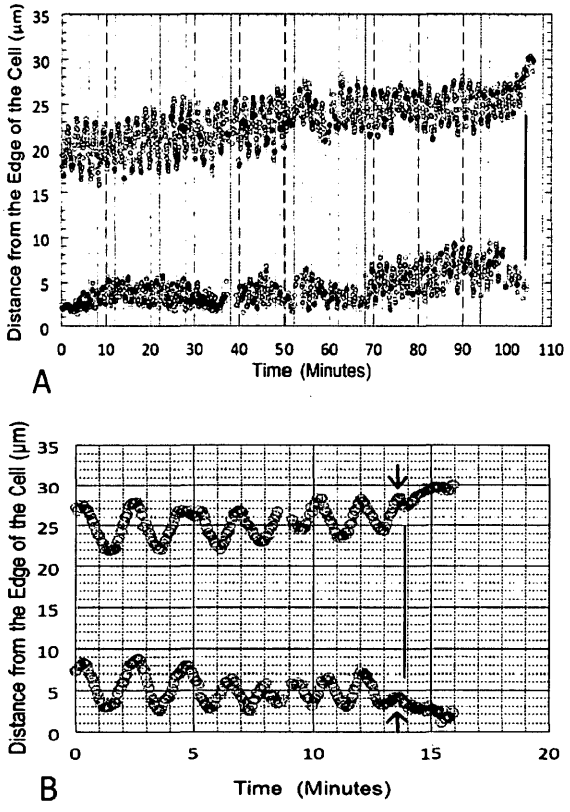

Figure 4.11 (a-b) Distance of the kinetochores of partner half-bivalents from the edge of the cell (pole) in μm versus time in minutes in a *Mesostoma* spermatocyte, illustrating anaphase. The thick black line represents that onset of anaphase. (a) Anaphase occurred after approximately 104 minutes of prometaphase bivalent oscillations. Bivalents separated into two half-bivalents as the kinetochores moved to the pole. (b) The both kinetochores moved approximately 2 μm away from the pole before the bivalent disjoined and each kinetochore moved to its respective pole. The black arrows point to segments in the graph where the kinetochores reversed direction when they disjoined.

Anaphase velocities in *Mesostoma* spermatocytes are within the range of anaphase chromosome velocities in other cell types (Carlson, 1977) but are considerably slower than oscillation velocities in the same cells (Table 4.5).

Table 4.5 Summary of the average velocities of kinetochore movement for bivalent kinetochore oscillations, anaphase chromosome movement, univalent movement and bivalent reorientations in control *Mesostoma* spermatocytes. ± refers to standard deviation.

Mesostoma Spermatocyte Control Cells				
Kinetochore Movement	Number of Cells	Number of Kinetochores Analyzed	Range of Velocities (μm/min)	Average Velocities (μm/min)
Oscillations	88	176	0.9 - 12.4	5.7 ± 2
Anaphase	16	37	0.1 - 3.4	1.2 ± 0.9
Univalent	12	22	2.6 - 21.1	9.4 ± 4.3
Bivalent Reorientations	12	16	4.9 - 14.1	8.2 ± 2.7

We analyzed distance versus time graphs to see if we could better understand when anaphase onset takes place based on possible irregularities in the sawtooth waves prior to anaphase. In the 5 sawtooth waves immediately preceding the final sawtooth wave prior to onset of anaphase there was no change in the amplitude or period and there was little to no change (less than 15% difference) in the velocity of kinetochore movement *to* the pole; however, there was a significant *decrease* (approximately 30-50%) in the velocity of kinetochore movement *away* from the pole, with the most drastic decrease (50%) seen in the 2 sawtooth waves immediately preceding anaphase onset. In 16 of the 20 cells we studied, anaphase occurred as half-bivalent kinetochores started to move away from pole: the half-bivalents disjoined and moved towards their respective spindle poles before reaching their furthest away from the pole position (Figure 4.11b). In

most (10/16) of these cells, bivalents disjoined after half-bivalent kinetochores moved approximately 2 μm away from the pole; bivalents also disjoined after half-bivalent kinetochores moved only 1 μm away from the pole (4/20), less than 1 μm away from the pole (1/20) or greater than 2 μm away from the pole (1/20). In the other 4 of the 20 cells we studied, anaphase occurred as half-bivalent kinetochores moved to the pole, the bivalents actually disjoining once the kinetochores reached their respective spindle poles (Figure 4.11b). This information does not help us predict when anaphase will occur when we are watching a live cell, but it does show that bivalents usually separate and enter into anaphase when half-bivalent kinetochores are moving away from the pole.

4.4.5 Second division.

We have observed meiosis II in one spermatocyte that we followed from the completion of meiosis I. The primary spermatoctye we originally followed (Figure 4.12a) in meiosis I entered anaphase after approximately an hour and twenty minutes. When we returned to the same cell 40 minutes later, a secondary spermatocyte was present (Figure 4.12b) and meiosis II was underway. The secondary spermatocyte then entered into anaphase approximately 15 minutes later (Figure 4.12c). Kinetochore oscillations were similar to those in meiosis I: average velocity of kinetochore movement to the pole was 6.5 μm/min and the average velocity of kinetochore movement away from the pole was 5.3 μm/min., the average distance the kinetochore moved away from the pole was 4.3 μm and the average period was 83 seconds (Table 4.2). Though we have data from only one

secondary spermatocyte, these oscillation parameters in second division were similar to those in primary spermatocytes, as seen in Table 4.2.

We now describe reorientations of bivalents, and movements of univalents in primary *Mesostoma* spermatocytes.

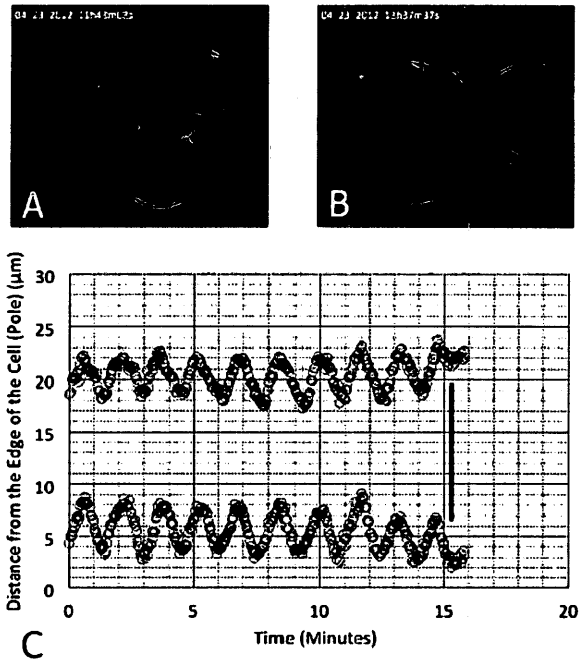

Figure 4.12 (a) Phase contrast image of a primary *Mesostoma* spermatocyte. (b) Phase contrast image of a secondary spermatocyte that was created following the completion of meiosis I of the primary spermatocyte in (a). (c) Distance of the kinetochores of partner half-bivalents from the edge of the cell (pole) in µm versus time in minutes for the secondary *Mesostoma* spermatocyte in (b).

4.4.6 Bivalent Reorientations.

We have observed 49 bivalent reorientations in time lapsed movies of 25 *Mesostoma* spermatocytes corresponding to 2492 minutes (41.5 hours) of filming; one example is seen in Supplementary Movie 1. We saw two kinds of bivalent reorientations: (1) bivalents that were mono-oriented when we first starting filming that subsequently

became bipolarly oriented;; (2) bipolarly oriented bivalents, with normal oscillations, that became mono-oriented after a half-bivalent kinetochore detached and re-attached to the opposite pole (i.e., the same pole as its partner). After the bipolar univalents became monopolar, bipolarity was re-established when one of the two monopolarly oriented kinetochores detached and re-oriented to the opposite pole; in these cells bipolarity was re-established either when the two kinetochores exchanged places or when the previously detached kinetochore returned to its original pole. Reorientations occur after stable bipolar orientation of the bivalents in question, not just after initial, perhaps incomplete, attachments, because we have filmed up to 75 minutes of normal oscillation behaviour before some detachments and reorientations.

In 8/49 cells with reorientations, mono-oriented bivalents that were mono-oriented when we started filming became bipolarly oriented during our filming sequence. We do not know how the initial monopolar orientation arose. In 7 of the 8 cells, no further reorientations took place once the mono-oriented bivalent became bipolarly oriented.

In 41/49 cells with reorientations, a kinetochore of a half-bivalent of a bipolarly oriented bivalent detached from its pole, moved towards the opposite pole and became mono-oriented. Most (37/41) of these mono-oriented bivalents returned to bipolarity within seconds to 15 minutes, but some (4/41) of these mono-oriented bivalents remained mono-oriented for as long as 30 minutes, with both kinetochores either resuming oscillations to the one pole or remaining stationary at the poles, never re-establishing bipolarity within this time frame. In the other (37/41) examples, when bivalents became

mono-oriented following the detachment of one of their half-bivalent kinetochores, one of the two kinetochores returned to the original pole. When returning to their original bipolar configuration it was often difficult to determine if the originally detached kinetochore or the sister kinetochore moved back to the original pole; we were able to identify which kinetochore moved back to the original pole of detachment in only 17/41 reorientations. In 13/17 of these reorientations the two kinetochores changed places (Figure 4.13a), whereas in 4/17 reorientations the originally detached kinetochore returned to its original pole (Figure 4.13d).

From distance versus time graphs, we determined that some reorienting kinetochores continued to oscillate (albeit with dampened amplitude) as they moved away from the pole, with linear movement between oscillations (e.g., Figure 4.13b, d), while other kinetochores move to the opposite pole with constant velocity (Figure 4.13c, d). When the detached kinetochore moved to the opposite pole, the oscillations of the partner kinetochore had reduced amplitudes and velocities (with unchanged periods), e.g., Figure 4.13c, d, and then stopped oscillating completely after the partner reached the pole.

Reorienting bivalent kinetochores that moved between spindle poles had velocities that averaged 2 μm/min faster than bivalent kinetochore oscillations, 8.2 ±2.7 (SD) μm/min (range 4.9 to 14.1 μm/min, n=16 kinetochores), compared to 5 μm/min for oscillations (Table 4.5). When 4 monopolar bivalents became bipolarly oriented, the kinetochore velocities were the same as movements of detached bipolarly oriented bivalents, 8.3 ±2.0 μm/min (range 6.3 to 10.3 μm/min).

4.4.7 Univalents.

We analyzed univalent inter-polar movements to determine if these excursions affect bivalent kinetochore oscillations. When univalents move from one pole to the other, they usually move very rapidly with constant velocity from one pole to the other, as seen in Figure 4.14a. In some cells however, the univalents paused briefly at the equator, for as little as 10 seconds and no more than 60 seconds, before continuing to move to the opposite spindle pole. We have seen 56 univalent excursions from pole to pole in approximately 1200 minutes of filmed cells. We observed 53 univalent excursions in 28 cells and multiple univalent excursions in 12 of those cells. From plots of 22 univalent excursions, the average velocity of univalent movement was 9.4 ±4.3 μm/min (range 2.6 to 21 μm/min) (Table 4.5). In cells in which multiple univalent excursions took place, the time between excursions varied from 2.5 to 26 minutes. In most of the cells we observed, there was only one univalent excursion during prometaphase but we have also observed anywhere from 2 univalent excursions to 7 univalents excursions in single prometaphase sequences (Figure 4.14b). Univalent movements did not affect the oscillation movements of the bivalents in the same cell, except for two excursions in 2/11 cells, one of which is illustrated in Figure 4.14c. No other oscillation parameters were affected, so we conclude that univalent segregation does not affect or interfere with bivalent kinetochore oscillations.

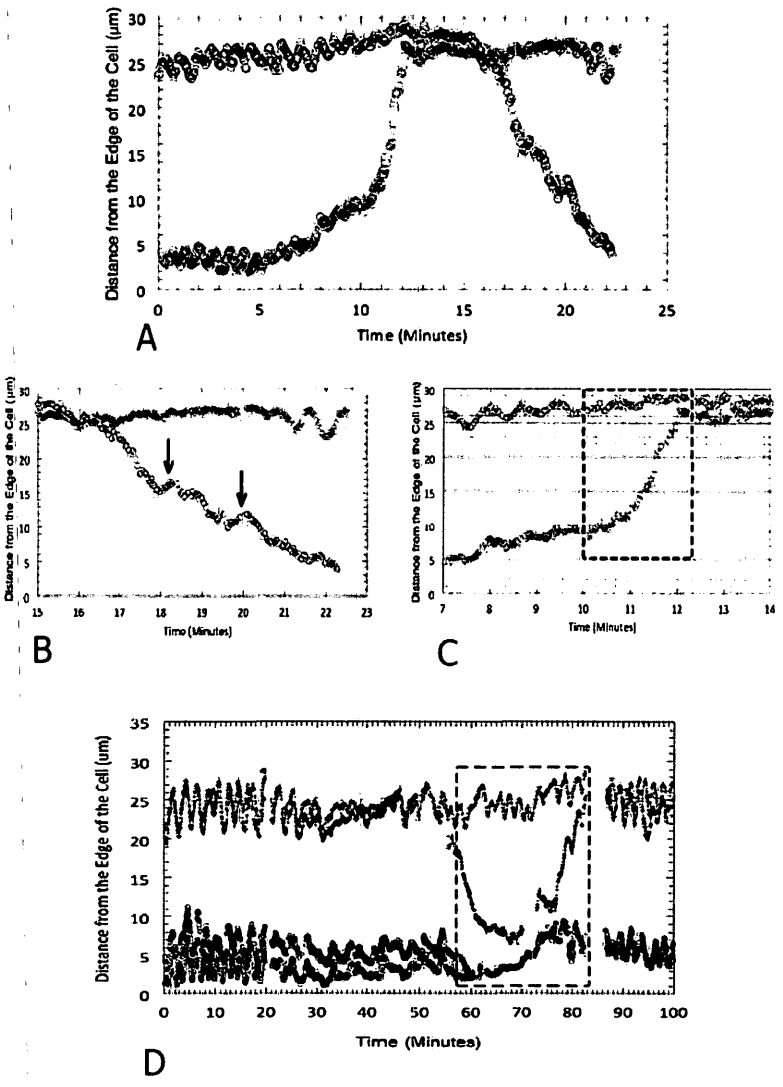

Figure 4.13 (a-d) Distance of the kinetochores of partner half-bivalents from the edge of the cell (pole) in µm versus time in minutes illustrating bivalents reorienting throughout prometaphase. (a) The lower half-bivalent kinetochore (**O**) detaches from lower pole, moves to the upper pole and attaches to it. Its partner half-bivalent kinetochore (**O**) then detaches from the upper pole and moves to the lower pole where it attaches. (b) Distance versus time from 15 to 25 minutes from Figure 4.13(a): the solid arrows point to the dampened oscillations of the kinetochore as it moves polewards. (c) Distance versus time from 7 to 14 minutes from Figure 4.13(a): the dashed box highlights that the upper half-bivalent (**O**) oscillates with a dampened amplitude as its partner half-bivalent (**O**) moves to the opposite pole with few or no oscillations. (d) The upper half-bivalent kinetochore (+) moves to the lower pole and then reorients and moves back to its original pole. The dashed box highlights that the lower half-bivalent (**O**) oscillates with a dampened amplitude as its partner half-bivalent (+) detaches and moves to the opposite pole.

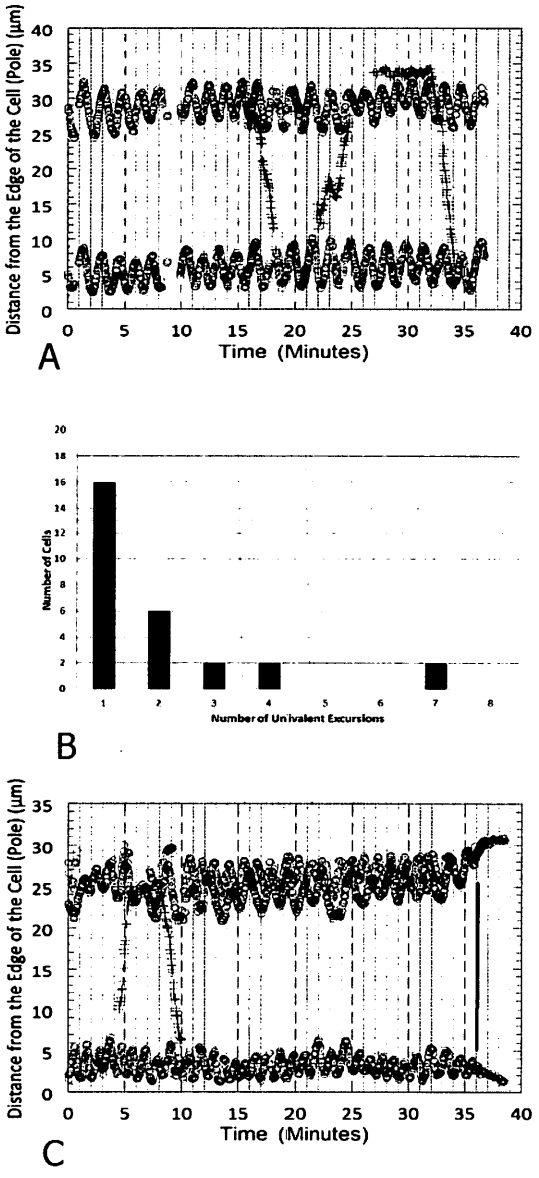

Figure 4.14 (a) Distance of the kinetochores of partner half-bivalents and univalents from the edge of the cell (pole) in µm versus time in minutes, illustrating three univalent excursions. In the first and second univalent excursions, the univalents move between spindle poles in a step-like fashion, whereas, in the third univalent excursion, the univalent moves to the lower spindle pole in a linear fashion. (b) Number of univalent excursions observed in single *Mesostoma* spermatocytes. (c) Distance of the kinetochores of partner half-bivalents and univalents from the edge of the cell (pole) in µm versus time in minutes illustrating two univalent excursions that decreased the amplitude of the kinetochore oscillations of the upper half-bivalent (**O**).

4.5 Discussion

We have described cell division in meiosis-I spermatocytes of *Mesostoma ehrenbergii* with the aim of laying the framework for experimental work on this system, with its several unique attributes. We described the regular oscillations of each bivalent that occur throughout prometaphase and until anaphase, and that there is no metaphase configuration recognisable as such; that the oscillations to the pole are faster than those away from the pole; that oscillating kinetochores periodically shift phase; that the free arms of the bivalents usually move with the kinetochores, but sometimes do not; that while the three bivalents appear to oscillate together, the oscillation parameters of each bivalent and of partner kinetochores in the same bivalent differ by more than 20% in 20-40% of the cells, so that the kinetochore oscillations seem independent. Anaphase most often occurs in the middle of an oscillation cycle, and anaphase movements are much slower than oscillation velocities (~1μm/min rather than 6μm/min). We described how bipolar bivalents periodically reorient, most often resulting in the partner kinetochores exchanging poles. We described the pole-to-pole movements of univalent chromosomes, and how these generally do not affect the oscillations of the bivalents.

The oscillations we observed in *Mesostoma* spermatocytes are similar to descriptions by Fuge, who was the first to describe and characterise the regular oscillations of the bivalents, despite being limited in his equipment and grant support (Fuge, 1987). Our observations agree with his in general – that there are continuous oscillations with high velocities, periodic changes in phase, etc. – but they also differ in some details (Table 4.6).

Table 4.6 Comparison of *Mesostoma* spermatocyte control cells from Fuge (1987, 1989) and our data.

	Mesostoma Spermatocyte Control Cells	
	Fuge (1987, 1989) European *M. ehrenbergii*	Our Data North American *M. ehrenbergii*
Average Velocity (Range including to the pole and away from pole)	8 to 10 μm/min	5 to 6 μm/min
Average Amplitude	5 to 7 μm	4 μm
Average Period	100 seconds	92.5 seconds
Amount of Time In-Phase: Amount of Time Out-of-Phase	1 : 4	3 : 1

Some of these differences can be attributed to the different species we studied. We studied a North American species of *M. ehrenbergii*, whereas, Fuge studied a European species of *M. ehrenbergii*. But we also differ in some interpretations. Fuge (1987) thought that the chromosomes in *Mesostoma* spermatocytes must be "elastic bodies under tension" as previously reported in grasshopper spermatocytes by Nicklas and Staechly (1967); therefore, as chromosomes move to the pole tension is created and when maximum tension is achieved, the elasticity in the chromosomes matches the poleward forces which results in chromosome movement away from the pole (Fuge, 1987). Based on our data, oscillations cannot be solely due to tension in the bivalent: oscillations continued even when chromosomes oscillated out-of-phase and when interkinetochore distances remained constant (Table 4.4, Figure 4.7). Fuge (1987) also thought that the oscillation parameters (velocity, period and amplitude) he studied were the same for all bivalents and thus that there must be interdependency between kinetochores, especially

since he observed a progressive amplification in the amplitude of all three bivalents throughout prometaphase. In our experiments, however, all parameters of the oscillations decreased during prometaphase, and kinetochores seemed to oscillate independently of each other since oscillation parameters differed between kinetochores by more than 20% (Table 4.3, Figure 4.4). While some of our results and interpretations differ from his, Fuge (1987, 1989, 1991) laid the groundwork in describing *Mesostoma* spermatocytes upon which we were able to build.

Anaphase chromosome movements started in the middle of oscillation cycles, most commonly when kinetochores moved away from the pole, interrupting the oscillatory movement away from pole. Anaphase chromosome velocities to the pole are much slower than oscillations, 1 μm/min compared to 6 μm/min; at first glance this might seem puzzling since microtubule depolymerisation acts as the rate-limiting step for movement velocity (Forer et al., 2003, Forer et al., 2008, Pickett-Heaps and Forer, 2009) and since both prometaphase and anaphase require depolymerisation of kinetochore microtubules. We think that something related to the kinetochore microtubules changes at or immediately prior to anaphase. It might be, for example, that during prometaphase oscillations kinetochore microtubules depolymerise at the kinetochore and "chew" their way to the pole as described by the PacMan model (Rieder and Salmon, 1994) but that during anaphase kinetochore microtubules depolymerise at the pole, as in the classic traction fibre theory or the "flux model" (Cameron et al., 2006). In general, one could explain the slower speeds during anaphase by the microtubule depolymerising enzymes at pole and kinetochore (Sharp and Ross, 2012) changing their depolymerisation rates at

anaphase; if the spindle matrix (Forer et al., 2008; Pickett-Heaps and Forer 2009; Johansen et al., 2011) propels microtubules and chromosomes poleward, the rate of movement would change depending on the rates of microtubule depolymerisation at the two ends of the microtubules.

Univalents periodically moved between spindle poles, sometimes up to 7 times in the same cell. Many cells have a 2:2 distribution of univalents at the poles from early prometaphase, but some have 3:1 or even 4:0 distributions. If pole-to-pole movements of univalents were required only to achieve distance segregation, then the cell would need at most 1 or 2 movements to have 1 X univalent and 1 Y univalent at each pole. In 6/28 cells, however, there were 3 or more excursions (Figure 4.14). Oakley attributed the more-than-needed number of excursions to the need to not only balance 1 X univalent and 1 Y univalent at each pole (distance segregation) but because there is non-random segregation of the univalents, requiring X1Y1 at one pole and X2Y2 at the other. Our data confirm that there are more-than-needed univalent movements in *Mesostoma* spermatocytes, which is consistent with Oakley's interpretation that there may be non-random segregation of the univalents. Perhaps relevant to this are the bivalent reorientations that occur in these cells.

Bivalent reorientations occur with reasonable frequency in the cells we studied: 49 reorientation in 2490 minutes of filming, or one reorientation every 50 minutes on average. This seems to us to be quite high, since we know of no other reports on any other not-treated cells that describe *any* reorientation of bipolarly oriented bivalents. The high frequency is not because this is correction of faulty initial attachment, because they

occurred after lengthy periods of normal oscillations and hence seemingly normal attachments, periods of up to 75 minutes. Thus we would expect the attachments to be stable once bipolar orientation is achieved. That there are so many bivalent reorientations, and that most reorientations (13/17) resulted in the sister kinetochores switching poles, may be related to the speculation by Oakley (1983, 1985) that univalent movements between the poles is used both to achieve non-random segregation (for example that male-derived and female-derived univalents must be at different poles). It may be that bipolar attachment of bivalents is necessary but not sufficient, that if directed, non-random segregation is required as well, then the reorientation of bivalents may be the mechanism used so that kinetochores of some bivalents can switch the poles to which they are oriented.

Bivalents oscillate regularly and continuously until anaphase in *Mesostoma* spermatocytes. In other cells described in the literature bivalents oscillate irregularly and only briefly throughout prometaphase before stabilizing at the metaphase plate (Pickett-Heaps et al., 1979; Pickett-Heaps and Tippit, 1980; Skibbens et al., 1993; Civelekoglu-Scholey et al., 2006; Jaqaman et al., 2010). This raises the question of whether *Mesostoma* spermatocytes require prometaphase oscillations in order to enter anaphase whereas other cells do not. Several lines of evidence show that oscillations are not required for anaphase onset. *Mesostoma* spermatocytes have entered into anaphase when one or more kinetochores are not moving, as described above; they also enter anaphase following Taxol treatment which stops all bivalent oscillations (unpublished) and when kinetochore movement is stopped with an optical trap (Ferraro-Gideon et al., 2013).

Therefore, the lengthy prometaphase oscillations observed in *Mesostoma* spermatocytes are not actually be required for anaphase onset.

During prometaphase oscillations in *Mesostoma* spermatocytes kinetochore movements to the pole are statistically faster than movements away from the pole. This is not necessarily the case in other cells. In more usual cells, the velocity of kinetochore movement to and away from the pole is the same, though different mechanisms have been thought to be required to produce these movements (Ault et al., 1991; Skibbens et al., 1993; Skibbens et al., 1995; Khodjakov and Rieder, 1996; Campas and Sens, 2009; Ke et al., 2009). In one model, to the pole and away from pole movement are both thought to be generated by tension in the kinetochore (Skibbens et al., 1993; Skibbens et al., 1995); in a different model away from pole movement is thought to be generated by polar ejection forces acting on the chromosome arms (Ault et al., 1991; Khodjakov and Rieder, 1996; Liu et al., 2007; Campas and Sens, 2009; Ke et al., 2009). Our data indicate that tension alone is not responsible for producing kinetochore oscillations, as discussed above, but a combination of these models may explain why kinetochore movement to the pole is significantly faster than kinetochore movement away from the pole in *Mesostoma* spermatocytes.

In summary, we have described cell division in meiosis-I spermatocytes of *Mesostoma ehrenbergii* and we have provided detailed description of the regular bivalent oscillations that occur throughout prometaphase; the periodic reorientations of bipolar bivalents; and the pole-to-pole movements of univalent chromosomes. We hope our descriptions help lay a foundation for further experimental work on these unique

oscillations, on trying to understand the distance segregation of univalents, on the possible non-random segregation of univalents and half-bivalents, on the normally-occurring reorientation of bipolarly oriented bivalents, and on mechanisms that control their precocious cleavage furrows.

4.6 Acknowledgements

This work was supported by grants from the Canadian Natural Sciences and Engineering Council to A.F.

4.7 References

Aist JR, Bayles CJ (1988) Video motion analysis of mitotic events in living cells of the fungus *Fusarium solani*. Cell Motil Cyto 9: 325-336

Ault JG, DeMarco AJ, Salmon ED, Rieder CL. (1991) Studies on the ejection properties of asters: astral microtubule turnover influences the oscillatory behaviour and positioning of mono-oriented chromosomes. J Cell Sci 99: 701-710

Bajer AS (1982) Functional autonomy of monopolar spindle and evidence for oscillatory movement in mitosis. J Cell Bio 93: 33-48.

Camenzind R, Nicklas RB (1968) The non-random segregation in spermatocytes of *Gryllotalpa hexadactyla*. A micromanipulation analysis. Chromosoma 24: 324-335

Cameron LA, Yang G, Cimini D, Canman JC, Kisurina-Evgenieva O, Khodjakov A, Danuser G, Salmon ED (2006) Kinesin 5-independent poleward flux of kinetochore microtubules in PtK1 cells. J Cell Biol 173: 173-179

Campas O, Sens P (2006) Chromosome oscillations in mitosis. Phys Rev Lett. 97: 1-4

Carlson JG (1977) Anaphase chromosome movement in the unequally dividing grasshopper neuroblast and its relation to anaphases of other cells. Chromosoma 64: 191-206

Cassimeris L, Rieder CL, Salmon ED (1994) Microtubule assembly and kinetochore directional instability in vertebrate monopolar spindles: implications for the mechanism of chromosome congression. J Cell Sci 107: 285-297

Civelekoglu-Scholey G, Sharp DJ, Mogilner A, Scholey JM (2006) Model of chromosome motility in *Drosophila* embryos: Adaptation of a general mechanism for rapid mitosis. Biophys J 90: 3966-3986

Dietz R 1956 Die Spermatocytenteilungen der Tipuliden. II. Graphische analyse der chromosomenbewegung während der prometaphase I im leben. Chromosoma 8: 183-211

Ferraro-Gideon J, Sheykhani R, Zhu Q, Duquette ML, Berns MW, Forer A (2013) Measurements of forces produced by the mitotic spindle using optical tweezers. Mol Biol Cell 24: 1375-1386.

Forer A, Koch C (1973) Influence of autosome movements and of sex chromosome movements on sex-chromosome segregation in crane fly spermatocytes. Chromosoma 40: 417-442

Forer A, Spurck T, Pickett-Heaps JD , Wilson PJ (2003) Structure of kinetochore fibres in crane-fly spermatocytes after irradiation with an ultraviolet microbeam: neither microtubules nor actin filaments remain in the irradiated region. Cell Motil Cytoskeleton 56: 173-192

Forer A, Pickett-Heaps JD, Spurck T (2008) What generates flux of tubulin in kinetochore microtubules? Protoplasma 232: 137-141

Forer A, Pickett-Heaps JD (2010) Precocious (pre-anaphase) cleavage furrows in *Mesostoma* spermatocytes. Eur J Cell Bio 89: 607-618

Forer A, Ferraro-Gideon J, Berns MW (2013) Distance segregation of sex chromosomes in crane-fly spermatocytes studied using laser microbeam irradiations. Protoplasma DOI 10.1007/s00709-013-0480-4

Fuge H (1987) Oscillatory movements of bipolar-oriented bivalent kinetochores and spindle forces in male meiosis of *Mesostoma ehrenbergii*. Eur J Cell Biol 44: 294-298

Fuge H (1989) Rapid kinetochore movements in *Mesostoma ehrenbergii* spermatocytes: action of antagonistic chromosome fibre. Cell Motil Cytoskeleton 13: 212-220

Fuge H (1991) Morphological aspects of chromosome spindle fibres in *Mesostoma*: "microtubular fir-tree" structures and microtubule association with kinetochores and chromatin. Protoplasma 160: 39-48

Gerbi SA (1986) Unusual chromosome movements in sciarid flies. Results and Problems in Cell Differentiation 13: 71-104

Hebert PDN, Beaton MJ (1990) Breeding systems and genome size of the rhabdocoel turbellaria *Mesostoma ehrenbergii.* Genome 33: 719-724

Hoang C, Ferraro-Gideon J, Gauthier K, Forer A (2013) Methods for rearing *Mesostoma ehrenbergii* in the laboratory for cell biology experiments, including identification of factors that influence production of different egg types. Cell Biol Int. Accepted.

Hughes-Schrader S (1969) Distance segregation and compound sex chromosomes in Mantispids (*Neuroptera: Mantispidae*). Chromosoma 27: 109-129

Husted L, Ruebush TK (1940) A comparative cytological and morphological study of *Mesostoma ehrenbergii ehrenbergii* and *Mesostoma ehrenbergii wardii*. J Morphol 67: 387-410

Jaqaman K, King EM, Amaro AC, Winter JR, Dorn JF, Elliot HL, Mchedlishvili N, McClelland SE, Porter IA, Posch M et al. (2010) Kinteochore alignment within the metaphase plate is regulated by centromere stiffness and microtubule depolymerise. J Cell Biol 188: 665-679.

Johansen KM, Forer A, Yao C, Girton J, Johansen J. (2011) Do nuclear envelope and intranuclear proteins reorganize during mitosis to form an elastic, hydrogel-like spindle matrix? Chromosome Res 19: 345-365.

Ke K, Cheng J, Hunt AJ (2009) The distribution of polar ejection forces determines the amplitude of chromosome directional instability. Curr Biol 19: 807-815

Khodjakov A, Rieder CL (1996) Kinetochores moving away from their associated pole do not exert a significant pushing force on the chromosome. J Cell Biol 135: 315-327

Khodjakov A, Cole RW, McEwan BF, Buttle KF, Rieder CL (1997) Chromosome fragments possessing only one kinetochore can congress to the spindle equator. J Cell Bio 136: 229-240

Nicklas RB, Staehly CA (1967) Chromosome micromanipulation. I. The mechanics of chromosome attachment to the spindle. Chromosoma 21: 1-16

Nicklas RB (1972) Chromosome micromanipulation IV. Polarized motions within the spindle and models for mitosis. Chromosoma 39: 1-26.

Nur U (1982) Destruction of specific heterochromatic chromosomes during spermatogenesis in the *Comstockiella* chromosome system (Coccoidea: Homoptera). Chromosoma (Berl.) 85: 519-530

Pickett-Heaps JD, Tippit DH, Andreozzi JA (1979) Cell division in the pinnate diatom Pinnularia. V- Observations on live cells. Biol Cellulaire 35: 295-304

Pickett-Heap JD, Tippit DH (1980) Light and electron microscopic oberservations on cell division in two large pinnate diatoms, Hantzschia and Nitzschia. I. Mitosis in vivo. Eur J Cell Bio 21: 1-11

Pickett-Heaps JD, Forer A (2009). Mitosis: spindle evolution and the matrix model. Protoplasma 235: 91-99

Oakley HA (1983) Male meiosis in *Mesostoma ehrenbergii ehrenbergii*. Kew Chromosome Conference II Editors PE Brandham, MD Bennett. George Allen and Unwin, London (Boston, Sydney) pp 195-199

Oakley HA (1985) Meiosis in *Mesostoma ehrenbergii ehrenbergii* (Turbellaria, Rhabdocoela) III. Univalent chromosome segregation during the first meiotic division in spermatocytes. Chromosoma 91: 95-100

Rieder CL, Salmon ED (1994) Motile kinetochores and polar ejection forces dictate chromosome position on the vertebrate mitotic spindle. J Cell Biol 124: 223-233

Schrader F (1921) The chromosomes of *Pseudococcus nipae*. Biological Bulletin 40: 259-270

Sharp DJ, Ross JL (2012) Microtubule-severing enzymes at the cutting edge. J Cell Sci 125: 2561-2569.

Skibbens RV, Skeen VP, Salmon ED (1993) Directional instability of kinetochore motility during chromosome congression and segregation in mitotic newt lung cells: A push-pull mechanism. J Cell Bio 122: 859-875

Skibbens RV, Rieder CL, Salmon ED (1995) Kinetochore motility after severing between sister centromeres using laser microsurgery: evidence that kinetochore directional instability and position is regulated by tension. J Cell Sci 108: 2537-2548

Wong R, Forer A (2003) Backward chromosome movement in crane-fly spermatocytes after UV microbeam irradiation of the interzone and a kinetochore. Cell Biol Int 28: 293-298

CHAPTER 5

TITLE: Effects of ultraviolet microbeam irradiations of kinetochore fibres and kinetochores in *Mesostoma ehrenbergii* spermatocytes

AUTHOR: Jessica Ferraro-Gideon[1]

AUTHORS AFFILIATIONS: [1]Department of Biology, York University, Toronto, ON M3J 1P3, Canada

CORRESPONDENCE INFORMATION:
Jessica Ferraro-Gideon
Biology Department, York University
4700 Keele St.
Toronto, ON
M3J1P3
(905) 736-2100 ext 44643
ferraroj@yorku.ca

RUNNING TITLE: UV microbeam irradiation effects on *Mesostoma* chromosome movements and precocious cleavage furrows (87 Characters)

KEYWORDS: *Mesostoma ehrenbergii*, UV Microbeam, Precocious Cleavage Furrow, Signalling in spindles, spindle fibres

WORD COUNT (not including references): 6296

5.1 Abstract

I used an ultraviolet microbeam to irradiate kinetochore fibres and kinetochores in *Mesostoma ehrenbergii* spermatocytes. In these cells, kinetochores oscillate for a period of 1-2 hours throughout prometaphase. I irradiated *kinetochore fibres* as the kinetochore moved to the pole or away from the pole. Kinetochores stopped moving following irradiation as the kinetochore moved in either direction, but they did not stop at the site of irradiation, but first moved to the pole and then stopped. Kinetochore movement recovered when kinetochore fibres were irradiated as the kinetochore moved to the pole but not as the kinetochore moved away from the pole. The results were different when *kinetochores* were irradiated: half-bivalent kinetochores and their partners stopped on the spot, where they were irradiated, but movement did not recover. Kinetochore fibre and kinetochore irradiations not only altered kinetochore movement in *Mesostoma* spermatocytes but shifted the position of the precocious cleavage furrow and/or altered the shape of the cell. These results suggest that different mechanisms are required to produce kinetochore movement to and away from the pole and suggest that there is signalling both between partner kinetochores, and between spindle components and the precocious cleavage furrow.

5.2 Introduction

I have studied the effects of ultraviolet (UV) microbeam irradiations on chromosome movement in *Mesostoma ehrenbergii* spermatocytes as the UV microbeam has proven to be a useful tool to target specific spindle components, such as kinetochore fibres and kinetochores, without damaging the surrounding area or killing the cell. The ultraviolet (UV) microbeam has been used for decades by cell biologists to study spindle structure and chromosome movement and it has been widely used by Forer and colleagues to conduct experiments that provide evidence that refutes current microtubule-based chromosome movement models and supports a non-microtubule-based, spindle matrix model to describe chromosome movement (Forer and Wilson, 1994; Forer et al., 2008; Picket-Heaps et al. 1996). Most microtubule-based models, including the Pac-Man model (Rieder and Salmon, 1994) and the "flux model" (Cameron et al., 2006), propose that the kinetochore fibre microtubules produce the force driving chromosome motion (Mitchison et al., 1986). The spindle matrix model, on the other hand, proposes that the forces driving both flux and chromosome-to-pole motion arise from a spindle matrix that utilizes actin-based motility and its motor myosin to exert external forces on kinetochore microtubules (Forer et al., 2008). The spindle matrix model considers microtubules as rigid fibres that limit the rate of movement and whose rate of depolymerisation, a consequence of force production, governs the velocity of chromosome-to-pole motion (Forer et al., 2003; Forer et al., 2008; Pickett-Heaps and Forer, 2009).

Forer and colleagues demonstrated in crane fly spermatocytes that chromosomes still moved to the pole after irradiation of kinetochore fibres even though their kinetochore microtubules were severed (Sillers and Forer, 1983; Forer and Wilson, 1994; Picket-Heaps et al. 1996) indicating that kinetochores do not "chew" their way to the spindle pole as suggested by the Pac-Man model. In other experiments, remnant kinetochore stubs elongated towards their pole following UV irradiation of kinetochore fibres, indicating that tubulin subunits are added at the kinetochore and flux towards the pole (Forer et al., 1997). In addition to using the UV microbeam to refute models such as Pac-Man and flux, Forer and colleagues performed experiments using the UV microbeam to provide evidence that non-microtubule components may be involved in driving chromosome-to-pole movement as well as to provide evidence that a spindle matrix exists. The addition of actin and myosin inhibitors blocked kinetochore stub elongation indicating that flux requires actin and myosin (Forer et al., 2007). In newt and PtK fibroblasts, spindle poles moved closer together after microtubules across the entire half-spindle were severed (Spurck et al., 1990; Snyder et al., 1991) which indicates that there is a tensile element that extends throughout the spindle in the absence of microtubule continuity (Forer et al., 2008). In other experiments, newt fibroblast chromosomes accelerated to the pole when Forer et al. (2008) severed the kinetochore microtubules, as would be expected in the absence of microtubules.

I conducted UV microbeam experiments on *Mesostoma ehrenbergii* spermatocytes. The results of my experiments support the findings of Forer and

colleagues (Sillers and Forer, 1983; Forer and Wilson, 1994; Picket-Heaps et al. 1996) and provide further evidence to support a spindle matrix model. In my experiments, kinetochores continued to move toward the pole following irradiation of kinetochore fibres, suggesting that the force driving chromosome-to-pole motion arises from a spindle matrix. In addition, irradiation of kinetochore fibres or kinetochores resulted in a shift in the position of the precocious "pre-anaphase" cleavage furrow and in some cells a complete loss of the furrow. This suggests that a tensile element, the spindle matrix, may extend throughout the spindle and that shifts in furrow position and altered cell shape may be a response to alterations of the spindle matrix.

5.3 Materials and Methods

5.3.1 Living Cell Preparations

Mesostoma ehrenbergii spermatocytes were obtained from a laboratory stock of animals that were originally reared from diapausing (overwintering) eggs. *Mesostoma* were reared according to the protocol described by Hoang et al. (2013). Briefly, subsequent to hatching of the diapausing eggs, adult worms were kept in 500 mL plastic jars filled with dechlorinated water at 25°C in an incubator with a 16h light: 8h dark cycle. The worms were daily fed laboratory-reared brine shrimp. We obtained spermatocytes from *Mesostoma* that were 3 to 4 weeks old, since testes are most meiotically active at this age (Oakley and Jones 1982, Oakley 1985, Croft and Jones 1989). Glass needles of various sizes attached to Tygon tubing (Fisher Scientific) were

used to suck the testes through the body wall. Testes were expelled from the needle into a drop of *Mesostoma* Ringer's solution (61 mM NaCl, 2.3 mM KCl, 0.5 mM CaCl2, and 2.3 mM phosphate buffer, pH 6.9) that contained fibrinogen (Sigma-Aldrich, St. Louis, MO), on a 0.35mm thick (2.7cm x 2.5cm) quartz coverslip using the methods previously described by Forer and Pickett-Heaps (2005). Once the cells were evenly distributed in fibrinogen, a drop of thrombin (Sigma-Aldrich, St. Louis, MO) was added to create a fibrin clot. The coverslip was placed in a perfusion chamber and perfused with *Mesostoma* Ringer's solution.

5.3.2 UV Microbeam

The phase-contrast UV microbeam apparatus was previously described (Wilson and Forer, 1987). Briefly, the UV microbeam apparatus was attached to a Carl Zeiss model D inverted microscope. A 100-W mercury arc lamp in a modified Zeiss lamp housing provided the source of UV. During irradiation, light from the lamp passes through the open shutter and is focussed onto the entrance slit of the monochromator. The beam leaving the monochromator is focussed onto a 200μm diameter pinhole. The light from the pinhole passes to a quartz beam splitter which reflects the irradiating beam toward the objective and is focussed onto the specimen being irradiated. Initially, green light (λ=546 nm) was used to focus the microbeam on a scratched piece of mirror. Once the microbeam was focussed on the mirror, the wavelength was changed to UV (λ=310 nm), and the mirror was replaced by a piece of uranyl acetate in order to produce a

fluorescent image (Czaban and Forer, 1991) of the focussed UV, the position of which then was marked on the TV monitor as the site of irradiation. A glycerine-immersion Zeiss Ultrafluar 100x phase-contrast lens (N.A. 0.85) was used to focus the microbeam to an approximately 2 μm diameter circle. Cells were irradiated for 5 to 30 seconds with UV light of wavelength 280 nm or 290 nm. The energy of each irradiation was measured using a calibrated photocell attached to a picoammeter as described by Wilson and Forer (1987). The dose of each irradiation was calculated as the total energy delivered to the spermatocyte per area (of the focussed pinhole) measured in ergs/μm^2.

5.3.3 Photocell Calibrations

To calibrate a photocell, a manufacturer's calibrated photocell was first used to take readings. Light passing through the monochromator onto the calibrated photocell was measured in amperes. As the manufacturer supplied amps per watt values for the photocell, the amperes produced were converted into watts which determined the light energy incident on the photocell. Multiple readings at wavelengths from 300 nm to 260 nm were taken using two other photocells. The readings from the two other photocells were compared to the readings from the calibrated photocell. One photocell was then placed at the microscope stage and the readings on the stage were compared to those of the photocell used during irradiation: this gave a conversion factor for light incident on the photocell which was used during irradiation to determine light incident on the

spermatocyte and hence the dose of each irradiation. The total energy delivered to the spermatocyte per area (of the pinhole) was then calculated in ergs/μm^2.

5.3.4 Data Analysis

Images of living cells were recorded on DVD and then time-lapsed into video sequences using Virtual Dub (www.virtualdub.org/). Images were analysed using WinImage, an in-house software program (Wong and Forer, 2003), by marking the position of the kinetochore and marking a fixed point, the edge of the cell, which is where the centriole is (Ferraro-Gideon et al., 2013). The on-screen pixel spacing of the marked positions were then converted by the program into micrometers based on images of a micrometer slide. The micrometer measurements at the different time points were imported into SlideWrite (www.slidewrite.com/) to plot distances versus time. For the illustrations, individual bitmap image files (BMP) of *Mesostoma* spermatocytes preceding irradiation and following irradiation were imported into Adobe Photoshop CS3. The brush tool was used to create outlines around the spermatocytes to determine if the position of the precocious cleavage furrow shifted following irradiation.

5.4 Results

5.4.1 *Mesostoma ehrenbergii* spermatocytes

Mesostoma spermatocytes have 5 pairs of chromosomes, 3 bivalents with bipolar orientation and 4 unpaired univalents (Oakley and Jones, 1982; Fuge, 1987; Croft and

Jones, 1989), shown in Figure 5.1. In *Mesostoma* spermatocytes, bivalent kinetochores execute fast oscillatory movement to and from the spindle poles (Fuge 1987, Fuge 1989, Fuge and Falke 1991) for approximately one to two hours, from early prometaphase until anaphase (Ferraro-Gideon et al., 2013).

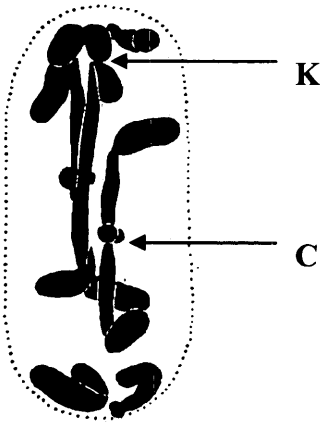

Figure 5.1. Picture of a fixed and sectioned *Mesostoma* spermatocyte taken from Husted and Ruebush (1940). Three bivalents and four univalents are visible. The arrow labelled (K) depicts the kinetochore and the arrow labelled (C) depicts the distally localised chiasma

Since there is no defined metaphase, the separation of half-bivalents to opposite poles (anaphase) usually occurs during an oscillation cycle (Ferraro-Gideon et al., 2013). Based on the cells used as controls for these experiments, kinetochores oscillate on average 4.6 μm to and away from the pole with an average velocity of 5.5 μm/min (range 1.6-14.1 μm/min), changing their direction of motion every 86 seconds (Table 5.1). More extensive data on controls cells that were analyzed throughout many years of observation are given in Ferraro-Gideon et al. (2013). Throughout prometaphase, univalent

chromosomes usually remain at the spindle poles but irregularly move between poles prior to anaphase onset (Oakley, 1983; Oakley, 1985), with velocities up to 20 μm/min.

Table 5.1. Velocity, amplitude and period of kinetochore movement to the pole and away from the pole of control cells in *Mesostoma* spermatocytes

Kinetochore Movement	Number of Kinetochores Measured	Range of Velocities (μm/min)	Average Velocity (μm/min)	Amplitude (μm)	Period (sec)
Away from the pole*	130	2.18-10.4	5.17±1.44	4.6 ±1.15	86 ±21.4
To the pole*	130	1.64-14.1	5.76 ±1.81		
Combined	260	1.64-14.1	5.48 ±1.66		
**Difference between to the pole and away from the pole kinetochore velocities is statistically significant at $p<0.01$, using Student's t-test.*					

5.4.2 Irradiation of a single kinetochore fibre

Ultraviolet microbeam experiments had not been previously conducted on *Mesostoma* spermatocytes. I irradiated single kinetochore spindle fibres with a wavelength of 290 nm as the kinetochore moved to or away from its spindle pole (Table 5.2). I varied the time of each irradiation from 5 to 30 seconds so the total energy delivered to the spermatocyte ranged between 1.0 to 2.0 ergs/μm^2. Kinetochores stopped moving after irradiation of their kinetochore fibre as the kinetochore moved in either direction. However, kinetochores did not stop on the spot, at their positions at the time of irradiation; rather, kinetochore movement stopped only after the kinetochore moved to the pole, at normal oscillation velocities, as graphically illustrated in Figures 5.2 and 5.3. Irradiations of single kinetochore fibres as the kinetochore moved to the pole resulted in

the temporary stoppage of movement at the pole of the half-bivalent associated with the irradiation. Irradiations of single kinetochore fibres as the kinetochore moved away from the pole, however, generally did not always result in stoppage of the kinetochore (Table 5.2). These inconsistencies were perhaps due to technical considerations as will be discussed later.

Table 5.2. Effects of UV microbeam irradiation on kinetochore movement following irradiation of the k-fibre as the kinetochore moves to the pole, irradiation of the k-fibre as the kinetochore moves away from the pole and irradiation of the kinetochore with wavelengths of 280nm and 290nm.

Irradiated *Mesostoma* Spermatocytes					**Kinetochores after Irradiation**
Irradiation	Total Number of Cells	Stopped Movement	Decreased Amplitude	No Effect	Number of Recovered Kinetochores
K-fibre as KT moves to the pole (290nm)	6	6	0	0	4/5
K-fibres as KT moves away from the pole (290nm)	13	5	3	5	0/5
Kinetochore (280nm)	9	9	0	0	0/9
Kinetochore (290nm)	4	2	0	2	0/2
***Chromosome movement is not altered when non-spindle components (chromosomes, chiasmata, univalents or cytoplasm) are irradiated (n=5).					

There was another difference dependent on the directionality of movement at the time of irradiation. Kinetochore movement resumed following kinetochore fibre irradiations only

when the irradiations occurred as the kinetochore moved to the pole. They did not resume after irradiations as the kinetochore moved away from the pole, as indicated in Table 5.2.

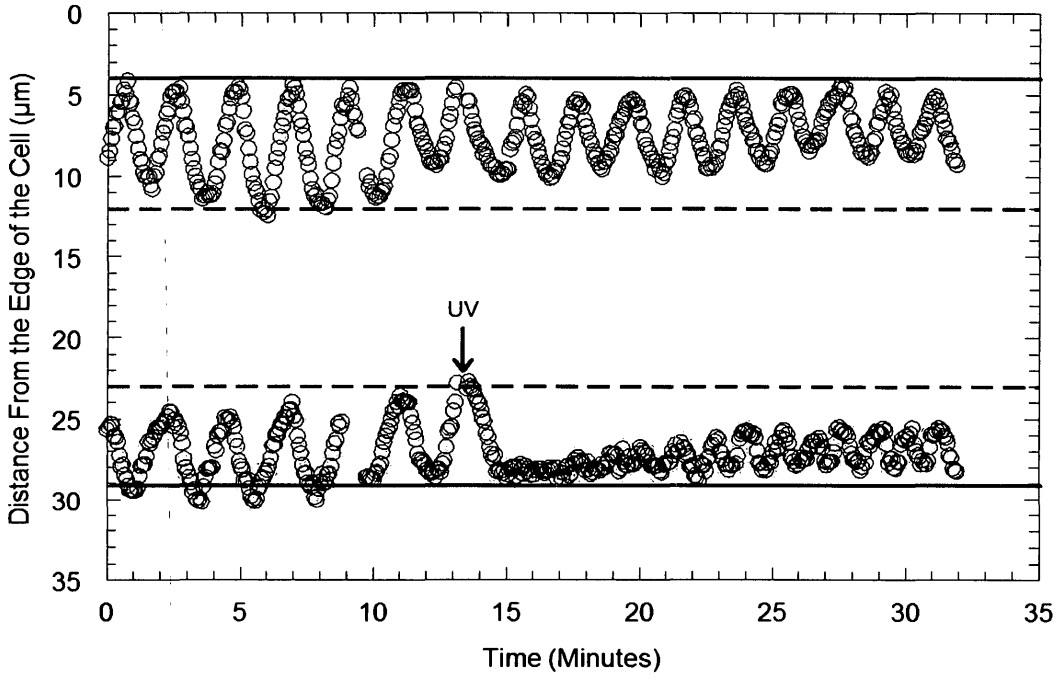

Figure 5.2. Single kinetochore fibre irradiation as the kinetochore moves to the pole in a *Mesostoma ehrenbergii* spermatocyte. Distance from the edge of the cell versus time for the irradiated half-bivalent and its partner. The arrow labelled UV indicates the time of irradiation (10s) for a single kinetochore fibre of the half-bivalent (O), as the kinetochore moves to the pole. Kinetochore movement to the pole was confirmed with a higher resolution image at the time of irradiation. The kinetochore associated with the irradiated half-bivalent stopped moving once it reached the pole and resumed oscillatory movement within approximately 5 minutes. The resumed movement has a decreased velocity, amplitude and period. The non-irradiated half-bivalent continues normal oscillatory movement with a period of 1-2 minutes, except the amplitude is decreased. The dotted lines are at the termini of the away-from-pole kinetochore oscillations prior to the irradiation. The poleward termini of the kinetochore oscillations prior to the irradiation are indicated by the solid lines.

Kinetochore movement resumed after approximately 5 minutes in 4/5 cells in which a kinetochore fibre was irradiated as the kinetochore moved to the pole. [In 1 cell, I did not

follow kinetochore movement long enough to determine if kinetochore movement resumed.] Recovered kinetochore oscillations were decreased an average of 23% in velocity, an average of 40% in amplitude and an average of 33% in period compared to pre-irradiation values.

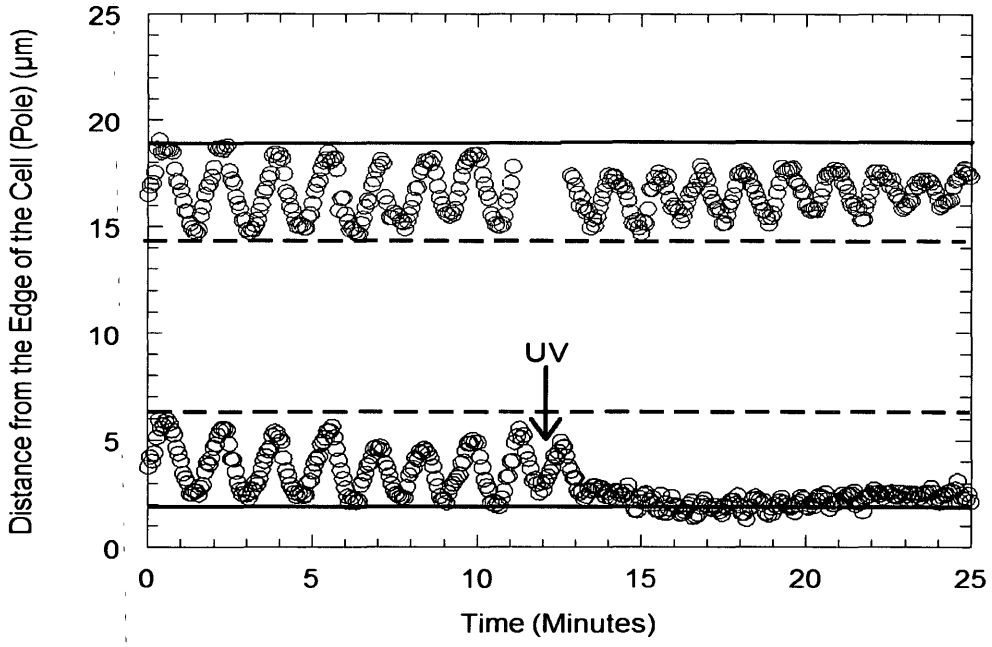

Figure 5.3. Single kinetochore fibre irradiation as the kinetochore moves away from the pole in a *Mesostoma ehrenbergii* spermatocyte. Distance from the edge of the cell versus time for the irradiated half-bivalent and its partner. The arrow labelled UV indicates the time of irradiation (12s) for a single kinetochore fibre of the half-bivalent (O), as the kinetochore moves away from the pole. The kinetochore continues to move away from the pole during the 12s irradiation but moves back to the pole immediately after the irradiation is complete. The kinetochore associated with the irradiated half-bivalent stopped moving once it reached the pole and movements did not resume. The partner half-bivalent continued normal oscillatory movement with a period of 1-2 minutes, except the amplitude is decreased. The dotted lines are at the termini of the away-from-pole kinetochore oscillations prior to the irradiation. The poleward termini of the kinetochore oscillations prior to the irradiation are indicated by the solid lines.

Kinetochore oscillations of the partners were normal after irradiation, except the oscillations decreased in amplitude (Figures 5.2 and 5.3). The reductions of partner oscillation amplitudes were different with the two directions of movement, however. For irradiation of the kinetochore fibre as the kinetochore moved to the pole, in all 3 cells with visible partners the movement to the pole continued to the before-irradiation positions but the away-from-the-pole movements did not: they terminated closer to the pole than they previously did (Figure 5.2). The converse was seen for irradiation of the kinetochore fibre as the kinetochore moved away from the pole; in both cells in which the partners were visible, the to-the-pole movements did not extend as close to the pole as before irradiation while the away-from-the-pole movement did (Figure 5.3). Overall, there are many similarities as well as differences on the affect of UV microbeam irradiations on kinetochore movement following irradiation of kinetochore fibres as the kinetochore moved to or away from the pole as outlined in Table 5.3.

There was exceptional kinetochore behaviour in one cell after irradiation of a single kinetochore fibre. In this cell, prior to irradiation a mono-oriented half-bivalent kinetochore moved from one pole to the other to achieve bi-polar orientation (Figure 5.4A-C). The reoriented kinetochore oscillated normally for 17 minutes and then its kinetochore fibre was irradiated (Figure 5.4D) with a dose of 4.8 ergs/μm^2, the highest dose of any irradiation. After the irradiation the associated kinetochore detached from the pole and moved to the opposite pole (Figure 5.4E) with a velocity nearly the same as the velocities of normal oscillation, as shown graphically in Figure 5.5. We assume that this

high UV power caused the kinetochore of the bivalent to become detached and move to the opposite pole. Unfortunately, I did not follow the cell longer than indicated in Figure 5.5.

Table 5.3. Comparison of the affect of UV microbeam irradiation on kinetochore movement following irradiation of kinetochore fibres as the kinetochores move to the pole or away from the pole.

	Type of Kinetochore Fibre Irradiation	
	Kinetochore Moved To the Pole	**Kinetochore Moved Away from Pole**
Wavelength Used	290nm	290nm
Affect of Irradiation on Kinetochore Movement	Stopped Kinetochore Movement	No Effect, Decrease in Amplitude of Oscillations, Stopped Kinetochore Movement
Position of Stopped Kinetochore Movement	At the Pole	At the Pole
Resumed Kinetochore Movement	Yes	No
Effect of Irradiation on Partner Kinetochore Movement	Decreased Amplitude of Oscillations	Decreased Amplitude of Oscillations
Direction in which the Terminus of Oscillations Decreased	Away from the Pole	To the Pole

5.4.3 Irradiation of a Kinetochore

Half-bivalent kinetochores were irradiated in *Mesostoma* spermatocytes with wavelengths of either 280nm or 290nm, as indicated in Table 5.2. After irradiation with

UV of wavelength 280nm, kinetochore movement stopped on the spot, in all 9 cells; the kinetochore then moved slowly to the pole and stopped at the pole (Figure 5.6).

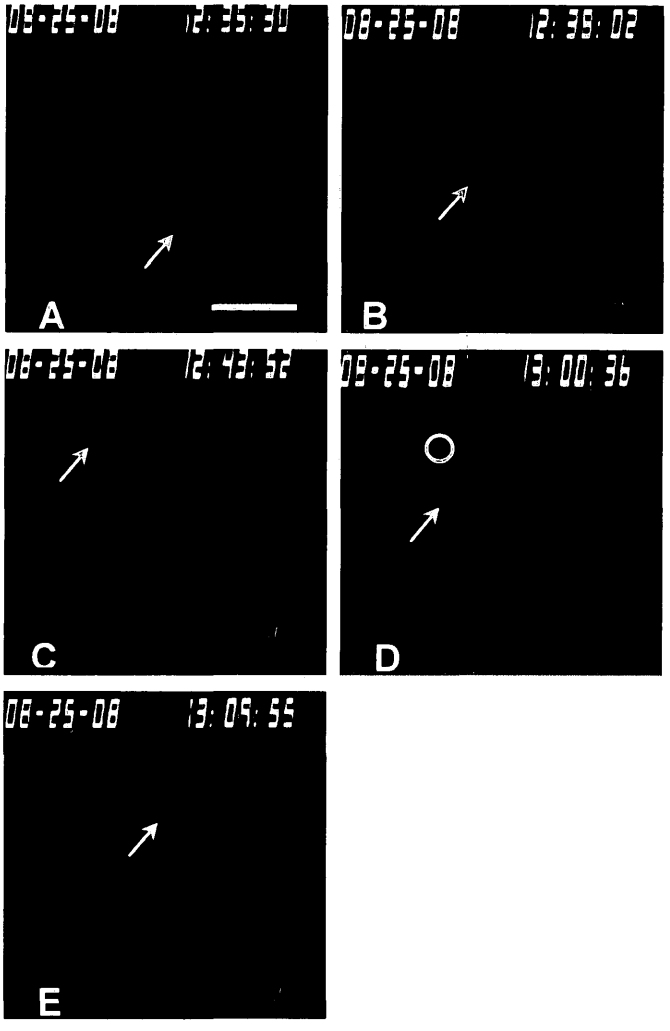

Figure 5.4. Phase-contrast microscope pictures of a *Mesostoma* spermatocyte. The arrow in each frame indicates the kinetochore of the half-bivalent. (A-C) The kinetochore of the half-bivalent extends to the opposite pole to achieve bipolar orientation. (D) Approximately 17 minutes later the kinetochore fibre was irradiated for 15s at 290nm as indicated by an O. (E) Following irradiation, the kinetochore associated with kinetochore fibre irradiation detached from the upper pole and moved back across the equator to the opposite pole. The white bar in (A) is 10μm.

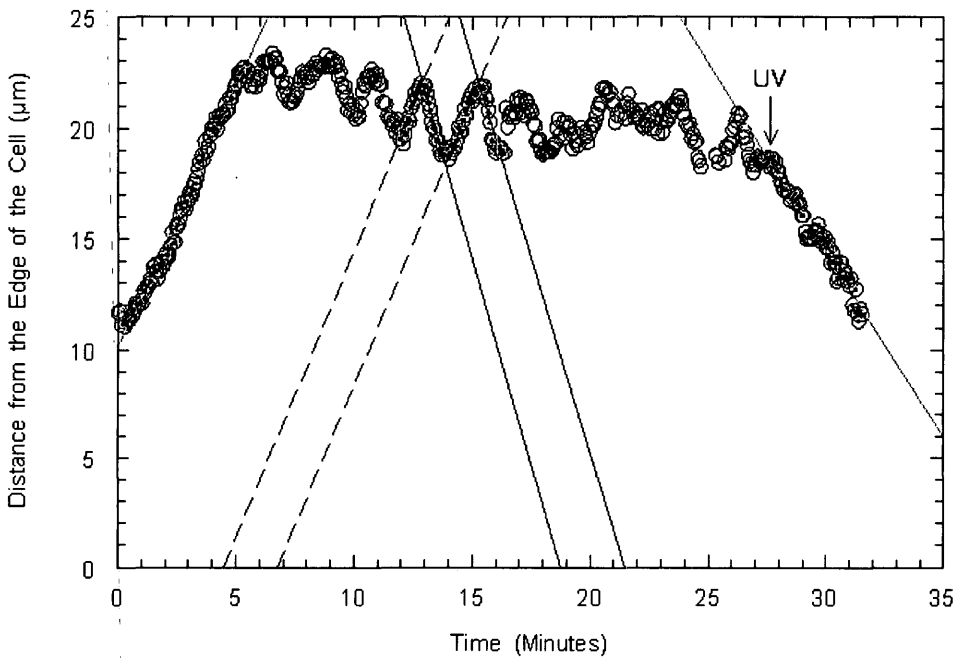

Figure 5.5. Distance from the pole versus time graph for the image sequence seen in Figure 5.4. The arrow labelled UV indicates the time of irradiation (15s). The graph illustrates the kinetochore of a half-bivalent orienting towards the opposite pole with a velocity of 2.3 µm/min and the detachment of the kinetochore associated with the kinetochore fibre irradiation towards the opposite pole following irradiation with a velocity of 1.7 µm/min. These velocities are slower than the average velocities of kinetochore movement to and away from the pole, 2.9 µm/min and 3.1 µm/min respectively.

The slow poleward movements of irradiated kinetochores had average velocities of 0.42±0.33 µm/min (n=5), one-twelfth the average velocities of normal oscillations. In 2 cells in which the partner kinetochore was visible, kinetochore movement of the partner decreased in amplitude immediately following irradiation. The partner then moved away from its pole as the irradiated kinetochore moved to its pole, both with the same velocity. The partner resumed oscillations with greatly reduced amplitude once the irradiated

kinetochore reached the pole (Figure 5.6), but no irradiated kinetochore ever resumed oscillations for as long as I followed them (up to 25 minutes).

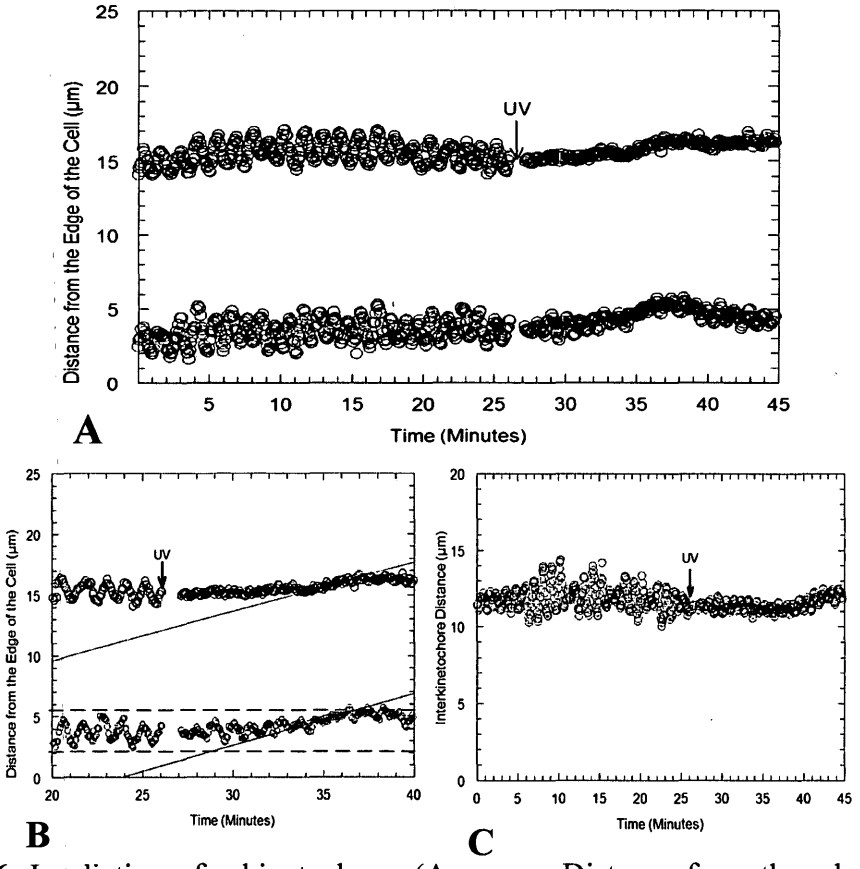

Figure 5.6. Irradiation of a kinetochore. (**A** and **B**) Distance from the edge of the cell versus time for the irradiated half-bivalent and its partner in a *Mesostoma ehrenbergii* spermatocyte. The arrow labelled UV indicates the time of irradiation (12s) for a kinetochore of the half-bivalent (**O**). The irradiated half-bivalent kinetochore stopped moving on the spot, then slowly moved to the pole with a velocity of 0.4 µm/min and stopped moving once it reached the pole. Kinetochore movement of the non-irradiated half-bivalent decreased in amplitude immediately following irradiation of the kinetochore of its partner half-bivalent, stopped oscillations briefly at 34 minutes (see **B**), moved away from its pole at a velocity of 0.4 µm/min, and once its partner reached the pole (at about 37 minutes) it resumed oscillation, though with reduced amplitude. The chromosome became longer, too. (**C**) Interkinetochore distance versus time for the irradiated half-bivalent and its partner in the same *Mesostoma ehrenbergii* spermatocyte showing that the overall chromosome length increased once the irradiated kinetochore reached the pole (at about 37 minutes).

I extended the kinetochore irradiation results to UV of wavelength 290nm, as different wavelengths (260nm-290nm) have been shown to have different effects on chromosome movement and on producing areas of reduced birefringence (Sillers and Forer, 1983). Effects were not consistent after I irradiated kinetochores with UV of wavelength 290nm: in 2/4 cells, kinetochore movement stopped and did not recover (Figure 5.7A) and in 2/4 cells, there was no effect on kinetochore movement (Figure 5.7B), as seen in Table 5.2. When kinetochore movement was stopped following irradiation, kinetochore movement stopped on the spot, the kinetochore then moved slowly towards the pole and stopped at the pole (Figure 5.7A) as seen consistently following irradiations of kinetochores with UV of wavelength 280nm. However, in one cell when kinetochore movement was not affected by UV of wavelength 290nm, I challenged the same kinetochore with UV of wavelength 280nm and it stopped on the spot following the second irradiation (Figure 5.7B),

5.4.4 Changes in the 'precocious' cleavage furrow and cell shape following irradiation

The cells in which single kinetochore fibres and kinetochores themselves were irradiated were analyzed to determine if the position of the 'precocious' cleavage furrow changes in response to irradiation of spindle components, as they do when the distribution of chromosomes changes (Forer and Pickett-Heaps, 2010). Cells that did not have furrows or furrows that could not be measured accurately were not included. In more than half the cells the cleavage furrow shifted position after irradiation, but the

results were variable in that there was either a shift toward the site of irradiation or a shift away from the site of irradiation (Table 5.4).

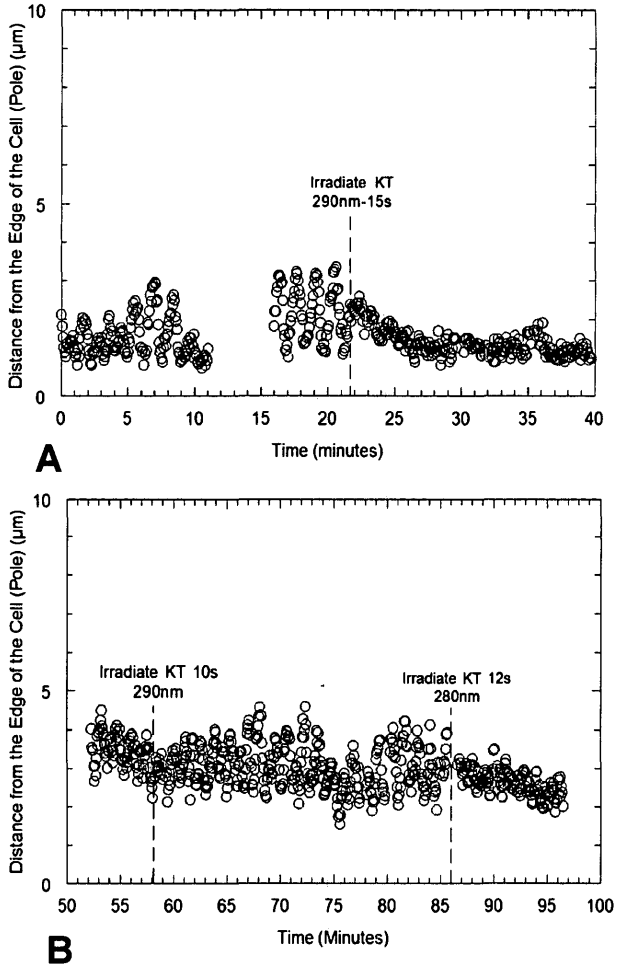

Figure 5.7. Irradiation of a kinetochore in a *Mesostoma* spermatocyte. Distance from the edge of the cell versus time for the irradiated half-bivalent. **(A)** The arrow labelled UV indicates the time of irradiation (15s) for a kinetochore of the half-bivalent (**O**). The irradiated half-bivalent kinetochore stopped moving on the spot, then slowly moved to the pole with a velocity of 0.18 µm/min and stopped moving once it reached the pole. **(B)** The arrow labelled UV indicates the time of irradiation (10s and 12s, respectively) for a kinetochore of the half-bivalent (**O**). The irradiated half-bivalent kinetochore continued oscillatory movement after irradiation with UV of wavelength 290nm but stopped moving on the spot after irradiation with UV of wavelength 280nm.

Table 5.4. Effects of UV microbeam irradiation on the position of the 'precocious' cleavage furrow and cell shape following irradiation of the k-fibre as the kinetochore moves to the pole, irradiation of the k-fibre as the kinetochore moves away from the pole and irradiation of the kinetochore. Changes in the position of the furrow or cell shape are independent of altered kinetochore movement. Cells that did not have furrows or furrows that could not be measured accurately were not included.

Irradiation	Total Number of Cells		Shifts *towards* Site of Irradiation		Shifts *away* from Site of Irradiation		No Change in Position		Change in Cell Shape	
	Total	Movement Altered	Total	Movement Altered	Total	Movement Altered	Total	Movement Altered	Total	Movement Altered
K-fibre as KT moves to the pole (290nm)	6	6	1	1	2	2	3	3	0	0
K-fibre as KT moves away from the pole (290nm)	12	7	2	2	5	3	5	2	5	4
Kinetochore (280nm)	8	8	2	2	3	3	3	3	6	6
Kinetochore (290nm)	2	1	1	1	0	0	1	0	2	1
TOTAL	**28**	**22**	**6** (21%)	**6** (27%)	**10** (36%)	**7** (32%)	**12** (43%)	**8** (36%)	**13** (46%)	**11** (50%)

***Cleavage furrows do not change position when non-spindle components (chromosomes, chiasmata, univalents and cytoplasm) are irradiated (n=5).

A shift in the cleavage furrow away from the site of irradiation is shown in Figure 5.8 and toward the site of irradiation in Figure 5.9. Spermatocytes sometimes changed shape after the irradiation, but only following irradiation of kinetochore fibres as the kinetochore moved away from the pole, or following irradiation of the kinetochore (Table 5.4). When the cell shape changed, immediately following irradiation the cleavage furrow moved from its position toward or away from the irradiation site; then the precocious furrow lost its indentation (Figure 5.10).

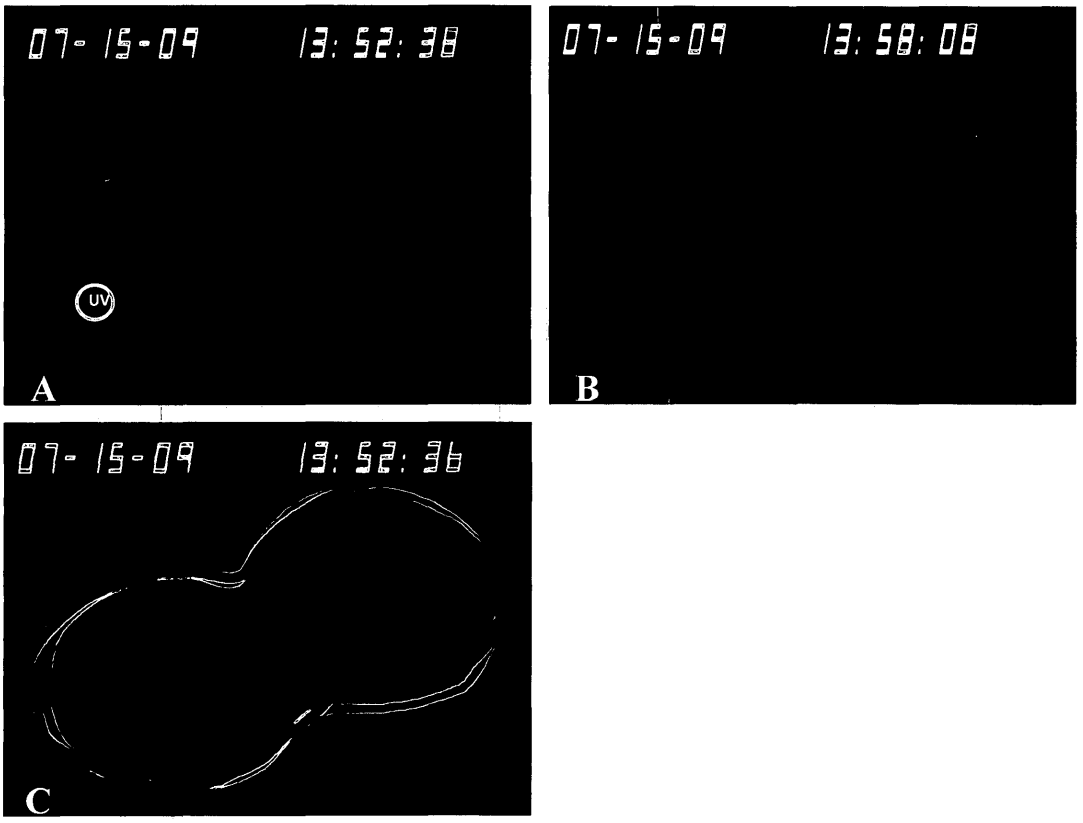

Figure 5.8. Phase contrast microscope pictures of a *Mesostoma* spermatocyte illustrating a change in the position of the cleavage furrow following irradiation of the k-fibre as the kinetochore moved away from the pole. (A) *Mesostoma* spermatocyte prior to irradiation. The circle indicates the site of irradiation. The k-fibre was irradiated for 12s starting at 13:54:20as the kinetochore moved away from the pole. (B) *Mesostoma* spermatocyte following irradiation. (C) The outlines were created using the brush tool on Photoshop. The yellow outline depicts the spermatocyte prior to irradiation and the purple outline depicts the spermatocyte after irradiation. The cleavage furrow moved away from the site of irradiation.

Shifts in the position of the cleavage furrow were not observed following irradiation of non-spindle components (n=5), including chromosomes, chiasmata, univalents and the cytoplasm; therefore shifts in the position of the cleavage furrow must be in response to altered spindle components.

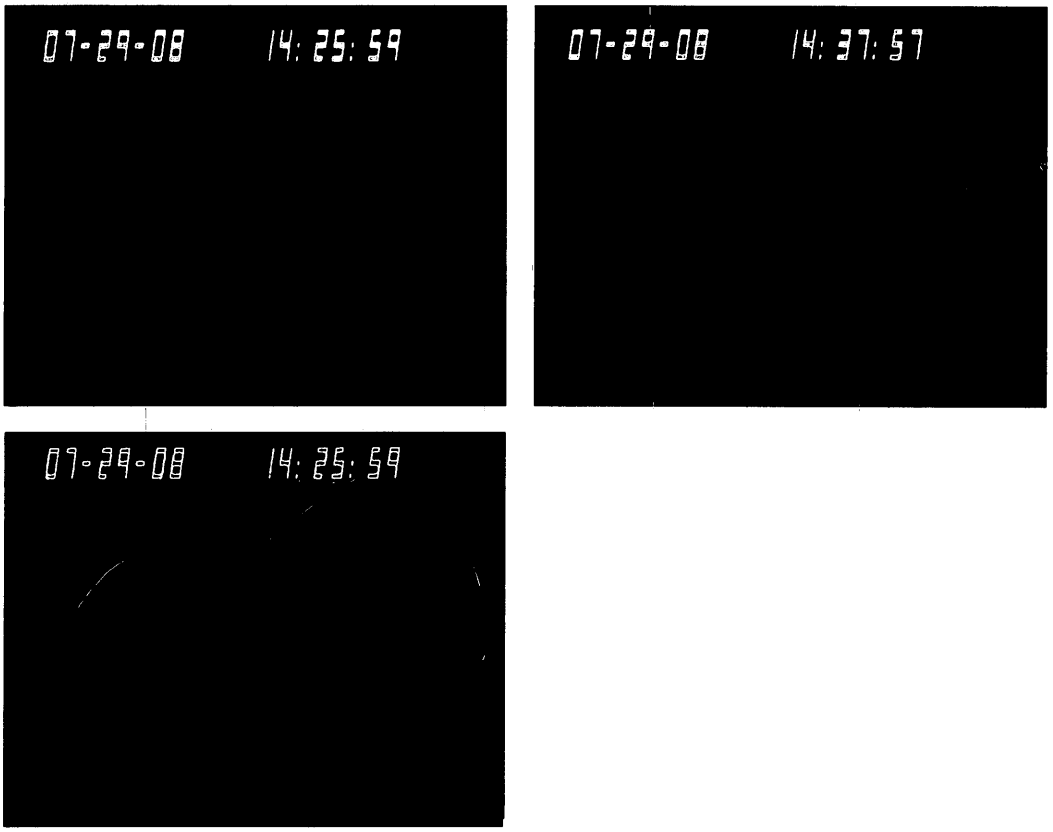

Figure 5.9. Phase contrast microscope pictures of a *Mesostoma* spermatocyte illustrating a change in the position of the cleavage furrow following irradiation of the k-fibre as the kinetochore moves to the pole. (A) *Mesostoma* spermatocyte prior to irradiation. The circle indicates the site of irradiation. The k-fibre was irradiated at 14:35:03 for 10s as the kinetochore moved to the pole. (B) *Mesostoma* spermatocyte following irradiation. Kinetochore stopped at the pole following irradiation and movement resumed after approximately 5 minutes. (C) The outlines were created using the brush tool on Photoshop. The yellow outline depicts the spermatocyte prior to irradiation and the pink outline depicts the spermatocyte after irradiation. The cleavage furrow moved toward the site of irradiation.

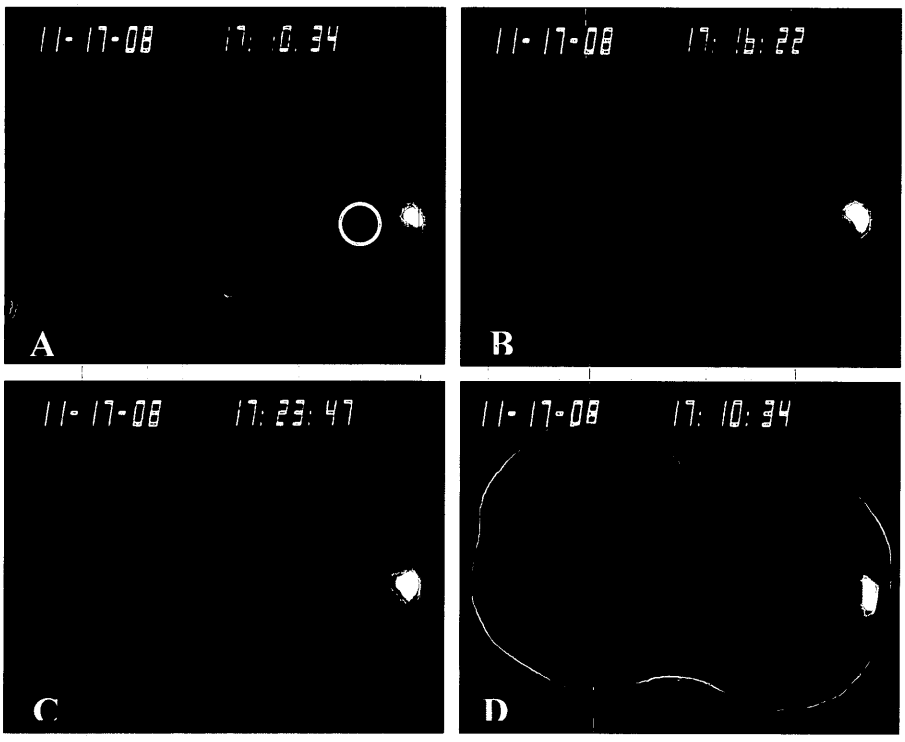

Figure 5.10. Phase contrast microscope pictures of a *Mesostoma* spermatocyte illustrating a change in the position of the cleavage furrow following irradiation of the kinetochore. (A) *Mesostoma* spermatocyte prior to irradiation. The circle indicates the site of irradiation. The kinetochore was irradiated at 17:14:36 for 20s. (B) *Mesostoma* spermatocyte immediately following irradiation. Kinetochore stopped at the pole and kinetochore movement did not resume. (C) *Mesostoma* spermatocyte, 9 minutes following irradiation of the kinetochore. (D) The outlines were created using the brush tool on Photoshop. The black outline depicts the spermatocyte prior to irradiation, the pink outline depicts the spermatocyte immediately after irradiation and the green outline depicts the spermatocyte 9 minutes after irradiation. The cleavage furrow shifts positions immediately after irradiation (pink outline). Ingression of the cleavage furrow is completely lost, the spermatocyte becomes round in shape and the poles moved closer together as seen by the green outline in comparison to the black outline.

Although shifts in the position of the cleavage furrow were observed only following irradiation of spindle components, shifts in the position of the cleavage furrow were independent of altered kinetochore movement following irradiation (Table 5.4). The cleavage furrow shifted its position following irradiation of spindle components in

spermatocytes both when kinetochore movement was altered by the irradiation and when kinetochore movement was not altered (Table 5.4). This suggests that the 'signal' to shift the furrow position is in response to alteration to some spindle component and not the stoppage of kinetochore oscillations.

A shift in the position of the cleavage furrow after irradiation of kinetochore fibres or kinetochores occurred predominately on one side of the spermatocyte and infrequently on both sides (Table 5.5).

Table 5.5. Position of the 'precocious' cleavage furrow after irradiation of k-fibres and kinetochores. The furrow can shift on both sides of the cell but primarily shifts only on one side. When the furrow shifts on one side, it can either shift on the side of the irradiation or on the side opposite to the irradiation.

		Kinetochore Fibre	Kinetochore	TOTAL	
Both Sides Shift		0	2		**2/15** (13%)
One Side Shifts	On UV Side	4	5	**9/13** (69%)	**13/15** (87%)
	Opposite to UV Side	3	1	**4/13** (31%)	

These one-sided shifts in the position of the furrow usually occur on the same side of the cell as the irradiation (Table 5.5) with an average shift of 1.2μm from its original position (Figure 5.11) either immediately or up to five minutes after irradiation of kinetochore fibres or kinetochores (Figure 5.12). Further studies using confocal immunofluorescence microscopy and electron microscopy could help us better understand which spindle

components need to be altered to alter kinetochore movement and which spindle components to change the position of the furrow.

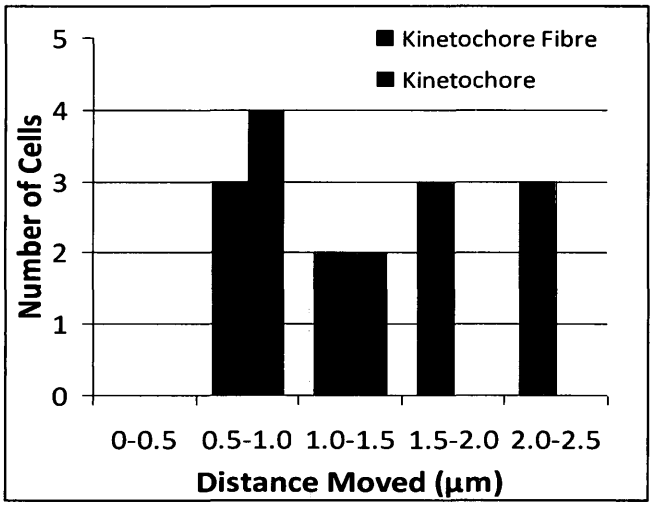

Figure 5.11. Distance the precocious' cleavage furrow moves following irradiation of the k-fibre as the kinetochore moves to the pole, irradiation of the k-fibre as the kinetochore moves away from the pole and irradiation of the kinetochore. The furrow shifts an average of 1.23μm.

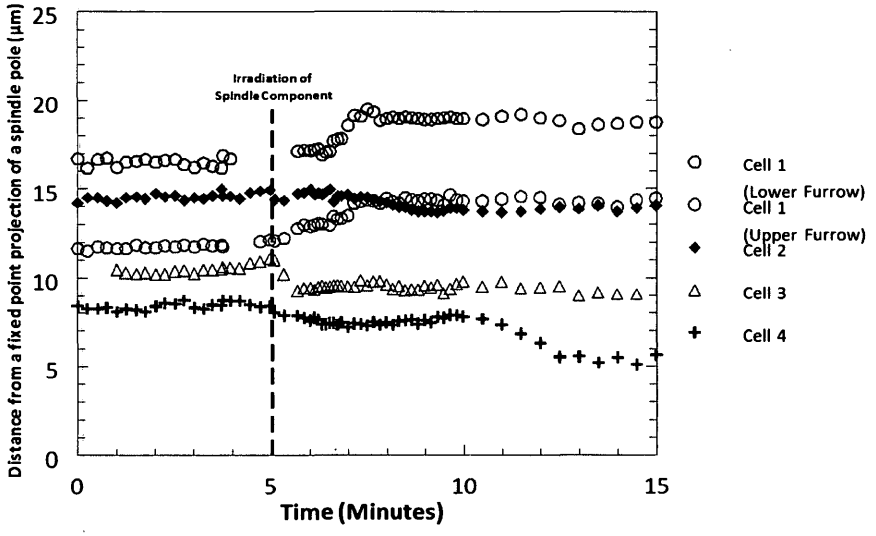

Figure 5.12. Time (minutes) it takes for the furrow to shift positions after irradiation of either a kinetochore fibre or kinetochore. The dotted line indicates the time of irradiation. The furrow shifted positions either immediately (Δ) or up to 5 minutes after irradiation (+).

5.5 Discussion

UV irradiation of kinetochore fibres and kinetochores in *Mesostoma* spermatocytes stopped kinetochore movement, shifted the position of the precocious cleavage furrow and altered the shape of the cell. Kinetochore movement was temporarily stopped after irradiation of single kinetochore fibres as the kinetochore moved to the pole but was irreversibly blocked following irradiation of kinetochores or after irradiations of kinetochore fibres as the kinetochore moved away from the pole. Partner kinetochore movement was stopped following irradiation of kinetochores only. UV irradiation of kinetochores or of kinetochore fibres as the kinetochore moved away from the pole seemed to have the strongest affect: kinetochore movement did not recover, the cleavage furrow regressed and the cell lost its shape.

Kinetochores moved to the pole and then stopped, even though their associated kinetochore fibre was irradiated (Figures 5.2 and 5.3). I do not know what the irradiations do; however, if the irradiations have depolymerised microtubules in the irradiated region in *Mesostoma* spermatocytes as in other cells-- crane fly spermatocytes, *Haemanthus*, PtK cells and newt fibroblast cells (Bajer and Molé-Bajer , 1986; Czaban et al., 1993; Forer et al., 2003; Snyder et al., 1991; Spurck et al., 1990; Wilson and Forer, 1988)-- then this suggests that kinetochore movement to the pole can occur in the absence of microtubules. If the irradiations do not depolymerise kinetochore microtubules, then they have altered something else that stops kinetochore movement. Either way, my data suggest that several components are involved in producing kinetochore movement in

Mesostoma spermatocytes. These results are in agreement with previous results obtained by Forer and colleagues in crane-fly spermatocytes; chromosomes continued to move to the pole following irradiation of kinetochore fibres that depolymerised kinetochore microtubules (Forer, 1966; Sillers and Forer, 1983; Spurck et al., 1997).

Irradiation of a single kinetochore fibre as the kinetochore moved in either direction resulted in stopped kinetochore movement at the pole; kinetochore movement, however, only resumed when single kinetochore fibres were irradiated as the kinetochore moved in one direction, to the pole (Table 5.3, Figure 5.2). These results suggest that kinetochore movement to and away from the pole are different and therefore, different mechanisms produce movement to and away from the pole in *Mesostoma* spermatocytes. If kinetochore movement stopped at the pole regardless of the direction the kinetochore was moving prior to the irradiation, then why did kinetochore movement only resume when the kinetochore fibre was irradiated when moving only in one direction? Since kinetochore movement was only temporarily stopped as the kinetochore moved to the pole, this suggests that the mechanism to produce poleward movement was repaired, allowing kinetochore movement to resume. In crane-fly spermatocytes, microtubules and actin were absent in the irradiated region following UV irradiation of kinetochore fibres (Forer et al., 2003). If both microtubules and actin work together to produce kinetochore movement in *Mesostoma* spermatocytes then damage to these components from UV irradiation must have different effects depending on the direction the kinetochore is moving at the time of the irradiation. Further studies using confocal immunofluorescence

microscopy and electron microscopy may help us better understand which mechanisms are involved in kinetochore movement to the pole and kinetochore movement away from the pole.

Irradiation of one kinetochore in *Mesostoma* spermatocytes stopped kinetochore movement of that one half-bivalent kinetochore and also stopped its partner. Since movements of partner kinetochores were not affected following irradiation of kinetochore fibres, kinetochores may play an important role in communication by 'signalling' to their partners. Signalling between kinetochores exists in crane-fly spermatocytes (Yin and Forer, 1996; Wong and Forer, 2003); irradiation of one kinetochore stopped kinetochore movement of all 6 half-bivalents (Ilagan and Forer, 1997). There are differences, however, between these two cells. In *Mesostoma* spermatocytes, the only kinetochore that is 'signalled' to is attached to the irradiated kinetochore: there is no signalling between kinetochores that are unattached since movement of these kinetochores is not affected. In crane-fly spermatocytes, the signalling occurs between unattached kinetochores since all six bivalents stop movement. There is another difference. Kinetochore movement of all 6 half-bivalents recovered in crane-fly spermatocytes, unlike stopped kinetochore movement of the irradiated half-bivalent kinetochore and its partner in *Mesostoma* spermatocytes. A physical linkage between kinetochores seems to be required for 'signalling' between kinetochores in *Mesostoma* spermatocytes. Fuge (1987, 1989) suggested that tension is required for kinetochore oscillations to take place in *Mesostoma* spermatocytes so one might think that kinetochores send signals based on the degree of

tension within this physical linkage. This does not seem to be the case, however, because there is a lack of tension after kinetochore fibres are UV irradiated and the one kinetochore is motionless at the pole. This indicates that partner kinetochores are affected following irradiation of kinetochores but not following irradiation of kinetochore fibres because of some 'signalling' property of the kinetochore. Signalling may also exist between spindle components and the precocious cleavage furrow in *Mesostoma* spermatocytes because irradiation of kinetochore fibres and of kinetochores both alter the position of the furrow. Changes in the position of the precocious cleavage furrow were originally observed in *Mesostoma* spermatocytes by Forer and Pickett-Heaps (2010) when the distribution of univalent chromosomes changed at the spindle poles. In other experiments, cleavage furrows shifted towards the aster-less pole in sand-dollar embryos following single centrosome irradiations (von Dassow et al., 2009). In both cell types, the furrow shifted towards the pole that either lost a univalent (Forer and Pickett-Heaps, 2010) or an aster (von Dassow et al., 2009). In the cells I studied, the furrow either shifted towards or away from the site of irradiation; therefore, different signals must be sent to the furrow from altered spindle components and segregating univalents. Signals sent to the furrow from altered spindle components are also independent of stopped kinetochore movement. This suggests that irradiations that alter spindle components stimulate signals that either stop kinetochore movement, or shift the position of the furrow, or both.

In addition to signalling between UV irradiated spindle components and the precocious cleavage furrow, shifts in furrow position and altered cell shape may be a response to the disruption in the structural tensegrity of the cell by the irradiation. As a result, the cell alters its shape until forces within the cell once again reach equilibrium (Ingber, 1993). An underlying spindle-like structure composed of the nuclear proteins Megator and Skeletor persists in *Drosophila* when microtubules are depolymerized, indicating that there is a basic spindle structure, a spindle matrix, independent from the spindle microtubules. In *Mesostoma* spermatocytes, the spindle matrix may respond to UV irradiation of spindle components by shifting the position of the furrow and altering cell shape to try to maintain the normal balance of forces within the spindle so non-irradiated bivalents can continue to oscillate normally. Based on my results however, it is still unclear which spindle components alter kinetochore movement and which spindle components change the position of the furrow. Further studies using confocal immunofluorescence microscopy on irradiated *Mesostoma* spermatocytes may help to better understand which spindle components are involved.

The UV microbeam experiments performed on *Mesostoma* spermatocytes suggest different mechanisms are required to produce kinetochore movement to and away from the pole. Signalling between kinetochores is present when there is a physical linkage connecting half-bivalent kinetochores and signalling between spindle components and the precocious cleavage furrow is responsible for spindle positioning and maintaining cell shape.

5.6 References

Bajer, A. and Molè-Bajer, J. (1961). UV microbeam irradiation of chromosomes during mitosis in endosperm. Exp Cell Res. **25**, 251-267.

Bajer, A. S. and Molé-Bajer, J. (1986). Reorganization of microtubules in endosperm cells and cell fragments of the higher plant *Haemanthus* in vivo. J. Cell Biol. **102**, 263-281.

Cameron, L.A., Yang, G, Cimini, D., Canman, J.C., Kisurina-Evgenieva, O., Khodjakov, A., Danuser, G. and Salmon, E.D. (2006). Kinesin 5-independent poleward flux of kinetochore microtubules in PtK1 cells. J Cell Biol. **173**, 173-179.

Croft, J.A. and Jones, G.H. (1989). Meiosis in *Mesostoma ehrenbergii ehrenbergii* IV. Recombination nodules in spermatocytes and a test of the correspondence of late recombination nodules and chiasmata. Genetics. **121**, 255-262.

Czaban, B. and Forer, A. (1991). Visualization of ultraviolet microbeam irradiation sites with uranyl acetate. Journal of Microsc. **164**, 61-65.

Czaban, B., Forer, A. and Bajer, A.S. (1993). Ultraviolet microbeam irradiation of chromosomal spindle fibres n *Haemanthus katherinae* endosperm. J Cell Sci. **105**, 571-587.

Ferraro-Gideon, J., Hoang, C., and Forer A. (2013). Meiosis-I in *Mesostoma ehrenbergii* spermatocytes includes distance segregation and inter-polar movements of univalents, and vigourous oscillations of bivalents. Protoplasma. Accepted.

Forer, A. (1966). Characterization of the mitotic traction system, and evidence that birefringent spindle fibres neither produce nor transmit force for chromosome movement. Chromosoma. **19**, 44-98.

Forer, A. and Pickett-Heaps, J. (2005). Fibrin clots keep non-adhering living cells in place on glass for perfusion or fixation. Cell Biol Int. **29**, 721–730.

Forer, A. and Wilson, P.J. (1994). A model for chromosome movement during mitosis. Protoplasma. **179**, 95-105.

Forer, A., Pickett-Heaps, J.D. and Spurck, T. (2008). What generates flux of tubulin in kinetochore microtubules? Protoplasma. **232**, 137-141.

Forer, A., Spurck, T., and Pickett-Heaps, J.D. (1997). Ultraviolet microbeam irradiations of spindle fibres in crane-fly spermatocytes and newt epithelial cells: resolution of previously conflicting observations. Protoplasma. **197,** 230–240.

Forer, A., Spurck, J.D. and Pickett-Heaps, J.D. (2007). Actin and myosin inhibitors block elongation of kinetochore fibre stubs in metaphase crane-fly spermatocytes. Protoplasma. **232**, 79-85.

Forer, A., Spurck, T., Pickett-Heaps, J.D. and Wilson, P.J. (2003). Structure of kinetochore fibres in crane-fly spermatocytes after irradiation with an ultraviolet microbeam: neither microtubules nor actin filaments remain in the irradiated region. Cell Motil Cytoskeleton. **56**, 173-192.

Fuge, H. (1987). Oscillatory movement of bipolar-oriented bivalent kinetochores and spindle forces in male meiosis of *Mesostoma ehrenbergii*. Euro J Cell Biol. **44,** 294-298.

Fuge, H. (1989). Rapid kinetochore movements in *Mesostoma ehrenbergii* spermatocytes: Action of antagonistic chromosome fibre. Cell Motil Cytoskeleton **13**, 212-220.

Fuge, H. and Falke, D. (1991). Morphological aspects of chromosome spindle fibres in *Mesostoma*: "Microtubular fir-tree" structures and microtubule association with kinetochores and chromatin. Protoplasma. **160**, 39-48.

Hoang, C., Ferraro-Gideon, J., Gauthier, H. and Forer, A. (2013). Methods for rearing *Mesostoma ehrenbergii* in the laboratory for cell biology experiments, including identification of factors that influence production of different egg types. Cell Biol Int. Accepted.

Ilagan, A.B. and Forer, A. (1997). Effects of ultraviolet-microbeam irradiation of kinetochores in crane-fly spermatocytes. Cell Motil Cytoskeleton. **36**, 266-275.

Ingber, D.E. (1993). Cellular tensegrity: defining new rules of biological design that govern the cytoskeletom. J Cell Sci. **104**, 613-627.

Izutsu, K. and Sato, H. (1992). Rapid backward movement of anaphase chromosomes whose kinetochore fibers were cut by ultraviolet microbeam irradiation. Protoplasma Suppl. **1**, 122-132.

Mitchison, T.J., Evans, L., Schulze, E. and Kirschner, M. (1986). Sites of microtubule assembly and disassembly in the mitotic spindle. Cell. **45**, 515-527.

Oakley, H. (1983). Male meiosis in *Mesostoma ehrenbergii ehrenbergii*. In: Kew Chromosome Conference II, ed. PE Brandham and MD Bennett. London: George Allen and Unwin, 195–199.

Oakley, H. (1985). Meiosis in *Mesostoma ehrenbergii ehrenbergii* (Turbellaria, Rhabdocoela) III. Univalent chromosome segregation during the first meiotic division in spermatocytes. Chromosoma. **91**, 95–100.

Oakley, H.A. and Jones, G.H. (1982). Meiosis in *Mesostoma ehrenbergii ehrenbergii* (Turbellaria, Rhabdocoela) I. Chromosome pairing, synaptonemal complexes and chiasma localisation in spermatogenesis. Chromosoma (Berl.). **85**, 311-322.

Pickett-Heaps, J.D., Forer, A. and Spurck, T. (1996). Rethinking anaphase:where "PAC-MAN" fails and why a role for the spindle matrix is likely. Protoplasma. **192**, 1–10.

Rieder, C.L. and Salmon, E.D. (1994). Motile kinetochores and polar ejection forces dictate chromosome position on the vertebrate mitotic spindle. J Cell Biol **124**, 223-233.

Sillers, P.J. and Forer, A. (1983). Action spectrum for changes in spindle fibre birefringence after ultraviolet microbeam irradiations of single chromosomal spindle fibres in crane-fly spermatocytes. J Cell Sci. **62**, 1-25.

Snyder, J.A., Armstrong, L., Stonington, O.G. Spurck, T.P., Pickett-Heaps, J.D. (1991). UV-microbeam irradiations of the mitotic spindle: spindle forces and structural analysis of lesions. Eur J Cell Biol. **55**, 122-132.

Spurck, T.P., Stonington, O.G., Snyder, J.A., Pickett-Heaps, J.D., Bajer, A., Mole-Bajer, J. (1990). UV microbeam irradiation of the mitotic spindle. II. Spindle fiber dynamics and force production. J Cell Biol. **111**: 1505-1518.

von Dassow, G., Verbrugghe, K.J.C., Miller, A.L., Sider, J.R., Bement, W.M. (2009). Action at a distance during cytokinesis. J Cell Biol. **187**, 831-845.

Wilson, P. and Forer, A. (1987). Irradiations of rabbit myofibrils with an ultraviolet microbeam. I. Effects of ultraviolet light on the myofibril components necessary for contraction. Biochem Cell Biology. **65**, 363-375.

Wilson, P.J. and Forer, A. (1988). Ultraviolet microbeam irradiations of chromosomal spindle fibres shears microtubules and permits study of the new free ends in vivo. J Cell Biol. **91**, 455-468.

Wong, R. and Forer, A. (2003). Signalling between chromosomes in crane fly spermatocytes studied using ultraviolet microbeam irradiation. Chromosome Res. **11**, 771–786.

Yin, B. And Forer, A. (1996). Coordinated movements between autosomal half-bivalents in crane-fly spermatocytes: evidence that 'stop' signals are sent between partner half-bivalents. J Cell Sci. **109**, 155-163.

CHAPTER 6

Measurements of forces produced by the mitotic spindle using optical tweezers

Jessica Ferraro-Gideon[a], Rozhan Sheykhani[a], Qingyuan Zhu[b], Michelle L. Duquette[b], Michael W. Berns[b,c], and Arthur Forer[a]

[a]Department of Biology, York University, Toronto, ON M3J 1P3, Canada; [b]Department of Bioengineering, University of California, San Diego, La Jolla, CA 92093; [c]Beckman Laser Institute and Department of Biomedical Engineering, University of California, Irvine, Irvine, CA 92697

6.1 ABSTRACT **We used a trapping laser to stop chromosome movements in *Mesostoma* and crane-fly spermatocytes and inward movements of spindle poles after laser cuts across *Potorous tridactylus* (rat kangaroo) kidney (PtK2) cell half-spindles. *Mesostoma* spermatocyte kinetochores execute oscillatory movements to and away from the spindle pole for 1–2 h, so we could trap kinetochores multiple times in the same spermatocyte. The trap was focused to a single point using a 63× oil immersion objective. Trap powers of 15–23 mW caused kinetochore oscillations to stop or decrease. Kinetochore oscillations resumed when the trap was released. In crane-fly spermatocytes trap powers of 56–85 mW stopped or slowed poleward chromosome movement. In PtK2 cells 8-mW trap power stopped the spindle pole from moving toward the equator. Forces in the traps were calculated using the equation $F = Q'P/c$, where P is the laser power and c is the speed of light. Use of appropriate Q' coefficients gave the forces for stopping pole movements as 0.3–2.3 pN and for stopping chromosome movements in *Mesostoma* spermatocytes and crane-fly spermatocytes as 2–3 and 6–10 pN, respectively. These forces are close to theoretical calculations of forces causing chromosome movements but 100 times lower than the 700 pN measured previously in grasshopper spermatocytes.**

Monitoring Editor
William Bement
University of Wisconsin

Received: Dec 21, 2012
Revised: Feb 28, 2013
Accepted: Mar 5, 2013

6.2 INTRODUCTION

This article deals with measurements of mitotic forces using optical traps. As put succinctly by Mitchison and Salmon (2001), "To understand spindle mechanics it has long been clear that we need to measure the forces acting in the spindle." Knowing the forces involved places important limits on the many models of how chromosomes move and of how spindle poles are kept apart (Mitchison *et al.*, 1986, 2005; Forer and Wilson, 1994; Pickett-Heaps *et al.*, 1996; Pickett-Heaps and Forer, 2009; Cameron *et al.*, 2006; Johansen and Johansen, 2007; Johansen *et al.*, 2011; Dumont and Mitchison, 2009; Goshima and Scholey, 2010).

The only direct attempt to measure the force to move anaphase chromosomes in living cells was in grasshopper spermatocytes (Nicklas, 1983). Nicklas (1983) used state-of-the-art techniques to make this measurement, and his experiments were instrumental in calling attention to the importance of determining mitotic forces. He hooked anaphase chromosomes with calibrated micromanipulation needles and calculated the force needed to slow or stop chromosome movement from the amount of bend in the needles. He concluded that whereas a force of 10^{-5} dynes (1 pN) "had little or no effect on chromosome velocity," to stop anaphase movement 100% of the time, he needed to apply 700 pN to the chromosome. These measured values are almost three orders of magnitude higher than theoretical values calculated using Stokes' law (Gruzdev, 1972), the Einstein–Stokes equation (Nicklas, 1965; Taylor, 1965; Alexander and Rieder, 1991), and, more recently, Young's modulus (Marshall *et al.*, 2001), as seen in Table 6.1. The calculations using Young's modulus require knowledge of the size and elasticity of the chromosome

This article was published online ahead of print in MBoC in Press (http://www.molbiolcell.org/cgi/doi/10.1091/mbc.E12-12-0901) on March 13, 2013.

Address correspondence to: Arthur Forer (aforer@yorku.ca); Michael W Berns (mwberns@uci.edu); Jessica Ferraro-Gideon (ferraroj@yorku.ca).

Abbreviation used: n, refractive index.

Reference	Organism	Force (pN)	Force (dyne)	Type of calculation	Viscosity used in calculation (cP)	Elasticity used in calculation (Pa)	Mitotic stage
Nicklas (1965)	Grasshopper	0.1	1×10^{-8}	Einstein–Stokes equation	100[a]		Anaphase
Taylor (1965)	Newt	0.12	1.2×10^{-8}	Einstein–Stokes equation	300[b]		Anaphase
Gruzdev (1972)	*Haemanthus*	0.06	6×10^{-9}	Stokes' equation	50[a]		Anaphase
Alexander and Rieder (1991)	Newt	10	1×10^{-6}	Einstein–Stokes equation	282[b]		Prometaphase
Marshall *et al.* (2001)	*Drosophila*	0.7	7×10^{-8}	Young's modulus		38	Anaphase
Nicklas (1983)	Grasshopper	700	7×10^{-5}	Measured value			Anaphase

[a]Viscosity values were assumed based on measurements of cytoplasmic viscosities.
[b]Viscosity was measured in the spindle using the Brownian motion of particles.

TABLE 6.1: Summary of the calculated and measured forces required to move chromosomes during mitosis in various organisms.

(Houchmandzadeh *et al.*, 1997); all others require knowledge of the velocity of chromosome movement, the size of the chromosome, and the viscosity of the spindle (Nicklas, 1965). The forces to move anaphase chromosomes were calculated as 0.1–0.7 pN, whereas the force calculated to move prometaphase chromosomes was considerably higher (10 pN). Prometaphase chromosomes move in those cells by sliding along microtubules, not with microtubules extending between kinetochores and the pole (Rieder and Alexander, 1990), and they move 10 times faster than anaphase chromosomes. Thus, as discussed by Marshall *et al.* (2001), if the force calculated by Alexander and Rieder (1991) is extrapolated to anaphase, it would be closer to 1 pN. Overall, then, the forces calculated as acting on the kinetochore during anaphase range from 0.1 to 1 pN. The greatest uncertainty in the calculations using viscosity is in determining the viscosity in the spindle per se instead of measuring Brownian motion of particles close to but outside the spindle (Taylor, 1965; Schaap and Forer, 1979; Alexander and Rieder, 1991). The calculation of 0.7 pN using Young's modulus does not use viscosity, however, but instead chromosomal elasticity, which gives added confidence that the theoretical value for force needed to move an anaphase chromosome is in the range 0.1–1.0 pN.

Because of the discrepancy between measurement and theory and the importance of verifying conclusions using different methods, we used optical trapping (optical tweezers) to measure mitotic forces in several phylogenetically diverse spindles: spermatocytes from the flatworm *Mesostoma*, spermatocytes from the crane fly *Nephrotoma suturalis*, and mitotic *Potorous tridactylus* (rat kangaroo) kidney (PtK) cells.

Optical tweezers produce force on small objects because of the refraction of light entering and leaving the object (Ashkin *et al.*, 1986). They have been used to estimate the drag force acting on chromosome fragments in newt cells (Liang *et al.*, 1994), the swimming force of sperm cells (Nascimento *et al.*, 2007), and the force of molecular motors driving mitochondria (Ashkin *et al.*, 1990), among other intracellular forces (Ashkin, 1997). The optical trap, a laser at wavelength 1064 nm, produces minimal optical damage to living cells (Ashkin *et al.*, 1987). The very slight absorption of this wavelength by water may result in 1°C rise in temperature per 100 mW in the focused spot (Liu *et al.*, 1994, 1995). The "trapped" object is held in the trap and moves when the trap moves. If there is an intracellular force on the object, the object will not be held in the trap unless the laser trap exerts more force than the intracellular force. In our experiments, the trap was focused onto either moving chromosomes or moving poles. The laser power (therefore, the corresponding force) was increased until the velocity of the chromosome or the pole decreased to zero. The stopping force was calculated from the laser power in the plane of focus of the microscope objective. This method gives values for the stopping force considerably closer to the theoretical values of 0.1–1 pN than to Nicklas' (1983) value of 700 pN.

6.3 RESULTS

6.3.1 *Mesostoma ehrenbergii* spermatocytes

Mesostoma spermatocytes have five pairs of chromosomes, three bivalents with bipolar orientation, and four unpaired univalents at the spindle poles (Oakley and Jones, 1982; Fuge, 1987; Croft and Jones, 1989), as shown in Figure 6.1A. *Mesostoma* spermatocytes do not have a defined metaphase. Instead, bivalent kinetochores oscillate to and from the spindle poles (Fuge, 1987, 1989) for at least 1 or 2 h from early prometaphase until anaphase (Figure 6.1, B and C). This occurs regularly over a distance of ~4 μm (range, 1–6 μm) and with a velocity that averages 6 μm/min (range, 1.63–11.6 μm/min). Microtubules extend between the poles and the kinetochores as the kinetochores oscillate (Figure 6.1, D–F; Fuge and Falke, 1991), and thus these movements are more like anaphase movements than prometaphase movements where chromosomes slide along microtubules. Each kinetochore changes direction at ~90-s intervals (Table 6.2). The univalent chromosomes remain at the poles throughout prometaphase and move between poles irregularly (Oakley, 1983, 1985) with velocities of up to 20 μm/min.

6.3.2 Trapping kinetochores in *Mesostoma* spermatocytes

Single kinetochores in prometaphase *Mesostoma* spermatocytes were trapped as the kinetochore either moved to or away from the pole. The trap was at the edge of the kinetochore (Figure 6.2A), which was identified by position, based on electron microscopy studies (Figure 6.1, D–F; Fuge and Falke, 1991). Laser powers were adjusted in the point of focus from 1 to >68 mW to determine the lowest power that would stop chromosome movement and allow chromosome movement to resume when the trap was turned off. Seventy-eight kinetochores were trapped. The minimum laser power to

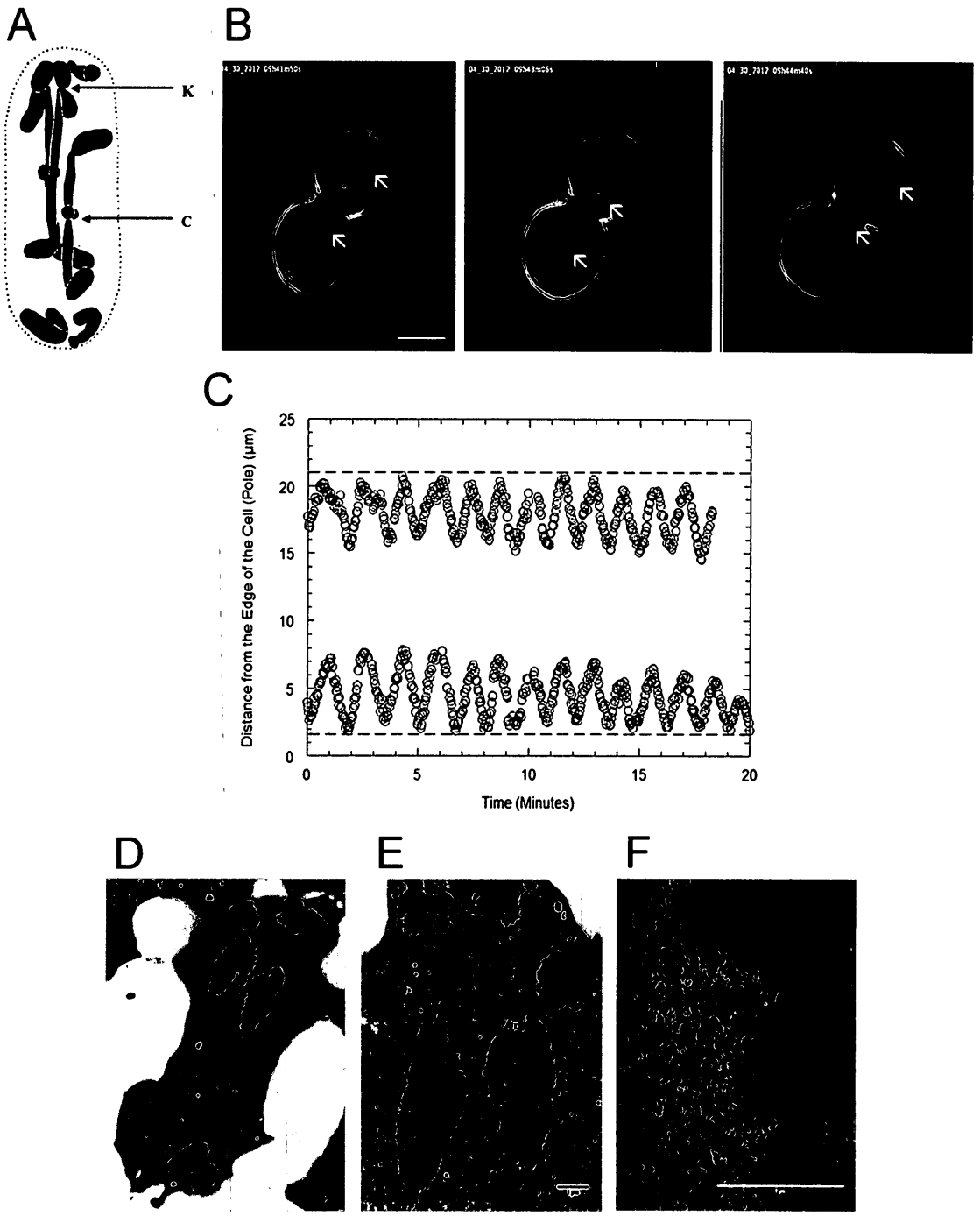

FIGURE 6.1: (A) Fixed and sectioned *Mesostoma* spermatocyte taken from Husted and Ruebush (1940), showing three bivalents and four univalents. The arrow labeled K points to the kinetochore of a bivalent, and the arrow labeled C points to a chiasma. (B) Montage of phase contrast microscope images of a *Mesostoma* spermatocyte, illustrating a bivalent as it moves to and away from the spindle poles during prometaphase/metaphase. The arrows indicate the position of the kinetochores. *Mesostoma* spermatocytes have a precocious cleavage furrow, which begins ingression when bivalents achieve bipolar orientation in prometaphase and then stalls, giving the spermatocytes a dumbbell-shaped appearance (Forer and Pickett-Heaps, 2010). Bar, 10 μm. (C) Distance of the kinetochores of partner half-bivalents from the edge of the cell (pole) in micrometers vs. time in minutes in an *M. ehrenbergii* spermatocyte. In this cell the average away-from-pole velocity is 6.9 μm/min and the average to-the-pole velocity is 7.5 μm/min. (D–F). Electron microscopy images of a *Mesostoma* spermatocyte. (D) A low-magnification overview image of a *Mesostoma* spermatocyte, illustrating two half-bivalents and two univalents at the upper pole. (E) Higher-magnification image of D illustrating the two kinetochores (K) of two half-bivalents and the centriole (C), which is embedded in the pericentriolar material. (F) Higher-magnification image of the kinetochore (K) of the right half-bivalent from E, illustrating microtubules terminating at the kinetochore. Bar, 1 μm.

Kinetochore movement	Number of KTs measured	Range of velocities (μm/min)	Average velocity (μm/min)	Amplitude (μm)	Period (s)
Away from the pole	74	1.63–9.83	5.19 ± 1.78	4.0 ± 1.15	89 ± 22.1
To the pole	73	1.92–11.6	6.41 ± 2.25		
Combined	147	1.63–11.6			

Average values ± SD. Difference between to-the-pole and away-from-the-pole kinetochore movement, $p = 0.0004$ ($t = 3.63$).

TABLE 6.2: Summary of the velocity, amplitude, and period of kinetochore movement to the pole and away from the pole of control cells in *Mesostoma* spermatocytes.

consistently either stop kinetochore movements or decrease oscillation amplitudes, after which kinetochores resumed movement when the laser was turned off, was 15–23 mW (Figure 6.3 and Table 6.3). The movement that resumed was not always normal: the amplitudes of the oscillations often were irregular and often were decreased by 1–3 μm. The absence of oscillations as regular as before trapping does not indicate damage to the kinetochore, because similar effects occur after treatments that affect solely spindle fibers: irregular oscillations with reduced amplitudes generally occur after recovery from ultraviolet microbeam irradiation of kinetochore fibers, as well as during initial recovery from Taxol treatment. Normal anaphase nonetheless occurs after either of these treatments (unpublished data).

In our experiments, when placed in the trap a kinetochore either immediately stopped moving (19 of 26) or stopped moving after oscillating with decreased amplitude (Figure 6.2B). When the trap stopped movement of one kinetochore, the sister (partner) kinetochore was not affected in 17 of 21 spermatocytes in which the sister kinetochore was visible (Figure 6.2B). Thus the effects are localized to the trapped region.

Chromosomes were trapped when moving to the pole and when moving away from the pole (Table 6.4). However, more data are needed to determine whether different forces are required. Cells generally were not followed long enough to see whether they entered anaphase, but anaphase was completed in four spermatocytes in which chromosomes were trapped using 5–23 mW. In two of four cells, bivalents entered anaphase as kinetochore movement was stopped by the trap (e.g., Figure 6.4). In the other spermatocytes (two of four), bivalents entered anaphase 5–15 min after being released from the trap. Thus the trap does not seem to harm either the trapped chromosomes or the cells.

A the cells.single univalent kinetochore was trapped as it moved from one spindle pole to the other. A trap power of 15 mW applied to the kinetochore caused the velocity to decrease from 2.4 to 0.33 μm/min and then stop (Figure 6.5). When the trap was removed, the univalent moved toward the pole with its original velocity (Figure 6.5). Therefore, 15 mW also stops movements of reorienting univalents, although we do not know whether univalents move because they slide along microtubules or because of fibers attached to their kinetochores.

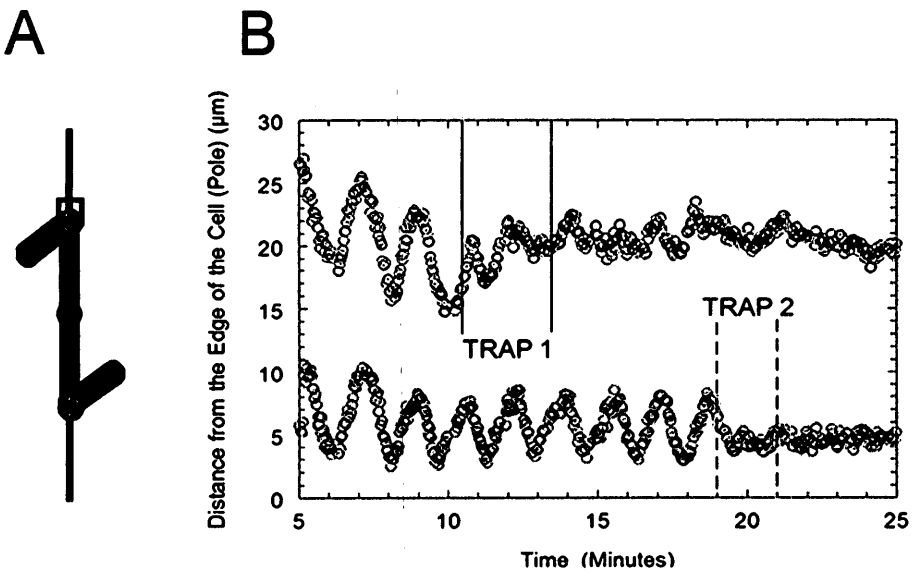

FIGURE 6.2: (A) Schematic of a bivalent from an *M. ehrenbergii* spermatocyte. The red and blue circles represent the positions of the kinetochores. The red square represents the position at which the optical tweezers were applied to the blue kinetochore. (B) Distance of the kinetochores of partner half-bivalents from the edge of the cell (pole) in micrometers vs. time in minutes in a *Mesostoma* spermatocyte. A power of 21.2 mW was applied to each kinetochore, first by trap 1 and then by trap 2. When trap 1 was applied, the amplitude of kinetochore (blue circles) movement away from the pole decreased and then stopped. When trap 1 was released, kinetochore movement resumed with irregular oscillations. When trap 2 was applied, kinetochore movement (red circles) decreased and then stopped. When trap 2 was released, kinetochore movement did not resume, but we may not have followed the kinetochore long enough to determine whether kinetochore movement would have resumed.

6.3.3 Trapping kinetochores in crane-fly spermatocytes

We extended our results to insects by measuring the laser power required to stop chromosome movement in crane-fly spermatocytes. For cells in anaphase I the traps were applied to the kinetochores, whose positions were known from previous polarizing and fluorescence microscope images (Forer, 1965; Wilson and Forer, 1989). For cells in prometaphase, bivalents were cut in two pieces with the cutting laser scissors (Harsono *et al.*, 2013); the resulting two pieces moved to opposite poles at the same speed as anaphase chromosomes. They were led by their kinetochores, and the movement was likely due to the same forces that propel anaphase chromosomes. The trap was placed at one kinetochore, and the chromosome piece moving to the other pole was used as a control. In our sample of 25 cells, consisting of 36 trapping experiments, chromosome movements were stopped consistently with trap powers of 56–85 mW (Figure 6.6 and Table 6.5). This is two to four times higher than the power needed to consistently stop kinetochore movements in *Mesostoma* spermatocytes.

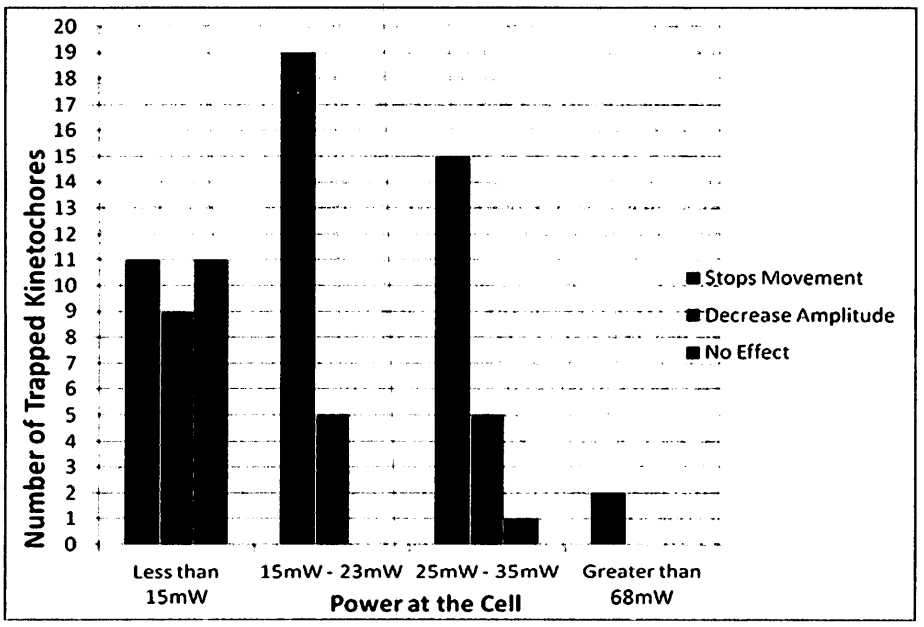

FIGURE 6.3: Power range in the trap (in milliwatts) used to stop kinetochore movement, decrease the amplitude of kinetochore movement, or have no effect on kinetochore movement.

6.3.4 Trapping spindle poles in PtK2 cells

Because the *Mesostoma* and crane-fly experiments were in meiotic invertebrate cells, we extended our studies to a mitotic vertebrate system. Laser microbeam cutting of metaphase spindles in tubulin-labeled PtK2 cells results in movement of spindle poles toward the spindle equator (Baker, 2010; Sheykhani *et al.*, 2013). We measured the laser power required to slow or stop movement of the spindle poles. Because spindle poles are held apart when poleward forces act on chromosomes, there must be equal and opposite forces on poles and kinetochores. Therefore the forces holding spindle poles apart are expected to be similar to the forces pulling the chromosomes poleward (e.g., McIntosh and Pfarr, 1991). In 13 of 16 control cells the pole on the cut side moved toward the equator within 10–30 s after irradiation; in 3 of 16 control cells movement began within 60–90 s (Figure 6.7A). The unirradiated pole moved toward the equator after this, resulting in a shorter but symmetric spindle (Figure 6.7B; Sheykhani *et al.*, 2013). A 7.8-mW trap was placed at one pole of metaphase PtK2 cells (Figure 6.7C) either before or after a laser microbeam cut was made across the entire half-spindle associated with that pole. The cells were followed 2–3 min after irradiation. Trapping the irradiated pole stopped the inward movement of the pole after irradiation in 4 of 6 cells (Figure 6.7D and Table 6.6). There was no change in fluorescence at the pole when the trap was applied, indicating that the trapping laser did not damage the spindles poles. In addition, normal microtubule immunofluorescence was seen when a 44.5-mW trap was applied to the kinetochore (Figure 6.8).

6.4 DISCUSSION

We report optical trap laser powers that stop kinetochore oscillations in *Mesostoma* spermatocytes, stop poleward chromosome movements in anaphase and prometaphase crane-fly spermatocytes, and stop the pole from moving after laser cuts across metaphase spindles in PtK2 vertebrate cells.

To convert milliwatts of laser power to trapping force, the basic formula is $F = nQP/c$, where F is the force, n is the refractive index of the object being trapped divided by the refractive index of the surroundings (Ashkin, 1992; Konig *et al.*, 1996), P is the power in the trap, and c is the speed of light. Q is a conversion factor that, for objects that absorb some of the trap, has a range of 0–1, where 1 is equivalent to total absorption (Ashkin, 1992; Svoboda and Block, 1994a; Konig *et al.*, 1996; Neuman and Block, 2004). Q is the fraction of momentum transferred to a trapped object, and its value determines whether an object will be trapped (Wright *et al.*, 1994). Of the elements of this equation, P is determined experimentally. There are reasonable estimates of n for spindles and chromosomes (Barer, 1957; Forer *et al.*, 1980). Q values are a bit more problematic but can be determined experimentally or calculated, but only for regularly shaped objects such as spheres (Svoboda and Block, 1994a; Gahagan and Swartzlander, 1998; Neuman and Block, 2004).

Our conversion of trap power to force relies on data of Liang *et al.* (1994), who trapped chromosomes in newt spindles and presented both the power used in the trap and the resultant forces that acted on the chromosomes. Chromosome shapes and relative refractive indices of spindles and chromosomes are similar in newt

Power at the focus (26% of power at back focal plane) (mW)	Trapping kinetochores in *M. ehrenbergii* spermatocytes							
	Stops movement and recovers	Stops movement and no recovery	Decreases amplitude	No effect	Total	Stopped kinetochore movement	Decreased amplitude	Stopped movement or decreased amplitude
<15	9 (29%)	2 (6%)	9 (29%)	11 (35%)	31	35%	29%	64%
15–23	7 (29%)	12 (50%)	5 (21%)	0	24	79%	21%	100%
25–35	0	15 (70%)	5 (25%)	1 (5%)	21	70%	25%	95%
>68	0	2 (100%)	0	0	2	100%	0%	100%
Total	16 (21%)	31 (40%)	19 (24%)	12 (15%)	78			

TABLE 6.3: Summary of the effect of varying powers in the trap on kinetochore movement when applied to the kinetochore in *Mesostoma* spermatocytes.

Power at the focus (26% of power at back focal plane) (mW)	A. Kinetochore moving to the pole				
	Stops movement and recovers	Stops movement and no recovery	Decreases amplitude	No effect	Total
<15	6 (32%)	1 (5%)	6 (32%)	6 (32%)	19
15–23	3 (20%)	8 (53%)	4 (27%)	0	15
25–35	0	9 (64%)	3 (21%)	2 (14%)	14
>68	0	2 (100%)	0	0	2
Total	9 (18%)	20 (40%)	13 (26%)	8 (16%)	50

Power at the focus (26% of power at back focal plane) (mW)	B. Kinetochore moving away from pole				
	Stops movement and recovers	Stops movement and no recovery	Decreases amplitude	No effect	Total
<15	2 (16%)	1 (8%)	4 (33%)	5 (42%)	12
15–23	4 (44%)	4 (44%)	1 (11%)	0	9
25–35	0	6 (86%)	0	1 (14%)	7
>68	0	0	0	0	0
Total	6 (21%)	11 (39%)	5 (19%)	6 (21%)	28

TABLE 6.4: The effect of varying powers in the trap on kinetochore movement in *Mesostoma* spermatocytes.

cells to those in most mitotic cells. To convert power to force, we used the basic formula $F = nQP/c$ and the power and force values from Liang *et al.* (1994) to calculate an equivalent Qn (Q') of 0.0341, and from this Q' value we converted our power values to piconewtons of the trap. The results (see Table 6.8 later in the paper) indicate that chromosome oscillations in *Mesostoma* spermatocytes are stopped (or "slowed") with trapping forces of 2–3 pN and poleward movements of crane-fly spermatocyte chromosomes are stopped or slowed with poleward forces of 6–10 pN. From other experiments in which forces and power were given, we calculated Q' values for other objects (Table 6.7) and used these to estimate the forces applied to PtK spindle poles to stop their movement toward the equator. Because centrioles are about the same size as mitochondria and both appear as phase dark dots in the cell cytoplasm, we used $Q' = 0.012$, the value for trapping mitochondria (Table 6.7). This assumes that the trap at the spindle pole acts on the centriolar apparatus (centrosome). It is possible that instead the trap might act on astral microtubules. We therefore also calculated force based on the Q' value of 0.09 for trapping microtubules (Table 6.7). Using these values, we calculated the forces pulling PtK spindle poles to the equator to be 0.31–2.3 pN (Table 6.8). These values are close to the forces that stop the invertebrate meiotic chromosomes.

It is significant that our values for the stopping force for chromosome movements are two orders of magnitude smaller than the 700 pN reported for grasshopper spermatocytes (Nicklas, 1983) but are close to the 0.1- to 1-pN theoretical forces calculated for stopping anaphase chromosomes (Table 6.1). The forces determined in our experiments are comparable to those of motor molecules and of motile sperm that were measured using optical tweezers: 1.7 pN for myosin (Molloy *et al.*, 1995); 2.6 pN for a single motor molecule driving mitochondria (Ashkin *et al.*, 1990); 5–6 pN for kinesin molecules (Svoboda and Block, 1994b); 9.2 pN for the unbinding of actin and myosin (Nishizaka *et al.*, 1995); and 44 pN for the motion of healthy sperm (Konig *et al.*, 1996). Because of the large difference between our values and those reported previously, we need to consider whether our numbers could be erroneously low. One consideration is to evaluate the force estimate of Liang *et al.* (1994) from which we derived Q'.

Liang *et al.* (1994) measured velocities of chromosome fragments moved through the cytoplasm by an optical trap; they estimated the force that they applied to the chromosomes from the maximum velocity, the viscosity of the cytoplasm, and the shapes of the chromosomes. The minimum value applied to the chromosomes by the trap was 30 pN. Large errors are not likely to have arisen from the velocities and shapes since they were measured directly from video images. The viscosity value of 280 cP was based

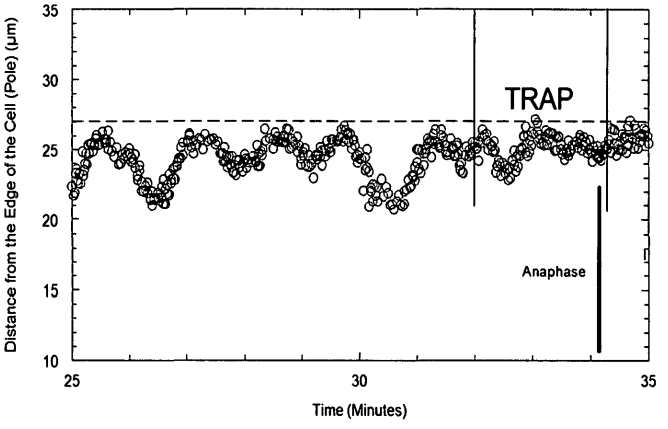

FIGURE 6.4: Distance of a kinetochore from the edge of the cell (pole) in micrometers vs. time in minutes in a *Mesostoma* spermatocyte. A power of 15.3 mW was applied by the trap to the kinetochore. The time the trap was turned on is represented by the first solid line, and the time the trap was turned off is represented by the second solid line. When the trap was applied, the amplitude of kinetochore movement (blue circles) away from the pole decreased and then stopped. The bivalent entered into anaphase before the trap was released from the kinetochore. The spindle pole is represented by the dashed line.

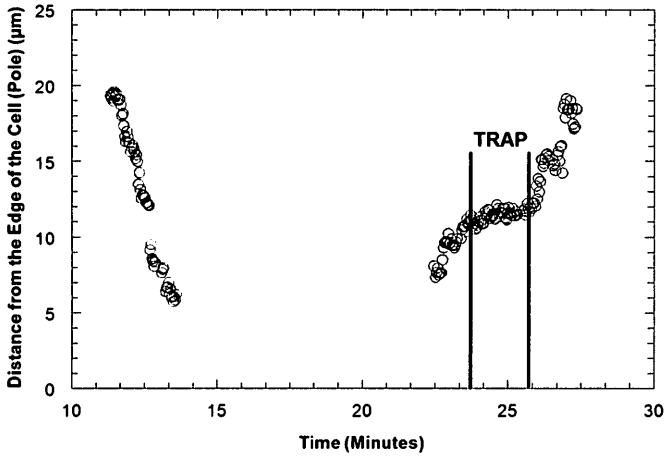

FIGURE 6.5: Distance of the kinetochore of a univalent from the edge of the cell (pole) in micrometers vs. time in minutes as the univalent moves from the upper spindle pole to the lower spindle pole and then from the lower spindle pole back to the upper spindle pole in a *Mesostoma* spermatocyte. The univalent (purple circles) moved from the upper pole to the lower pole with a velocity of ~7.0 μm/min. A power of 15 mW in the trap, illustrated by the two vertical lines, was applied as the univalent reoriented and segregated from the lower pole back to the upper pole. The trap caused the univalent to decrease in velocity to 0.33 μm/min and then stop. When the trap was released, the univalent moved to the upper pole with its original velocity.

on measurements of Alexander and Rieder (1991). This viscosity is <10% different from the 300 cP measured by Taylor (1965) for spindles of the same cell type. Other estimates of spindle viscosity in other cell types are lower than this (e.g., Schaap and Forer, 1979;

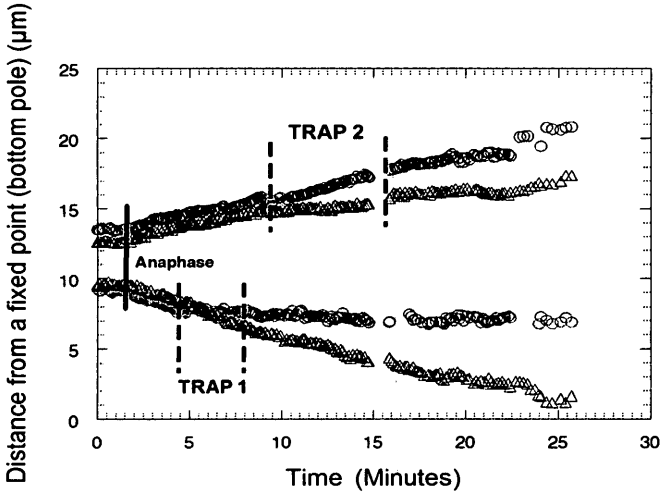

FIGURE 6.6: Distance of the kinetochores of two partner half-bivalents in anaphase from a fixed point (bottom pole) in micrometers vs. time in minutes in a crane-fly spermatocyte. A power of 49.4 mW was applied to the lower half-bivalent kinetochore (red circles) and then 62.4 mW to the upper half-bivalent kinetochore (blue triangles). When trap 1 was applied, chromosome movement (red circles) stopped and the partner half-bivalent was not affected. When trap 1 was released, chromosome movement resumed with a slower velocity. When trap 2 was applied, chromosome movement (blue triangles) stopped and its partner was not affected. When trap 2 was released, chromosome movement resumed with a slower velocity.

Table 6.1). Thus any error in the viscosity would be on the high side, and reducing their viscosity value would decrease our force estimates and not increase them. With regard to the power in the trap, Liang *et al.* (1994) recorded the power of the trap as 440 mW "at the microscope objective." Because in an earlier article (Liang *et al.*, 1993) the trap power was measured "at the objective focal plane," we reduced 440 mW to 264 mW for our conversion of power to force to take into account the 60% transmission of the objective (Liu *et al.*, 1995, 1996). The power measurement should not introduce much error into our determination. The final consideration is whether the refractive index ratio in the calculation might be erroneous. The largest the ratio can be for aqueous biological material is 1.17, the ratio of a solid (n = 1.56) to that of water (n = 1.33), or a ratio of 1.15 for spindle refractive indices of 1.36 (Forer *et al.*, 1980). Errors in this refractive index ratio (n) thus could not give rise to differences of more than 10–15% in the final force calculation. Overall, although we would not argue that our estimates of force are necessarily accurate to within <50%, especially considering the biological variability (Tables 6.3 and 6.5), we do not think that errors from converting trapping power to force on chromosomes can account for the two-orders-of-magnitude difference between our values and those of Nicklas (1983). A possible explanation for the differences between our values and those of Nicklas (1983) is that the laser trap did not stop movement because of its force but rather because it either damaged the kinetochore directly or damaged kinetochore microtubules (Liu *et al.*, 1995; Neuman and Block, 2004). Several lines of evidence argue against this. The trapping laser wavelength (1064 nm) has minimal effect on biological specimens because cells and their organelles are generally transparent to this wavelength (Liang *et al.*, 1996; Neuman and Block, 2004). Damage from the trap is extremely unlikely because after being released from the trap the stopped *Mesostoma* spermatocyte kinetochores resume movements and the cells enter anaphase. In addition, previous studies demonstrated that cells survive and can be cloned into viable populations after exposure to this wavelength (Liu *et al.*, 1996). Using the same wavelength, an average temperature increase of 1.0°C/100 mW was measured when trapping motile sperm heads, but this increase in temperature did not alter the cellular DNA of the sperm (Liu *et al.*, 1996). If anything, in our experiments, a temperature increase of a few degrees should speed up chromosome movement, not retard it. In addition, for equivalent trapping powers (4–160 mW), *Escherichia coli* were able to reproduce while in the trap, yeast were able to bud into clumps while in the trap, and there was no change in the flexibility of red blood cells or damage to organelles of protozoa after trapping (Ashkin *et al.*, 1987; Ashkin, 1992; Aufderheide *et al.*, 1992). Furthermore, microtubules were unaf-fected when kinesin-coated beads were trapped with optical tweezers in vitro (Kuo and Sheetz, 1993). Microtubules were unaffected when they were bent with optical tweezers to measure flexural rigidity, and after release from the trap the microtubules returned to their original positions (Kurachi *et al.*, 1995; Felgner *et al.*, 1996). Further, in our experiments, PtK cell microtubules were not damaged by powers used to trap *Mesostoma* and crane-fly spermatocyte kinetochores (21 and 44.5 mW; Figure 6.8). Furthermore, in *Mesostoma* spermatocytes, chromosome movement resumed immediately after the trap was turned off (at powers <23 mW). In addition, movements of other chromosomes or partner half-bivalents were not affected in either *Mesostoma* or crane-fly spermatocytes. Bivalents in *Mesostoma* spermatocytes entered into anaphase even in the presence of the trap (Figure 6.4), and anaphase crane-fly spermatocyte chromosomes resumed movement when released from

Power at the objective (26% of power at back focal plane) (mW)	Cut prometaphase bivalent or anaphase chromosome movement							
	Stops movement and recovers	Stops movement and no Recovery	Decrease in velocity	No effect	Total	Percentage of stopped KT movement (%)	Percentage of decreased velocity (%)	Stopped movement or decreased velocity (%)
25–55	8 (50%)	0	3 (19%)	5 (31%)	16	50	19	69
56–85	9 (69%)	1 (8%)	2 (15%)	1 (8%)	13	77	15	92
86–140	3 (43%)	1 (14%)	2 (29%)	1 (14%)	7	57	29	86
Total	20 (56%)	2 (6%)	7 (19%)	7 (19%)	36			

TABLE 6.5: Summary of the effect of varying powers in the trap on chromosome movement when applied to the kinetochore of anaphase chromosomes or cut prometaphase bivalents in crane-fly spermatocytes.

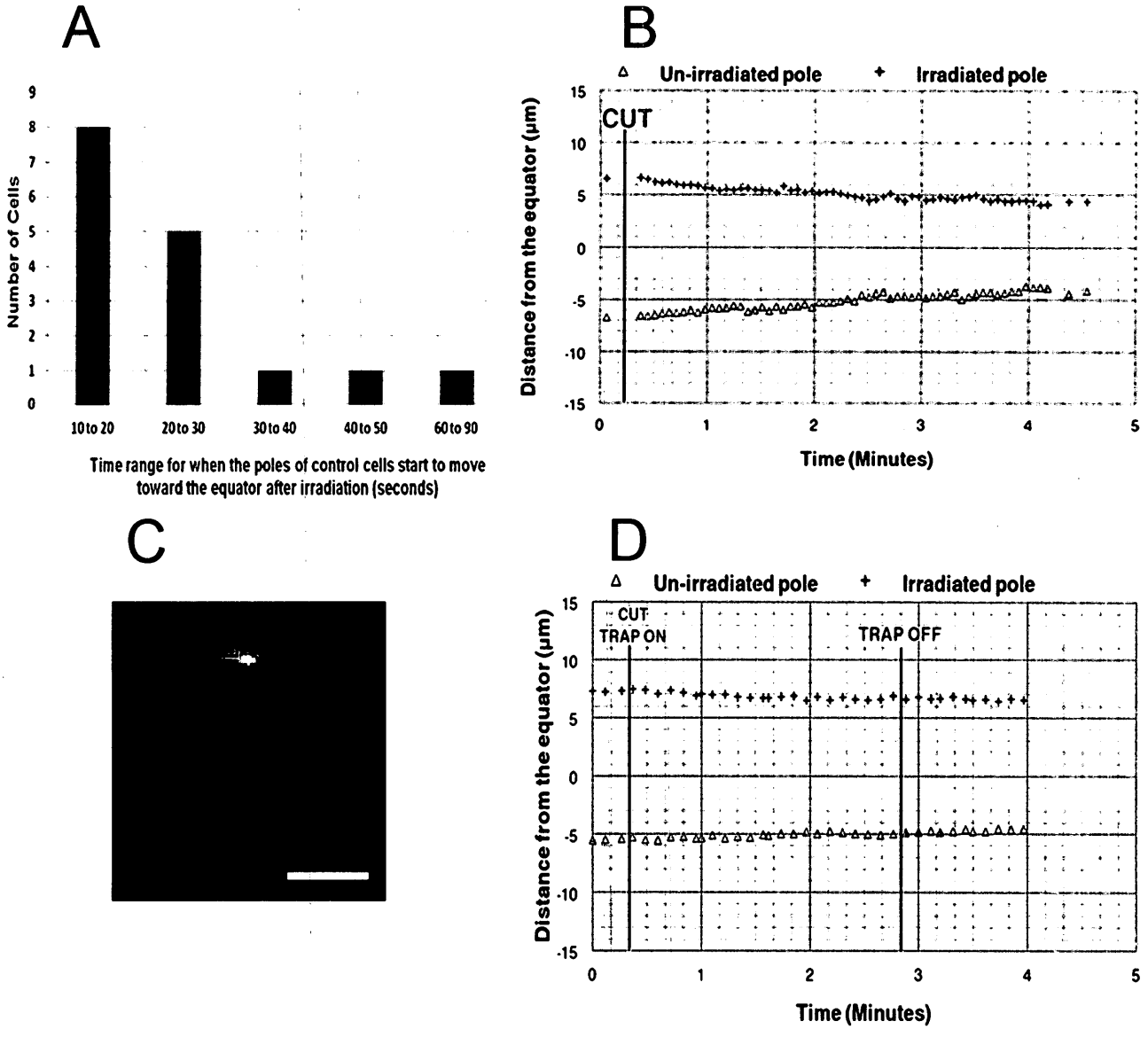

FIGURE 6.7: (A) Time range required (in seconds) for the irradiated pole to start to move toward the equator after laser microbeam irradiation during metaphase in PtK2 cells. (B) Distance of the irradiated and unirradiated poles from the equator in micrometers vs. time in minutes. The vertical line represents the time of the irradiation. The pole on the irradiated side moved toward the equator first soon after the irradiation. (C) PtK2 irradiated cell illustrating the position of the trap (red square) at the spindle pole and the line cut across the spindle. Bar, 10 µm. (D) Distance of the irradiated and unirradiated poles from the equator in micrometers vs. time in minutes. The vertical lines represent the time of the irradiation when the trap was turned on and when the trap was turned off. A trapping power of 7.8 mW was applied to the spindle pole of the irradiated metaphase half-spindle. When the trap was applied, the irradiated pole and the unirradiated pole did not move toward the equator.

	Control cells	Trapped cells
Number of cells with movement of irradiated pole	16	2
Number of cells with no movement of either pole	0	4
Total	16	6

TABLE 6.6: Summary of the laser microbeam irradiation on the irradiated half-spindle in control PtK2 cells and in trapped PtK2 cells with a power of 7.8 mW.

the trap (Figure 6.6). This large body of data supports the conclusion that chromosome movements were stopped because of the trapping force acting on the chromosome, not because of deleterious effects of the trap. Therefore optical damage to the cells is unlikely to have caused the discrepancy between our force measurements and those reported by Nicklas (1983).

It does not seem likely that the discrepancy between our measured force values and those of Nicklas (1983) is due to species differences between grasshopper spermatocytes and the cells that we used, because the mitotic forces we measured were similar in *Mesostoma* spermatocytes, crane-fly spermatocytes, and PtK2 cells. This includes a diverse phylogenetic range of organisms and cell types. In fact, the similarity in forces in this broad range of spindles suggests that the amount of force needed to move chromosomes on either the meiotic or mitotic spindle might be evolutionarily conserved.

We do not know why there is such a large discrepancy between our experiments and those of Nicklas (1983), but our results are more in line with the theoretical calculations of others (Table 6.1). It is conceivable that in Nicklas (1983) stretching of the membrane might have given rise to erroneously high values. When hooking a chromosome with a needle, the needle never enters the cell but instead stretches the membrane and hooks the chromosome, like working inside a balloon from the outside. Nicklas (1983) described experiments designed to rule out contributions to his measurements from forces needed to stretch membranes. Notwithstanding those experiments, it still is conceivable that an artificially high measured force arises from stretching the cell membrane since stretching cell membranes by 0.5–1 μm requires forces of 100–900 pN as measured using atomic force microscopy (Matzke *et al.*, 2001; Silberberg *et al.*, 2009; Schillers *et al.*, 2010). Whether or not this speculation is valid, our results point to the need for further investigation into the magnitude of mitotic/meiotic forces since our results indicate that they may be considerably lower than the higher value that has been generally accepted.

FIGURE 6.8: (A) Differential interference contrast image of a PtK cell, illustrating the position of the trap at the interface between the kinetochore and the kinetochore microtubules. The trap is represented by the red square. The trap was applied for 4 min with a power of 44.5 mW. (B) The PtK cell from Figure 6.4E stained with tubulin antibody. No damage to the microtubules is visible in the region in which the trap was applied (red square). Bar, 10 μm.

6.5 MATERIALS AND METHODS

6.5.1 Live-cell preparations

Living *Mesostoma* spermatocytes were obtained from a laboratory stock of *Mesostoma ehrenbergii* that originally was reared from diapausing (overwintering) eggs. Adult animals were kept in 500-ml plastic jars filled with dechlorinated water at 25°C in incubators with a 16 h light:8 h dark cycle and daily fed live brine shrimp. We obtained spermatocytes from animals that were 3–4 wk old and had ~1–3 overwintering eggs. Testes were removed by inserting through the body wall of the animal a glass needle pulled from 10-μl pipettes (Fisher Scientific, Pittsburgh, PA) and then sucking testes up via Tygon tubing (Fisher Scientific) that was attached to the needle. Testes were expelled from the needle into a drop of *Mesostoma* Ringer's solution (61 mM NaCl, 2.3 mM KCl, 0.5 mM $CaCl_2$, and 2.3 mM phosphate buffer, pH 6.9) that contained fibrinogen (Calbiochem, La Jolla, CA) on a glass coverslip, as previously described (Forer and Pickett-Heaps, 2005). When the cells were evenly dispersed in the fibrinogen, a drop of thrombin (Sigma-Aldrich, St. Louis, MO) was added to create a fibrin clot. The coverslip was then placed in a perfusion chamber (Forer and Pickett-Heaps, 2005) and perfused with *Mesostoma* Ringer's solution.

Living crane-fly spermatocytes were obtained from a laboratory stock of crane flies (*Nephrotoma suturalis* Loew). Briefly, we dissected the testes of IV-instar larvae under Halocarbon 95S oil, rinsed the testes in insect Ringer's solution (0.13 M NaCl, 5 mM KCl, 1 mM $CaCl_2$, 0.02 M phosphate buffer, pH 6.9), and placed them in a fibrin clot as described. The coverslip was then placed in a perfusion chamber and perfused with insect Ringer's solution.

6.5.2 Cell culture

P. tridactylus kidney epithelial cells (#CCL 56; American Type Culture Collection, Manassas, VA) expressing enhanced cyan fluorescing protein (ECFP) tagged to the α-subunit of tubulin as previously described (Botvinick *et al.*, 2004; Sheykhani *et al.*, 2013) were grown in Life Technologies (Carlsbad, CA) advanced DMEM F-12 supplemented with L-glutamine and 3% fetal bovine serum. Briefly, the cells were incubated at 37°C with 5% CO_2. A fibrinogen-thrombin clot was used as previously described to adhere the cells to the coverslip before irradiation (Forer and Pickett-Heaps, 2005; Snyder *et al.*, 2010, Sheykhani *et al.*, 2013). Irradiations were performed at room temperature (18–20°C).

6.5.3 Trapping and cutting

The optical setup used in this study was described previously (Shi *et al.*, 2012; Harsono *et al.*, 2013). Briefly, the system was based on an inverted microscope Axio Observer (Zeiss, Jena, Germany) with a 1064-nm continuous wave Nd:YVO_4 laser (Millennia IR; Newport Co., Irvine, CA) for trapping and a 200-fs pulsed laser (Mai Tai; Newport Co.) tuned at 730 nm for cutting. Both laser beams are expanded to fill the back aperture of the objective (Zeiss Plan-Apochromat 63/1.40 Oil Ph3). The transmission of this objective was determined to be 26% at 1064 nm and 74% at 730 nm using a multiobjective measuring procedure

Reference	Object being trapped	Q' (calculated)	Stated power	Force estimated by an independent method (pN)	Wavelength used (nm)
		Coated beads			
Sato *et al.* (1991)	3-μm beads (latex)	0.18	5 mW	3	1330
Wright *et al.* (1993)	1-μm beads (silica)	0.017	0.1 mW	0.0056	1064
	10-μm beads (polystyrene)	0.16	0.56 mW	0.3	
Svoboda and Block (1994b)	Kinesin-coated beads	0.03	62.5 mW	5–6	1064
Yin *et al.* (1995)	RNA polymerase–coated beads	0.05	82 mW	13.6	Not given
Simmons *et al.* (1996)	3-μm beads	0.12	100 mW	40	1064
		Biological specimens			
Ashkin *et al.* (1990)	Mitochondria	0.012	63 mW	2.6	Not given
Liang *et al.* (1994)	Chromosome fragments	0.034	264 mW	30	1064
Kurachi *et al.* (1995)	Microtubules	0.09	1 mW	0.3	647.1
			25 mW	7.5	
Konig *et al.* (1996)	Sperm heads	0.16	150 mW	82	800
Kellermayer *et al.* (1998)	Unfolding titin	0.08	1.5 W	400	1064

Q' values were calculated using the equation $Q' = cF/P$.

TABLE 6.7: Comparison of Q' values calculated from articles that gave values for laser power and its equivalent force.

previously described (Gomez-Godinez *et al.*, 2010). Half-wave plates are motorized to adjust the power of each laser. The beams are steered by fast-scanning mirrors (FSM300; Newport Co.) such that the focus of both the laser trap and the laser scissors can be readily located and moved within the sample plane. The cutting and trapping beams are combined by a long-pass dichroic beam splitter and then coupled into the microscope by a custom laser entry port. Images were recorded live by an ORCA R2 camera (Hamamatsu, Hamamatsu Japan) at variable intervals ranging from 2 to 10 s.

The power in the trap plane of focus was varied from <15 to >68 mW at the cell when the trap was applied to the kinetochore of prometaphase/metaphase half-bivalents in *Mesostoma* spermatocytes. The power at the focal plane was 25–140 mW when the trap was applied to the kinetochore of anaphase chromosomes or of pieces of cut prometaphase bivalents in crane-fly spermatocytes and 7.8 mW when the trap was applied to spindle poles in PtK2 cells. Trapping time varied from 30 s to >5 min.

6.5.4 Data analysis

The tagged image file format (TIFF) and portable network graphic (PNG) images that were taken every 2–10 s using the LabVIEW (National Instruments, Austin, TX) program throughout the duration of the experiment were cropped, stamped with date and time, and converted to bitmap image files (BMP) using IrfanView (www.irfanview.com/). The BMP images were converted into time-lapsed

	Power (mW)	Force (pN)			
		$Q' = 0.0341$	$Q' = 0.012$	$Q' = 0.09$	No Q'
Mesostoma spermatocyte	15–23	1.7–2.6			
Crane-fly spermatocyte	56–85	6.3–9.6			
PtK2 pole movement	7.8		0.31	2.34	
PtK2 anaphase chromatid movement[a] (Liang *et al.* 1991)	36	4			
Theoretical force values	N/A				0.06–10
Previously measured value	N/A				700

The theoretical and previously measured force values are included for comparison. N/A, not applicable.

[a]A trap of 60 mW to chromatid arms at the start of anaphase reversibly stopped anaphase chromatid movement. The authors used 60 mW measured at the objective, and because of the 60% transmission of the lens, the power was 36 mW at the specimen.

TABLE 6.8: Forces calculated using $F = Q'P/c$, with appropriate Q' values derived from the literature (see the text).

video sequences using VirtualDub (www.virtualdub.org/). Single frames from the time-lapsed videos were exported into WinImage, an in-house software program (Wong and Forer, 2003), and the positions to be measured were recorded. The user marked the positions to be measured, and the computer program converted the on-screen pixel spacing into micrometers. The micrometer measurements at the different time points were imported into SlideWrite (www.slidewrite.com/) to plot distance versus time. The slope of the line of best fit was used to calculate velocities.

6.5.5 Fluorescence staining, confocal microscopy, and electron microscopy

After trapping the edge of the kinetochore with laser powers of 21 and 44.5 mW for 4 min, we lysed PtK cells at room temperature in a cytoskeleton-stabilizing lysis buffer (100 mM piperazine *N,N*-bis(2-ethanesulfonic acid), 10 mM ethylene glycol tetraacetic acid; 5 mM $MgSO_4$; 5% dimethyl sulfoxide; 1% Nonidet P-40; pH 6.9) while the trap was still on. Lysed cells were fixed for 5 min in 0.25% glutaraldehyde in phosphate-buffered saline (PBS), rinsed in PBS (two times for 5 min each), kept in sodium borohydride (1 mg/ml; two times for 8–10 min) to neutralize free aldehyde groups, and then rinsed again with PBS (two times for 5 min each). Trapped cells were stained with YL1/2 rat monoclonal antibody specific for tyrosinated α-tubulin (Kilmartin *et al.*, 1982) diluted (1:200), followed by Alexa 594 goat anti-rat immunoglobulin (Invitrogen, Burlington, Canada) diluted 1:100. All staining steps were in MatTek glass-bottom dishes (MatTek, Ashland, MA). Cells were rinsed with PBS containing 0.1% Triton X-100 before addition of tubulin antibody. The incubation time for each antibody was 1 h. Preparations were kept in the dark during the incubation periods to prevent light inactivation of the fluorochromes. All dilution of antibodies was done in PBS. After staining and before mounting, the glass coverslip was removed from the dish using coverslip removal fluid (MatTek). Coverslips were mounted in Mowiol (Calbiochem, Billerica, MA) solution (Osborn and Weber, 1982) containing paraphenylene diamine as an antifading agent (Fabian and Forer, 2005) and stored at 4°C in the dark.

Cells were studied using an Olympus FluoView 300 confocal microscope (Olympus, Tokyo, Japan), with HeNe laser at 543 nm, using an Olympus Plan Apo 60× oil immersion objective (numerical aperture, 1.4). Images, collected with FluoView software, were further processed using ImageJ (National Institutes of Health, Bethesda, MD) and Photoshop (Adobe, San Jose, CA). Image adjustments for publication were only of brightness and contrast.

Control cells in perfusion chambers were fixed for electron microscopy as described by Forer and Pickett-Heaps (2010). Briefly, cells were fixed in 2% glutaraldehyde, postfixed in 4% osmium tetroxide, dehydrated, and embedded in epoxy resin; the hardened epoxy resin was removed from the coverslips, and individual cells were marked and sectioned.

6.6 ACKNOWLEDGMENTS

We are grateful to Linda Shi (University of California, San Diego, La Jolla, CA) for her help and guidance with the Robolase microscope and Jagesh Shah (Harvard University, Cambridge, MA) for constructing and providing the ECFP PtK2 cells. This work was supported by grants from the Canadian Natural Sciences and Engineering Council to A.F., York University Fieldwork and Research Cost Funds to J.F., and the Beckman Laser Institute Foundation and a grant from the Air Force Office of Scientific Research FA9550-10-1-0538 to M.B.

6.7 REFERENCES

Alexander SP, Rieder CL (1991). Chromosome motion during attachment to the vertebrate spindle: initial saltatory-like behavior of chromosomes and quantitative analysis of force production by nascent kinetochore fibres. J Cell Biol 113, 805–815.

Ashkin A (1992). Forces of a single-beam gradient laser trap on a dielectic sphere in the ray optics regime. Biophys J 61, 569–582.

Ashkin A (1997). Optical trapping and manipulation of neutral particles using lasers. Proc Natl Acad Sci USA 94, 4853–4860.

Ashkin A, Dziedzic JM, Bjorkholm JE, Chu S (1986). Observation of a single-beam gradient force optical trap for dielectric particles. Opt Lett 11, 288–290.

Ashkin A, Dziedzic JM, Yamane T (1987). Optical trapping and manipulation of single cells using infrared laser beams. Nature 330, 769–771.

Ashkin A, Schutze K, Dziedzic JM, Euteneuer U, Schliwa M (1990). Force generation of organelle transport measured in vivo by an infrared laser trap. Nature 348, 346–348.

Aufderheide KJ, Du Q, Fry ES (1992). Directed positioning of nuclei in living *Paramecium tetraurelia*: use of the laser optical force trap for developmental biology. Dev Genet 13, 235–240.

Baker N (2010). Optical studies on cell division (mitosis). PhD Thesis. La Jolla, CA: University of California, San Diego.

Barer R (1957). Refractometry and interferometry of living cells. J Opt Soc Am 47, 545–556.

Botvinick EL, Venugopalan V, Shah JV, Liaw LH, Berns MW (2004). Controlled ablation of microtubules using a picosecond laser. Biophys J 87, 4203–4212.

Cameron LA, Yang G, Cimini D, Canman JC, Kisurina-Evgenieva O, Khodjakov A, Danuser G, Salmon ED (2006). Kinesin 5-independent poleward flux of kinetochore microtubules in PtK1 cells. J Cell Biol 173, 173–179.

Croft JA, Jones GH (1989). Meiosis in *Mesostoma ehrenbergii ehrenbergii* IV. Recombination nodules in spermatocytes and a test of the correspondence of late recombination nodules and chiasmata. Genetics 121, 255–262.

Dumont S, Mitchison TJ (2009). Force and length in the mitotic spindle. Curr Biol 19, R749–R761.

Fabian L, Forer A (2005). Redundant mechanisms for anaphase chromosome movements: crane-fly spermatocyte spindles normally use actin filaments but also can function without them. Protoplasma 225, 169–184.

Felgner H, Frank R, Schliwa M (1996). Flexural rigidity of microtubules measured with the use of optical tweezers. J Cell Sci 109, 509–516.

Forer A (1965). Local reduction of spindle fibre birefringence in living *Nephrotoma suturalis* (Loew) spermatoctyes induced by ultraviolet microbeam irradiation. J Cell Biol 25, 95–117.

Forer A, Larson DE, Zimmerman AM (1980). Experimental determinations of tubulin in the in vivo mitotic apparatus of sea urchin zygotes. Can J Biochem Cell Biol 58, 1277–1285.

Forer A, Pickett-Heaps J (2005). Fibrin clots keep non-adhering living cells in place on glass for perfusion or fixation. Cell Biol Int 29, 721–730.

Forer A, Pickett-Heaps J (2010). Precocious (pre-anaphase) cleavage furrows in *Mesostoma* spermatocytes. Eur J Cell Biol 89, 607–618.

Forer A, Wilson PJ (1994). A model for chromosome movement during mitosis. Protoplasma 179, 95–105.

Fuge H (1987). Oscillatory movement of bipolar-oriented bivalent kinetochores and spindle forces in male meiosis of *Mesostoma ehrenbergii*. Eur J Cell Biol 44, 294–298.

Fuge H (1989). Rapid kinetochore movements in *Mesostoma ehrenbergii* spermatocytes: action of antagonistic chromosome fibre. Cell Motil Cytoskeleton 13, 212–220.

Fuge H, Falke D (1991). Morphological aspects of chromosome spindle fibres in *Mesostoma*: "microtubular fir-tree" structures and microtubule association with kinetochores and chromatin. Protoplasma 160, 39–48.

Gahagan KT, Swartzlander GA (1998). Trapping of low-index microparticles in an optical vortex. J Opt Soc Am B 15, 524–534.

Gomez-Godinez V, Wu T, Sherman AJ, Lee CS, Liaw LH, Zhongsheng Y, Yokomori K, Berns MW (2010). Analysis of DNA double-strand break response and chromatin structure in mitosis using laser microirradiation. Nucleic Acids Res 38, e202.

Goshima G, Scholey JM (2010). Control of mitotic spindle length. Annu Rev Cell Dev Biol 26, 21–57.

Gruzdev AD (1972). Critical review of some hypotheses concerning anaphase chromosome movements. Tsitologiya 14, 141–149.

Harsono MS, Zhu Q, Shi LZ, Duquette M, Berns MW (2013). Development of a dual joystick-controlled laser trapping and cutting system for optical micromanipulation of chromosomes inside living cells. J Biophotonics 6, 197–204.

Houchmandzadeh B, Marko JF, Chatenay D, Libchaber A (1997). Elasticity and structure of eukaryote chromosomes studied by micromanipulation and micropipette aspiration. J Cell Biol 139, 1–12.
Husted L, Ruebush TK (1940). A comparative cytological and morphological study of *Mesotoma ehrenbergii* and *Mesotoma ehrenbergii wardii*. J Morphol 67, 387–410.
Johansen KM, Forer A, Yao C, Girton J, Johansen J (2011). Do nuclear envelope and intranuclear proteins reorganize during mitosis to form an elastic, hydrogel-like spindle matrix? Chromosome Res 19, 345–365.
Johansen KM, Johansen J (2007). Cell and molecular biology of the spindle matrix. Int Rev Cytol 263, 155–206.
Kellermayer MSZ, Smith SB, Bustamante C, Granzier HL (1998). Complete unfolding of the titin molecule under external force. J Struct Biol 122, 197–205.
Kilmartin JV, Wright B, Milstein C (1982). Rat monoclonal antitubulin antibodies derived by using a new nonsecreting rat cell line. J Cell Biol 93, 576–582.
Konig K, Svaasand L, Liu Y, Sonek G, Patrizio P, Tadir Y, Berns MW, Tromberg BJ (1996). Determination of motility forces of human spermatozoa using 800nm optical trap. Mol Cell Biol 42, 501–509.
Kuo SC, Sheetz MP (1993). Force of single kinesin molecules measured with optical tweezers. Science 260, 232–234.
Kurachi M, Hoshi M, Tashiro H (1995). Buckling of a single microtubule by optical trapping forces: direct measurement of microtubule rigidity. Cell Motil Cytoskeleton 30, 221–228.
Liang H, Vu KT, Krishnan P, Trang TC, Shin D, Kimel S, Berns MW (1996). Wavelength dependence of cell cloning efficiency after optical trapping. Biophys J 70, 1529–1533.
Liang H, Wright WH, Cheng S, He W, Berns MW (1993). Micromanipulation of chromosomes in PTK2 cells using laser microsurgery (optical scalpel) in combination with laser-induced optical force (optical tweezers). Exp Cell Res 204, 110–120.
Liang H, Wright WH, He W, Berns MW (1991). Micromanipulation of mitotic chromosomes in PTK2 cells using laser-induced optical forces ("optical tweezers"). Exp Cell Res 197, 21–35.
Liang H, Wright WH, Rieder CL, Salmon ED, Profeta G, Andrews J, Liu Y, Sonek G, Berns MW (1994). Directed movement of chromosome arms and fragments in mitotic newt lung cells using optical scissors and optical tweezers. Exp Cell Res 213, 308–312.
Liu Y, Cheng DK, Sonek GJ, Berns MW, Chapman CF, Tromberg BJ (1995). Evidence for localized heating induced by infrared optical tweezers. Biophys J 68, 2137–2144.
Liu Y, Cheng K, Sonek GJ, Berns MW, Tromberg BJ (1994). Microfluorometric technique for the determination of localized heating in organic particles. Appl Phys Lett 65, 919–921.
Liu Y, Sonek J, Berns MW, Tromberg BJ (1996). Physiological monitoring of optically trapped cells: assessing the effects of confinement by 1064-nm laser tweezers using microfluorometry. Biophys J 71, 2158–2167.
Marshall WF, Marko JF, Agard DA, Sedat JW (2001). Chromosome elasticity and mitotic polar ejection force measured in living *Drosophila* embryos by four-dimensional microscopy-based motion analysis. Curr Biol 11, 569–578.
Matzke R, Jacobson K, Radmacher M (2001). Direct, high-resolution measurements of furrow stiffening during division of adherent cells. Nat Cell Biol 3, 607–610.
McIntosh JR, Pfarr CM (1991). Mitotic motors. J Cell Biol 115, 577–585.
Mitchison T, Evans L, Schulze E, Kirschner M (1986). Sites of microtubule assembly and disassembly in the mitotic spindle. Cell 45, 515–527.
Mitchison TJ, Maddox P, Gaetz J, Groen A, Shirasu M, Desai A, Salmon ED, Kapoor TM (2005). Roles of polymerization dynamics, opposed motors, and a tensile element in governing the length of *Xenopus* extract meiotic spindles. Mol Biol Cell 16, 3064–3076.
Mitchison TJ, Salmon ED (2001). Mitosis: a history of division. Nat Cell Biol 3, E17–E21.
Molloy JE, Burns JE, Kendrick-Jones J, Tregear RT, White DCS (1995). Movement and force produced by a single myosin head. Nature 378, 209–212.
Nascimento JM, Shi LZ, Meyers S, Gagneux P, Loskutoff NM, Botvinick EL, Berns MW (2007). The use of optical tweezers to study sperm competition and motility in primates. J R Soc Interface 5, 297–302.
Neuman KC, Block SM (2004). Optical trapping. Rev Sci Instrum 75, 2787–2809.
Nicklas RB (1965). Chromosome velocity during mitosis as a function of chromosome size and position. J Cell Biol 25, 119–135.
Nicklas RB (1983). Measurements of the force produced by the mitotic spindle in anaphase. J Cell Biol 97, 542–548.
Nishizaka T, Miyata H, Yoshikawa H, Ishiwata S, Kinosit K (1995). Unbinding force of a single motor molecule of muscle measured using optical tweezers. Nature 377, 251–254.
Oakley H (1983). Male meiosis in *Mesostoma ehrenbergii ehrenbergii*. In: Kew Chromosome Conference II, ed. PE Brandham and MD Bennett. London: George Allen and Unwin, 195–199.
Oakley H (1985). Meiosis in *Mesostoma ehrenbergii ehrenbergii* (Turbellaria, Rhabdocoela) III. Univalent chromosome segregation during the first meiotic division in spermatocytes. Chromosoma 91, 95–100.
Oakley HA, Jones GH (1982). Meiosis in *Mesostoma ehrenbergii ehrenbergii* (Turbellaria, Rhabdocoela) I. Chromosome pairing, synaptonemal complexes and chiasma localisation in spermatogenesis. Chromosoma 85, 311–322.
Osborn M, Weber K (1982). Immunofluorescence and immunocytochemical procedures with affinity purified antibodies: tubulin-containing structures. Methods Cell Biol 24, 97–132.
Pickett-Heaps J, Forer A (2009). Mitosis: spindle evolution and the matrix model. Protoplasma 235, 91–99.
Pickett-Heaps JD, Forer A, Spurck T (1996). Rethinking anaphase: where "Pac-Man" fails and why a role for the spindle matrix is likely. Protoplasma 192, 1–10.
Rieder CL, Alexander SP (1990). Kinetochores are transported poleward along a single astral microtubule during chromosome attachment to the spindle in newt lung cells. J Cell Biol 110, 81–95.
Sato S, Ohyumi M, Shibata H, Inaba H, Ogawa Y (1991). Optical trapping of small particles using a 1.3-μm compact InGaAsP diode laser. Opt Lett 16, 282–284.
Schaap CJ, Forer A (1979). Temperature effects on anaphase chromosome movement in the spermatoctyes of two species crane flies (*Nephrotoma suturalis* Loew and *Nephrotoma ferruginea* Fabricius). J Cell Sci 39, 29–52.
Schillers H, Walte, Urbanova K, Oberleithner H (2010). Real-time monitoring of cell elasticity reveals oscillating myosin activity. Biophys J 99, 3639–3646.
Sheykhani R, Baker N, Gomez-Godinez V, Liaw LH, Shah J, Berns MW, Forer A (2013). The role of actin and myosin in PtK2 spindle length changes induced by laser microbeam irradiations across the spindle. Cytoskeleton (Hoboken), DOI: 10.1002/cm.21104.
Shi LZ *et al.* (2012). Integrated optical systems for laser nanosurgery and optical trapping to study cell structure and function. In: Current Microscopy Contributions to Advances in Science and Technology, ed. A. Mendez-Vilas, Badajoz, Spain: Formatex, 685–695.
Silberberg YR, Yakubov GE, Horton MA, Pelling AE (2009). Cell nanomechanics and focal adhesions are regulated by retinol and conjugated linoleic acid in a dose-dependent manner. Nanotechnology 20, 285103.
Simmons RM, Finer JT, Chu S, Spudich JA (1996). Quantitative measurements of force and displacement using an optical trap. Biophys J 70, 1813–1822.
Snyder JA, Ha Y, Olsofka C, Wahdan R (2010). Both actin and myosin inhibitors affect spindle architecture in PtK1 cells: does an actomyosin system contribute to mitotic spindle forces by regulating attachment and movements of chromosomes in mammalian cells? Protoplasma 240, 57–68.
Svoboda K, Block SM (1994a). Biological applications of optical forces. Annu Rev Biophys Biomol Struct 23, 247–285.
Svoboda K, Block SM (1994b). Force and velocity measured for single kinesin molecules. Cell 77, 773–784.
Taylor EW (1965). Brownian and saltatory movements of cytoplasmic granules and the movement of anaphase chromosomes. In: Proceedings of the Fourth International Congress on Rheology, ed. AL Copley, New York: Interscience, Part 4, 175–191.
Wilson PJ, Forer A (1989). Acetylated a-tubulin in spermatogenic cells of the crane fly *Nephrotorna suturalis*: kinetochore microtubules are selectively acetylated. Cell Motil Cytoskeleton 14, 237–250.
Wong R, Forer A (2003). Signalling between chromosomes in crane fly spermatocytes studied using ultraviolet microbeam irradiation. Chromosome Res 11, 771–786.
Wright WH, Sonek GJ, Berns MW (1993). Radiation trapping forces on microspheres with optical tweezers. Appl Phys Lett 63, 715–717.
Wright WH, Sonek GJ, Berns MW (1994). Parametric study of the force on microspheres held by optical tweezers. Appl Opt 33, 1735–1748.
Yin H, Wang MD, Svoboda K, Landick R, Bloc SM, Gelles J (1995). Transcription against an applied force. Science 270, 1653–1657.

CHAPTER 7

TITLE: Effects of laser microbeam irradiations of kinetochore fibres, kinetochores and other spindle components in *Mesostoma ehrenbergii* spermatocytes

AUTHOR: Jessica Ferraro-Gideon[1]

AUTHORS AFFILIATIONS: [1]Department of Biology, York University, Toronto, ON M3J 1P3, Canada

CORRESPONDENCE INFORMATION:
Jessica Ferraro-Gideon
Biology Department, York University
4700 Keele St.
Toronto, ON
M3J1P3
(416) 736-2100 ext 44643
ferraroj@yorku.ca

RUNNING TITLE: Laser microbeam irradiation effects on *Mesostoma* chromosome movements (62 Characters)

KEYWORDS: *Mesostoma ehrenbergii*, Optical Scissors, Signalling between kinetochores, spindle fibres

WORD COUNT (not including references): 6296

7.1 Abstract

I used an optical cutting laser to irradiate kinetochore fibres, sever kinetochores, cut bivalents in half and sever bivalent arms in *Mesostoma ehrenbergii* spermatocytes. I irradiated *kinetochore fibres* with low doses (less than 39 mW) and high doses (greater than 42 mW) of laser power as the kinetochore moved to the pole or away from the pole. Following **low power** irradiations kinetochores sometimes stopped moving or oscillated with dampened amplitude but usually they detached, moved to the opposite pole and then returned to the original pole and resumed normal oscillations. Following **high power** irradiations kinetochores detached and moved to the opposite pole, but they did not return to the original pole and did not resume normal oscillations. When detached kinetochores moved toward the opposite pole, the kinetochore that returned to the original pole was always the one that was detached, not its partner. The direction of kinetochore movement when its kinetochore fibre was irradiated with a laser power less than 39 mW determined the position where the kinetochore stopped moving or which end of the oscillation cycle was truncated. When *kinetochores* were severed from bivalents, either the severed kinetochores and their partner kinetochores stopped moving, or the severed kinetochores and all the other 5 half-bivalent kinetochores stopped moving and did not recover. These results suggest that different mechanisms are required to produce kinetochore movement to and away from the pole, that there is non-random segregation of bivalents, and that there is signalling both between partner kinetochores and between half-bivalent kinetochores on different chromsomes.

7.2 Introduction

I have studied the effects of laser microbeam irradiations on chromosome movement in *Mesostoma ehrenbergii* spermatocytes. The optical cutting laser (also known as 'optical scissors') was only recently developed and utilized to study chromosome movement in a variety of cell types (Berns et al., 1971; Khodjakov and Rieder, 1996; McNeill and Berns 1981; Rieder et al., 1986;; Skibbens et al., 1995). Although the ultraviolet microbeam has been used by cell biologists for a century and has been advantageous in studying chromosome movement (Bajer and Mole-Bajer, 1961; Bloom et al., 1955; Forer, 1966; Urtez et al., 1954; Zirkle, 1970), the optical cutting laser allows cell biologists to perform experiments to sever, ablate and dissect a variety of spindle components, experiments that could not be performed with the UV microbeam.

To determine which components are involved in the force production driving chromosome movement, I used the UV microbeam at varying wavelengths (280-290nm) and powers to irradiate single kinetochore fibres or kinetochores. The UV microbeam results pointed to differences between the components that move chromosomes to the pole compared with those that move the chromosome away from the pole: the irradiations blocked movement away from the pole but allowed continued movement to the pole. To further study which components are involved in the force production driving chromosome movement, I used an optical cutting laser to irradiate kinetochore fibres as the kinetochore moved to the pole or away from the pole, to ablate single kinetochores, to cut bivalents in half or to sever bivalent arms. I performed these experiments on

Mesostoma spermatoctyes as bivalent kinetochores oscillate for a period of 1-2 hours and multiple experiments could be performed on individual spermatocytes.

Previous results have suggested that kinetochore movement to the pole is different from kinetochore movement away from the pole, bivalents non-randomly segregate during prometaphase and signalling between kinetochores may exist. I hoped that the laser microbeam experiments would allow me to test these findings.

7.3 Materials and Methods

7.3.1 Living Cell Preparations

Mesostoma ehrenbergii were reared according to the protocol described by Hoang et al. (2013), but modified to fit the conditions in a different laboratory. Briefly, adult worms were kept in scintillation vials filled with dechlorinated water at room temperature with variable light:dark cycles. The worms were fed laboratory-reared brine shrimp every other day. Spermatocytes were obtained from *Mesostoma* with clearish-white testes that were approximately 3 to 4 weeks old and had 1-3 overwintering eggs. Testes were sucked through the body wall of the worms using 10μL glass needles attached to Tygon tubing (Fisher Scientific). Using the methods previously described by Forer and Pickett-Heaps (2005), testes were expelled and evenly distributed in a drop of *Mesostoma* Ringer's solution (61 mM NaCl, 2.3 mM KCl, 0.5 mM CaCl2, and 2.3 mM phosphate buffer, pH 6.9) that contained fibrinogen (Calbiochem) on a glass coverslip. A drop of thrombin (Sigma-Aldrich, St. Louis, MO) was added then added to create a fibrin clot. The

coverslip was placed in a holder over a well filled with *Mesostoma* Ringer's solution and the preparation was sealed with wax.

7.3.2 Optical Cutting Laser

The optical cutting laser setup has been described previously (Harsono et al., 2012; Shi et al., 2012). Briefly, a 200 femtosecond pulsed laser (Mai Tai, Newport, Co., Irvine, CA, USA) tuned at 730 nm attached to an Axio Observer inverted microscope (Zeiss, Germany) was used for cutting. The objective (Zeiss Plan-Apochromat 63/1.40 Oil Ph3, Zeiss, Germany) used for these experiments transmits 74% of the laser power from the back focal plane to the cell. The power of the laser was adjusted using motorized half-wave plates and the beam was steered by fast-scanning mirrors (FSM300, Newport Co., Irive, CA, USA) so the focus of the optical cutting laser scissors could be located and moved within the sample plane. Live images were recorded at 2 second intervals using an ORCA R2 camera (Hamamatsu, Japan).

The power in the optical cutting laser was varied from 21 mW to 45 mW at the back focal plane (15 mW to 33 mW at the cell) to irradiate kinetochore fibres, kinetochores, cut bivalents in half and sever arms of bivalent in *Mesostoma* spermatocytes. No z-series, a z-series of 1 (focus in 1 plane above and 1 plane below the plane of focus) or a z-series of 3 (three planes above and three planes below) was used to either cut a single focal plane or multiple focal planes spaced about 0.2 μm apart.

7.3.3 Data Analysis

Images were taken every 2 seconds using a LabView National Instruments program throughout the duration of the experiment. The images were saved in Tagged Image File Format (TIFF) and Portable Network Graphic (PNG) format. These images were then converted to Bitmap image files (BMP), cropped and stamped with date and time, using the freeware program, Irfanview. Time-lapsed video sequences were created from these BMP files using the freeware program Virtual Dub. Single frames from the time-lapsed videos were exported into WinImage, a software program developed by Raymond Wong, and the positions of the kinetochore and the bivalent arms were measured from a fixed point at the edge of the cell. WinImage was used to mark their positions and convert these measurements into micrometres. These measurements were then imported into SlideWrite, a commercially available software program, which was used to plot distance versus time graphs.

7.4 Results

7.4.1 *Mesostoma ehrenbergii* spermatocytes

Mesostoma spermatocytes have 5 pairs of chromosomes, 3 bivalents with bipolar orientation and 4 unpaired univalents (Oakley and Jones 1982, Fuge 1987, Croft and Jones 1989), shown in Figure 7.1. In *Mesostoma* spermatocytes, bivalent kinetochores execute fast oscillatory movement to and from the spindle poles (Fuge 1987, Fuge 1989,

Fuge and Falke 1991) for up to 2 hours, from early prometaphase until anaphase (Ferraro-Gideon et al, 2013).

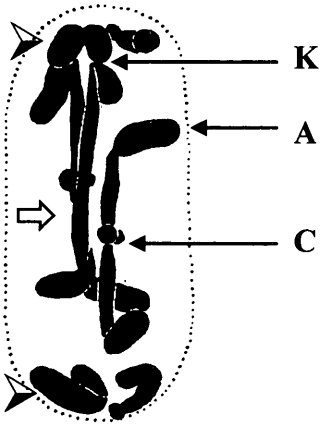

Figure 7.1. Picture of a fixed and sectioned *Mesostoma* spermatocyte taken from Husted and Ruebush (1940). Three bivalents and four univalents are visible. The arrowheads depict the univalents and the white arrow points to a bivalent. The arrow labelled (K) depicts the kinetochore, the arrow labelled (A) points to a bivalent arm, and the arrow labelled (C) points to a distally localised chiasma.

Anaphase onset can occur at any time throughout prometaphase since there is no defined metaphase; half-bivalent separation to opposite poles signifies anaphase (Ferraro-Gideon et al., 2013). Univalent chromosomes, on the other hand, usually remain at the spindle poles throughout prometaphase and only sometimes move between spindle poles prior to anaphase onset (Oakley, 1983; Oakley, 1985). In the 15 cells used as controls for these experiments, kinetochores oscillated on average 5.7 μm to and away from the pole with an average velocity of 6.6 μm/min (range 3.2-11.5 μm/min), changing their direction of motion every 50 seconds (Table 7.1). Because only a relatively small number of control

cells were analyzed for these experiments, velocity, amplitude and period are higher than in the larger number of controls cells described in Ferraro-Gideon et al. (2013).

Table 7.1. Velocity, amplitude and period of kinetochore movement to the pole and away from the pole of control cells in *Mesostoma* spermatocytes

Kinetochore Movement	**Number of Kinetochores Measured**	**Range of Velocities (μm/min)**	**Average Velocity (μm/min)**	**Average Amplitude (μm)**	**Average Period (sec)**
Away from the pole*	47	3.24-8.92	6.15±1.44	5.7±1.6 (4.0-9.0)	100±25 (60-150)
To the pole*	47	3.17-11.5	6.98±1.77		
Combined	94 (n=15)	3.17-11.5	6.57±1.61		
**Difference between to the pole and away from the pole kinetochore velocities is statistically significant at $p<0.01$, using Student's t-test.*					

7.4.2 Laser Microbeam Irradiation of Single Kinetochore Fibres

I irradiated kinetochore fibres with a laser of wavelength 730 nm as the kinetochore moved to or away from its spindle pole (Table 7.2) and varied the power in the laser (21 mw to 45 mW) and for different cuts varied the number of focal planes (no z-series up to z-series=3). Low dose (less than 42 mW) irradiations usually (18/23) caused the kinetochores to detach from the pole (e.g., Figure 7.2) but sometimes (5/23) caused oscillations with dampened amplitude, or stopped movement (Table 7.2A). When kinetochores detached from their pole, they moved up to 14 μm towards the opposite pole and then back towards their original pole of attachment either immediately after reaching their furthest away from the pole position or up to 6 minutes later (Table 7.3). When detached kinetochores moved back towards their original pole, in 18 cells, they either

moved towards the pole in one linear motion (Figure 7.3A) or they moved towards the pole in a step-like motion (Figure 7.3B).

Table 7.2. Effects of laser microbeam irradiation on kinetochore movement following irradiation of the k-fibre as the kinetochore moves to the pole or moves away from the pole. (A) Low power (21 mw to 39 mW) irradiations. (B) High power (42 to 45 mW) irradiations.

A. Low Power Kinetochore Fibre Irradiations							
Type of Kinetochore Fibre Irradiation	**Total Number of Cells**	**Kinetochore Detached from its Pole**		**Kinetochores Did Not Detach**			
				Decreased Amplitude of Kinetochore Oscillations		**Stopped Kinetochore Movement**	
		Oscillations Recovered	Oscillations did not Recover	Away from the Pole	At the Pole	Recovers	No Recovery
Kinetochore moves Away from the Pole	17	14 (82%)	0	2 (12%)	0	0	1 (6%)
Kinetochore moves To the Pole	6	4 (66%)	0	0	1 (17%)	1 (17%)	0

B. High Power Kinetochore Fibre Irradiations							
Type of Kinetochore Fibre Irradiation	**Total Number of Cells**	**Kinetochore Detached from its Pole**		**Kinetochores Did Not Detach**			
				Decreased Amplitude of Kinetochore Oscillations		**Stopped Kinetochore Movement**	
		Oscillations Recovered	Oscillations did not Recover	Away from the Pole	At the Pole	Recovers	No Recovery
Kinetochore moves Away from the Pole	3	0	3 (100%)	0	0	0	0
Kinetochore moves To the Pole	2	0	2 (100%)	0	0	0	0

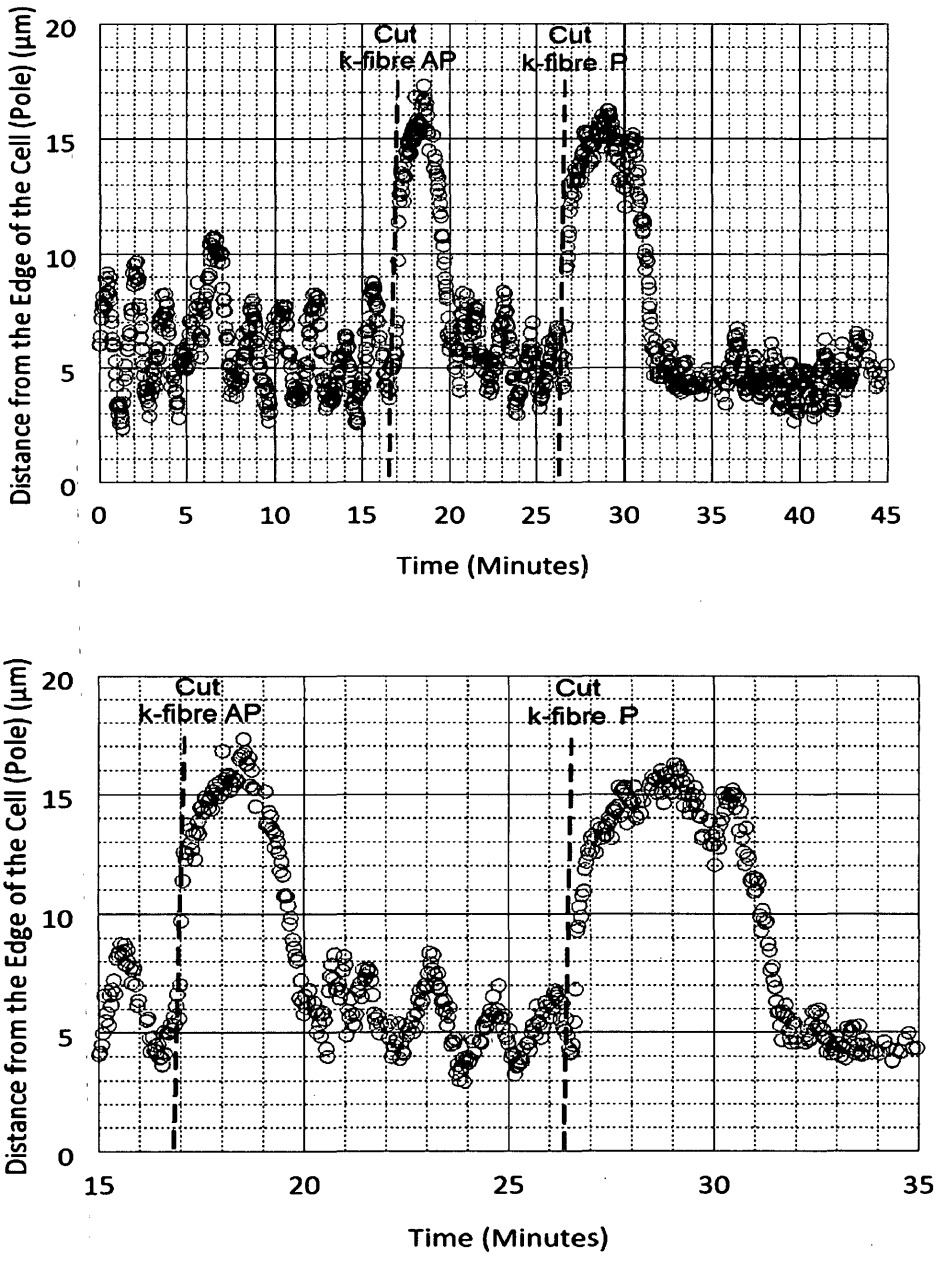

Figure 7.2. (A-B) Single kinetochore fibre cutting with a power of 21mW and a z-series of 1 as the kinetochore moved away from the pole and then as the kinetochore moved to the pole in a *Mesostoma ehrenbergii* spermatocyte. Distance from the edge of the cell (pole) in µm versus time in minutues for the irradiated half-bivalent. The dashed line indicates the time of each cut. Kinetochores detached from the pole when their kinetochore fibres were severed, re-attached and then resumed kinetochore oscillations.

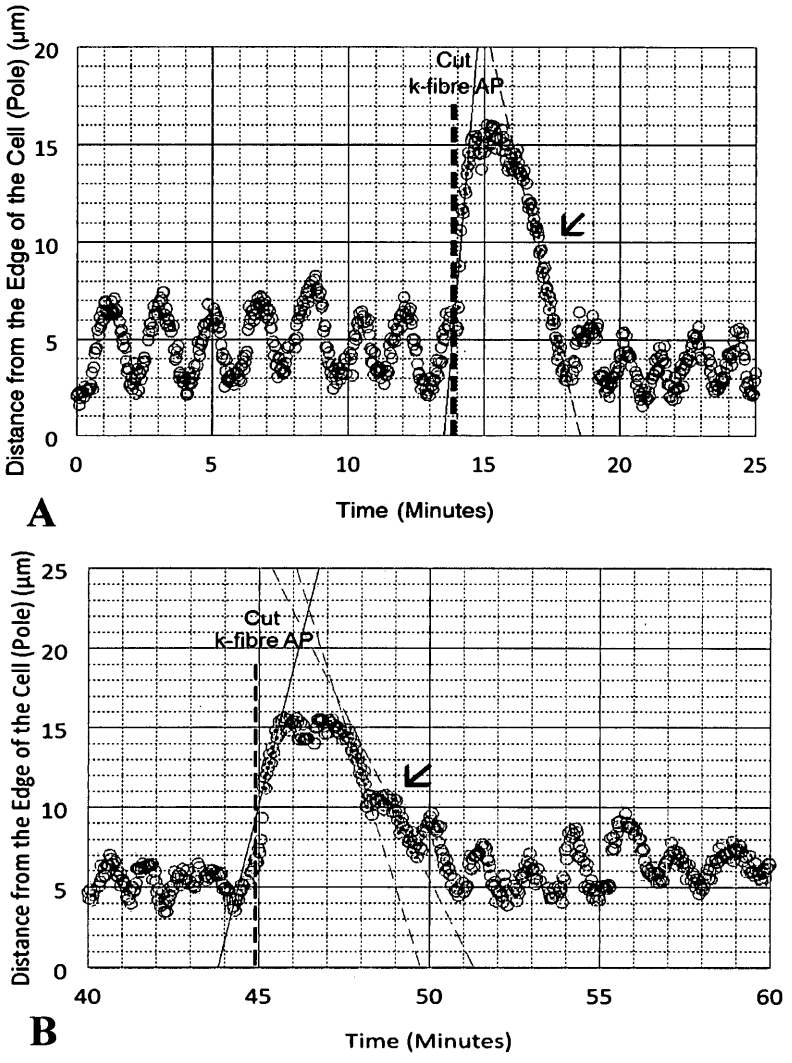

Figure 7.3. (A-B) Single kinetochore fibre cutting as the kinetochore moved away from the pole in a *Mesostoma ehrenbergii* spermatocyte. Distance from the edge of the cell (pole) in µm versus time in minutes for the irradiated half-bivalent. The dashed line indicates the time of cut. (A) The half-bivalent kinetochore whose kinetochore fibre was severed with a power of 32mW and a z-series of 1 detached from the pole and then moved back toward its pole in one linear motion. (B) The half-bivalent kinetochore whose kinetochore fibre was severed with a power of 38mW and no z-series detached from the pole and then moved back toward its pole in a step-like motion. Kinetochore movement of the detached kinetochore as it moved back to the pole pointed to by the black arrow points.

Once detached kinetochores reached their original pole of attachment and re-established bipolar orientation, kinetochore movement recovered (Table 7.2; e.g., Figure 7.3): the oscillations of half the kinetochores were the same as before cutting and the other half had decreased amplitude (e.g., Figure 7.4).

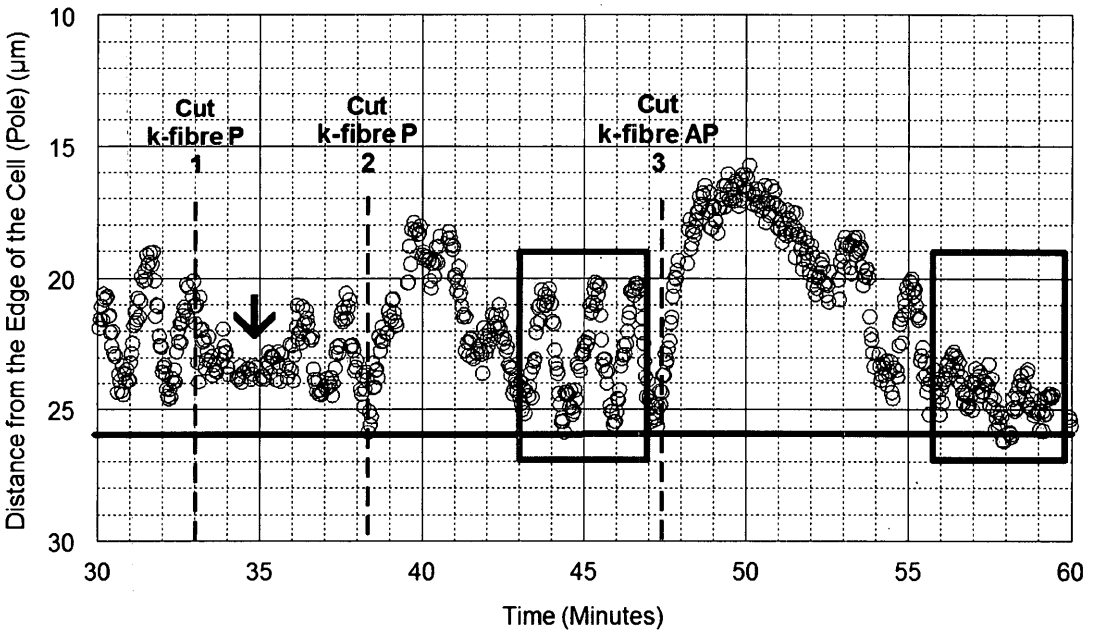

Figure 7.4. Single kinetochore fibre cutting with a power of 37mW as the kinetochore moved to the pole and then as the kinetochore moved away from the pole in a *Mesostoma ehrenbergii* spermatocyte. Distance from the edge of the cell (pole) in µm versus time in minutes for the irradiated half-bivalent. The black solid line indicates the position of the spindle pole. The dashed line indicates the time of each of the cuts. When the kinetochore fibre was severed as: 1. the kinetochore moved to the pole, kinetochore movement temporarily stopped at the pole and recovered; 2. the kinetochore moved to the pole, the kinetochore detached from the pole, immediately moved back to the pole and recovered with normal oscillations; and 3. the kinetochore moved away from the pole, the kinetochore detached from the pole, moved back toward the pole after approximately 3 minutes and then oscillated with a dampened amplitude. The black arrow points to stopped kinetochore movement at the pole. The solid gray boxes envelope recovered kinetochore movement after the detached kinetochore re-attaches to its pole. The first box illustrates recovered kinetochore movement with normal oscillations and the second box illustrates recovered kinetochore movement with a decrease in the amplitude of oscillations.

Kinetochore detachment from the pole was independent of the direction of motion of the kinetochore and occurred when kinetochore fibres were severed as the kinetochore moved in either direction (Figure 7.2, Figure 7.4). Some effects of the severing did depend on direction of kinetochore motion at the time of severing, however. The velocity the detached kinetochore moved towards the opposite pole was dependent on the direction of motion of the kinetochore. Detached kinetochores accelerated towards the opposite pole when kinetochore fibres were severed as the kinetochore moved away from the pole but moved at oscillation velocities or slower when kinetochore fibres were severed as the kinetochore moved to the pole (Table 7.4). When the detached kinetochore moved back towards its original pole, kinetochore movement was always slower than oscillation velocities (Table 7.4). When the severing caused cessation of oscillations, the positions at which the kinetochore stopped moving depended on the direction of motion: those moving toward the pole stopped at the pole end of the oscillation cycle (Figure 7.4) and those moving away from the pole stopped at the away-from-pole end of the oscillation cycle. When the severing dampened the amplitudes of oscillation, the dampening was at the pole end of the oscillation for kinetochores moving to the pole and was at the opposite end for kinetochores moving away from the pole.

These results were for the 23 cells listed in Table 7.2A, when I used a laser power of 21 mW to 39 mW at the back focal plane. There were different effects on kinetochore movement when higher powers (greater than 42mW) were used and kinetochore fibres were cut in several focal planes (z-series of 3). When these parameters were used to

irradiate 5 kinetochore fibres: kinetochores detached, they moved to the opposite pole, and sat there motionless, with no oscillations (Figure 7.5).

Table 7.3. Comparison of the velocity, distance travelled and time of recovered movement after kinetochore fibres were severed as the kinetochore moved in either direction. Values are standard deviations.

Detached Kinetochore Movement in *Mesostoma* Spermatocyte				
Detached Kinetochore Movement	**Range of Velocities (μm/min)**	**Average Velocities (μm/min)**	**Average Distance Travelled Away from the Original Pole (μm)**	**Average Time KT Movement Recovered (min)**
KT movement Away from the Original Pole after k-fibres were severed	1.4 - 21.5	8.0 ± 4.4 (n=24)	9.3 ± 3.4 (4.0 - 14.0) (n=24)	1.4 (0 - 6) (n=20)
Recovered KT movement to the Original Pole after k-fibres were severed	2.7 - 6.6	4.5 ± 1.3 (n=15)		

Kinetochore movement may not have recovered in these cells because the combination of high power and multiple Z planes may have irreversibly damaged the spindle; spindle damage was clearly visible in 2 cells by the presence of a sniglet (Cole et al., 1995) after the kinetochore fibre was cut.

In sum, lower and higher laser powers have different effects on kinetochore movement; and the effects of higher powers may be due to damage to the cell. Lower powers detached the kinetochores, but the same kinetochores returned to their original poles and resumed oscillation, either with normal or dampened amplitudes. Table 7.5 summarises the effects after severing kinetochore fibres when the kinetochores were moving in the two directions.

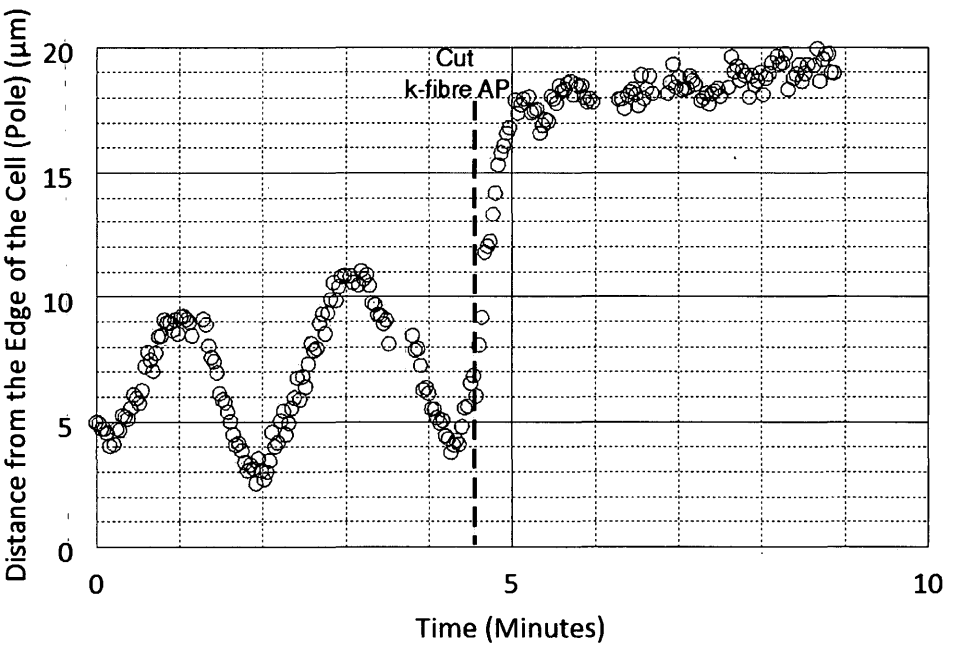

Figure 7.5. Single kinetochore fibre cutting as the kinetochore moved away from the pole with a power of 45mW and a z-series of 3 in a *Mesostoma* spermatocyte. Distance from the edge of the cell (pole) in µm versus time in minutes for the irradiated half-bivalent. The dashed line indicates the time of the cut. The kinetochore detached from the pole when its kinetochore fibre was severed and remained motionless at the opposite pole during the period of this experiment.

Table 7.4. Comparison of the number of cells in which movement of the detached and recovered kinetochore accelerated or moved at original velocities or slower towards the pole when the kinetochore fibre was severed as the kinetochore moved to the pole or away from the pole

Direction kinetochore was Moving when K-fibre was Cut	Movement of Detached Kinetochore towards the Opposite Spindle Pole		Recovered Kinetochore Movement towards the Original Spindle Pole	
	Accelerated	Moved at Original Velocity or Slower	Accelerated	Moved at Original Velocity or Slower
To the Pole	0	4	0	3
Away from the Pole	9	5	0	8

Table 7.5. Comparison of the effect of laser microbeam cuts on kinetochore movement.

	When the Kinetochore Fibre was Cut	
	Kinetochore Moved To the Pole	**Kinetochore Moved Away from Pole**
Effect of Laser cutting on Kinetochore Movement- Low Power (37 – 39 mW)	1.Detached Kinetochores & Movement Recovered 2. Stopped Movement 3. Decreased Amplitude of Oscillations	1.Detached Kinetochores & Movement Recovered 2. Stopped Movement 3. Decreased Amplitude of Oscillations
Velocity of Detached Kinetochore Movement	Oscillation Velocity or Slower	Faster than Oscillation Velocity
Position of Stopped Kinetochore Movement	At the Pole	Away from the Pole
Stopped Kinetochore Movement Recovered	Yes	No
Decreased Amplitude	At the Pole	Away from the Pole
Effect of Laser cutting on Kinetochore Movement- High Power (42 – 45 mW)	1.Detached Kinetochores & No Recovered Movement	1.Detached Kinetochores & No Recovered Movement

7.4.3 Laser Microbeam Irradiations of Single Kinetochores, Bivalents and Bivalent Arms

In addition to irradiating single kinetochore fibres, I severed half-bivalent kinetochores, I cut bivalents in half, and I severed the arms of half-bivalents (Table 7.6). It was very difficult to sever kinetochores or cut bivalents in half because bivalents are continuously oscillating and they move past the laser line faster than a single line laser cut is completed, so to cut the chromosome multiple laser cuts were sometimes required. I severed a kinetochore in 6 cells, and in 5 of them the severed kinetochore moved to the pole at about the same speed as during oscillations. In 3 of these cells, its partner kinetochore also moved to its pole and stopped, as graphically illustrated in Figure 7.6 where measurements were made from a fixed point (pole) to the edge of the cut bivalent (not to its partner kinetochore). Time lapsed videos confirm that the partner kinetochore moved to its pole and stopped. There was no effect on kinetochore movement in one cell when the kinetochore was severed. This could be because the kinetochore was not completely severed from the bivalent.

I cut bivalents in half in 3 cells, and in 2 of them both kinetochores moved to the pole, stopped, and did not recover (Table 7.6, Figure 7.7). Half-bivalent kinetochores moved to the pole with the same speed as oscillations. Kinetochore movements of the other two bivalents in the same cell were not affected when a bivalent was cut in half. In 1/3 cells, there was no effect on kinetochore movement when the bivalent was cut in half. This could be because the bivalent was not completely severed and a connection between the half-bivalents still existed.

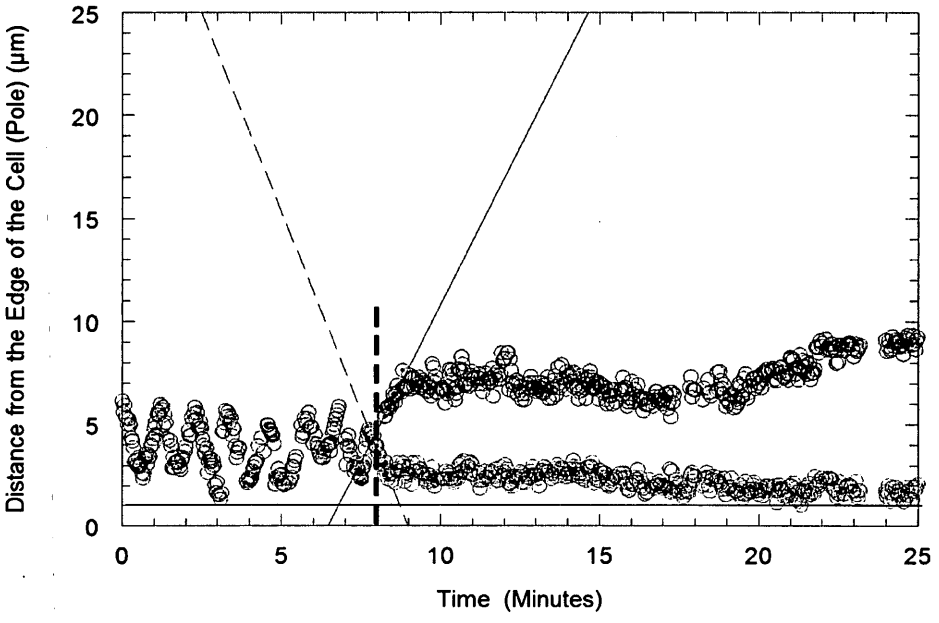

Figure 7.6. Single kinetochore is severed in a *Mesostoma* spermatocyte. Distance from the edge of the cell (pole) in µm versus time in minutes for the severed half-bivalent (O). The dashed line indicates the time of cut with a laser power of 37mW at the back focal plane for a single kinetochore. Following the cut, the kinetochore (O) moved to the pole with a velocity of 3.8µm/min and stopped. The cut bivalent (O) moved away from its respective pole with a velocity of 3.1µm/min. Once the non-severed kinetochore reached the pole, it stopped and did not recover. Measurements were taken from the pole to the bottom of the severed half-bivalent not from the pole to the partner kinetochore. The pole is indicated by the solid line.

I severed the arm of a half-bivalent in 8 cells. In 3/8 cells, the severed arm moved backward across the equator toward its partner half-bivalent and stopped; movement of the severed arm toward its partner may indicate that a connection exists between the two arms, similar to the 'tethers' that connect separating half-bivalent arms in crane fly spermatocytes (LaFountain et al., 2002).. In 5/8 cells, on the other hand, the severed arm continued to oscillate (in 3 cells) or remained stationary (in 2 cells). When the severed arm continued to oscillate, it oscillated between its associated kinetochore and its partner, first moving closer to one kinetochore and then the other.

Table 7.6. Effects of laser microbeam irradiation on kinetochore movement after half-bivalent kinetochores were severed or bivalents were cut in half.

Type of Cut	Number of KTs Analyzed	Stopped Kinetochore Movement of the Half-Bivalent associated with the Irradiation		Stopped Kinetochore Movement of the Partner Half-Bivalent		No Effect on Kinetochore Movement
		At the Pole	At its Away from Pole Position	At the Pole	At its Away from Pole Position	
Kinetochore	6	5	0	5	0	1
Cut bivalent in Half	3	2	0	2	0	1
TOTAL	**9**	**7**	**0**	**7**	**0**	**2**

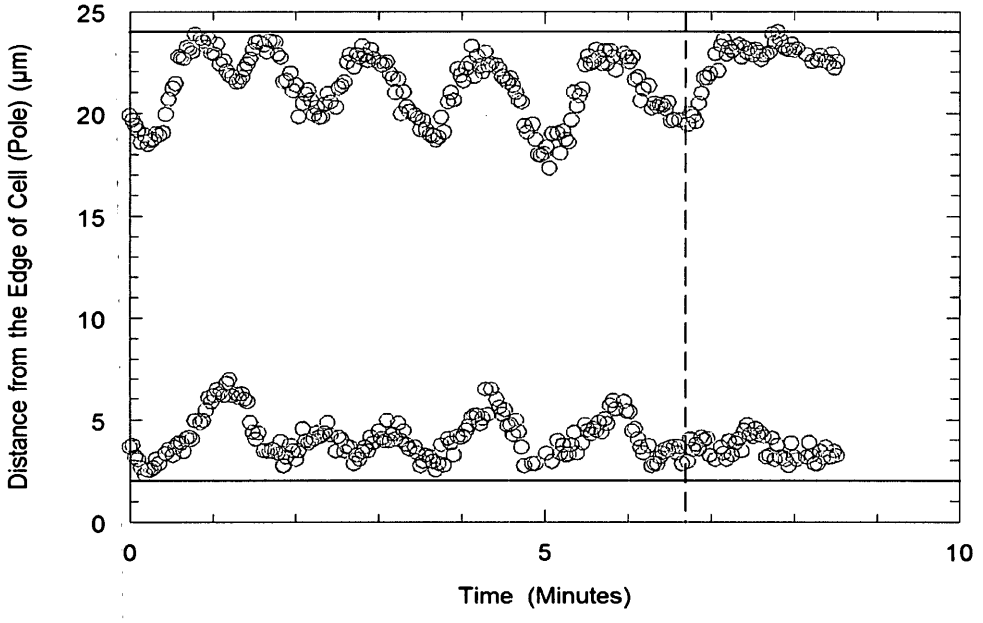

Figure 7.7. Single bivalent is severed in half in a *Mesostoma* spermatocyte. Distance from the edge of the cell (pole) in µm versus time in minutes for the two half-bivalents (O). The dashed line indicates the time that the bivalent is severed in half. During its normal oscillations the half-bivalent moving to the upper pole, moves to the pole with an average velocity of 8.1µm/min. When the bivalent is severed in half, the half-bivalent moving to the upper pole, moves to the pole with a velocity of 8.8 µm/min and stops. The half-bivalent moving to the lower pole, remains at the pole and does not recover. The poles are indicated by the solid lines.

The severed arm may have continued to oscillate between the two kinetochores because the arm was not completely severed from its associated kinetochore and the remaining weak attachment prevented it from moving completely across the equator towards its partner. The severed arm may have remained stationary, even though it was completely severed from its bivalent, because that specific arm was not tethered to its partner, similar to crane fly spermatocytes that only have tethers between 2 of their 4 bivalent arms. Since, 6/8 cells had connections between partner arms, "tethers" seem to exist between half-bivalent arms in *Mesostoma* spermatocytes as they do in crane fly spermatocytes (LaFountain et al., 2002), the only two organisms studied in this regard. .

7.4.4 Laser Microbeam Irradiation of Single Univalent Kinetochore Fibres

I irradiated in front of a univalent with a laser power of 34 mW and a z-series of 1, as the univalent moved from one spindle pole to the other with the hope of severing any kinetochore fibre attachments. I only performed this experiment once as univalents move so rapidly between spindle poles that it is sometimes difficult to spot a univalent moving and when I do, there is not enough space between the pole and the univalent kinetochore to irradiate the kinetochore fibre. As the univalent moved from one spindle pole to the other, I irradiated in front of the univalent kinetochore twice (Figure 7.8). Following the first irradiation, kinetochore movement temporarily slowed from 5.7 μm/min to 1.6 μm/min and following the second irradiation, kinetochore movement temporarily stopped (Figure 7.8). When the univalent resumed movement to the pole

approximately 1 minute later, the univalent accelerated to the pole with a velocity of 6.5 μm/min. I do not know if I severed the kinetochore fibre attachment between the pole and the univalent kinetochore but because kinetochore movement slowed and also stopped following irradiation, I assume that I did sever microtubules. Confocal immunofluorescence microscopy studies need to be done to determine which spindle components are being altered by the irradiation.

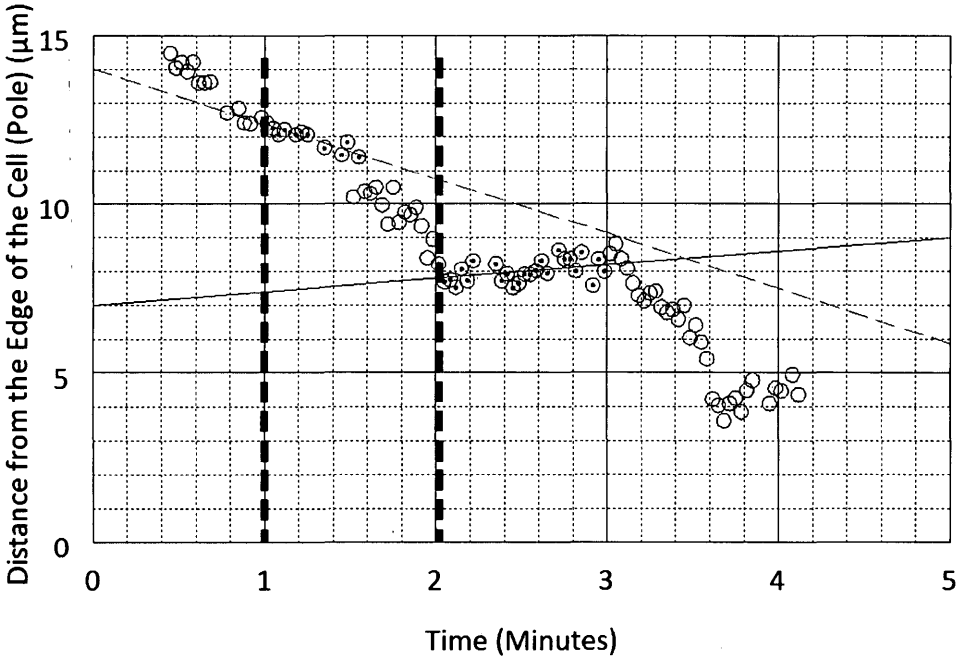

Figure 7.8. Single univalent kinetochore fibre irradiation as the kinetochore moved from one spindle pole to the other with a power of 34 mW and a z-series of 1 in a *Mesostoma* spermatocyte. Distance from the edge of the cell (pole) in μm versus time in minutes for the irradiated univalent. The dashed lines indicates the time of the cuts. Kinetochore movement slowed from 4.1 μm /min to 1.6 μm/min after the first cut and then temporarily stopped after the second cut. The univalent then accelerated to the pole with a velocity of 6.5 μm/min.

7.5 Discussion

Laser microbeam irradiation of kinetochore fibres as the kinetochore moved in either direction in *Mesostoma* spermatocytes detached kinetochores, stopped kinetochore movement or decreased the amplitude of kinetochore oscillations. Detached kinetochores recovered and resumed normal oscillations when low doses were used to sever kinetochore fibres as the kinetochore moved in either direction but kinetochores did not recover when higher doses were used (Table 7.2). The direction the kinetochore was moving when single kinetochore fibres were severed when kinetochores did not detach determined the position the kinetochore stopped moving and the position kinetochores oscillated with decreased amplitude (Table 7.4, eg. Figure 7.4). Half-bivalent kinetochores and their partner kinetochores moved to opposite poles and stopped when single kinetochores were severed and half-bivalents were cut in half.

The kinetochore of the half-bivalent connected to the laser-irradiated fibre moved past its maximum distance away from the pole toward the opposite pole when its kinetochore fibre was severed. I assume this is because the fibre was severed and the chromosome was detached from the pole. The kinetochore then moved to its original pole and obtained bipolar orientation (presumably because it reattached to its original pole) and oscillated normally (Figures 7.2, 7.3 and 7.4). Bivalents in *Mesostoma* spermatocytes often detach and reorient during prometaphase/metaphase (Ferraro-Gideon et al., 2013); this behaviour is similar to bivalents whose kinetochore fibres were severed. When a half-bivalent reorients under normal circumstances however, its partner kinetochore switches poles and moves back to the original pole but when kinetochore fibres are

severed, the same, detached kinetochore moves back to its original pole. Since partner kinetochores do not switch poles when kinetochore fibres are severed but do when bivalents reorient, this suggests that bivalent segregation in *Mesostoma* spermatocytes is non-random, similar to the suggested non-random segregation of univalents in *Mesostoma* spermatocytes that was suggested by Oakley (1983, 1985) and later by Ferraro-Gideon et al. (2013).

Low power irradiations of a single kinetochore fibre as the kinetochore moved in either direction resulted in the detachment and recovery of the half-bivalent connected to the laser-irradiated fibre. Although it would appear that there is no difference between kinetochore movement to the pole and kinetochore movement away from the pole; there were differences in velocities of poleward movement depending on the direction of motion at the time the fibre was severed. Directionality differences also were seen when half-bivalent kinetochores did not detach following laser microbeam irradiation. The position the kinetochore stopped depended on the direction of motion of the kinetochore when kinetochore fibres were irradiated, as did the side of the oscillation 'wave' that decreased in amplitude (Table 7.6). I assume that when kinetochores detached from the pole microtubules were completely severed so there would be the same affect on kinetochore movement regardless of the direction the kinetochore was moving. I assume that when kinetochores did not detach from the pole the microtubules and non-microtubule components were not completely severed but only altered in some way, so there would be a different affect on kinetochore movement depending on the direction the kinetochore was moving. Therefore, these results may support the UV microbeam results

showing that there is a difference between kinetochore movement to the pole and away from the pole. Further studies using confocal immunofluorescence microscopy may help determine which components are severed when kinetochores detach from the pole and which components are altered when kinetochore movement stops or amplitude decreases.

Severing a half-bivalent kinetochore in *Mesostoma* spermatocytes stopped kinetochore movement of the severed kinetochore and its partner at the pole. The results of UV microbeam irradiations of kinetochores in *Mesostoma* spermatocytes and in crane fly spermatocytes (Yin and Forer, 1996; Wong and Forer, 2003) suggest that kinetochores may play an important role in communication; UV irradiation of a single kinetochore stopped kinetochore movement of the irradiated kinetochore and its partner in *Mesostoma* spermatocytes and stopped kinetochore movement all 6 half-bivalents in crane-fly spermatocytes (Ilagan and Forer, 1997). Following UV microbeam irradiations of kinetochores it was suggested that there are differences between these two cells: signalling between kinetochores requires a direct physical linkage between partner half-bivalents in *Mesostoma* spermatocytes, whereas, signalling occurs between all chromosomes in crane fly spermatocytes, suggesting an indirect link. The laser microbeam results however might suggest that signalling can occur between kinetochores that are not physically linked in *Mesostoma* spermatocytes or it may suggest that a connection is required between the kinetochore and the bivalent for kinetochore oscillations to take place. Thus opposing forces across the bivalent (at the two kinetochores) may be necessary for oscillations. Therefore, severing a kinetochore may not be a good indicator as to whether or not signals are transmitted between kinetochores

in *Mesostoma* spermatocytes. Instead laser microbeam experiments should be repeated by ablating kinetochores not severing them.

The laser microbeam experiments performed on *Mesostoma* spermatocytes suggest different mechanisms are required to produce kinetochore movement to and away from the pole. Bivalent reorientations that occur throughout prometaphase are non-random. If signalling between kinetochores is present, it may not require physical linkage connecting half-bivalent kinetochores to stop kinetochore movement of partner half-bivalents.

7.6 References

Bajer, A. and Mole-Bajer, J. (1961). UV microbeam irradiation of chromosomes during mitosis in endosperm. Exp Cell Res. **25**, 251-267.

Berns, M.W., Cheng, W.K., Floyd, A.D. and Ohnuki, Y. (1971) Cell division after laser microirradition of mitotic chromosomes. Nature. **233**, 122-123.

Bloom, W., Zirkle, R.E. and Uretz, R.B. (1955). Irradiation of parts of individual cells. III. Effects of chromosomal and extrachromosomal irradiation on chromosome movements. Ann NY Acad Sci. **59**, 503-513.

Cole, R.W., Khodjakov, A., Wright, W.H., Rieder, C.L. (1995). A differential interference contrast-based light microscopic system for laser microsurgery and optical trapping of selected chromosomes during mitosis *in vivo*. J Microsc Soc Am. **1**, 203–215.

Ferraro-Gideon, J., Hoang, C., and Forer A. (2013). Meiosis-I in *Mesostoma ehrenbergii* spermatocytes includes distance segregation and inter-polar movements of univalents, and vigorous oscillations of bivalents. Protoplasma. Accepted.

Forer, A. (1966). Characterization of the mitotic traction system, and evidence that birefringent spindle fibres neither produce nor transmit force for chromosome movement. Chromosoma. **19**, 44-98.

Forer, A. and Pickett-Heaps, J. (2005). Fibrin clots keep non-adhering living cells in place on glass for perfusion or fixation. Cell Biol Int. **29**, 721–730.

Fuge, H. (1987). Oscillatory movement of bipolar-oriented bivalent kinetochores and spindle forces in male meiosis of *Mesostoma ehrenbergii*. Euro J Cell Bio. **44**, 294-298.

Fuge, H. (1989). Rapid kinetochore movements in *Mesostoma ehrenbergii* spermatocytes: action of antagonistic chromosome fibre. Cell Motil Cytoskeleton. **13**, 212-220.

Fuge, H. and Falke, D. (1991). Morphological aspects of chromosome spindle fibres in *Mesostoma*: "microtubular fir-tree" structures and microtubule association with kinetochores and chromatin. Protoplasma. **160**, 39-48.

Harsono, M.S., Zhu, Q., Shi, L.Z., Duquette, M., and Berns, M.W. (2013). Development of a dual joystick-controlled laser trapping and cutting system for optical micromanipulation of chromosomes inside living cells. J Biophotonics. **6**, 197-204.

Ilagan, A.B. and Forer, A. (1997). Effects of ultraviolet-microbeam irradiation of kinetochores in crane-fly spermatocytes. Cell Motil Cytoskeleton. **36**, 266-275.

Khodjakov, A. and Rieder, C.L. (1996). Kinetochores moving away from their associated pole do not exert a significant pushing force on the chromosome. J Cell Biol. **135**, 315-327.

McNeill, P.A. and Berns, M.W. (1981). Chromosome behavior after laser microirradiation of a single kinetochore in mitotic PTK2 cells. J Cell Biol. **88**, 543-553.

Oakley, H.A. (1983). Male meiosis in *Mesostoma ehrenbergii ehrenbergii*. Kew Chromosome Conference II Editors PE Brandham, MD Bennett. George Allen and Unwin, London (Boston, Sydney) pp 195-199.

Oakley, H.A. (1985). Meiosis in *Mesostoma ehrenbergii ehrenbergii* (Turbellaria, Rhabdocoela) III. univalent chromosome segregation during the first meiotic division in spermatocytes. Chromosoma. **91,** 95-100.

Shi, L.Z., Zhu, Q., Wu, T., Duquette, M., Gomez, V., Chandsawangbhuwana, C., Harsono, M.S., Hyun, N., Baker, N., Nascimento, J, *et al.* (2012). Integrated optical systems for laser nanosurgery and optical trapping to study cell structure and function. In: Current Microscopy Contributions to Advances in Science and Technology, A. Mendez-Vilas (ed.). Badajoz, Spain: Formatex, Microscopy Book Series – Number 5.

Skibbens, R.V., Rieder, C.L. and Salmon, E.D. (1995). Kinetochore motility after severing between sister centromeres using laser microsurgery: evidence that kinetochore directional instability and position is regulated by tension. J Cell Sci. **108**, 2537-2548.

Uretz, R.B., Bloom, W. and Zirkle, R.E. (1954). Irradiation of parts of individual cells. II. Effects of an ultraviolet microbeam focused on parts of chromosomes. Science. **120**, 197-199.

Wong, R. and Forer, A. (2003). Signalling between chromosomes in crane fly spermatocytes studied using ultraviolet microbeam irradiation. Chromosome Res. **11**, 771–786.

Yin, B. And Forer, A. (1996). Coordinated movements between autosomal half-bivalents in crane-fly spermatocytes: evidence that 'stop' signals are sent between partner half-bivalents. J Cell Sci. **109**, 155-163.

Zirkle, R.E. (1970). Ultraviolet-microbeam irradiation of newt-cell cytoplasm: spindle destruction, false anaphase, and delay of true anaphase. Radiat Res. **42**, 516-537.

CHAPTER 8

8.1 General Discussion

The purpose of my thesis is to study and better understand which components are involved in the force production driving chromosome movement during meiosis I. I have used a variety of different tools including, an ultraviolet microbeam, a laser microbeam (optical scissors) and an optical trapping laser (optical tweezers) to irradiate, sever and manipulate different components of the spindle in *Mesostoma ehrenbergii* spermatocytes. Since *Mesostoma* have large spermatocytes with few easily distinguishable bivalents that have regular and persistent kinetochore oscillations, they make an ideal organism for studying chromosome movement. Their continuous kinetochore oscillations allow me to perform multiple experiments on the same spermatocyte, therefore producing numerous replications in a short time period.

8.2 Conclusions

During my PhD thesis, I first had to learn how to rear *Mesostoma* en masse in the laboratory and then develop a protocol for maintaining these stocks. This protocol is described in (Chapter 3), an article by Hoang et al. (2013). We determined that *Mesostoma* will continue to produce subitaneous eggs when they are reared at 25°C and daily fed brine shrimp. We also determined that light:dark cycles do not influence subitaneous egg production in *Mesostoma.* Since we have been able to determine which parameters allow the continued production of subitaneous eggs, we have now reared

these worms to 46 generations. Because there are only a handful of articles in the literature that describe cell division in this organism, a first step was to characterise meiosis-I in *Mesostoma* spermatocytes in greater detail, described in (Chapter 4), an article by Ferraro-Gideon et al. (2013a). Since I learned how to rear and maintain large stocks of *Mesostoma* in the laboratory, I had sufficient animals for experimentation and I was able to study and characterise bivalent kinetochore oscillations, anaphase chromosome movements, bivalent reorientations and univalent movements in their spermatoctyes.

Our main conclusions were that bivalent kinetochore movement to the pole is significantly faster than kinetochore movement away from the pole. The movement parameters, namely velocity, period and amplitude, are more than 20% different for partner kinetochores, kinetochores to the same pole and kinetochores moving to opposite poles. Anaphase chromosome movement is approximately $1/5^{th}$ to $1/6^{th}$ the speed of bivalent kinetochore oscillations in the same cell. Mono-oriented bivalents seen at the start of filming generally become bipolarly oriented, and bipolarly oriented bivalents periodically become mono-oriented, and, in most cells, partner kinetochores switch poles before re-attaching. Univalent excursions are not common (56 excursions in 1200 minutes), but when they do occur, 2 up to 7 univalent excursions can occur in one cell. From these observations, I conclude that kinetochore movement to the pole is different from kinetochore movement away from the pole; oscillations of kinetochores in the same cell are independent; there is distance segregation of bivalents and univalents; and

multiple bivalent reorientations and univalent excursions may be due to non-random segregation of chromosomes.

The first set of experiments I performed on *Mesostoma* spermatocytes involved UV microbeam irradiation of kinetochore fibres and kinetochores using methods used by Forer and colleagues (Sillers and Forer, 1983; Wilson and Forer; 1987). From my UV microbeam results, I observed that not only was kinetochore movement altered following irradiation of kinetochore fibres and kinetochores but the precocious cleavage furrow shifted positions and in some cells there was a complete loss of cell shape following irradiation. After UV irradiation of kinetochore fibres as the kinetochore moved in either direction, kinetochores moved to the pole and stopped moving. They did not stop moving at the position they were in when the fibre was irradiated. Kinetochore movement resumed following irradiations of kinetochore fibres as the kinetochore moved to the pole but did not resume following irradiations of kinetochore fibres as the kinetochore moved away from the pole. UV irradiation of kinetochores stopped kinetochore movement on the spot, the kinetochore slowly moved to the pole and stopped at the pole, but movement did not resume. Kinetochore oscillations of non-irradiated partners were normal following irradiation of kinetochore fibres except for decreased amplitudes; kinetochore oscillations of non-irradiated partners decreased in amplitude and then stopped following irradiation of kinetochores. Irradiation of kinetochore fibres and kinetochores, shifted the position of the precocious, "pre-anaphase", cleavage furrow either toward or away from the site of irradiation and in some cells, there was a complete loss of ingression of the

furrow and a change in cell shape following irradiation of kinetochore fibres as the kinetochore moved away from pole and following irradiation of kinetochores. The results from my UV microbeam experiments demonstrated that kinetochore movement to the pole is due to different mechanisms than kinetochore movement away from the pole; kinetochore movement to the pole was not affected following irradiation of kinetochore fibres as the kinetochore moved in either direction; and the precocious cleavage furrow shifts its position when spindle components are altered, To try to better understand these results, I tried to fix and stain cells for confocal immunofluorescence microscopy. Despite considerable effort no reliable method was developed to fix and stain *Mesostoma* spermatocytes for immunofluorescence.

Using the UV microbeam I was not able to answer all the questions I wanted to answer during my thesis. I wanted to do experiments that let me sever chromosomes, trap bivalent kinetochores, and ablate kinetochores of bivalents and univalents to ask: can bivalents oscillate independently if they are severed in half or severed closer to one kinetochore? Are the forces that act on the kinetochore as it moves to the pole different from those that act as it moves away from the pole, as my earlier experiments might indicate? Will a univalent move from one pole to the other if its kinetochore is ablated? Does ablating a kinetochore give the same result as inactivating it using UV? I was given the privilege to use laser microbeams in Dr. Michael Berns' laboratory at the University of California, San Diego (UCSD) where I performed laser microbeam experiments as well as optical trapping laser experiments, to try to answer some of these questions. I

spent approximately 10 weeks total working in his UCSD laboratory, during 4 trips, during which time I performed optical cutting and optical trapping experiments on *Mesostoma* spermatoctyes and also on crane-fly spermatocytes and PtK2 cells. I used his optical cutting laser to sever single kinetochore fibres, to sever bivalents, to sever the arms of bivalents and to sever kinetochores but I focused most of my attention on optical trapping experiments in *Mesostoma* spermatocytes. Since chromosome movement in *Mesostoma* spermatocytes stopped when the trap was applied and resumed when the trap was released as the kinetochore moved in either direction depending on the power in the trap, I calculated the force required to stop chromosome movement. I measured the forces on a phylogenetically diverse group of cells and found that the force required to stop chromosome movement is considerably lower than originally thought (Chapter 7, an article by Ferraro-Gideon et al., 2013b). Less force was required to stop chromosome movement in *Mesostoma* spermatocytes than in crane fly spermatocytes and even less force was required to stop the irradiated spindle pole from moving in PtK2 cells. Although the force required to stop chromosome movement or pole movement was different amongst these three organisms, these forces are still one one-hundredth times lower than originally measured (Nicklas, 1983) and are closer to the theoretical calculations of force (Alexander and Rieder, 1991; Gruzdev, 1972; Marshall *et al.*, 2001; Nicklas, 1965; Taylor, 1965).

Once I completed the optical laser trapping experiments, I conducted experiments using the optical cutting laser. As my time to perform these experiments was limited and

because of experimental difficulties with the optical cutting laser (the vertical focus was not accurate), I focused my attention on cutting kinetochores fibres as the kinetochore moved in either direction. I managed however to perform other cutting experiments but I was able to obtain only a few replicates of each. These cutting experiments included: severing bivalents in half, cutting arms of bivalents and severing bivalent kinetochores. When single kinetochore fibres were laser irradiated as the kinetochore moved in either direction, the half-bivalent kinetochore associated with the irradiation detached from the pole and moved towards the opposite pole. Following irradiation of kinetochore fibres with lower doses of laser power as the kinetochore moved away from the pole or to the pole, the half-bivalent kinetochore always moved back towards it original pole, re-attached and resumed normal oscillations. However, following irradiation of the kinetochore fibre with higher doses of laser power as the kinetochore moved in either direction, the half-bivalent kinetochore remained detached and did not recover movement. I assume that kinetochores detached from the pole because the laser microbeam severed kinetochore microtubules. In the other optical cutting experiments that I performed, kinetochores moved to the pole and stopped when bivalents were severed in half: they did not oscillate after the two kinetochores were physically separated. Cut bivalent arms usually remained stationary but in some cells, the cut piece of arm moved toward its partner, perhaps indicating the presence of tethers between half-bivalent arms. Because I do not have more than 3 replicates of each experiment, these results should be considered as still preliminary until further replications are done.

Based on the results I obtained from characterizing kinetochore oscillations in *Mesostoma* spermatocytes (Chapter 4) and conducting UV microbeam (Chapter 5), optical laser trapping (Chapter 6) and optical microbeam (Chapter 7) experiments, I suggest that kinetochore movement to the pole is different from kinetochore movement away from the pole, partner kinetochore oscillations are independent and there is non-random segregation of univalents and bivalents, as I now discuss in turn.

I suggest that kinetochore movement to the pole is different from kinetochore movement away from the pole based on the following results. Kinetochore movement to the pole is significantly faster than kinetochore movement away from the pole. UV microbeam irradiation of kinetochore fibres as the kinetochore moved in either direction stopped kinetochore movement at the pole: movement away from the pole was blocked whereas movement to the pole continued. After kinetochores stopped at the pole, resumption of oscillations depended on the direction of movement at the time of irradiation, indicating differences in the mechanisms of movement in the two directions. Laser microbeam irradiations severed kinetochore fibres as the kinetochore moved in either direction, stopping kinetochore movement or decreasing the amplitude of kinetochore oscillations. The position at which the kinetochore stopped or oscillated was different depending on the direction of kinetochore motion at the time the fibre was severed. The results from my optical laser trapping experiments suggest that less force is required to trap kinetochores and stop movement to the pole than to trap kinetochores and stop movement away from the poles. The effects of UV microbeam irradiation on the

precocious cleavage furrow (shifting position or regressing) depended on the direction of kinetochore motion at the time of irradiation. All these results suggest that different mechanisms as well as different spindle components are required for kinetochore movement to the pole and for kinetochore movement away from the pole. I hope that confocal immunofluorescence microscopy studies will support these conclusions which will in turn allow me to create a model to explain how kinetochores move to the pole and how kinetochores move away from the pole.

I suggest that partner kinetochore oscillations are independent based on the following results. The kinetochore oscillation parameters (velocity, period and amplitude) that I studied in control *Mesostoma* spermatocytes are more than 20% different for partner kinetochores. After UV microbeam irradiation of kinetochore fibres or optically trapping a kinetochore, the experimental kinetochore stopped oscillating while the partner kept on oscillating. These results suggest that partner kinetochore oscillations are independent. However, I also obtained results that suggest that signaling may occur between partner kinetochores. Kinetochore movement of both partner half-bivalents stopped when one kinetochore was irradiated with the UV microbeam or when a bivalent is severed with the laser microbeam. These results suggests that signals may be transmitted between kinetochores to terminate kinetochore oscillations; therefore, when a kinetochore is inactivated or damaged by UV irradiation or laser ablation it signals to its partner to stop oscillating.

I suggest that there is non-random segregation of chromosomes based on the following results. When kinetochore fibres were severed with the laser microbeam, the kinetochore detached from the pole and moved toward the opposite pole. The detached kinetochore then moved back to its **original** pole. In control cells, when bivalents reorient, partner kinetochores usually **switch** poles. The difference between the two results suggests that there is a specific, non-random segregation of half-bivalents in these cells. In *Mesostoma* spermatocytes, multiple univalent excursions can occur in one cell as univalents move between spindle poles. The numbers of excursions far exceed the numbers required to achieve one of each kind of univalent at each pole. This suggests that a specific, non-random segregation of univalents is required, and only when this is achieved will a spermatocyte enter into anaphase. Since a specific orientation of univalents and bivalents is required, this suggests that both univalent segregation and half-bivalent segregation is non-random.

In my thesis, I have developed methods to rear *Mesostoma ehrenbergii* in the laboratory; I have further characterized chromosome movements in their spermatocytes; I have used the UV microbeam to irradiate spindle fibres and kinetochores (Chapter 5), the optical trapping laser to trap chromosomes (Chapter 6) and the optical cutting laser to cut kinetochore fibres, bivalents and kinetochores (Chapter 7). I have used these tools to study chromosome movement and the structure of the spindle in *Mesostoma* spermatoctyes, included in 4 journal articles and data in two other chapters that will eventually be submitted to journals. Perhaps the most important experiment was

determining that the force produced by the spindle to stop chromosome movement is one one-hundredth times lower than originally measured by Nicklas (1983). The force originally calculated by Nicklas (1983) had been widely accepted for the past 30 years and had not been previously disputed, so this would be of major importance in studying the forces involved in chromosome movement in mitotic and meiotic cells. We can learn much about meiosis I by further studying *Mesostoma* spermatocytes and I now want to discuss some of the experiments that might be done in the future..

8.3 Future Experiments

Mesostoma ehrenbergii spermatocytes offer a unique system for studying bivalent kinetochore oscillations, distance segregation of bivalents and univalents and precocious, "pre-anaphase", cleavage furrows. Although these phenomena may exist separately in other organisms, *Mesostoma* spermatocytes allow researchers to study each of these phenomena in one meiotic system. Meiosis in *Mesostoma* spermatocytes has only been studied by Oakley (1983, 1985), Fuge (1987, 1989, 1991) and Forer and Pickett-Heaps (2010), and although experiments performed by these researchers have laid the groundwork for studying meiosis in this organism, they have ultimately only scratched the surface to begin to understand this unconventional meiotic system. I will now describe possible experiments that can be performed on *Mesostoma* spermatocytes that will allow cell biologists to better understand each of these unique phenomena.

8.3.1 Possible experiments to perform using an Ultraviolet Microbeam

I have irradiated kinetochore fibres with a wavelength of 290nm and kinetochores with wavelengths of 280nm and 290nm. Since I do not know which components are altered following irradiation of kinetochores or kinetochore fibres with these wavelengths, confocal immunofluorescence microscopy studies should be performed on *Mesostoma* spermatocytes that have been UV irradiated to see which components are altered following irradiation. Depending on the results obtained from the immunofluorescence studies, it may be helpful to repeat these experiments using different wavelengths of UV (260nm-290nm) to see how chromosome movement is altered following these irradiations and if these wavelengths alter different spindle components (Sillers and Forer, 1983). By understanding which components are altered following UV irradiation and how altering these components affects chromosome movement, a model could be developed to explain how kinetochores move to the pole and away from the pole.

UV microbeam irradiations of kinetochore fibres should be repeated using higher doses of UV. Higher doses of UV caused the kinetochore to detach from the pole in one cell (Chapter 5), different from the results obtained using lower doses of UV. Perhaps using higher doses would allow us to sever kinetochore fibres using a UV microbeam, and allow us to study reorientations in more detail.

Since the UV microbeam has only been used to irradiate kinetochore fibres and kinetochores, the UV microbeam should also be used to irradiate other spindle components, including the spindle pole and univalent kinetochores. Following irradiation of kinetochore fibres or kinetochores, the furrow shifted its position and in some cells, the furrow regressed. Therefore, one could irradiate other spindle components in *Mesostoma* spermatocytes to determine if the furrow also shifts its position or regresses following irradiation; and one could determine if irradiation of other spindle components alters bivalent kinetochore oscillations.

8.3.2 Possible experiments to perform using an Optical Cutting Laser and an Optical Trapping Laser

I have severed kinetochore fibres as the kinetochore moved to the pole and moved away from the pole. The results obtained when the kinetochore fibre was severed with high power irradiations as the kinetochore moved in either direction were consistent: the kinetochore detached, stopped away from its pole and did not recover. The results obtained when the kinetochore fibre was severed with low power irradiations as the kinetochore moved in either direction, however, were not consistent: the kinetochore detached, then moved back toward its pole, re-attached and resumed oscillations or the kinetochore did not detach and kinetochore movement stopped or kinetochores oscillated with dampened amplitude. Because this was only observed in 28 cells total (20 as the kinetochore moved away from the pole and 8 as the kinetochore moved to the pole) further replications are required to solidify these results.

In addition to severing bivalent kinetochore fibres, the optical cutting laser can be used to: sever bivalents, sever arms of bivalents, ablate kinetochores, sever kinetochore fibres as a univalent moves from one pole to the other, and sever kinetochore fibres as bivalents enter anaphase. Severing bivalents in half would allow us to determine if partner half-bivalents move independently of one another and if the attachment of partners is required to send either 'stop' or 'go' signals to each other to continue oscillations.

It was originally suggested by Fuge (1987, 1989) that tension is required for kinetochore oscillations to take place in *Mesostoma* spermatocytes. Based on the results from my UV microbeam and laser microbeam experiments, I cannot suggest one way or another if tension is required for kinetochore oscillations in *Mesostoma* spermatocytes. To determine if tension or physical attachment of half-bivalents is required for kinetochore oscillations, we could trap the middle of the bivalent with an optical trapping laser and then sever the bivalent below the trap. The power in the trap would apply force (tension) on the cut bivalent. If tension is required for kinetochore oscillations, the cut half-bivalent would continue to oscillate in the presence of the trap but if physical attachment of half-bivalents is required, the cut half-bivalent would not oscillate even in the presence of the trap.

By severing the arms of bivalents in *Mesostoma* spermatocytes one could determine if a connection exists between the two arms, called "tethers" by LaFountain et al. (2002), as observed in crane-fly spermatocytes. By severing the arms of bivalents in

Mesostoma spermatocytes, one could also test the ejection force model which considers that ejection forces acting on bivalent arms propel kinetochores away from the pole (Bajer, 1982; Skibbens et al., 1993). Severing the arms of bivalents in *Mesostoma* spermatocytes, could also provide a direct comparison between the *Mesostoma* spermatocytes Fuge studied and the *Mesostoma* spermatocytes we study; since two of the bivalents in the *Mesostoma* spermatocytes studied by Fuge did not have bivalent arms. This experiment would test whether a lack of bivalent arms could account for the differences observed between the cells we studied and the cells studied by Fuge.

Kinetochore oscillations in *Mesostoma* spermatocytes are much faster than chromosome movement to the pole during anaphase (Chapter 4). To determine if different mechanisms and spindle components are involved in kinetochore oscillations during prometaphase and chromosome movement during anaphase, we could irradiate kinetochore fibres with an UV microbeam or sever kinetochore fibres using a laser microbeam. If chromosome movement during anaphase uses different spindle components and mechanism than kinetochore oscillations, the results will be different. Chromosome movement may accelerate to the pole during anaphase following UV irradiation or laser irradiation of kinetochore fibres as observed in other cell types (Forer et al., 2008). This experiment would probably be very difficult however, as we cannot determine when a cell will enter into anaphase and determine whether there was an effect, because anaphase only lasts a few minutes and the distances travelled are small.

Univalent excursions between spindle poles are not observed in every *Mesosotma* spermatocyte but if we could spot a univalent segregating from one pole to the other and sever its kinetochore fibre, this would allow us to determine if univalent movement stops, slows or accelerates once its kinetochore fibre is severed. Ablation of a kinetochore or severing the kinetochore fibre of a univalent as a univalent segregates between poles could also determine if there is an end on attachment between univalent kinetochores and kinetochore microtubules or if univalent kinetochores slide along microtubules. The difficulty with these experiments is that there would only be a short period of time to sever kinetochore fibres or kinetochores as univalent segregation between spindle poles is very fast.

8.3.3 Possible experiments to perform using confocal immunofluorescence microscopy

Mesostoma spermatocytes have not been well studied in the literature and we have only recently characterized kinetochore movements, anaphase chromosome movements and univalent movement in this organism. Little is still known about the structure of the spindle. Although we have characterized kinetochore movement in this organism, we still cannot explain the mechanisms utilized for these movements to occur. Therefore, it is important for us to understand the structure of the spindle. In order to do this, we need to fix *Mesostoma* spermatocytes and stain them for a variety of different spindle components, including: tubulin, acetylated tubulin, actin, myosin, spindle matrix proteins (ex. skeletor, megator, chromator), cleavage furrow proteins (ex. anillin, Aurora

B) and enzymes involved in kinetochore movement located at the kinetochore and/or the pole (ex. katanin, spastin, fidgetin). Once we can better understand how the spindle is structured, which components comprise the spindle and where each of these components is located, we can place chemical and structural restrictions on models that explain how bivalent kinetochores oscillate; how anaphase chromosomes move; how cleavage furrows shift positions or complete cytokinesis after the cell enters into anaphase; and how univalents segregate from one pole to the other.

Many of the UV microbeam and laser microbeam experiments that were suggested in *Mesostoma* spermatocytes should be extended using confocal immunofluorescence microscopy and/or electron microscopy to see which components are damaged. In most of the UV microbeam and laser microbeam experiments, kinetochore fibres are being altered by the irradiation. We know this because kinetochore movement is affected. We do not know, however, how the kinetochore fibre is altered. Immunofluorescence microscopy would allow us to determine which spindle components are affected following irradiation of a single kinetochore fibre after UV microbeam irradiation or laser microbeam irradiation. Using confocal microsocopy and staining for tubulin, actin and myosin, we could determine which of these components are altered following UV irradiation and laser irradiation of both kinetochore fibres and kinetochores and which components of these components are altered following irradiation of kinetochore fibres as the kinetochore moves to the pole and away from the pole. Electron microscopy could

also be used to confirm the effects of UV irradiation and laser irradiation on microtubules.

8.3.4 Possible experiments to perform using micromanipulation

We know that distance segregation of univalents (Oakley, 1983, 1985) and bivalents takes place in *Mesostoma* spermatocytes; we do not know, however, if non-random segregation of univalents and bivalents occurs as suggested by Oakley (1983, 1985) and as I suggested above. Therefore, if we could move univalents between spindle poles or reorient bivalents, we would be able to determine if the same univalent or the same half-bivalent kinetochore returns to its original pole or if a different univalent or the partner half-bivalent kinetochore moves to the opposite pole as in control *Mesostoma* spermatocytes (Chapter 4).

Micromanipulation experiments can also be used to study the cleavage furrow. By moving univalents from one pole to the other or reorienting bivalents with a micromanipulation needle, one could also study shifts in the position of the cleavage furrow in response to changes in the number of univalents and bivalents or one could move the needle between the pole and furrow to see if there are connections between them that when broken cause the furrow to shift position.

8.3.5 Possible experiments to perform using pharmacological agents

Preliminary drug treatment experiments have been performed on *Mesostoma* spermatocytes (unpublished data). Drug treatment experiments allow us to study which

components are involved in the force production driving chromosome movement. By targeting specific spindle components with drugs that inhibit or stabilize spindle components, we can determine if those particular spindle components are involved in chromosome movement. If non-microtubule components are involved in producing the force driving chromosome-to-pole motion as suggested by the spindle matrix model (Pickett-Heaps et al., 1997), and as suggested by some of my experiments (Chapter 5 and Chapter 6), then treatment with anti-actin drugs (Cytochalasin D or Latrunculin B) or anti-myosin drugs (BDM or Y-27632) might be expected to stop chromosome movement. These experiments would not only allow us to see if microtubules, actin and myosin are involved in chromosome movement but it would allow us to see if they are involved in the positioning of the precocious cleavage furrow and maintaining the cell shape.

8.3.6 Other possible experiments to perform on *Mesostoma* spermatocytes

Since *Mesostoma* are transparent and produce viviparous eggs, it may be possible to inject genes that code for GFP-tubulin directly into these eggs and then rear these worms to see if we can obtain GFP-labeled tubulin in the spindle. Since kinetochore fibres in *Mesostoma* spermatocytes are difficult to stain, using GFP-labeled tubulin would allow us to easily observe spindle fibres using fluorescence microscopy. Therefore, if we performed UV microbeam or laser microbeam experiments we would be able to determine if microtubules were altered or severed following kinetochore fibre ablation. Although this may be a difficult project to pursue, fluorescently labeled spindle fibres would be useful for the study of chromosome movement in this organism.

I have tried to list many possible experiments that could be performed on *Mesostoma* spermatocytes. These spermatocytes offer a unique system for studying meiosis and there are numerous experiments that can be performed. I hope that other labs will take advantage of our ability to grow the animals in the lab and join me in trying to understand these cells.

8.4 References

Alexander, S. P. and Rieder, C.L. (1991). Chromosome motion during attachment to the vertebrate spindle: initial saltatory-like behavior of chromosomes and quantitative analysis of force production by nascent kinetochore fibres. J. Cell Biol. **113,** 805-815.

Bajer, A.S. (1982). Functional autonomy of monopolar spindle and evidence for oscillatory movement in mitosis. J Cell Biol. **93**, 33-48.

Ferraro-Gideon, J., Hoang, C. and Forer, A. (2013a). Meiosis-I in *Mesostoma ehrenbergii* spermatocytes includes distance segregation and inter-polar movements of univalents, and vigourous oscillations of bivalents. Protoplasma. (Accepted)

Ferraro-Gideon, J., Sheykhani, R., Zhu, Q., Duquette, M.L., Berns, M.W. and Forer, A. (2013b) Measurements of forces produced by the mitotic spindle using optical tweezers. Mol Biol Cell. **24**, 1375-1386.

Foe, V.E. and von Dassow, G. (2008). Stable and dynamic microtubules coordinately shape the myosin activation zone during cytokinetic furrow formation. J Cell Biol. **183**, 457-470.

Forer, A. and Pickett-Heaps, J. (2010). Precocious (pre-anaphase) cleavage furrows in *Mesostoma* spermatocytes. Eur J Cell Biol. **89**, 607-618.

Forer, A., Pickett-Heaps, J.D. and Spurck, T. (2008). What generates flux of tubulin in kinetochore microtubules? Protoplasma. **232**, 137-141.

Fuge, H. (1987). Oscillatory movement of bipolar-oriented bivalent kinetochores and spindle forces in male meiosis of *Mesostoma ehrenbergii*. Euro J Cell Biol. **44,** 294-298.

Fuge, H. (1989). Rapid kinetochore movements in *Mesostoma ehrenbergii* spermatocytes: Action of antagonistic chromosome fibre. Cell Motil Cytoskeleton **13**, 212-220.

Fuge, H. and Falke, D. (1991). Morphological aspects of chromosome spindle fibres in *Mesostoma*: "Microtubular fir-tree" structures and microtubule association with kinetochores and chromatin. Protoplasma. **160**, 39-48.

Gruzdev, A.D. (1972). Critical review of some hypotheses concerning anaphase chromosome movements. Tsitologiya. **14**, 141-149.

Hoang, C., Ferraro-Gideon, J., Gauthier, K. and Forer, A. (2013). Methods for rearing *Mesostoma ehrenbergii* in the laboratory for cell biology experiments, including identification of factors that influence production of different egg types. Cell Biol Int. Accepted

LaFountain, J.R., Cole, R.W. and Rieder, C.L. (2002). Partner telomeres during anaphase in crane-fly spermatocytes are connected by an elastic tether that exerts a backward force and resists poleward motion. J Cell Sci. **115**, 1541-1549.

Marshall, W.F., Marko, J.F., Agard, D.A. and Sedat, J.W. (2001). Chromosome elasticity and mitotic polar ejection force measured in living *Drosophila* embryos by four-dimensional microscopy-based motion analysis. Curr. Biol. **11,** 569-578.

Nicklas, R.B. (1965). Chromosome velocity during mitosis as a function of chromosome size and position. J. Cell Biol. **25**, 119-135.

Nicklas, B. (1983). Measurements of the force produced by the mitotic spindle in anaphase. J Cell Biol. **97**: 542-548.

Oakley, H.A. (1983). Male meiosis in *Mesostoma ehrenbergii ehrenbergii*. Kew Chromosome Conference II Editors PE Brandham, MD Bennett. George Allen and Unwin, London (Boston, Sydney) pp 195-199.

Oakley, H.A. (1985). Meiosis in *Mesostoma ehrenbergii ehrenbergii* (Turbellaria, Rhabdocoela) III. univalent chromosome segregation during the first meiotic division in spermatocytes. Chromosoma. **91,** 95-100.

Pickett-Heaps, J.D., Forer, A. and Spurck, T. (1997). Traction fibre: toward a "tensegral model of the spindle". Cell Motil Cytoskeleton. **37**, 1-6.

Sillers, P.J. and Forer, A. (1983). Action spectrum for changes in spindle birefringence after ultraviolet microbeam irradiations of single chromosomal spindle fibres in crane-fly spermatocytes. J Cell Sci. **62**, 1-15.

Skibbens, R.V., Skeen, V.P. and Salmon, E.D. (1993). Directional instability of kinetochore motility during chromosome congression and segregation in mitotic newt lung cells: a push-pull mechanism. J Cell Biol. 122, 859-875.

Taylor, E.W. (1965). Brownian and saltatory movements of cytoplasmic granules and the movement of anaphase chromosomes. In: Proceedings of the Fourth International Congress on Rheology, ed. AL Copley, New York: Interscience, Part 4, 175–191.

Wilson, P. and Forer, A. (1987). Irradiations of rabbit myofibrils with an ultraviolet microbeam. I. Effects of ultraviolet light on the myofibril components necessary for contraction. Biochem Cell Bio. **65**, 363-375.

APPENDIX 1

TABLE A.1: Literature studies on the formation of S eggs or D eggs in different rearing conditions, with a summary of conclusions. A study on egg type production in a closely related species, *M. lingua* is also included. Temperatures that are reported as ratios are the ratios of the temperatures the animals are incubated in during the light and dark phase respectively, of the photoperiod. Some rearing conditions were not specified (n/a).

Experiment	Photoperiod (light/dark cycle)	Temperature	Food Source	Feeding regime	Number of animals/ ml of water	Container	Water medium
Studies on egg type production in M. ehrenbergii							
Beisner et al., 1997	12/12 hr	18 °C or 24 ° C	*Daphnia*	Fed 1, 5, 15, or 25 *Daphnia* daily or fed 5 *Daphnia* every second day	1/ 15 ml of water	Glass chamber	Filtered pond water
	Conclusions: I. Temperature has different effects on worms hatching from D eggs (1st generation) and worms hatching from S eggs (subsequent generations). a. 1st generation worms were more likely to become S worms at 18 °C. b. Worms from subsequent generations were more likely to become S worms at 24 °C. II. Amount of food fed to the worms has different effects on worms hatching from D eggs (1st generation) and worms hatching from S eggs (subsequent generations). a. 1st generation worms were more likely to become S worms when fed less (5 Daphnia every second day). b. In subsequent generations, worms were more likely to become S worms when fed less and at 24 °C but at 18 °C, worms only became S worms when they were well fed (15 Daphnia per day).						
De Beauchamp, 1926	n/a	Temp. range: 18-20 °C or 13-15 °C	n/a	n/a	n/a	n/a	n/a
Fiore, 1971	12/12 hr	23 °C	n/a	n/a	10/ 100ml of water	n/a	n/a
	Conclusions: I. When young worms were reared with adult worms (even when they were separated by a net made from nylon mesh), the young worms were less likely to become S worms.						
Fiore and Iaolè, 1973	12/12 hr	23 °C	*Daphnia*	n/a	a) Reared in isolation: 1/ 5-7ml of water b) Reared	a) Reared in isolation: test tubes b) Reare	n/a

					in groups: 60-70ml of water	d in groups: glass bowls	
	Conclusions: I. When worms were reared in isolation (therefore, all offspring arose through self-fertilization) and separate lines were maintained, certain lines had a higher percentage of S worms in all generations despite similar environmental conditions while other lines became extinct, suggesting genetic influences. II. Worms reared individually were more likely to become S worms compared to worms reared in groups of more than 2 worms. Worms reared in pairs were not significantly different in percentages of S worms than worms reared individually. III. Density did not have a significant influence on whether worms became S worms or D worms. IV. Poorly fed worms were more likely to become S worms compared to well fed worms. V. 5%:95% oxygen:nitrogen ratio increased the chance of worms bearing S eggs compared to 20%:80% oxygen:nitrogen ratio.						
Heitkamp, 1977	8 /16 hr or 12/ 12 hr	14/9 °C, 9/13 °C, 22/15 °C, 26/19 °C, or 30/22 °C	*Daphnia*	Fed daily	Isolated or in pairs / 60-70 ml water	Trays	n/a
	Conclusions: I. Temperature has different effects on worms hatching from D eggs (1st generation) and worms hatching from S eggs (subsequent generations) a. 1st generation worms all produced S eggs regardless of temperatures between 10-25 °C b. Worms from subsequent generations tend to produce S eggs only at temperatures higher than 20 °C						
Steinmann and Bresslau, 1913	n/a	n/a	n/a	n/a	n/a	n/a	n/a
	Conclusions: I. Endogenous factors cause all worms to overwinter and only bear D eggs after a certain number of generations (usually around 6).						
Study on egg type production in a closely related species, M. lingua.							
Heitkamp, 1972	n/a	30/22 °C, 26/18 °C, 13/7 °C or 9/4 °C	*Daphnia*	Fed daily or fed once every fifth day	5-50 animals/ 1250ml of water	n/a	n/a
	Conclusions: I. In *M. lingua,* population densities of more than 15-20 animals per 1250ml of water at +20 °C promote the production of D eggs. Crowding effect was dependent on temperature- at higher temperatures (30/22 °C and 26/18 °C), 1250ml of water can support 40-50 animals without any effect while at lower temperatures (13/7 ° C and 9/4 °C), the crowding effect is seen for more than 5-10 individuals per 1250 ml of water. II. In *M. lingua,* poorly fed worms (fed 1/5th day) were more likely to become S worms						

APPENDIX 2

Immunofluorescence of control Mesostoma spermatocytes.

Mesostoma spermatocytes are difficult to both fix and stain for immunofluorescence. The shape of the spermatocyte changes and the furrow regresses when fixed with conventional lysis buffer (1% NP40, 5% DMSO). Because of this, I tried numerous fixation methods including: 0.25% Glutaraldehyde in lysis buffer, 2.5% Formaldehyde, 2.5% Formaldehyde followed by lysis buffer, 2.5% Formaldehyde followed by 0.25% Glutaraldehdye and a lysis buffer that I developed based on a protocol from Foe and von Dassow (2008) that contains 1% Triton-X, 0.2% Glutaraldehyde and 2% Formaldehyde and that requires 24 hours at each staining step. As a control for developing fixation methods for *Mesostoma* spermatocytes, I tried these fixation methods on crane-fly spermatocytes using antibodies that were previously found to strongly label spindle components in crane-fly spermatocytes. I found that the von Dassow lysis buffer was the best fixation method to stain for both tubulin and actin (Figure A1) whereas other fixation methods stained well only for tubulin (Figure A2a) or only for actin (Figure A2b). As the lysis buffer I developed based on the protocol from Foe and von Dassow (2008) was found to be the best method for fixation of crane-fly spermatocytes I used the same protocol to stain *Mesostoma* spermatocytes. When scanning *Mesostoma* preparations after fixation, I noticed that in some cells there was a change in cell shape and, in particular, a regression of the furrow (Figure A3). Consequently, I will continue to look for a fixation method for immunofluorescence for which there is no change in cell shape. Some *Mesostoma* spermatocytes however, did not change shape following fixation

so I stained them for tyrosylated tubulin (Figure A4 and A5), acetylated α-tubulin (Figure A5) and actin (Figure A4), with good results. As little is known about the dynamics of the spindle in *Mesostoma* spermatocytes, I wanted to determine the arrangement of microtubules, the stability of microtubules, the site of nucleation of microtubules and confirm the presence of non-microtubule components in the spindle and precocious cleavage furrow. To determine the arrangement of microtubules, I stained *Mesostoma* spermatocytes against tyrosylated tubulin: as seen in Figure A15a, microtubules originate from the microtubule organizing centres which are brightly stained and located at either pole. Spindle microtubules extend outward toward the equator on either side of the bivalents as well as insert into the kinetochores (Figure A4c) and as previously seen by Fuge and Falke (1991) in electron microscopy sections. As indicated by the arrow in Figure A4a, microtubules also extend the entire length of the spermatocyte. These microtubules might be used for sliding, as univalents move between poles to achieve proper orientation prior to the onset of anaphase and these movements may be due to sliding along microtubules. I hypothesized that the kinetochore microtubules like the ones observed in Figure A4a would not be stable since kinetochores in *Mesostoma* spermatocytes oscillate rapidly to and from the spindle pole, changing direction every 1-2 minutes. Acetylation of tubulin occurs only after polymerisation and only when microtubules are stable, which takes 5 minutes or more after microtubules are newly polymerized (Wilson and Forer, 1989). I used 6-11B-1 monoclonal antibody (Piperno et al 1987) to determine if kinetochore microtubules in *Mesostoma* spermatocytes are acetylated. As seen in Figure A5a-b, acetylated tubulin was localized only to microtubule

organizing centres. This confirms that kinetochore microtubules in *Mesostoma* spermatocytes are not stable, different from crane-fly spermatocytes (Wilson and Forer 1989) and other cells, but similar to PtK_2 cells (Piperno et al 1987). Acetylation also has been used in other cell types as a marker for the site of addition and/or subtraction of tubulin subunits from kinetochore microtubules (Wilson and Forer 1989, Wilson et al 1994). The localization of acetylated tubulin to microtubule organizing centres in *Mesostoma* spermatocytes only indicates that tubulin subunits are acetylated at the spindle poles and does not indicate if the site of addition and/or subtraction of tubulin subunits is at the kinetochore or at the spindle poles. Lastly, I wanted to confirm the presence of non-microtubule components in the spindle and precocious cleavage furrow in *Mesostoma* spermatocytes; however, staining for actin has been difficult as both phallodin and antibodies to actin don't seem to penetrate through the spermatocyte to stain the spindle. Some actin staining is visible at the cleavage furrow as seen in Figure 4b; however, many *Mesostoma* spermatocytes did not stain for actin. We know that actin is present in the spindle of *Mesostoma* spermatocytes as treatment with drug inhibitors to actin alter chromosome movement and cause the regression of the cleavage furrow (Forer unpublished data). With improved fixation to preserve the ingression of the furrow and the shape of the cell, I hope that it will also improve staining of non-microtubule components so I will be able to determine the distribution of these components within the spindle.

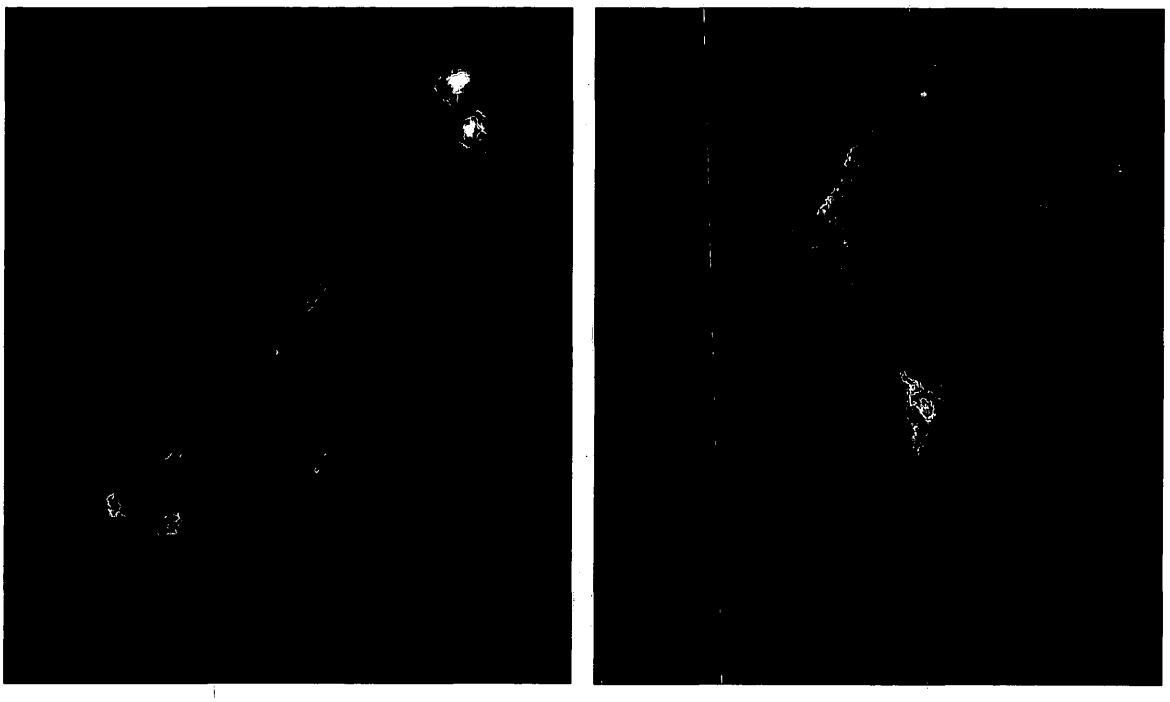

Figure A1. Confocal immunoflorescence images of a crane fly spermatocyte fixed with von Dassow lysis buffer (1% Triton-X, 0.2% Glutaraldehyde, 2% Formaldehyde). (A) Crane fly spermatocyte stained with YL1/2 (1:100) for tyrosinated tubulin. (B) Crane fly spermatocyte stained with 0.66μM Alexa 488 Phallodin. The sex chromosome kinetochore fibres and asters stained well for tubulin as seen in (A). There is only some staining of the cortex and cleavage furrow for actin as seen in (B) as glutaraldehyde used in the fixative prevents Phallodin from fully penetrating the spermatocyte.

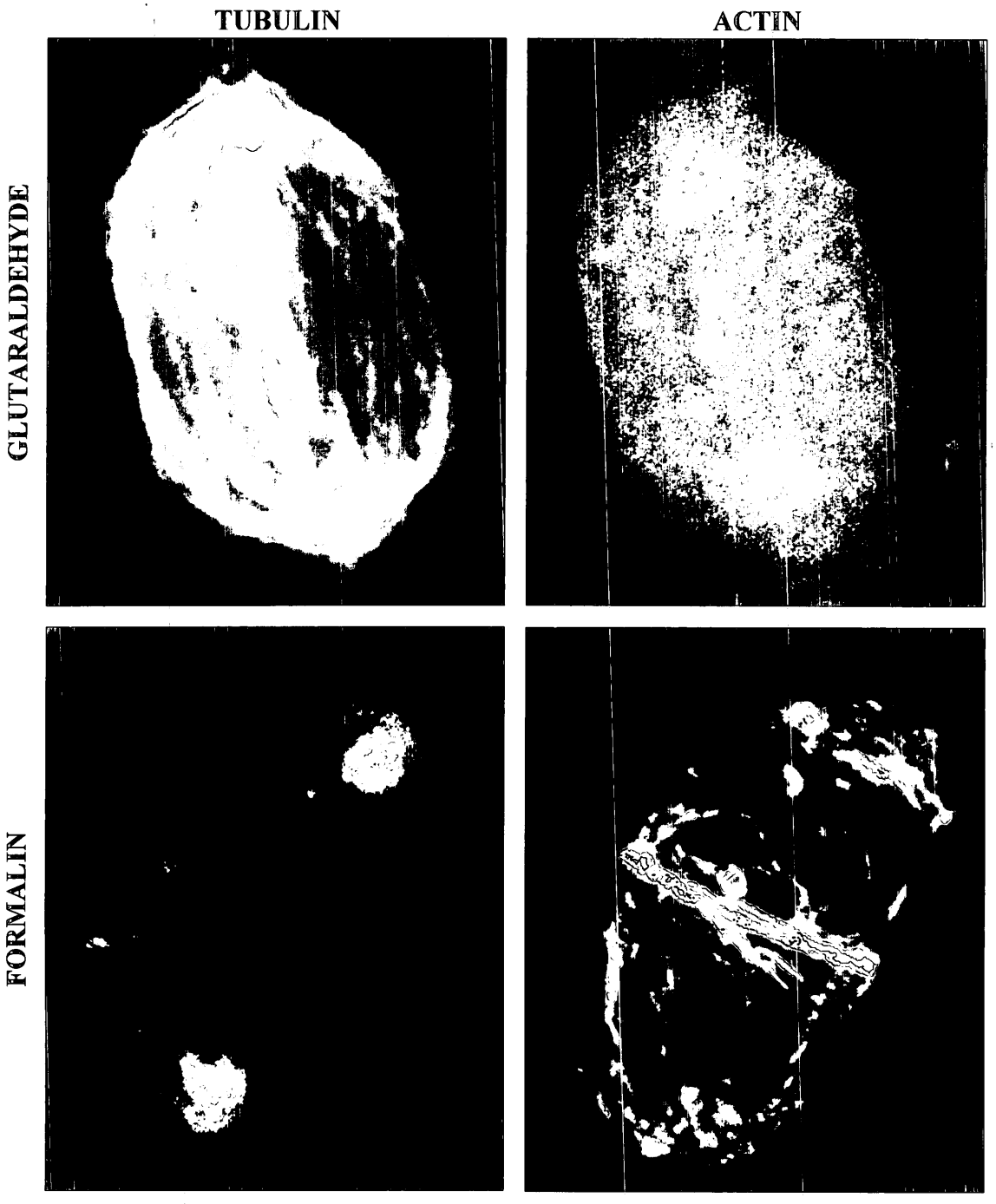

Figure A2. (A) Confocal immunoflorescence images of a crane fly spermatocyte fixed with von Dassow lysis buffer that does not contain 2.5% formaldehyde and stained with YL1/2 (1:100) for tyrosinated tubulin and 0.66μM Alexa 488 Phallodin. (B)) Confocal immunoflorescence images of a crane fly spermatocyte fixed with 2.5% formaldehyde and stained with YL1/2 (1:100) for tyrosinated tubulin and 0.66μM Alexa 488 Phallodin.

BEFORE VON DASSOW LYSIS AFTER VON DASSOW LYSIS

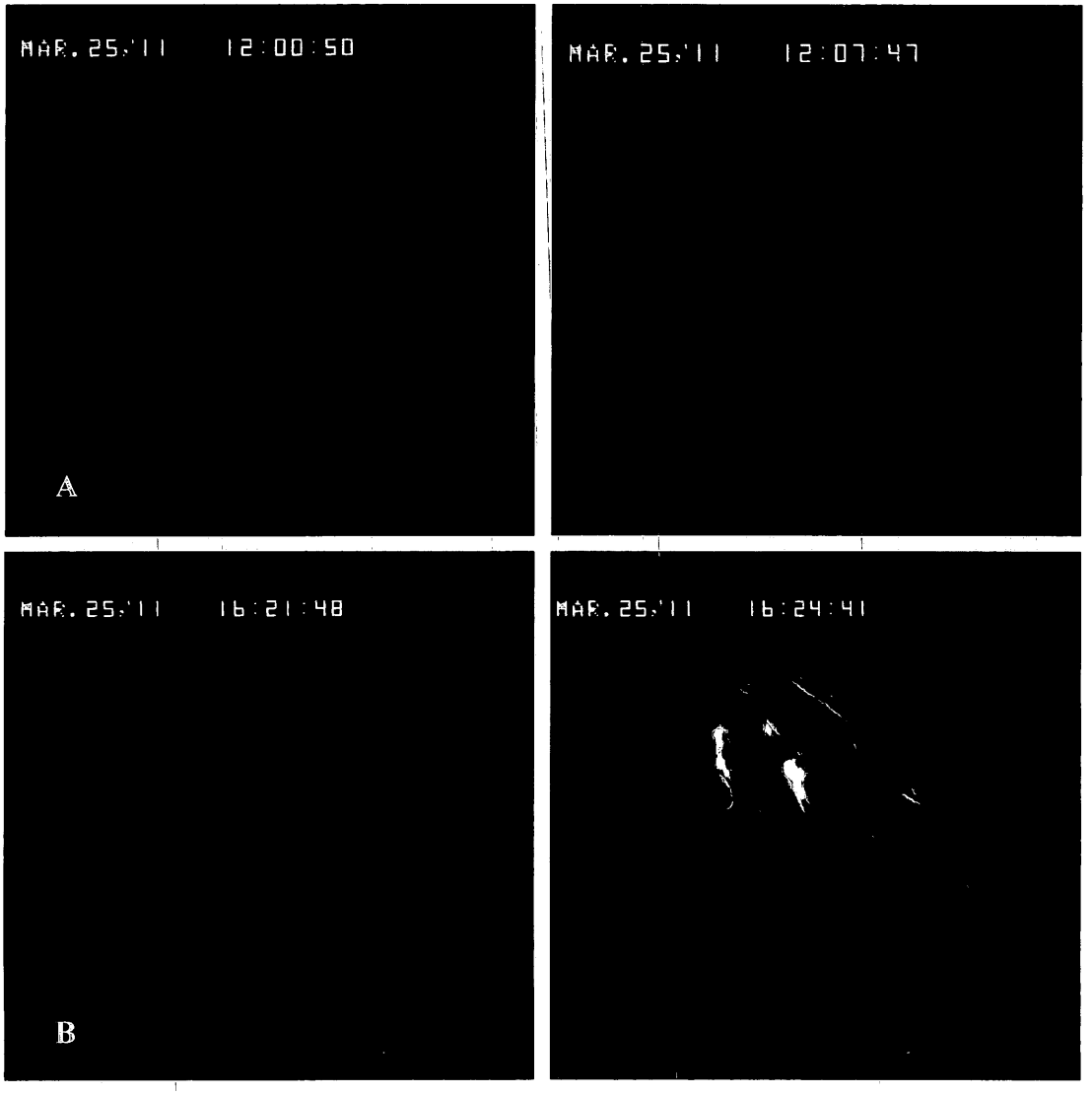

Figure A3. Phase-contrast images of *Mesostoma* spermatocytes before fixation and after fixation with von Dassow lysis buffer. (A) *Mesostoma* spermatocyte becomes rounded in shape and the upper pole comes in. (B) *Mesostoma* spermatocyte retains its shape but the furrow on left side regresses.

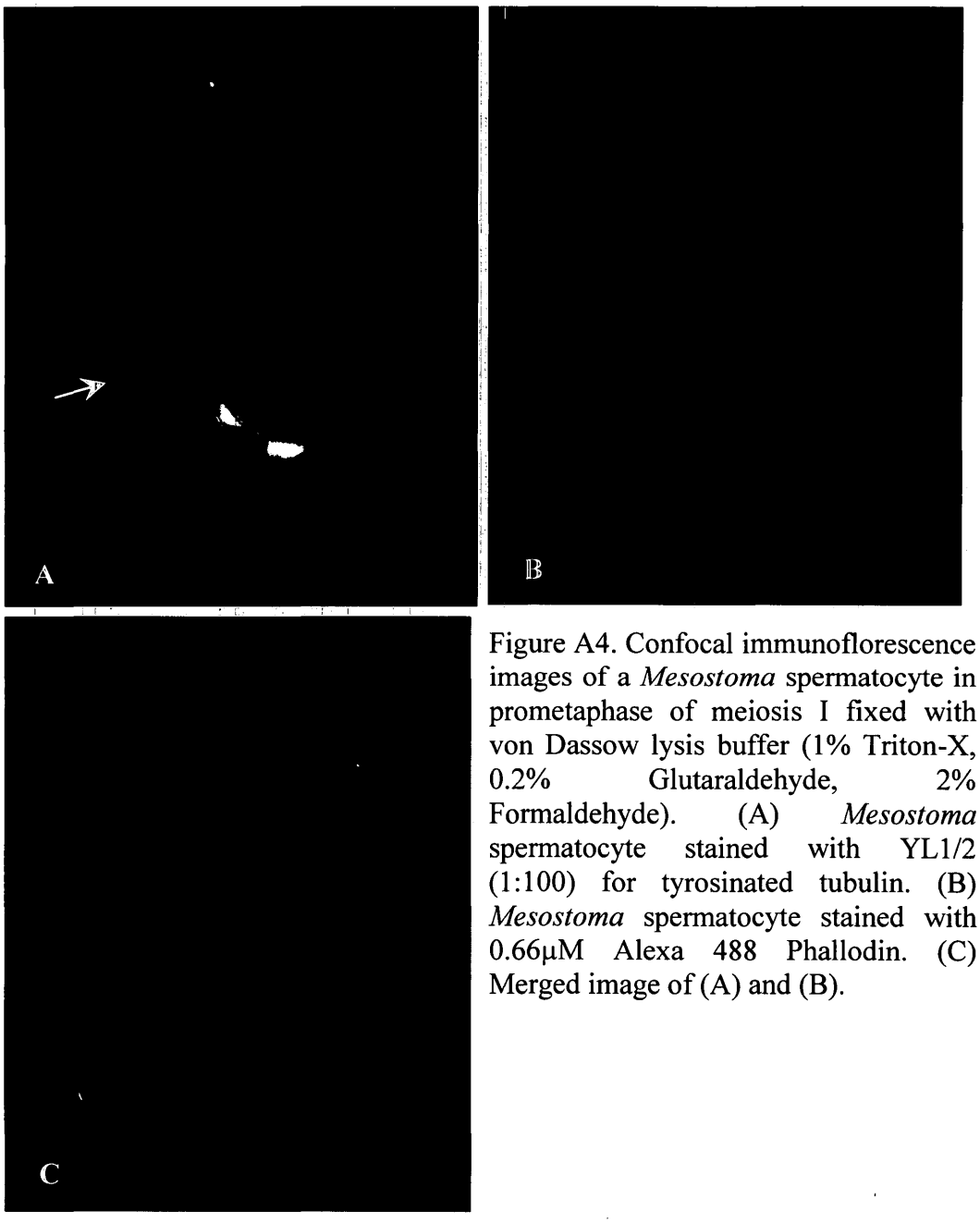

Figure A4. Confocal immunoflorescence images of a *Mesostoma* spermatocyte in prometaphase of meiosis I fixed with von Dassow lysis buffer (1% Triton-X, 0.2% Glutaraldehyde, 2% Formaldehyde). (A) *Mesostoma* spermatocyte stained with YL1/2 (1:100) for tyrosinated tubulin. (B) *Mesostoma* spermatocyte stained with 0.66μM Alexa 488 Phallodin. (C) Merged image of (A) and (B).

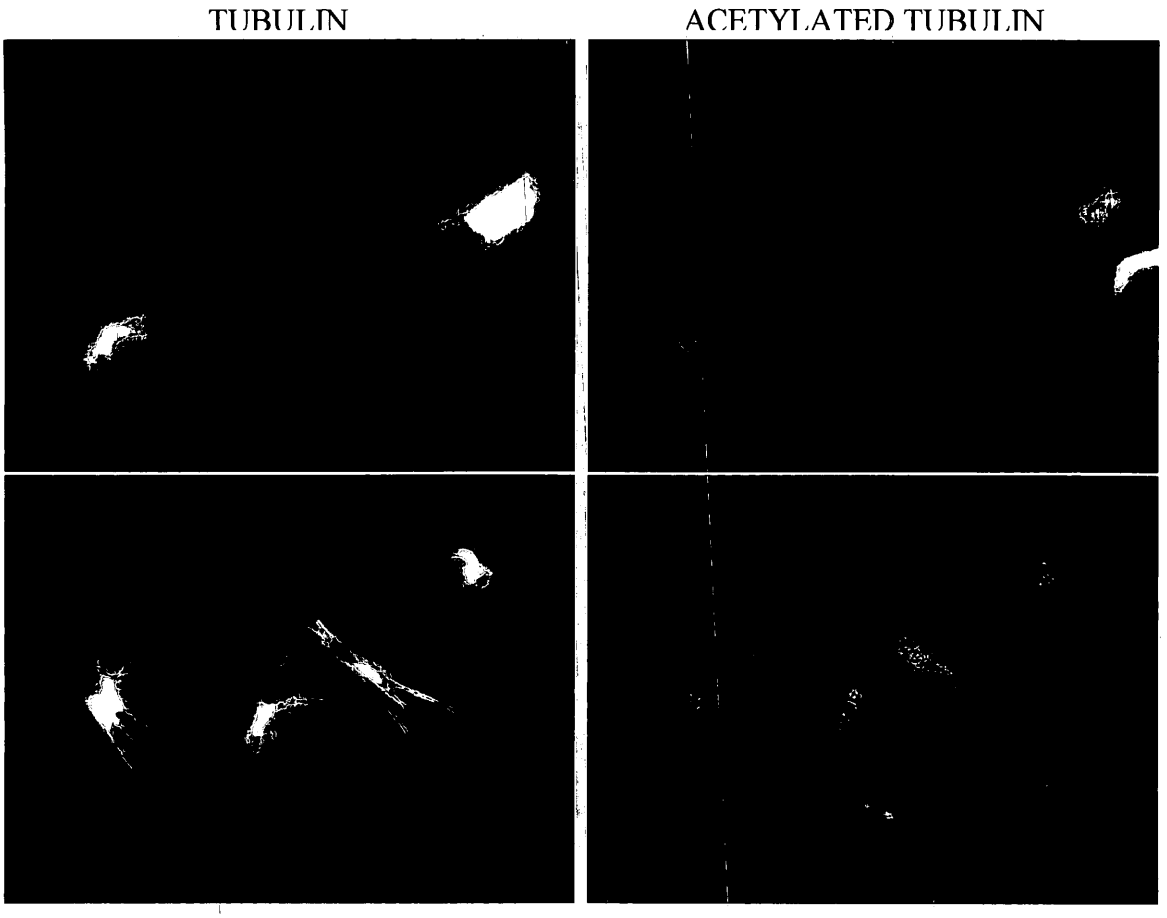

Figure A5. Confocal immunoflorescence images of *Mesostoma* spermatocytes fixed with von Dassow lysis buffer (1% Triton-X, 0.2% Glutaraldehyde, 2% Formaldehyde) and stained for tyrosinated tubulin (YL1/2, 1:100) and acetylated tubulin (6-11B-1, 1:200). (A) *Mesostoma* spermatocyte in prometaphase I of meiosis. (B) Early *Mesostoma* spermatocyte.

References

Croft JA and Jones GH. (1989) Meiosis in *Mesostoma ehrenbergii ehrenbergii* IV. Recombination nodules in spermatocytes and a test of the correspondence of late recombination nodules and chiasmata. *Genetics* **121**: 255-262.

Foe VE and von Dassow G. (2008) Stable and dynamic microtubules coordinately shape the myosin activation zone during cytokinetic furrow formation. *Journal of Cell Biology* **183**: 457-470.

Forer A and Pickett-Heaps J. (2010) Precocious (pre-anaphase) cleavage furrows in *Mesostoma* spermatocytes. *European Journal of Cell Biology* **89**:607-618.

Fuge H. (1987) Oscillatory movement of bipolar-oriented bivalent kinetochores and spindle forces in male meiosis of *Mesostoma ehrenbergii*. *European Journal of Cell Biology* **44**: 294-298.

Fuge H. (1989) Rapid kinetochore movements in *Mesostoma ehrenbergii* spermatocytes: Action of antagonistic chromosome fibre. *Cell Motility and the Cytoskeleton* **13**: 212-220.

Fuge H and Falke D. (1991) Morphological aspects of chromosome spindle fibres in *Mesostoma*: "Microtubular fir-tree" structures and microtubule association with kinetochores and chromatin. *Protoplasma* **160**: 39-48.

Ingber DE. (1993) Cellular tensegrity: defining new rules of biological design that govern the cytoskeleton. *Journal of Cell Science* **104**: 613-627.

Oakley HA and Jones GH. (1982) Meiosis in *Mesostoma ehrenbergii ehrenbergii* (Turbellaria, Rhabdocoela) I. Chromosome pairing, synaptonemal complexes and chiasma localisation in spermatogenesis. *Chromosoma (Berl.)* **85**: 311-322.

Piperno G, LeDixt M and Chang X. (1987) Microtubules containing acetylated a-tubulin in mammalian cells in culture. *Journal of Cell Biology* **104**: 289-302.

Sillers PJ and Forer A. (1983) Action spectrum for changes in spindle fibre birefringence after ultraviolet microbeam irradiations of single chromosomal spindle fibres in crane-fly spermatocytes. *Journal of Cell Science* **62**: 1-25.

Wilson PJ and Forer A. (1989). Acetylated alpha tubulin in spermatogenic cells of the crane fly *Nephrotoma suturalis*: kinetochore microtubules are selectively acetylated. *Cell Motility and Cytoskeleton* **14**: 237-250.

Wilson PJ, Forer A and Leggiardo C. (1994) Evidence that kinetochore microtubules in crane-fly spermatocytes disassemble during anaphase primarily at the poleward end. *Journal of Cell Science* **107**: 3015-3027.